PROCEEDINGS

2021 AUSTRALIAN GEOMECHANICS SOCIETY VICTORIAN SYMPOSIUM

Innovations in Geotechnical Design

Thursday, 21 October 2021, 8:30am – 5:00pm

An online-only event

AUSTRALIAN GEOMECHANICS SOCIETY
VICTORIA CHAPTER

CHADWICK GEOTECHNICS

PREFACE

The Victorian chapter of the Australian Geomechanics Society (AGS) is pleased to announce a one-day symposium titled "Innovations in Geotechnical Design" which is to be held on 21 October 2021. The event platform changed to an online-only event due to development of new restriction due to COVID-19 pandemic. This event will bring together geotechnical and other civil engineering professionals to share and discuss their knowledge and experiences related to geotechnical design and the latest technology and innovative methods.

Victoria's construction industry is still up and running, recovering quite well from the hiccups of the pandemic and several lock-downs. To catch up with the fast pace of global advancement in technology, incorporating more and more of the emerging and innovative methods in geotechnical design and construction seems to be the way forward, facing the challenges in the built environment. This symposium will present overviews of the state-of-the-art practices innovations in design, including new research, case studies, advanced technology and simulations related to various geo-structure systems, as well as reliability, safety, and observational design implemented in Victorian projects.

The symposium will bring together professional engineers, researchers, specialist contractors, regulators, educators and students to share and discuss their experiences on the above topics. This will be a great networking opportunity post-pandemic.

SYMPOSIUM ORGANISING COMMITTEE*

Alireza Mohammadinia (Co-Chair)

Mike Shackleton (Co-Chair)

Frazer Saunders

Richard Flynn

Negin Yousefpour

Yuqi Tan

Marvin Bedary

Stephen Wall

*a sub-committee of the AGS Victoria committee

SPONSORS

PLATINUM

Chadwicks Geotechnics

GOLD

Global Synthetics Pty Ltd

Insitu Geotech Services (IGS)

TECHNICAL REVIEWERS

All technical papers in these proceedings, excluding the keynote addresses, were peer reviewed. The reviewers are acknowledged and listed below:

Alireza Mohammadinia (Editor)

Chris Coulson

Joel Gniel

Daniel King

Ken Wright

Ramtin Tajeddin

Sanjive Narendranathan

Mahdi Miri Disfani

Jayantha Kodikara

Rob Day

A technical society of

AUSTRALIAN GEOMECHANICS SOCIETY

ENGINEERS AUSTRALIA

CONTENTS

ABOUT THE KEYNOTE SPEAKERS

JINSONG HUANG

Professor
The University of Newcastle

Jinsong Huang is a professor at the Priority Research Centre for Geotechnical Science and Engineering, the University of Newcastle. His research interests include risk assessment in geotechnical engineering and computational geomechanics. He has published over 100 journal papers on the risk assessment of slope stability and landslides, the modelling of spatial variability, stress integration techniques for elastoplastic models, the contact dynamics of granular media, the analysis of hydraulic fracturing and the predictive maintenance of railway tracks. He received a Regional Contribution Award from the International Association of Computer Methods and Advances in Geomechanics at its international conference in Kyoto in 2014 and the GEOSNet Award from the Geotechnical Safety Network in 2017. He will serve as the conference chair of the 8th International Symposium on Geotechnical Safety and Risk to be held at the University of Newcastle in December 2022.

JULIAN SEIDEL

Managing Director
Foundation QA

Dr. Julian Seidel has 42 years professional experience as a geotechnical engineer specialising in deep foundations, with particular expertise in pile dynamics and rock socketed piles. Julian graduated dux of Civil Engineering at Monash University in 1979, and 15 years later completed his PhD thesis "The analysis and design of pile shafts in weak rock" at Monash University under Chris Haberfield and Ian Johnston.

Julian has been employed over this time with GHD, Golder Associates, VicRoads, Pile Dynamics in the USA, Wagstaff Piling and Monash University. In 1999, he commenced his own consultancy Foundation QA, which later morphed into FSG. In 2020, Julian left FSG to continue his expert consulting activities under the Foundation QA brand in south east Asia on major infrastructure, legal disputes and insurance claims.

Google Scholar lists 70 of Julian's journal and conference papers, with over 1000 citations. He continues to pursue his personal research interests and to reinvigorate his publishing activities which have been put aside for many years.

CHRIS LYONS

Principal Geotechnical Engineer
Suburban Rail Loop Authority

Chris has over 24 years experience as a geotechnical engineer working across a wide range of infrastructure and commercial developments projects. He has worked on numerous major projects around the globe and has been involved in all stages of project works ranging from investigations, detailed design for construction and high-level project coordination. Chris has extensive experience covering the design of various types of deep and shallow foundations, ground improvement, advanced soil modelling, retaining walls and slope stabilisation works for both static and seismic loadings. Chris' recent areas of focus have been in ground movement damage assessments, dynamic rockfall modelling and integration of digital technology into geotechnical engineering workflows. Chris is currently work for Suburban Rail Loop Authority as the projects Principal Geotechnical Engineer.

SCOTT TAYLOR

Director Engineering
Major Road Projects Victoria

Scott currently leads the Engineering Team at Major Road Projects Victoria (MRPV), as the Director, Engineering His role oversees all engineering and technical aspects of the projects within the MRPV portfolio, with the aim of managing and mitigating technical risks.

Scott has worked in both the government and private sectors with a focus on Bridge Design and Design Management. Project Highlights include the West Gate Bridge Strengthening Project, leading the Design team for the M80 Ring Road Upgrade – Sunshine Ave to Calder Fwy which included the EJ Whitten Bridge widening, and the Ballarat Rail Upgrade Project. Scott is currently a member of the Victorian Division Committee for Engineers Australia, and a non-Executive Director of We Ride Australia. Scott also has a strong research background, having obtained a PhD in 2004 in the area of structural dynamics and computational methodologies.

SCHEDULE

8:30 am – Welcome and opening remarks

SESSION 1
SERVICEABILITY, RELIABILITY AND SAFETY IN DESIGN

8:40 AM **KEYNOTE ADDRESS**
Use of probabilistic methods in geotechnical engineering
Jinsong Huang (The University of Newcastle)

9:20 am **Presentation**
Reliability-based geotechnical design in an Australian context
Andrew Lochaden (Golder Associates)

9:35 am **Presentation**
Application of soil nail wall to roadway widening using GFRP rebars as per Australian design guidelines
Jay Lee (GS E&C Australia - formerly AECOM Melbourne)

9:50 am **Presentation**
Risk Prediction Model for Formation of Underground Cavities and Sinkholes due to Defective Sewer Pipes
Samanthi Indiketiya (Chadwick Geotechnics, Formerly Swinburne University of Technology)

10:05 am **Sponsor presentation**
Insitu Geotech Services – A Day in the Life of IGS

10:15 am **Questions**

10:25 am **Morning tea**

SESSION 2
INSTRUMENTATION AND MONITORING IN DESIGN

10:50 AM **KEYNOTE ADDRESS**
Ground truth, control and design of driven piles: implementing old ways with a new twist
Julian Seidel (Foundation QA)

11:30 am **Presentation**
The Application of 3D Finite Element Method in the Design of Large Piled Foundation System - Case Study: Melbourne Cement Facility
Kaveh Ranjbar (FSG Geotechnics and Foundations)

11:45 am **Presentation**
Pile Testing Verification – an Alternative Approach
Dion Denes (Golder Associates)

12:00 pm **Sponsor presentation**
Chadwick Geotechnics:
Innovation – Little things = Big WINS

12:10 pm **Questions**

12:20 pm **Lunch**

SESSION 3
OPTIMIZATION OF RISK AND SAFETY IN DESIGN

1:20 PM **KEYNOTE ADDRESS**
Using geotechnical innovation to reduce project risk
Chris Lyons (Suburban Rail Loop Authority)

2:00 pm **Presentation**
Design methodology and input parameters applicable to foundation design for large complex towers
Ying Tay (Golder Associates)

2:15 pm **Presentation**
Optimisation of Temporary Support Design for the Northern Portal Cut & Cover Tunnel
Jawad Zeerak (EIC Activities)

2:30 pm **Sponsor presentation**
Global Geosynthetics:
Innovative design approach for working platforms and hard stands
Amir Shahkolahi

2:40 pm **Questions**

2:50 pm **Afternoon tea**

SESSION 4
THE ROLE OF DESIGN IN INFRASTRUCTURE PROJECTS

3:15 PM **KEYNOTE ADDRESS**
Supporting Innovative Design and Construction
Scott R Taylor (Major Road Projects Victoria)

3:55 pm **Presentation**
BIM to Numerical Modelling Interoperability for Geotechnical Design of Underground Metro Station
Mengqi Huang (Monash University)

4:10 pm **Presentation**
On best practices for trackbed design
Negin Yousefpour (The University of Melbourne)

4:25 pm **Questions**

4:35 pm **Closing address**

4:45 pm **Finish**

Go to table of contents

SPONSORS

PLATINUM SPONSOR

CHADWICK GEOTECHNICS

GOLD SPONSORS

INSITU GEOTECH SERVICES
reducing geotechnical uncertainty

Global Synthetics
LEADERS IN GEOSYNTHETICS

CHADWICK
GEOTECHNICS

General Services

Chadwick Geotechnics is a leading supplier of services to the Geotechnical, Civil and Environmental disciplines across Australia, its Territories, and throughout the Asia Pacific region.

Key capabilities include:

Field Engineering

- Construction Engineering
- Onsite & Offsite Logging
- Factual Investigations & Reporting
- Bearing Assessments/Plate Load Testing
- Earthworks Supervision & Monitoring

Laboratory

- NATA Accredited
- Construction Materials Testing
- Triaxial and Consolidation Testing
- Thermal Resistivity Testing
- Rock Testing

Drilling

- Solid/Percussion/Direct Push
- Geotechnical and Environmental Systems
- NDD (Non Destructive Digging)

Instrumentation

- Optimisation
- Supply
- Installation
- Monitoring
- Telemetry

Think Act Be Safe

bsi. ISO 45001 Occupational Health and Safety Management

Engineering • Laboratory • Drilling • Instrumentation

Chadwick Geotechnics Pty Ltd
Melbourne | www.chadwickgeotechnics.com.au | info@chadwickgeotechnics.com.au

SESSION 1

SERVICEABILITY, RELIABILITY AND SAFETY IN DESIGN

Keynote Address

Use of probabilistic methods in geotechnical engineering

Jinsong Huang M.AGS M. ASCE

Discipline of Civil, Surveying and Environmental Engineering, College of Engineering, Science and Environment, The University of Newcastle, Callaghan NSW 2308, Australia; PH: +61 2 4921 5118; email: Jinsong.huang@newcastle.edu.au

ABSTRACT

Due to the intrinsic inhomogeneous nature of soils and rocks, the minimal site investigations, and the need to extrapolate available information over a large domain, geotechnical designs have inevitable uncertainties. To be conservative, geotechnical engineers traditionally use a safety factor to account for uncertainties. A more rigorous way of considering uncertainties is to use probabilistic methods. To promote the use of probabilistic methods in geotechnical engineering, this paper tries to address the following commonly encountered questions: 1) Why do we need to use probabilistic methods? 2) How can we use probabilistic methods if we don't have enough test data? 3) How much field/test data do we need? 4) How can we use multiple sources of information? 5) How can we use monitoring data to predict future performance?

Keywords: probabilistic methods, geotechnical engineering, limited data, Bayesian methods, prediction

1 INTRODUCTION

In recent years, there has been a remarkable increase in activity and interest in the use of probabilistic methodologies applied to more traditional areas of geotechnical engineering. This growth has manifested itself in many forms and spans both academe and practice within the geotechnical engineering community, for example, more dedicated conferences, short courses for practitioners, and new journals and books. However, there are still some reluctances. This paper tries to promote the use of probabilistic methods in geotechnical engineering by addressing some commonly encountered questions.

2 WHY DO WE NEED TO USE PROBABILISTIC METHODS?

2.1 Limited site investigation data

Soils and rocks in their natural state are among the most variable of all engineering materials, and geotechnical engineers must often "make do" with materials that present themselves at a particular site. In a perfect world with no economic constraints, we would drill numerous boreholes and take multiple samples back to the laboratory for measurement of standard soil properties such as permeability, compressibility, and shear strength. Armed with all this in-formation, we could then perform our design of a seepage problem, foundation, or slope and be very confident of our predictions. In reality we must usually deal with very limited site investigation data, and the traditional approach for dealing with this uncertainty in geotechnical design has been through the use of characteristic values of the soil properties coupled with a generous factor of safety.

If we were to plot the multitude of data from the hypothetical site investigation as a histogram for one of the properties, we would likely see a broad range of values in the form of a bell-shaped curve. The most likely values of the property would be somewhere in the middle, but a significant number of samples would display higher and lower values too. This variability inherent in soils and rocks suggests that geotechnical systems are highly amenable to a statistical interpretation. This is quite a different philosophy from the traditional approach mentioned previously. In the probabilistic approach, we input soil properties characterised in terms of their means and variances leading to estimates of the probability of failure or reliability of a design.

2.2 Probability of failure is more meaningful than factor of safety

It is common to apply the same factor of safety for different types of application without regard to the degree of uncertainty or failure consequence involved. In this case, the factor of safety can be misleading because a higher factor of safety doesn't necessarily mean the structure is safer.

Considering two examples of drained slope stability, they both have the same geometry as shown in Figure 1. The characteristic values of the soil properties in the two examples are shown in Eq. (1) and (2) respectively.

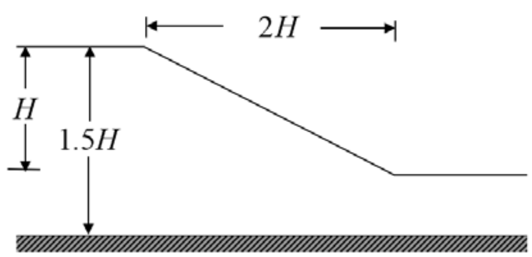

Figure 1. Slope profile

$$\phi' = 23^\circ \qquad \frac{c'}{\gamma H} = 0.048 \tag{1}$$

$$\phi' = 32^\circ \qquad \frac{c'}{\gamma H} = 0.048 \tag{2}$$

where c' and ϕ' are drained cohesion and friction angle respectively, and γ is unit weight of soil.

According to the stability charts in Michalowski (2002), the factor of safety for the two slopes can be found as 1.5 and 2.0 respectively. We may think that the second slope is safer than the first one because of a higher factor of safety. However, if we use a probabilistic approach, we may find that the mean and standard deviation of factor of safety for the two slopes are $\mu_{FS} = 1.5$, $\sigma_{FS} = 0.18$ (slope 1), and $\mu_{FS} = 2.0$, $\sigma_{FS} = 0.5$ (slope 2). Assuming the factor of safety is normally distributed, one can easily calculate the corresponding probabilities of failure of the two slopes are 0.27% and 2.27% respectively. It is clear that the second slope is actually less safe than the first one because of a higher probability of failure. The main reason why factor of safety can be misleading is that it uses only one parameter to quantify safety level. In probabilistic approaches, however, two parameters are used to quantify not only the mean safety level but also the standard deviation.

The factor of safety cannot provide meaningful information for risk assessment. For the two examples we just considered, both factors of safety are bigger than one which means both slopes are safe. By looking at the factor of safety along, it is hard for engineers to choose among the two slopes.

On the contrary, when probabilities are coupled with consequences of design failure, we can assess the risk associated with the design. For the examples we just considered, if the construction cost and consequence of design failure are estimated as shown in Table 1, the risk of the two designs can be estimated as Risk= construction cost + probability of failure × consequence.

It can be seen from Table 1 that the second slope with a higher probability of failure has lower risk than the first slope. However, if the consequence increases from 10M to 100M, the first slope with a lower probability of failure will have a lower risk than the second slope. This is consistent with the common sense that for important project, we need to lower the probability of failure to reduce risk.

Table 1: Risk assessment of slope failure

	Slope 1		Slope 2	
Construction cost (million dollar)	1		0.5	
Probability of failure	0.27%		2.27%	
Consequence (million dollar)	10	100	10	100
Risk (million dollar)	1.027	1.27	0.727	2.77

3 HOW CAN WE USE PROBABILISTIC METHODS IF WE DON'T HAVE ENOUGH TEST DATA?

We actually have two schools of statistics. The first one is frequentist approach. Frequentist says that we need to have enough data to draw a statistical conclusion, for example, a probability distribution. This is the dominant statistical practice during the 20th century.

The other approach is Bayesian methods. Bayesian says that before we do any test, we have some prior knowledge about the test we are looking at. And data can be used to update our prior knowledge. Bayesian methods started getting popular in 21st century, although it was published 200 years ago. It is now widely used in computer science, medical science, social science and so on.

The Bayesian approach has special significance to engineering design where available information is invariably limited and subjective judgement is often necessary. In the case of parameter estimation, we may often have some knowledge (perhaps inferred intuitively from experience) of the possible values, or range of values, of a parameter; moreover, we may also have some intuitive judgment on the values that are more likely to occur than others.

In Bayesian statistics, site investigation information, laboratory test data, in situ test data and load tests results are used as evidence to update prior knowledge, predictions and designs. The posterior distribution of the parameters is calculated based on Bayes' theorem:

$$P(\theta \mid D) = \frac{L(D \mid \theta)P(\theta)}{P(D)} \tag{3}$$

where θ denotes the parameters to be updated, D the data collected, $P(\theta)$ the prior probability distribution of the parameters, $L(D \mid \theta)$ the likelihood probability distribution and $P(D)$ the probability distribution of the evidence.

To demonstrate how Bayes' theorem can be used when test data are limited, let's consider load testing of pile capacity. Before any test is performed, engineers can look in the literature or similar projects for the initial assessment of the pile capacity (y). For simplicity, let's assume the pile capacity is normally distributed with mean μ and standard deviation σ. The standard deviation σ can be estimated based on the variability of the site (e.g., Kay (1978)). The mean pile capacity μ is uncertain, and is initially estimated using the prior probability distribution expressed by

$$f'(\mu) \sim N(\mu_0, \sigma_0) \tag{4}$$

where $N()$ represents the Normal distribution, and μ_0 and σ_0 are the mean and standard deviation of μ (mean of mean pile capacity, standard deviation of mean pile capacity). The parameters μ_0 and σ_0 were assumed to be associated with prediction methods (a static or dynamic method).

Suppose n pile capacity tests have been performed and the results are denoted as the vector $\hat{\mathbf{y}}$. The posterior distribution of μ can be obtained by Bayes' rule:

$$f''(\mu|\hat{\mathbf{y}}) = \frac{P(\hat{\mathbf{y}}|\mu)f'(\mu)}{P(\mathbf{y})} \quad (5)$$

$$\propto \exp\left(-\frac{\left(\mu - \frac{n\sigma_0^2\bar{y}+\sigma^2\mu_0}{n\sigma_0^2+\sigma^2}\right)^2}{2\left(\frac{\sigma_0^2\sigma^2}{n\sigma_0^2+\sigma^2}\right)}\right)$$

where $\bar{y}$ is the average value of $\hat{\mathbf{y}}$.

A detailed derivation of Eq. (5) can be found in Huang et al. (2016).

The posterior mean and standard deviation of μ are

$$\mu_1 = \frac{n\sigma_0^2\bar{y}+\sigma^2\mu_0}{n\sigma_0^2+\sigma^2} \quad (6)$$

and

$$\sigma_1 = \frac{\sigma_0^2\sigma^2}{n\sigma_0^2+\sigma^2} \quad (7)$$

Let us assume the prior mean and standard deviation of μ are $\mu_0 = 1.3$ and $\sigma_0 = 0.5$ and suppose five load tests have been conducted. The average capacity of tested piles is $\bar{y} = 0.8$. According to Eqs. (6) and (7), the posterior mean and standard deviation of μ are

$$\mu_1 = \frac{n\sigma_0^2\bar{y}+\sigma^2\mu_0}{n\sigma_0^2+\sigma^2} = \frac{5\times0.5^2\times0.8+0.2^2\times1.3}{5\times0.5^2+0.2^2} = 0.82$$

and

$$\sigma_1 = \frac{\sigma_0\sigma}{\sqrt{n\sigma_0^2+\sigma^2}} = \frac{0.5\times0.2}{\sqrt{5\times0.5^2+0.2^2}} = 0.09$$

The uncertainty of the mean capacity (μ) has been reduced significantly from $\sigma_0 = 0.5$ to $\sigma_1 = 0.09$ by the five load tests. It is interesting to note that even when we have only one test, we can still use Eqs. (6) and (7).

4 HOW MUCH FIELD/TEST DATA DO WE NEED?

Suppose we want to do an excavation on a site as shown in Figure 2(a) and the final slope profile is shown in Figure 2(b). The grayscale in Figure 2(b) represents different undrained strengths.

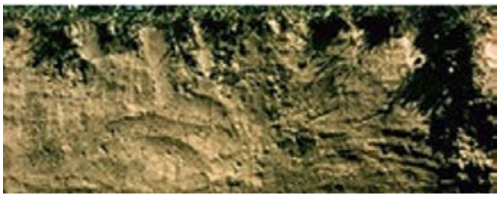

(a)

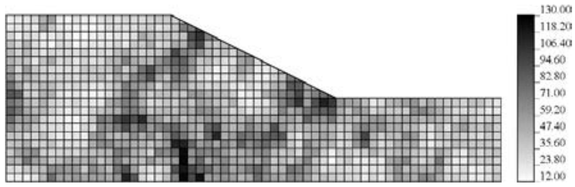

(b)

Figure 2. True in-situ distribution of undrained shear strength

Before we do the excavation or test, we actually don't know the undrained shear strength distribution in Figure 2(b). We can look in the literature for the statistics of the undrained shear strength of the soil in this particular site. And based on the statistics, we can use random field theory to guess the possible spatial distributions of the undrained shear strengths and perform a set of Monte Carlo simulations as shown in Figure 3. We generate a set of realisations of the slope, some of them will fail (e.g., Figure 3 a), some will not (e.g., Figure 3 b). If you divide the total number of failures by the total number of simulations, we can estimate the probability of failure, which is 17% in this case.

For the same slope, if we perform a cone penetration test as indicated by the red box in Figure 4, we then know the undrained shear strength of this column. Now we have statistics of the undrained shear strengths plus some test data. Based on the statistics and data, we can perform a set of conditional Monte Carlo simulations (e.g., Yang et al. 2019). Conditional means that the values of the known undrained shear strengths will not change from simulation to simulation, but fixed. From a set of conditional Monte Carlo simulations, we can estimate the probability of failure, which is 6% in this case.

If we perform a second CPT, we will know two columns of undrained shear strengths as shown in Figure 5. We can perform another set of conditional Monte Carlo simulations, and estimate the probability of failure, which is 0.7%. If we perform a third CPT, the estimated probability of failure is essentially close to zero as shown in Figure 6. If we keep doing test, eventually we will know the undrained shear strength distribution everywhere. And it turns out that the slope is actually safe. we can see based on three CPTs, we can reach a very reliable prediction of the slope stability. Please note that this conclusion only holds for this particular slope. For a different slope, the slope may fail, and we may need different number of CPTs to find it out. But the same methodology can be used to study how much tests do we need to draw a reliable prediction.

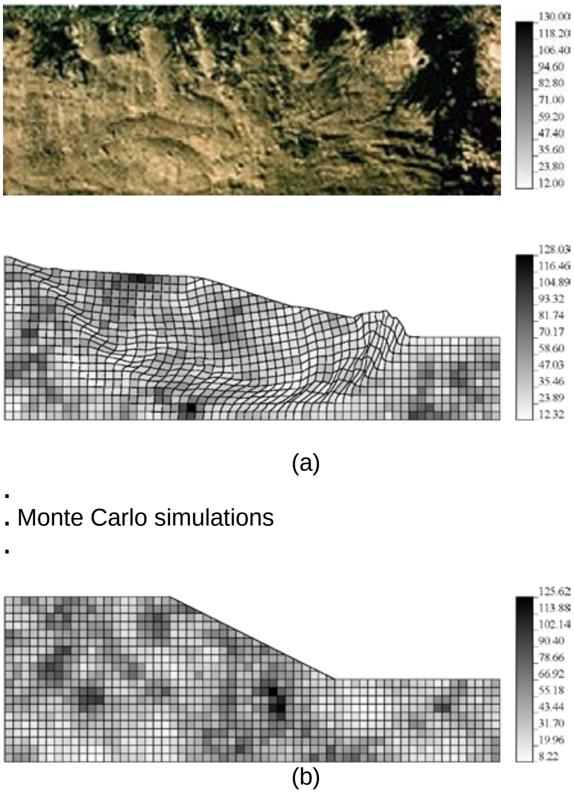

Figure 3. Unconditional Monte Carlo simulations based on the statistics in the literature

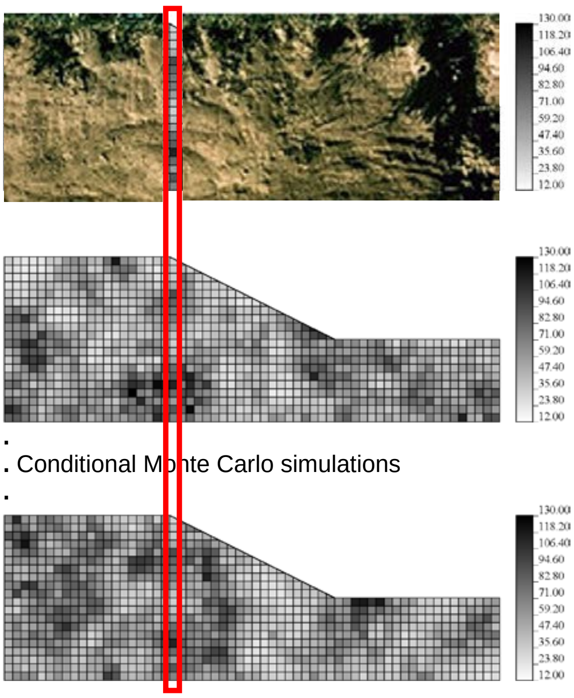

Figure 4. Conditional Monte Carlo simulations based on the statistics and one CPT test

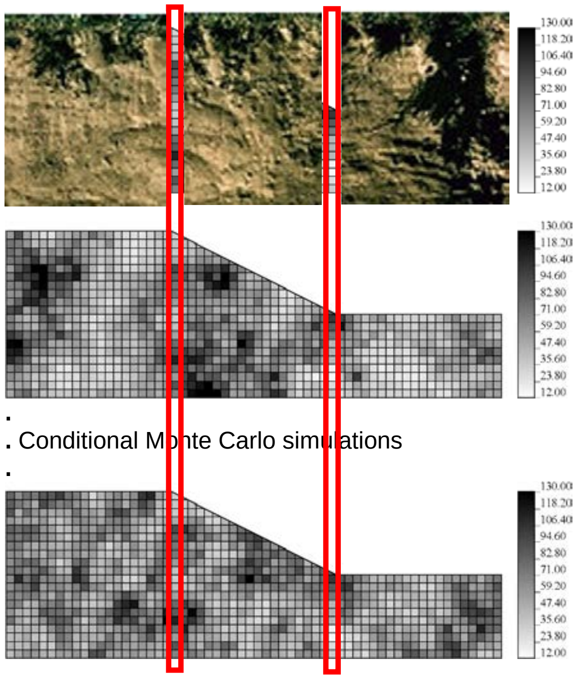

Figure 5. Conditional Monte Carlo simulations based on the statistics and two CPT tests

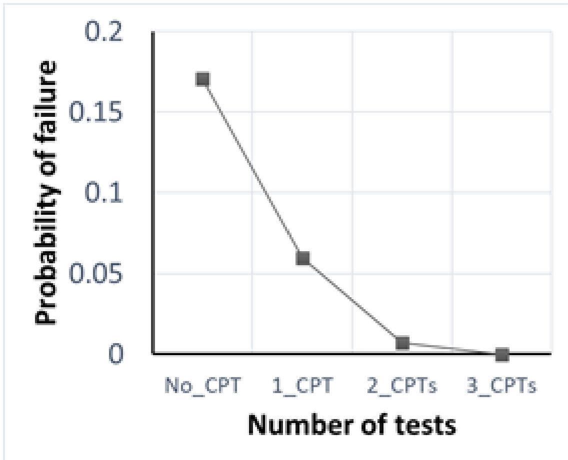

Figure 6. Probability of failure verse number of CPT tests

Generally speaking the approaches that we use to assess the safety of structures can be summarised in Table 2. It can be seen from Table 2 that probabilistic approaches can use test data directly, thus can reduce the uncertainty in our prediction. Recently Machine learning approaches become popular in geotechnical engineering. It is noted however, that Machine learning approaches use test data only, while probabilistic approaches can be combined with mechanical models (e.g., finite element model).

Table 2: Risk assessment of slope failure

Approach	Input data
Deterministic	Characteristic values
Unconditional probabilistic analysis	Mean, standard deviation, spatial correlation structure
Conditional probabilistic analysis	Mean, standard deviation, spatial correlation structure, test data
Machine learning	Test data

5 HOW CAN WE USE MULTIPLE SOURCES OF INFORMATION?

Site characterisation is a fundamental step of collecting geotechnical information for proper design, construction and long term performance of all types of civil and geotechnical structures. Current site investigation practice in geotechnical engineering often involves two steps: 1) a geophysical site investigation or a desk-top study of existing geophysical data; and 2) a dedicated *in situ* geotechnical investigation including several boreholes and laboratory testing at the intended location of the future structure. Each type of investigation explores a specific volume of the subsoil and has different degrees of uncertainty. Geophysics provides a wide variety of tools which can help to identify the subsoil stratigraphy. Data are obtained on a two- (or three-) dimensional section of the ground, often with low resolution. On the other hand, *in situ* tests are performed along a one-dimensional line with depth and laboratory tests performed at point locations within the ground. These tests provide direct measurements of physical and mechanical properties, but cover only a small volume of the subsoil. In current engineering practice, the integration of geophysical data with geotechnical data is done manually, often by visual inspection based largely on engineering judgement and experience, which does not only introduce additional human error, but also causes loss of information. For example, the geophysical data is used to find the desirable locations of geotechnical tests, but often ignored in deriving geotechnical properties.

A more scientific integration of geophysical data with geotechnical data can be done based on Bayes' theorem. Figure 7 shows a one dimensional cone tip resistance profile obtained by a CPT test. On top of that, it also shows a two dimensional shear wave velocity profile obtained by multi channel surface wave (MASW) test. If we can use CPT and MASW test results together, it will help to reduce the uncertainties in our model.

Huang et al. (2018) developed a Bayesian updating approach, which can combine multiple sources of information automatically. If we use the CPT test result only, we can use random field theory to estimate the mean, standard deviation and spatial correlation length using the CPT results and then use conditional random fields to guess the possible soil profiles. Figure 8 shows the soil profile based on conditional random field and the CPT test only. It can be seen from Figure 8 that at the place where we have CPT test, the mean cone tip resistance is the same as we tested by CPT and the standard deviation of cone tip resistance is low. However, at the places where we don't have any test, the mean cone tip resistance is similar to and informed only by the CTP test results, and the standard deviation of cone tip resistance is large. This means that we have less confidence on the profile of cone tip resistance based on one CPT only.

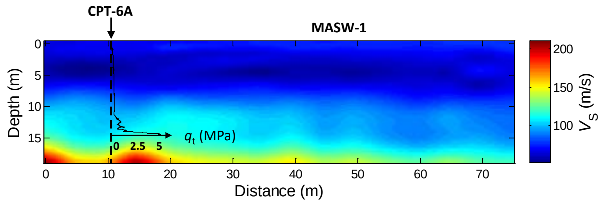

Figure 7. Geotechnical CPT test and geophysical multi channel surface wave test

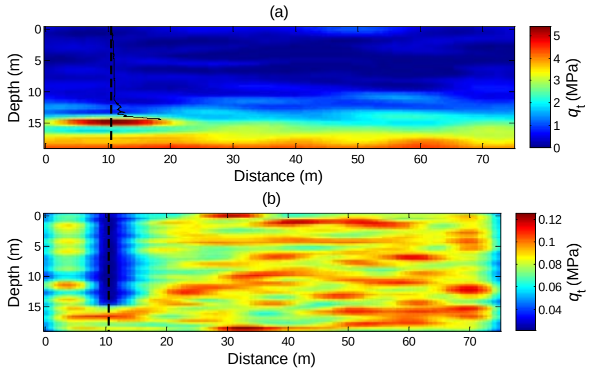

Figure 8. Soil profile based on one CPT test, a) mean cone tip resistance, b) standard deviation of cone tip resistance.

If we use the CPT and MASW test results together, we can have a higher confidence on the cone tip resistance profile. Figure 9 shows the soil profile based on Bayesian updating and both CPT and MASW test results. It can be seen from Figure 9 that at the place where we have CPT test, the mean cone tip resistance is still the same as we tested by CPT and the standard deviation of cone tip resistance is low. However, at the places where we don't have CPT test, the mean cone tip resistance is informed by the MASW results, and the standard deviation of cone tip resistance is reduced.

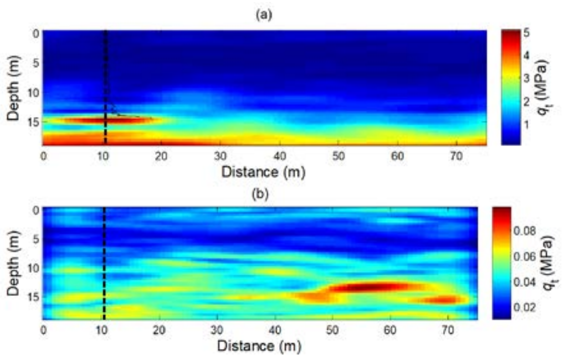

Figure 9. Soil profile based on CPT and MASW test results, a) mean cone tip resistance, b) standard deviation of cone tip resistance.

6 HOW DO WE USE MONITORING DATA TO PREDICT FUTURE PERFORMANCE?

In design stage, we predict the safety level of the structures based in lab and field test results. After construction, the behaviour of the structure most of the time is different from our prediction. For important projects such as large dams and bridges, we usually install some sensors or devices to monitor the behaviour of the structure. In this case, we need to use the monitoring data to reassess the safety level of the structure. This is called back analysis.

Another example where back analysis becomes important is embankment built on soft soils. Due to variations in a soft soil profile and its properties, the actually settlement behaviour is usually different from the performance anticipated in design. If the decision on the settlement behaviour (i.e., quicker or slower than expected) can be made sooner, then a smaller amount of surcharge is required and road construction can start earlier, which leads to significant financial benefits.

Table 3 lists some of the most commonly used back analysis methods. The simplest back analysis is manual calibration where engineers try to minimise the different between observation D and model output $g(\theta)$. Least square method is probably the most widely used method for back analysis because it always provides a solution no matter how complicated the problem is. Least square is actually a special case of the Maximum Likelihood method where measurement error is normally distributed with zero mean. In contrast to the Maximum Likelihood method, Maximum A Posterior method not only consider the likelihood, but also the prior distribution of the parameters. Bayesian back analysis is the most generic type of back analysis. Instead of solving for the set of parameters that maximum posterior probability density as in the Maximum A Posterior method, Bayesian updating samples the whole posterior probability density function. The most commonly used method for this purpose is the Markov chain Monte Carlo method.

Table 3: Commonly used methods for back analysis

Method	Formula
Manual calibration	$\text{Min } D - g(\theta)$
Least square	$\text{Min}\left(D - g(\theta)\right)^2$
Maximum Likelihood	$\text{Max } L\left(\dfrac{D - g(\theta) - \mu_e}{\sigma_e}\right)$
Maximum A Posterior	$\text{Max } L\left(\dfrac{D - g(\theta) - \mu_e}{\sigma_e}\right) P(\theta)$
Bayesian updating	$P(\theta \mid D) \propto L\left(\dfrac{D - g(\theta) - \mu_e}{\sigma_e}\right) P(\theta)$

Bayesian updating can use prior knowledge (e.g., lab and field test results) and monitoring data in a rigorous framework. It can also consider measurement errors and provide confidence interval on the predictions. A proof-of-concept application of Bayesian updating for embankment settlement prediction can be found in Kelly et al. (2015). Zheng et al. (2018) used Bayesian updating with laboratory data, field test data, and monitoring data to yield accurate predictions during the construction and consolidation periods for the test embankment built at Ballina, New South Wales, Australia. The results show that surface settlement can be well predicted using 116 days of observed settlements, while the pore pressure can be predicted using 292 days of pore pressure measurements. The predictions are shown to converge to the field measurements, regardless of some assumptions about the measurement errors. It is also demonstrated that incorporating more monitoring data into the Bayesian updating process enables more accurate predictions.

7 CONCLUSIONS

Deterministic factor of safety approach has been used in geotechnical engineering for many decades. Although probabilistic approaches can provide more information for risk assessment, there are still quite some resistances to the use of probabilistic approaches. The most common excuse for not using probabilistic approach is lack of data. This paper has shown that Bayesian approaches can be used even when we have only one test result. Bayesian approaches are also useful for combining different types of test results and back analysis based on monitoring data. It is anticipated that probabilistic approaches will become more and more popular in geotechnical engineering to supplement, not replace the factor of safety approach.

8 ACKNOWLEDGEMENTS

The research supports by the Australian Government through the Australian Research Council's Discovery Projects funding scheme (project DP190101592) and Linkage funding scheme (project LP200100367) are acknowledged.

REFERENCES

Huang, et al. (2016). "Updating reliability of single piles and pile groups by load tests." Computers and Geotechnics 73: 221-230.

Huang, et al. (2018). "Probabilistic characterization of two-dimensional soil profile by integrating cone penetration test (CPT) with multi-channel analysis of surface wave (MASW) data." Canadian Geotechnical Journal 55(8): 1168-1181.

Kay (1978). "Safety Factor Evaluation for Single Piles in Sand." Journal of the Geotechnical Engineering Division-Asce 104(1): 148-149.

Kelly, et al. (2015). "Bayesian updating for one-dimensional consolidation measurements." Canadian Geotechnical Journal 52(9): 1318-1330.

Michalowski (2002). "Stability Charts for Uniform Slopes." Journal of Geotechnical and Geoenvironmental Engineering 128(4): 351-355.

Yang, et al. (2019). "Importance of soil property sampling location in slope stability assessment." Canadian Geotechnical Journal 56(3): 335-346.

Zheng, et al. (2018). "Embankment prediction using testing data and monitored behaviour: A Bayesian updating approach." Computers and Geotechnics 93: 150-162.

Reliability-based geotechnical design in an Australian context

A. L. E. Lochaden[1] and S. Buttling[2]

[1] Principal Geotechnical Engineer, Golder Associates Pty Ltd, Melbourne, PO Box 6079, Hawthorn East, VIC 3121; PH (+61) 3 8862 3500; FAX (+61) 3 8862 3501; email: alochaden@golder.com.au
[2] Principal, National Geotechnical Consultants, PO Box 485, The Gap, QLD 4061; PH (+61) 7 3300 0088; email: stephen.buttling@ngconsult.com.au

ABSTRACT

The design philosophy adopted by the international geo-engineering community over the last few decades has largely evolved from working stress design (WSD), in which a single or lumped factor of safety (FoS) is adopted, to a load and resistance factor design (LRFD) approach. In LRFD, partial factors are applied to actions (i.e. loads), soil parameters and / or resistances. These partial factors vary in magnitude depending on the relative uncertainty of each parameter to which they are applied. The approach adopted in Australia has differed, with both WSD and LRFD approaches being widely used. In the authors' experience, there is limited awareness in the Australian geo-engineering community of the relationship between the concept of reliability and the partial factors adopted in LRFD, and therefore of the potential benefits of undertaking reliability-based design (RBD). The outcome of this is that RBD, in which the uncertainty of the variables which may affect the design is individually assessed, is rarely undertaken. This paper discusses the concept of RBD and its place within the framework of Australian Standards and presents practical means of adopting RBD with accompanying examples from the literature. The intention of the paper is to encourage practitioners to consider uncertainty in geotechnical design more rigorously, whilst acknowledging the importance of maintaining engineering judgement in design.

Keywords: geotechnical design, working stress, limit state, reliability.

1 INTRODUCTION

At its simplest, the purpose of any geotechnical design is to ensure that the risk of failure is sufficiently low to be deemed acceptable. Failure may be the catastrophic collapse of a retaining wall for example, but could also be an unacceptable degree of cracking in a building due to the excessive movement of the footing system.

Historically, the geo-engineering professional has considered this risk by applying a lumped FoS to a calculated ultimate resistance, i.e. WSD. This methodology has largely been replaced internationally by LRFD, in which various factors are applied to actions (including loads), soil parameters and / or resistances, the magnitude of which are typically defined in national design standards and are a function of the expected relative uncertainty of the variable under consideration. The introduction of LRFD brought with it a lexicon which was new (and in some cases, potentially unnecessary), and which remains frustrating to many geo-engineering professionals.

If LRFD is considered to be an evolution of WSD, RBD may be considered to be an evolution of LRFD. RBD involves the rigorous assessment of the uncertainty of the variables on which a design is dependent. RBD has been discussed in the literature for over 40 years, but its adoption as a design methodology has been slow. However, it is now included in some international design standards, including the Canadian Highway Bridge Design Code (Canadian Standards Association, 2014).

This paper sets out the current state of geotechnical design in Australia, describes the relationship between LRFD and RBD, and presents ways in which RBD can be adopted in practice.

2 THE STATE OF GEOTECHNICAL DESIGN IN AUSTRALIA

National Standards exist to ensure that the balance between cost and safe / serviceable structures is appropriately achieved, and that a similar level of reliability is achieved in design undertaken by different practitioners. The state of geotechnical design in Australia, within the framework of national design standards, is somewhat unusual for a number of related reasons.

Firstly, whereas the UK, previously through BS 8004 (BSI, 1986) which encompassed all types of foundations and now through Eurocode 7 (BSI, 2004), and the United States through AASHTO (2017), have complete and overarching design standards, there are a limited number of Australian Standards for the design of various geotechnical elements, for example AS2159 (Standards Australia, 2009) for piled foundations, AS2870 (Standards Australia, 2011) for residential slabs and footings, and AS4678 (Standards Australia, 2002) for (predominantly gravity) retaining walls.

Secondly, relevant Australian Standards have not been published for commonly encountered design scenarios such as slopes and shallow footings including raft foundations for high rise buildings (other than residential slabs and footings, as described above), although AS5100.3 (Standards Australia, 2017a) is sometimes adopted for shallow footing design for infrastructure projects.

Thirdly, whilst most international design standards have moved from WSD to LRFD, Australia has effectively maintained both approaches. For example, pile foundations are typically designed using a limit state approach to AS2159, whereas slopes are typically designed using a lumped FoS approach.

To further complicate matters, the analysis tools commonly adopted in geotechnical design have changed over the last number of years such that parts of the national design standards have lost some of their relevance. For example, embedded retaining walls are now commonly designed using tools such as WALLAP and PLAXIS 2D. However, both AS4678 (Standards Australia, 2002) and AS5100.3 (Standards Australia, 2017a) provide insufficient guidance on how such soil-structure interaction analyses should be undertaken. Although beyond the scope of this paper, the reader is directed to Haberfield (2017), for example.

3 THE RELATIONSHIP BETWEEN RBD AND LRFD

3.1 Introduction

As stated in Section 2, design must balance cost with the safety / serviceability of a structure. Regardless of the various design methodologies which may be adopted, or whether the design is a structural or a geotechnical one, an appropriate design must establish that the design resistance is not less than the design actions (applied loads).

The degree of safety of a structure has traditionally been assessed in a deterministic manner by engineering professionals in terms of a calculated FoS. The engineering professional undertakes this assessment using either what he / she considers to be appropriate values for applied loads and resistances to take account of their potential variability, or what the relevant design standard mandates. This is illustrated in Figure 1, in which the margin of safety is defined as the difference between the resistance and the loads. However, this methodology neglects to robustly consider the potential variability of both the applied loads and the resistances.

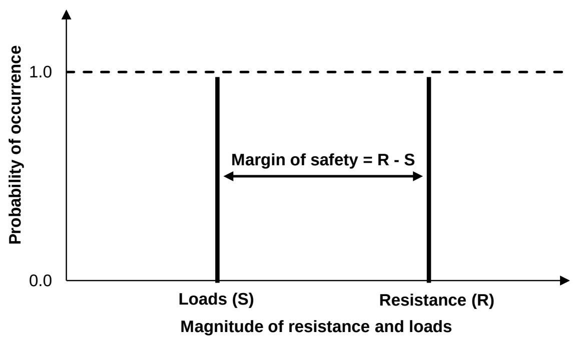

Figure 1. Graphical illustration of margin of safety for WSD (after Becker, 1996)

3.2 Load and resistance factor design

LRFD requires the engineering professional to demonstrate that serviceability and ultimate limit states (SLS and ULS, respectively) are not exceeded. In simple terms, the purpose of the SLS check is to assess if movement beyond an allowable limit occurs, whilst the purpose of the ULS is to ensure that collapse will not occur.

As set out in Becker (1996b), the partial factors which are applied in LRFD may be based on calibration using one or a combination of:

- Previous experience.
- WSD approach.
- Reliability theory (as discussed in Section 3.2).

One of the benefits of LRFD over WSD is that the engineering professional is required to apply partial factors to individual components of load and resistance, thereby allowing the higher risk of variation in (say) live loads compared to (say) the self-weight of concrete to be considered in the design. This is not possible in WSD, as a single lumped FoS is applied.

LRFD has been subject to criticism by Australian practitioners, for example Day (2001), Pells (2011), Day *et al.* (2007), and Wong *et al*. (2007). It is acknowledged that many of the arguments made in these references are valid, but note that a discussion of these arguments lies outside the scope of this paper. It is noted that despite the criticisms set out in these references, Wong *et al*. (2007) state that "…*despite these difficulties, there is definitely a place for limit state design in geotechnical engineering*" and "*the use of limit state design…has benefits as long as the underlying design principles and soil-structure interaction effects are properly understood and communicated*".

3.3 Reliability based design

Reliability theory was introduced initially as a design concept for structural engineering, and subsequently for geotechnical engineering, primarily to counter this lack of robust consideration of the potential variability. The use of reliability theory in the field of geotechnical engineering is not new – it was the subject of the 17th Terzaghi Lecture in 1981 (Whitman, 1984).

The requirement for this more robust consideration is discussed below with reference to Figure 2. This has previously been presented in the literature (including Becker, 1996a). Loads and resistances are variables and are not defined by a single value as considered in the deterministic approach described in Section 3.1. Sources of geotechnical uncertainty include spatial variation, measurement error, transformation error (for example, the calculation of undrained shear strength of a cohesive material from Cone Penetration Test data), and model calculation uncertainty (i.e. the degree to which the analytical model represents the true behaviour of the system).

By plotting both the load and resistance frequency distributions on a single plot, the relatively low probability of a combination of high loads and low resistance which would result in failure is represented by the intersection of the load and resistance frequency distributions.
In Figure 2:

- Cases (a) and (b) are two curves representing the frequency distributions of resistance which have the same design value, but differing standard deviations, noting that the standard deviation for Case (a) is less than that for Case (b).
- Case (a) represents a condition whereby the resistance is well defined (i.e. the frequency distribution curve is relatively narrow). This could be the case where a significant amount of geotechnical investigation has been undertaken at a site and where there is relatively small variability in the geotechnical data. The area of intersection (in green) of the load and resistance curves is relatively small and therefore the probability of failure is relatively low.
- Case (b) represents a condition whereby the resistance is not well defined (i.e. the frequency

distribution curve is relatively broad). This could be the case where little geotechnical investigation has been undertaken at a site and where there is relatively high variability in the geotechnical data. The area of intersection of the load and resistance curves (the combined green and red areas) is relatively large and therefore so is the probability of failure.

- The higher probability of failure of Case (b) compared to Case (a) is not captured by the traditional FoS approach, as the mean margin of safety (and therefore FoS) for both Cases (a) and (b) is the same.

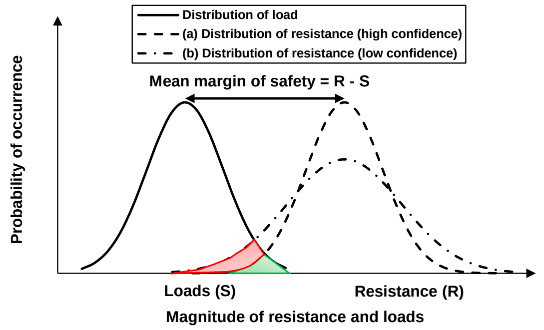

Figure 2. Variation of loads and resistance (after Becker, 1996a and Green, 1989)

The intention of RBD is to provide adequate confidence that the probability of failure (P_f) is sufficiently low. RBD allows a more consistent assessment of reliability to be calculated compared to either WSD or LRFD. Although the theory of reliability analysis lie beyond the scope of this paper, reliability analysis requires assumptions to be made in relation to the frequency distributions of the loads and resistances (for example the normal distributions shown in Figure 2), and therefore the P_f calculated should not be considered to be the "true" probability of failure, but a reasonable estimate. Furthermore, as with any design, reliability analysis requires the engineering professional to use appropriate means of calculation, interpretation of geotechnical data, etc..

As an alternative to P_f, the likelihood of failure may be expressed in terms of the reliability index (β), which is a description of the safety of the structure normalised by its uncertainty. A higher β value indicates a more robust design. The target β for a specific structure should be based on a number of considerations, but primarily the consequences of failure (for example, risk to life and economic consequences). The target β for Australian structures for various considerations is set out in AS5104 (Standards Australia, 2017b), and which includes an appendix focussed on geotechnical engineering.

The concept of β is explained in Low (2005) with reference to Figure 3 and the First Order Reliability Method (FORM, also known as the Hasofer-Lind method, Hasofer and Lind, 1974), demonstrated using the example of the rotational failure of a gravity wall, as follows:

- The ellipses in Figure 3 represent combinations of the effective angle of friction (φ') of the retained material and of the soil-wall interface friction angle (δ) which have the same probability of occurring concurrently.
- The ellipses are centred about characteristic values of φ' and δ.
- The "critical combination" is the most probable combination of φ' and δ which would result in failure, and is the shortest distance on the plot from the characteristic values of φ' and δ to the failure surface.
- β is defined as the quotient of the shortest distance from the centre of the ellipse to the failure surface (R in Figure 3) and one standard deviation (r in Figure 3).

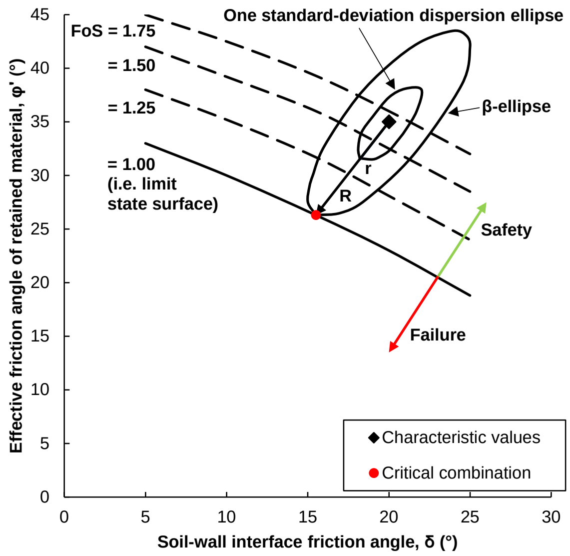

Figure 3. Definition of β (after Low, 2005)

More than two variables can be considered in reliability analyses, the first step being the replacement of the ellipses by ellipsoids in three dimensions. However, to allow graphical representation in two-dimensional space, the example above has been limited to two variables only.

If for some design scenario the calculated β value was too low, the engineering professional could increase the strength and size of structural members while leaving the uncertainty changed. This would result in an increase in the distance from the characteristic points to the failure surface (R) and leave r unchanged, thereby increasing the calculated β value. An alternative solution would be to leave the strength and size of structural members unchanged and decrease the uncertainty, for example by undertaking more and / or higher quality geotechnical investigations. This would cause a reduction in the radius of the one standard-deviation dispersion ellipse (r), also resulting in an increase in the calculated β value.

The partial factors presented in national design standards and which are required to be adopted in LRDF may have been (but are not always) calculated based on reliability analysis, as discussed in Section 3.2. The benefit of the presentation of partial factors within national design standards is that the engineering professional is not required to undertake reliability analyses for a design, and can instead use the provided partial factors to achieve the required level of reliability. However, in deriving partial factors to be applied for all potential scenarios to achieve adequate reliability, reasonable ranges of uncertainty must be considered. This means that in some design situations, the partial factors presented in national design standards will result in a β for a structure which is greater than that required, i.e. the resulting design will be overly conservative. A site-specific RBD therefore presents the engineering professional with the potential opportunity to adopt lower partial factors, if:

- The engineering professional has the expertise to undertake such an analysis,
- Sufficient geotechnical investigation data are available to undertake a valid statistical assessment of the data, and
- The relevant national design standard allows it.

4 UNDERTAKING RBD IN PRACTICE

4.1 Introduction

The purpose of Section 4 is to demonstrate the way in which RBD may be adopted in practice. Practical examples of RBD for various commonly encountered geotechnical design scenarios are summarised.

Whilst there are many examples in the literature of reliability assessments which have been undertaken using both non-commercially available finite element software (for example, Fenton and Griffiths, 2003), and bespoke software coupled with commercially available software (for example, Schweckendiek *et al*., 2007), it is the authors' opinion that these are unlikely to be practical for the majority of consulting geo-engineering professionals considering the current level of maturity of RBD in both Victoria and Australia more widely. The focus has therefore been on more routine examples.

4.2 Design approach and methodologies

Fenton *et al*. (2016) present a general methodology for the adoption of RBD which is common to many geotechnical design scenarios. This methodology includes the following (albeit high-level) steps:

- Identify the limit state under consideration, for example bearing capacity of a shallow footing.
- Describe the relevant parameters (for example effective cohesion, c' and φ') statistically by using appropriate frequency distribution curves.
- Use a numerical model to assess for many scenarios if the limit state is exceeded.
- Assess the probability of failure based on the number of cases which result in the limit state being exceeded.

Of the above steps, a typical geo-engineering professional will likely be least familiar with the assessment of frequency distribution curves and with the identification of a suitable numerical model to assess the limit states for the purposes of a reliability analysis.

An assessment of an appropriate frequency distribution requires a working knowledge of statistics. Ideally, the geo-engineering professional would have a thorough understanding of the site conditions from an appropriate site investigation, with many data points to allow an appropriate frequency distribution to be identified (e.g. normal, log-normal, etc.). However, this is not always practical and so the geo-engineering professional may use information presented in the literature in relation to the mean and coefficient of variation of various soil properties (refer Uzielli *et al*., 2006 for example). It is noted that the coefficient of variation (COV) is the quotient of the standard deviation and mean of the sample, and is a description of its relative dispersion.

Baecher and Christian (2003) present a summary of various numerical methodologies which can be adopted for the practical adoption of RBD, some of which are summarised below.

- First Order Second Moment (FOSM) method.
- Point Estimate method.
- FORM.
- Monte Carlo simulation.

Many geo-engineering professionals will reasonably endeavour to adopt reliability based methodologies within the software with which they are familiar and which is commonly adopted in the industry. The SLOPE/W software, for example, allows the user to undertake Monte Carlo simulations. Whilst the application PROBANA has been used in the past to undertake FORM and Monte Carlo analysis coupled with PLAXIS 2D, the authors understand that this application is neither commercially available nor supported by more recent versions of PLAXIS 2D (Bentley Systems, personal communication, 10 August 2021).

4.3 Design examples – shallow footing

Cherubini (1990) presents a closed-form solution for the probabilistic evaluation of the bearing capacity of a shallow foundation for a cohesionless soil with φ' ≤ 35°. φ' only is considered as an independent variable. The frequency distribution of the ultimate bearing capacity, calculated using numerical integration, is presented for various standard deviations of φ'.

Low and Tang (1997) present a more sophisticated reliability analysis of a shallow footing. As the methodology is similar to that set out in Low (2005) and discussed in Section 4.5, this is not discussed further herein.

4.4 Design example – pile group

Randolph and Buttling (2022) demonstrate how the Monte Carlo method, scripted using Python, can be applied to undertake a probabilistic analysis of a pile group analysed using the spreadsheet program PIGLET. In the example presented by Randolph and Buttling (2022), a number of inputs to the pile group analysis are treated as random variables, including the shear modulus (both axial and lateral) of the soil in which the piles are constructed, the axial capacity of the piles, and the normalised lateral pile head displacement at which the secant stiffness is 50% of the initial tangent value. As the analysis undertaken was a test case (and not a design to be constructed), the range of the random variables used as inputs to the probabilistic analysis was expressed through the use of published COV data, rather than a statistical assessment of site-specific geotechnical investigation data.

The Python subroutine was used to carry out 100,000 analyses for 38 load cases, which took approximately 150 minutes on a standard computer. It was found that the pile group lateral displacement limit of 50 mm (considered as a ULS case) was exceeded by 0.33% of the simulations, giving a β value of 2.72. This compares with a value of 3.1 recommended in AS5104 (Standards Australia, 2017b) for Class 2 structures with a high cost of safety measures. A typical bridge such as a highway bridge would probably be defined as a Class 3 structure in which case β would be required to be 3.3. As noted above, for the test case of the subroutine the site specific soil data was not used, but it was considered that β could relatively easily be raised to 3.3 if required, such as by a better site investigation, for example using a dilatometer or pressuremeter to measure the in situ modulus and its variability.

4.5 Design examples – retaining walls

Low (2005) presents reliability analyses of two types of retaining walls which were undertaken using FORM within Microsoft Excel and its built-in optimisation program application Solver. The reliability analyses were undertaken on both a gravity retaining wall (Figure 5) to assess the ULS failure modes of rotation and sliding, and an anchored retaining wall (Figure 6) to assess the ULS failure mode of rotation. Low (2005) provides detailed information on how the methodology was undertaken and includes a link from which the relevant Microsoft Excel files may be downloaded.

For the case of the gravity retaining wall, limiting equations for rotation and sliding (referred to as performance functions) are derived from basic physics and geo-mechanics. Three variables are considered: φ', δ and base adhesion. The degree of correlation between φ' and δ is also considered, and the degree to which the reliability is sensitive to each variable is assessed. β is calculated using the Solver application described above.

For the case of the anchored retaining wall, nine variables were considered in the assessment of the required wall embedment to achieve a target β. These variables included soil unit weight, surcharge pressure, depth to groundwater and the yield force of the anchor. In a similar manner to the gravity retaining wall case, the equations for force and moment equilibrium are used as performance functions, and a reliability assessment undertaken.

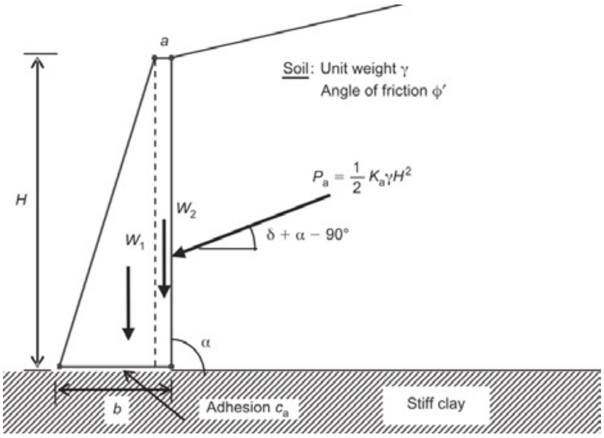

Figure 5. Reliability analysis of gravity retaining wall (from Low, 2005)

Low (2005) concludes that the calculated β values using FORM are in good agreement with those calculated from an alternative Monte Carlo simulation, but with significantly less computational effort.

5 DISCUSSION AND SUMMARY

If RBD is to be adopted more widely in the geotechnical industry in Australia, a number of issues need to be addressed. These include:

- Increased focus on appropriate statistics in undergraduate geo-engineering courses.
- Upskilling of the knowledge of relevant statistics of currently practising geo-engineering professionals.
- Further research into the benefits that RBD has over WSD and LRFD, and clear communication of these benefits to clients such that the additional high-quality site investigations required for RBD are approved.

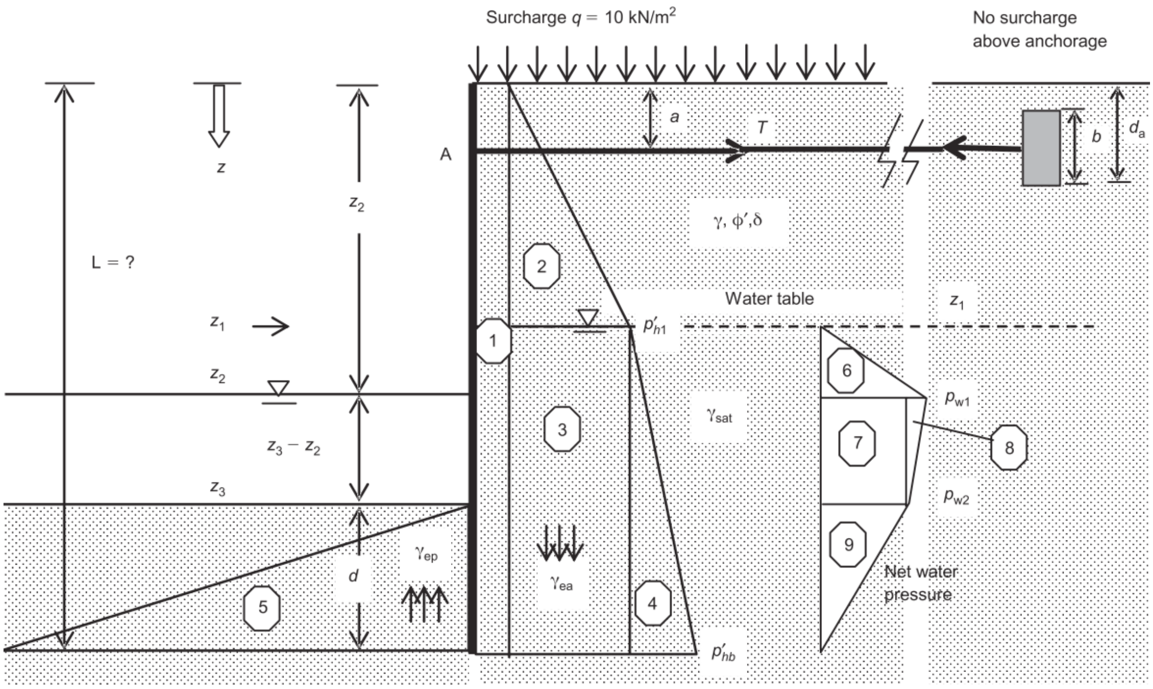

Figure 6. Reliability analysis of anchored retaining wall (from Low, 2005)

- The improvements in recent years in the way in which electronic site investigation data are gathered and manipulated has allowed significant efficiencies to be gained in the management of geotechnical data. The time and budget gained through these improved efficiencies needs to be re-invested in more sophisticated interpretation methodologies to allow RBD to be undertaken.
- Greater engagement with RBD by the Australian geo-engineering community.
- Increased co-operation between industry and academia in relation to how RBD may be adopted in practice, e.g. the Recent Trends in Geotechnical and Geo-Environmental Engineering and Education (RTGEE) workshops.
- Development of an overarching Australian Standard for geotechnical design, similar to that which exists in Europe and the USA, which addresses the concept of RBD.

Subject to the above, the authors consider that RBD has the potential to be a highly useful design tool for the geo-engineering professional. Notwithstanding this, the authors consider that, as described by Becker (1996a):

- Whilst probability and statistics are useful tools if properly applied, they must not become a substitute for trying to understand the behaviour of geotechnical materials.
- Geotechnical design must not become overly distracted by levels of safety and their quantification, but instead focus on the understanding of the basic failure mechanisms and fundamental material behaviour.

REFERENCES

AASHTO (2017). "AASHTO LRFD bridge design specifications". Washington DC, USA.

Baecher, G.B. Christian, J.T. (2003). "Reliability and Statistics in Geotechnical Engineering".

Becker, D.E. (1996a). "18th Canadian Geotechnical Colloquium: limit state design for foundations. Part I. An overview of the foundation design process". Canadian Geotechnical Journal, 33, pp. 956-983.

Becker, D.E. (1996b). "18th Canadian Geotechnical Colloquium: limit state design for foundations. Part II. Development for the National Building Code of Canada". Canadian Geotechnical Journal, 33, pp. 984-1007.

British Standards Institution (BSI) (1986). "Code of Practice for Foundations".

British Standards Institution (BSI) (2004). "Eurocode 7: Geotechnical design".

Canadian Standards Association (2014). "Canadian Highway Bridge Design Code". CAN/CSA-S6-06, Mississauga, Ontario.

Cherubini, C. (1990). "A closed-form probabilistic solution for evaluating the bearing capacity of shallow foundations". Canadian Geotechnical Journal, vol. 27, pp. 526-529.

Day, R.A. (2001). "Factored material properties and limit state loads – unlikely extreme or impossible pretence". Geotechnical Engineering, vol. 149, no. 4, pp. 209-210.

Day, R.A., Wong, P.K. and Poulos, H.G. (2007) "Fifteen years of geotechnical limit state design in Australia. Part I – soil retaining structures". Proceedings of 10th Australia New Zealand Conference on Geomechanics, Brisbane, pp. 596-601.

Fenton, G.A. and Griffiths, D.V. (2003). Bearing-capacity prediction of spatially random c - φ soils. Canadian Geotechnical Journal, 40, pp. 54-65.

Fenton, G.A., Naghini, F., Dundas, D., Bathurst, R.J. and Griffiths, D.V. (2016). "Reliability-based geotechnical design in 2014 Canadian Highway Bridge Design Code". Canadian Geotechnical Journal, 53, pp. 236-251.

Green, R. (1989). Limit states design: some thoughts. Proceedings of the Symposium on Limit States Design in Foundation Engineering. Canadian Geotechnical Society – Southern Ontario Section, Toronto, May 26-27, pp. 91-116.

Haberfield, C.M. (2017). Practical applications of soil structure interaction analysis. Gregory Tschebotarioff Lecture 2017, ISSMGE. 19th International Conference on Soil Mechanics and Geotechnical Engineering, Seoul, pp. 81-100.

Hasofer, A.M. and Lind, N. (1974). Exact and invariant second-moment code format. J. Eng. Mech., 100(1), pp. 111-121.

Low, B.K. (2005). Reliability-based design applied to retaining walls. Geotechnique, vol. 55 no. 1 pp. 63-75.

Low, B.K. and Tang, W.H. (1997). Automated reliability based design of footing foundations. Proceedings of the 7th international conference on structural safety and reliability. ICOSSAR '97, Kyoto, Japan, vol. 3 pp. 1837-1840.

Pells, P.J.N. (2011). "Against limit state design in rock". Tunnels & Tunnelling International, February edition, pp. 34-38.

Randolph, M.F. and Buttling, S. (2022). "An investigation of probabilistic analysis in relation to the design of pile groups". Proceedings of the 20th International Conference on Soil Mechanics and Geotechnical Engineering, Sydney, Australia (awaiting publication).

Schweckendiek, T. Courage, W.M.G., and van Gelder, P.H.A.J.M. "Reliability of sheet pile walls and the influence of corrosion – structural reliability analysis with finite elements". Proceedings of the European Safety and Reliability Conference (ESREL 2007), Stavanger, Norway, 25-27 June, pp. 1791-1799.

Standards Australia (2002). "Earth-retaining structures, AS 4678:2002". Sydney, NSW.

Standards Australia (2009). "Piling – design and installation, AS 2159". Sydney, NSW.

Standards Australia (2011). "Residential slabs and footings, AS 2870". Sydney, NSW.

Standards Australia (2017a). "Bridge design, part 3: foundation and soil-supporting structures, AS 5100.3". Sydney, NSW.

Standards Australia (2017b). "General principles on reliability for structures, AS 5104". Sydney, NSW.

Uzielli, M., Lacasse, S., Nadim, F. and Phoon, K.K. (2006). "Soil variability analysis for geotechnical practice". Characteristic and engineering properties of natural soils, vol. 3, pp. 1653-1752.

Whitman, R.V. (1984). "Evaluating calculated risk in geotechnical engineering". J. Geotech. Engrg., 110, pp. 143-188.

Wong, P.K., Day, R.A. and Poulos, H.G. (2007) "Fifteen years of geotechnical limit state design in Australia. Part II – foundations". Proceedings of 10th Australia New Zealand Conference on Geomechanics, Brisbane.

Application of soil nail wall to roadway widening using GFRP rebars as per Australian design guidelines

J. Lee[1], PhD, PE, CPEng, FIEAust, E. Lee[2], ME, MIEAust, M. Leong[3], ME, M. Wei[4], PhD, CPEng, FIEAust

[1]Executive Director, GS E&C Australia, (formerly AECOM, Melbourne), Level 3, 100 Walker Street, North Sydney, NSW 2060; PH (02) 9135-2961; email: jeawoo.lee@gsenc.com
[2]Senior Geotechnical Engineer, AECOM, Level 10, 727 Collins Street, Docklands, VIC 3008; PH (03) 9653-8705; email: erin.lee@aecom.com
[3]Design Manager, CPB Contractors, Level 6, 567 Collins Street, Melbourne, VIC 3008; PH (03) 9228-7000; email: melvyn.Leong@cpbcon.com.au
[4]Technical Principal, EIC Activities, Level 6, 567 Collins Street, Melbourne, VIC 3008; PH (03) 9228-7700; email: michael.wei@eicactiv.com

ABSTRACT

This paper presents the application of soil nail wall technology to roadway widening. An arterial road upgrade project in Melbourne consists of widening the freeway in the northern part of Melbourne, including massive cuts into a hillside on the southern side of the existing freeway. Cuts up to 12 meters necessitated the use of retaining walls at 1H:10V batter to stay within the right of way. A soil nail retaining wall was adopted to facilitate reduced excavation, less impact on the existing slope, and improved construction speed with a top-down process. The soil nail retaining wall is 520 m long with a maximum height of approximately 12 meters, including the undercut for pavement and drainage. The ground comprises clay fill overlying residual clay and subsequent weathering profiles of basalt from Newer Volcanics group, partly overlying Brighton Group sediments. Eleven boreholes were drilled sufficiently below the bottom of the wall. Laboratory tests were conducted to estimate the soil and rock strength, including triaxial compression tests with pore pressure measurement to determine effective strength parameters for Brighton group clayey soil. The design employed Glass Fibre Reinforced Polymer (GFRP) bars to enhance the work efficiency by removing encapsulation of steel bars, the durability of which was reviewed for the 100 year design life with the proven data provided by the manufacturer. The soil nail retaining wall was designed as per AS5100.3 and AS4678 guidelines selectively depending on the importance of the wall with reference to VicRoads Specification Section 683 and FHWA-NHI-14-007.

Keywords: retaining wall, GFRP permanent nail, roadway widening, Australian design guidelines for soil nail walls

1 INTRODUCTION

An arterial road upgrade project in Melbourne consists of widening the freeway in the northern part of Melbourne, including massive cuts into a hillside on the southern side of the existing freeway. Cuts up to 12 meters necessitated the use of retaining walls to stay within the right of way. The reference design provided a reinforced concrete wall on piles to form the retaining wall, which provokes construction risks due to significant excavation to be committed adjacent to the live road. Comparing various retaining wall options, the detailed design adopted a soil nail retaining wall in light of several advantages over other earth retention systems, including reduced excavation, less impact on the existing slope, and improved construction speed with a top-down process. The soil nail retaining wall is 520 m long with a maximum height of approximately 12 meters, including the undercut for pavement and drainage. The ground comprises clay fill overlying residual clay and subsequent weathering profiles of basalt from Newer Volcanics group, partly overlying Brighton Group sediments.

Eleven boreholes were drilled sufficiently below the bottom of the wall along the wall alignment. Test pits were dug to inform the depth of unsupported cut. Laboratory tests were conducted to estimate the soil and rock strength, including triaxial compression tests with pore pressure measurement to determine effective strength parameters for Brighton group clayey soil. The design employed Glass Fibre Reinforced Polymer (GFRP) rebars as opposed to steel bars, which had been used for most soil nail walls in roadway projects, to enhance the work efficiency by removing encapsulation of steel bars. The durability of GFRP rebars was reviewed for the 100-year design life with the proven data provided by the manufacturer. The soil nail retaining wall was designed as per AS5100.3 and AS4678 guidelines selectively depending on the importance of the wall with reference to VicRoads Specification Section 683 and FHWA-NHI-14-007. This paper addresses the implication of Australian design guidelines for soil nailed walls using GFRP bars, soil nail bond strength determination, the impact of excavation on adjacent existing structures, and the integration of road barriers into the wall.

2 SITE CONDITIONS

2.1 Ground conditions

The ground conditions have been inferred from eleven boreholes drilled along/close to the wall alignment up to a depth equal to the wall height below the base of the wall. Six test pits were dug up to 3 m deep, which informs the design of unsupported exaction. A review of geological maps of the area and the available geotechnical information indicates that the soils and rock of the Quaternary age Newer Volcanics are underlain by Tertiary age sediments.

Boreholes drilled on-site demonstrate ground conditions comprising fill varying in depth between 1.5 m and 4.0 m, overlying natural residual soil and basalt of Newer Volcanics Group. The borehole logs long plot is displayed along the soil nail wall alignment in Figure 1. As shown in Figure 1, the boreholes near the western/eastern end of the soil nail wall indicate that the Newer Volcanics are underlain by cemented sandy clay of Tertiary age sediments, which forms part of the ground behind the wall. The residual clays encountered within these boreholes are of very stiff to hard consistency. The weathering of the basalt varies from highly to moderately weathered with low to high strength. Based on the available geotechnical information, the basalt is identified to be highly jointed and fractured. Existing groundwater data available on-site suggests the groundwater levels are below the base of the soil nail wall.

2.2 Laboratory soil and rock testing and rock mass quality

Considering limited information on relationships between effective soil strength parameters and in-situ sounding tests, such as SPT "N" on hard sandy clay of Tertiary age sediments, consolidated undrained triaxial tests with pore pressure measurement were conducted on the undisturbed samples taken from hard sandy clay encountered in boreholes near the western and eastern ends (BH01, 02 and 09). The results of the triaxial tests are displayed in the form of p-q' plot, as shown in Figure 2.

The effective cohesion tested greater than 40 kPa, indicating the clay is highly over-consolidated throughout the boreholes, with plasticity tests on the samples indicating low plasticity. Observation on rock cores and laboratory test results on basalt core samples indicate the rock mass quality of the basalt pertaining to Class IV Poor rock in Rock Mass Rating by Bieniawski (1989) and Blocky/Disturbed/Seamy to Disintegrated on GSI chart by Hoek (1994) as shown in Figure 3.

Uniaxial compression strength (UCS) of basalt tested between 8 and 35 MPa. The UCS and Point Load Strength (Is50) relationship appeared to be UCS = 8 x Is_{50} sitewide.

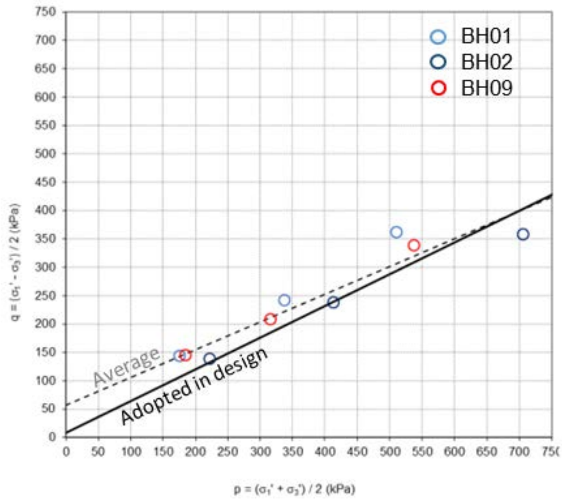

Figure 2. P-q' plot from CU triaxial tests with pore pressure measurement

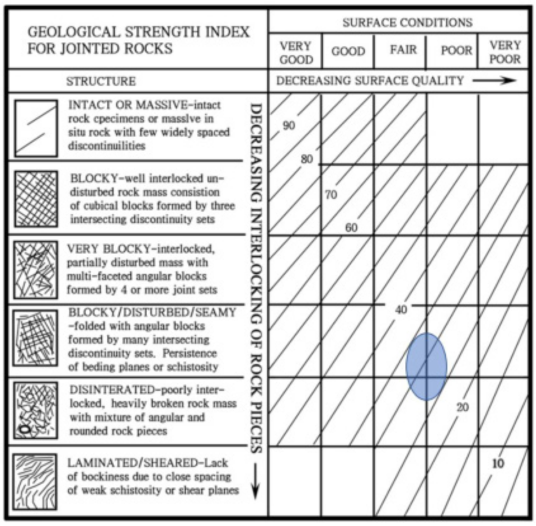

Figure 3. Rock mass quality on GSI chart by Hoek

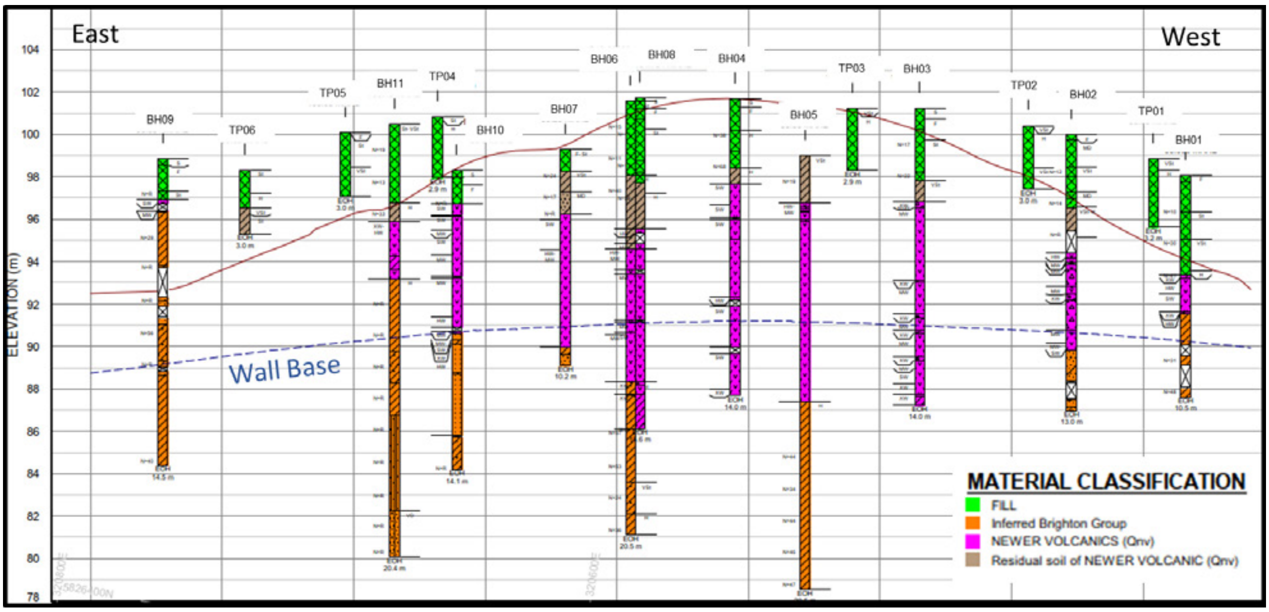

Figure 1. Borehole long plot along the wall

2.3 Restrictions Imposed by Adjacent Structures

The wall alignment neighbours existing structures, which imposes constraints, including:

- proximity to the existing transmission tower that is approximately 8 m south of the crest of the proposed soil nail wall for which the asset owner required the design to ensure minimum clearance of 0.5 m between the closest soil nail and the tower footing and maximum vertical tolerance of 5 mm for the transmission tower;
- existing soil nail wall, the face of which needs to be dismantled to tie in with; and
- proximity to the existing bridge at the eastern end of the wall.

Design and construction measures have been made to manage the tolerance of the wall deflection in proximity to the existing transmission tower by complying with the design requirement as per AS5100 and numerically predicting the wall deflection, which has been ensured with the monitoring during the construction. More stringent design requirements out of AS5100 and AS4678 have applied for the design where the wall extends up to 30 m from the existing bridge abutment or existing assets of high importance with reference to VicRoads Road Structure Inspection Manual (2018). The implication of design codes is further discussed in Section 3.2.

In addition, the traffic barriers adjoining the bottom of the soil nail wall shall be designed to act as independent systems or to prove no detriment to the soil nail wall in the event of any collision with the traffic barrier where the barriers and the wall are integrated. To this end, the impact load is considered to be taken by the traffic barrier designed as an independent system to the soil nail wall, hence no damage to the integrity of the wall or load transfer to the wall. This is further discussed in Section 3.3.1.

2.4 Other Wall Features

The retaining wall requires a balustrade or other barrier to alleviate the risk of a person falling from the top of it as depicted in Figure 4. The extension at the top of the soil nail wall, which forms a safety barrier upstand, is assumed to be constructed at the same time as the upper-most nails. This barrier upstand is subjected to wind loading and handrail loading from AS5100 Cl 12.5 (a-c).

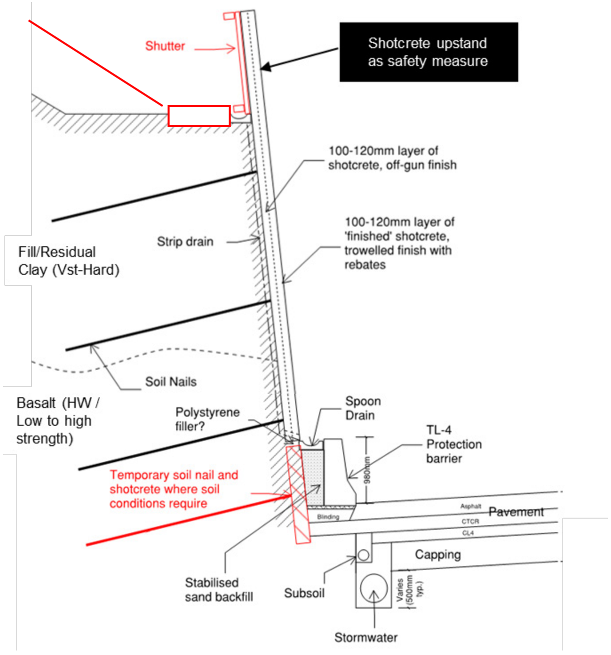

Figure 4. Typical cross-section of soil nail wall featuring barrier and shotcrete upstand

3 DESIGN CONSIDERATIONS

3.1 Design soil/rock parameters and bond strength

Geotechnical material parameters adopted for design have been derived based on the available geotechnical information, including both in-situ and laboratory tests, and practically accepted correlations in literature (e.g. Burt 2005), as summarised in Table 1. The highly weathered (Hw) to moderately weathered (Mw) basalt strength parameters are determined based on the empirical relations between the RMR class and Mohr-Coulomb failure criterion strength parameters and Mohr-Coulomb strength parameters equivalent to Hoek and Brown strength for rock mass.
The soil nail bond strength was determined from the lesser of empirical bond stress presented in literature such as CIRIA report C637 (CIRIA 2005) and effective stress based estimation employing the effective strength design parameters in Table 1.

Table 1: Geotechnical design parameters

Material	Unit Weight, kN/m^3	Effective Cohesion, kPa	Effective Friction Angle, degrees	Undrained shear strength, kPa	Young's Modulus, kPa	Soil Nail Ultimate Bond Stress, kPa	Bond stress based on
Existing Fill	19	5	28	75	20	50	Average normal effective stress
Newer Volcanics Residual Clay (Very stiff to hard)	19	10	28	100	30	60	Average normal effective stress
Basalt – Hw to Mw	22	80	32	-	300	300	Empirical adhesive strength
Inferred Brighton Group – cemented sandy clay (hard)	19	15	35	200	60	80	Average normal effective stress

The adhesion between the nail grout and Hw basalt for the rotary-drilled hole was determined with reference to empirical literature charts such as those in FHWA (FHWA 2003). The nail verification pull-out tests conducted during the installation of nails have verified the design ultimate bond stress to be adequate.

3.2 Soil Nail Wall Design as per AS4678 and AS5100 for Soil Nail Retaining Walls

The soil nail wall design has been completed predominantly relying on the stability of soil nail walls, which has been analysed using the 2D limit equilibrium software Slide2 by Rocscience and the 2D finite element software PLAXIS 2020 with the strength reduction method employed.

Static stability design has primarily adopted the limit state method with material strength partial factors and load factors adopted in accordance with AS 4678-2002 as summarised in Table 2 and Table 3, achieving a minimum global “factor of safety” (“FoS”) of 1.0 in both short-term (i.e. during construction) and long-term static conditions.

Table 2: Partial Factors as per AS4678

Partial Factor Items	Existing Fill	In-situ Material
Effective friction angle, ϕ_ϕ	0.9	0.85
Effective cohesion, ϕ_c	0.75	0.7
Undrained shear strength, ϕ_{uc}	0.5	0.5

Table 3: Load Factors as per AS4678

Partial Factor Items	Factor adopted
Dead load behind wall	1.25
Dead load ahead of wall	0.8
Traffic load behind wall	1.5

The following design reduction factors have been considered for the global stability analysis in as per AS4678-2002 or other standards as stated below:

- Tendon structural capacity reduction factor = 0.4 as per VicRoads Section 683 (06.b.vii);
- Pull-out (bond) resistance reduction factor for rock nails = ϕ_k x ϕ_b = 0.56;

where:

- o Importance category reduction factor, ϕ_k = 0.8 (AS4678-2002 Table B1);
- o Minimum material reduction factor ϕ_b = 0.7 (AS4678-2002 Table B2) for the bond between rock and grout;
- o Pull-out resistance reduction factor for soil nail = ϕ_n x ϕ_b =0.63;

where:

- o Structure classification design factor, ϕ_n = 0.9 for structure classification C (AS4678-2002 Table 5.2); and
- o Minimum material reduction factor, ϕ_b = 0.7 (AS4678-2002 Table B2) for the bond between soil and grout;

The bond capacity within the first 1 m length of nail has been ignored in the design as per VicRoads Section 683.

For the design sections in proximity to important structures, the design has adopted the working stress method as per AS 5100.3-2017, achieving a minimum global FoS of 1.8 in long-term
Condition. The important structures sections include:

- located within 30 m of the existing road bridge
- located within 30 m of the existing transmission tower.

Seismic stability has been analysed based on the working stress method, achieving a minimum global FoS of 1.2. The stability analysis has taken into account possible construction staging with 0.5 m excavation below each row of nails prior to installing the subsequent row of nails and 1.5 m over-excavation below the pavement level at the end of the excavation included. The short term analysis accounting for ‘during-construction cases’, including those subject to the build-up of temporary water pressure and seismic loading, has been performed employing undrained soil design parameters, which have been switched to effective stress design parameters for the long term stability analysis.

As shown in Figure 5, the long term analysis has been carried out excluding the bottom row of soil/rock nails behind the road protection barrier that is considered sacrificial for collision so that the wall stability is independent of the bottom row soil/rock nails. As a result, the minimum global “FoS” has been calculated to be between 1.1 and 1.4 for the sections designed as per AS4678 and 1.9 for those as per AS5100 in long term conditions.

On the other hand, the strength reduction method in the finite element models has generated the minimum global FoS slightly higher than that from the conventional limit equilibrium method. The working stress method analysis against all the sections designed as per AS4678 or AS5100 has indicated the minimum global FoS greater than 1.5 specified as the design criteria in FHWA-NHI-14-007 and CIRIA report C637.

The nails have been laid out at spacings of 1.5 m in soils and 1.8 m in Hw to Mw basalt with lengths up to 0.9 H at maximum. The hole diameter has been set to 125 mm in soils and 105 mm in Hw to Mw basalt.

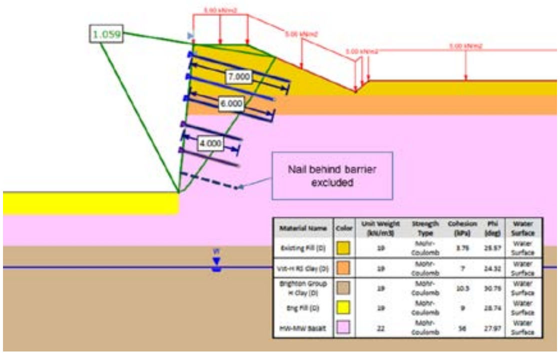

Figure 5. Soil Nail Wall Stability Analysis with the bottom nail excluded

3.3 Deformation Analysis Considering Interaction with Adjacent Structures

The Finite Element analysis undertaken has also assessed the deformation of the soil nail walls, including the influence of collision loading and its impact on the existing structures in proximity. The maximum lateral wall deflection has been estimated to be less than 0.3 % of the wall height, which results in insignificant settlement behind the wall in terms of serviceability. Particular attention has been paid to whether the soil nailing induced ground deformation adversely impacts the structure adjacent to the wall.

3.3.1 Collision loading impact assessment

As per the VicRoads regulation on external loads acting on a retaining wall, the road protection barriers in front of the soil nail wall are to be designed to be structurally independent of the soil nail wall from the collision loads. The geotechnical information indicated that the materials behind road barriers consist of Hw to Mw weathered basalt or highly over-consolidated sandy clay. No structural component was required as part of the retaining wall to support the ground after excavation. The facing was assumed to be redundant (i.e. no replacement required) behind the barrier in the event of a vehicle collision. A joint placed in the facing behind the top of the barrier split the facing into two pieces structurally. A 25 mm thick compressible layer was also included to prevent the load transfer from the barrier to the shotcrete. The road protection barriers have been placed without an extended foundation, piled or slab footing where the assumed design ground condition is present.

The impact of collision loading has been assessed using PLAXIS 2D for the design sections. The road protection barrier was modelled with concrete properties embedded 100 mm into the finished road level. The result has shown no sign of local instability and a negligible increase in either ground deformation or working load in nails.

3.3.2 Asset impact assessment

A 220 kV transmission tower has been identified where the wall height becomes the highest. With the proposed wall slope of 1H in 10V, the closest tower leg is approximately 8 m behind the crest of the soil nail wall. The available information on the tower has informed that each foot of the transmission tower is founded on a circular trapezoid pad footing with the upper surface diameter of 1.1 m and the base diameter of 1.4 m at 2.6 m below ground surface at the time of construction. Due to proximity to the soil nail wall, the transmission tower might be subject to ground movement induced by the excavation during soil nail wall construction. The asset owner of the existing transmission tower requested the conditions described in Section 2.3 to be met. The PLAXIS 2D model developed for asset impact assessment is presented in Figure 6. The material underneath the tower footings is assumed to be residual soil clay with very stiff to hard consistency. Two transmission tower footings with 6.7 m apart centre to centre are included in the analysis.

Due to the uncertainty of the transmission tower loads on the footing, an allowable bearing pressure of 440 kPa on residual clay has been taken as the footing foundation load. The upper row of soil nails is 6 m long at an inclination of 15°, maintaining sufficiently more than 500 mm from the tower footing, which has been accepted by the asset owner.

The PLAXIS analysis result has shown the maximum differential movement under the footings less than 3 mm across the neighbouring footings, which is within the tolerance of 5 mm.

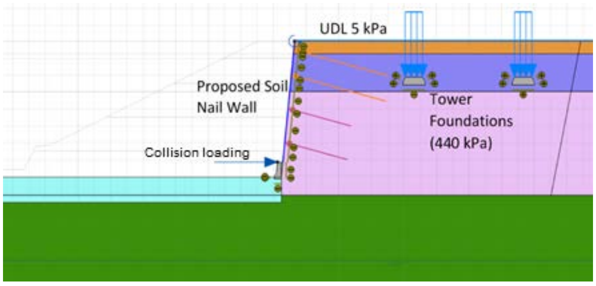

Figure 6. Soil Nail Wall Stability Analysis with the bottom nail excluded

3.3.3 Interference with Existing Nails

The presence of existing soil nails was expected to introduce interface constraints with the soil nails proposed at the section tying in to the existing soil nail wall. PLAXIS 2D analysis was carried out to assess the impact of removing the existing soil nail walls based on the information shown on the historical design drawings. The existing soil nails exposed within the excavation for each lift were assumed to be cut prior to the installation of the new soil nails, with the existing soil nail behind the new wall remaining in place without ground disturbance and a new row of soil nails installed.

The critical section comprising the tallest heights of the retaining walls (existing retaining wall height of 6.6 m and new retaining wall height of 8.8 m) was modelled, as shown in Figure 7. The result of the impact analysis using PLAXIS 2D has indicated a low likelihood of disturbance to the stability of the soil nail walls by the removal of the existing nails in a sequential manner.

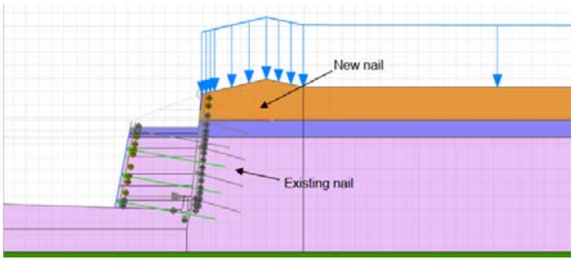

Figure 7. Soil Nail Wall Stability Analysis with the bottom nail excluded

3.4 Facing Design

The wall facing comprises double shotcrete layers - structural facing overlain by aesthetic facing. The structural facing has been designed in accordance with FHWA-NHI-14-007. The working stress-based PLAXIS analysis outcomes have informed the structural capacity assessment with the employment of a lumped load factor of 1.5 as per AS5100.3.

4 USE OF GFRP BARS

4.1 Longevity of GFRP Bars

The lightweight properties of GFRP rebars make handling and installation easy and safe compared with conventional steel rebars. Their inherent non-corrosive properties have additional benefits from a durability perspective, as no additional corrosion protection is required (CIRIA 2005). Although the application of GFRP rebars to permanent soil nail walls is yet to be long enough to attest to the longevity over a 100-year design life, indicative testing conducted by others has suggested that vinyl ester resin GRP should have a long life in a cementitious environment (Johnson 1998). Mechanical testing to inform the 100-year design life is usually based on creep rupture testing. This testing is used to estimate indicative sustainable loads over a period of 106 hours (>114 years) assuming the linear degradation of the ultimate tensile strength (UTS) of the GRP due to creep. This testing is undertaken in the absence of embedment material around the soil nails. The indicative performance is therefore based on an allowable applied load on the GRP bars of less than the creep rupture strength estimates at 100 years and the indicative performance of the Vinyl Ester resin GRP in the cement mortar bedding.

The vinyl ester resin GRP Bluey BluGeo GRP60-20 mm bar was identified in the testing performed by Mohamed and Benmokrane (Mohamed and Benmokrane 2018) to have an indicative 106 hour creep rupture strength of 58% of the original UTS. Theoretically, where the load is applied less than the 106 hour creep rupture strength and the mortar and soil nail bar bond is maintained over the design life, the properties of the GRP are not considered unduly affected by the environment, which the soil nail should then have adequate durability for the nominated 100-year design life. In addition, according to the manufacture information, the product should comply with VicRoads Section 683.

4.2 Implication of GFRP bars on Soil Nail wall design

For the sake of comparison between GFRP and conventional steel nails as to their implication to the design of soil nail wall, PLAXIS2D and SLIDE models have been analysed over one of the design sections with respect to the minimum global FoS, maximum horizontal wall displacement, and maximum axial nail force adopting the parameters tabulated in Table 4.

Table 4 Properties of GRP and Steel

Items	BluGeo GRP60	DSI GEWI® Threadbar
Diameter (mm)	25	20
Young's Modulus (GPa)	60	200
Ultimate Tensile Strength (kN)	350	157
Unit Weight (kg/m)	0.9	2.47
Structural Reduction Factor	0.40 (1)	0.648 (2)

[1] As per VicRoads Standard Specification 683
[2] As per AS 4678-2002 Earth-retaining structures

The use of GFRP nails in lieu of conventional steel nails results in the following:

- decreases in axial nail force up to 30% due to lower elastic modulus of GRP nails than that of steel nails.
- marginal increases of soil nail wall horizontal displacement up to 7% due to the lower elastic modulus of GRP nails than that of steel nails.
- no change in the factor of safety against wall instability.

5 CONCLUSIONS

A soil nail wall up to 12 m high has been successfully designed and constructed adjacent to one of the busiest arterial roads in the Greater Melbourne area as part of a freeway widening project. The application of soil nailing utilising GFRP rebars to the retaining wall has provided significant benefit to the project from either the design or construction perspective, including:

- Meeting the design requirements with innovative material replacing conventional steel rebars
- Relieving burden on the design concerning corrosion of conventional steel rebars
- Minimising disruption to the adjacent live arterial road by reducing temporary earthworks, which is facilitated by top down staging of soil nailing
- Speeding up the nailing installation progress, leading to construction time saving
- Enhancing work efficiency by reducing the burden to handle heavy steel products and encapsulating steel rebars

Lastly, although the case study presented demonstrates the applicability of GFRP soil nails for use in retaining walls with significant benefit design and construction-wise, the use of GFRP nails will be better convinced with further research on the long term performance in the future. Monitoring the wall profile at regular intervals over a long period may help understand the long term behaviour of the wall reinforced with GFRP rebars

REFERENCES

Australian Standard (2002), AS4678-2002.
Australian Standard (2017), AS5100-2017.
Bentley Systems (2020), PLAXIS User Manual.
Bieniawski, Z. T. (1989). Engineering Rock Mass Classifications. Wiley-Interscience. p. 272.
CIRIA (2005) Soil Nailing - best practice guidance, CIRIA Report C637, CIRIA.
Hoek, E. (1994) Strength of Rock and Rock Masses, ISRM News Journal, Vo 2(2), pp. 4-16.
Johnson, P. E. & Carf, G. B. (1998), The use of soil nails for the construction and repair of retaining walls, Transport Research Laboratory 373.
Look, B. G. (2007) Handbook of GeotechnicalInvestigation and Design Tables, Taylor & Francis.
Mohamed, K. And Benmokrane, P. (2018) Creep Rupture of BluGeo GRP60-20mm GFRP Bars of Size 6 (Designated diameter of 20 mm), NSERC Research Chair in Innovative FRP Composite Materials for Infrastructure, University of Sherbrooke.
VicRoads (2018), Road Structures Inspection Manual.
VicRoads (2019), VicRoads Standard Specification 683 – soil nail walls.

Risk Prediction Model for Formation of Underground Cavities and Sinkholes due to Defective Sewer Pipes

S.R. Indiketiya[1], P. Jegatheesan[2] and R. Kuwano[3]

[1]Former PhD Student, Swinburne University of Technology, Hawthorn, Melbourne, Vic 3122, Australia; email: samanthi.uom@gmail.com
[2]Former Senior Lecturer, Swinburne University of Technology, Hawthorn, Melbourne, Vic 3122, Australia; email: piratheepan.jegatheesan@yahoo.com
[3] The University of Tokyo, Meguro-ku, Tokyo 153-8505, Japan; email: kuwano@iis.u-tokyo.ac.jp

ABSTRACT

Sinkhole formation due to internal erosion around defective sewer pipes is identified as a serious threat in urban infrastructure system. Post-repair and rehabilitation after pipe failure are not effective as emergency pipe repairs are very costly and pipe failure leads to various public and environmental consequences. Only a few studies have been conducted on the prediction of the risk of ground erosion around pipe defects. Therefore, the main objective of this article is to propose a model which can predict the risk of formation of sinkholes around sewer pipelines based on the weighted factors method when a pipe defect is certain. The proposed methodology relies on different factors which contribute to void development and severity of the consequences. The Risk of Erosion (ROE) combines the effect of Likelihood of Erosion void formation (LOE) and Consequence of Erosion cavity formation and ground failure (COE). The LOE rating is related to many parameters, including soil properties, hydraulic conditions, and pipe defect characteristics, while the COE rating is related to the environmental, economic, and social consequences of pipe failure. Therefore, this model, which can predict the risk of developing a sinkhole close to an existing pipe defect, will enable sewer assets maintenance teams to evaluate each pipe and prioritize the maintenance and rehabilitation work based on the risk to each pipe.

Keywords: Sinkholes, Risk Prediction Model, Sewer Rehabilitation, Internal Erosion

1 INTRODUCTION

Wastewater and stormwater collection systems are critical components of urban infrastructure systems in any country. Failure of deteriorated buried sewer pipes can occur in two ways. One process is when the soil backfill in the vicinity of a pipe defect is gradually eroded, the pipe will bend and collapse due to loss of confinement from the ground (Balkaya et al. 2012). The second process occurs when the cracks are formed at either sides or the crown of the pipe. Voids can develop above the pipe while the pipe is still well supported from the bottom. In this case, erosion may propagate towards the ground surface causing a sinkhole which eventually breaks most of the other buried service lines (Sato and Kuwano 2015).

Many studies have been conducted on sewer deterioration and risk prediction models for pipe failures (Yan and Vairavamoorthy 2003; Baah et al. 2015; Emilio 2015). To the author's best knowledge, only one risk prediction model is available in the literature (Kaddoura and Zayed 2017) which proposed a model that can predict the risk of void erosion present outside sewer pipelines. This is based on weighted factors method using Fuzzy theory. However, this model has several limitations. It does not account few a few other critical factors which control the process of cavity formation such as the relative density or compaction of the ground and the influence of rainfall. Moreover, the erosion susceptibility of clay has been considered as higher than fine sand and silt which is contradicting with available literature (Rogers 1986, Indiketiya 2019). The model only predicts the probability of erosion void presence outside sewer pipes and the risk due to consequences of erosion void formation is not accounted for the overall risk.

Therefore, it will be useful to develop an efficient model which can predict the overall risk of developing erosion voids in defective sewers which can be useful to sewer asserts management teams for allocating priorities in rehabilitation projects and for sewer and storm water pipe designers to design high stability backfill design considering the erosion resistance of the backfill.

2 METHODOLOGY

2.1 Risk assessment method

Most of the risk assessments conducted for sewer failures as outlined in available literature have considered some form of likelihood or probability of failure, consequence of failure and risk of failure. Emilio (2015) adopted a similar method to predict the risk of failure of sewer pipes. Therefore, modified version of the same approach is used in this study to predict the risk of erosion void formation (ROE) which combines the likelihood of erosion void formation (LOE) and consequence of erosion void formation (COE) in sewer pipes. The risk assessment involved identifying influencing parameters for LOE and COE then quantifying the LOE and COE by assigning critical scores based on the literature and by allocating factor weights based on experts' opinion. After both ratings were determined, they were multiplied together to find the risk score for ROE as shown in Equation 1.

$$\text{ROE} = \text{LOE} * \text{COE} \quad (1)$$

Following an extensive literature review, seven most influencing parameters which control the erosion initiation and progression through pipe defects were identified for the LOE function as shown in Equation 2. The contribution from each factor to LOE, λ_i was estimated based on the expert's belief where, each $0 \leq \lambda_i \leq 1$ and $\Sigma\lambda_i = 1$.

$$\text{LOE} = \lambda_1.\text{Soil type score} + \lambda_2.\text{Relative density of backfill score} + \lambda_3.\text{Depth of sewer pipe score} + \lambda_4.\text{Location of GWT score} + \lambda_5.\text{Pipe defect size score} + \lambda_6.\text{Frequency and magnitude of sewer exfiltration score} + \lambda_7.\text{Frequency and magnitude of rainfall score} \quad (2)$$

The consequences of the erosion void formation and sinkhole formation are very similar to the consequences of the pipe failures. Therefore, four parameters which have been commonly adopted in previous risk prediction models for pipe deterioration (Baah et al. 2015; Emilio 2015) were selected for COE of this model. Selected four factors to represent environmental, economic, and social impacts of the pipe location are depicted in Equation 3. Where, μi was estimated based on the expert's belief while satisfying $0 \le \mu_i \le 1$ and $\Sigma\mu_i = 1$.

$$COE = \mu_1.\text{Environmental-pipe diameter score} + \mu_2.\text{Economic-commercial zone score}) + \mu_3.\text{Social-critical infrastructure score}) + \mu_4.\text{Social-traffic volume score}) \quad (3)$$

2.2 Assigning critically scores for LOE

The condition of each pipe is evaluated for the LOE based on seven factors and each parameter was assessed and scored between 0 and 4 as given in Table 1 to Table 7. Therefore, the overall risk of LOE of pipe will also be scored out of 4 as $0 \le \lambda_i \le 1$ and $\Sigma\lambda i = 1$. as depicted in Equation 2. The scoring criteria for each of the seven factors are summarized through section 2.2.1 to 2.2.7.

2.2.1 Soil Characteristics

The soil type, its particle-size distribution and plasticity are identified as key parameters which controls the initiation of erosion through pipe cracks (Rogers 1986; Sato and Kuwano 2015; Indiketiya 2019). Considering all those data, soil types were arranged into a hierarchy based on the erosion resistance through underground openings and tabulated as shown in Table 1.

Table 1. Scoring for soil type

Soil type (USCS specification)	Attribute	Score
GW, GC, CH	Excellent	0
CL-CH, SC, GM	Good	1
SW, CL, GP	Fair	2
SM, CL-ML, MH	Poor	3
SM, ML, SP, Dispersive Clay	Worst	4

2.2.2 Relative density of the backfill

The importance of having a higher relative density to minimise erosion potential in non-cohesive material has also been discussed by Rogers (1986) and Renuka (2012). Most of the sewer pipe construction specifications have recommended minimum compaction of 70% relative density for pipe embedment (United States Department of the Interior 1996; WSA 02-2002-2.3-MRWA Edition 2002). Therefore, considering the experimental results from above researchers, different scores were assigned to each pipe backfill density as displayed in Table 2.

Table 2. Scoring for density of backfill

Relative density (Non-Cohesive Soil)	Attribute	Score
>90%	Excellent	0
70%-90%	Good	1
60-70%	Fair	2
35-60%	Poor	3
<35%	Worst	4

2.2.3 The depth of the sewer

Pipes which are closer to ground surface are often disturbed and damaged due to heavy traffic, construction works and maintenance of other underground services (Davies et al. 2001). In addition, O'Reilly et al. (1989) found out that the defect rate decreases with the increasing of the pipeline depth. The chance of erosion initiation and propagation also could increase at a lower depth due to lower confining pressure and faster rain infiltration through the opening. Kaddoura and Zayed (2017), also proposed a depth categorisation for sewer pipes in his void erosion prediction model. Based on the above-mentioned discussion and studies, pipes are scored based on it's depth in LOE function as displayed in the Table 3.

Table 3. Scoring for depth of the pipeline

The depth of the sewer (m)	Attribute	Score
> 4	Excellent	0
2-4	Good	1
1.2-2	Fair	2
0.6-1.2	Poor	3
0-0.6	Worst	4

2.2.4 Location of the GWT

If the GWL exists above the sewer pipeline or above any structural defect, there is a higher possibility of infiltration and soil migrating to the sewer pipeline (Davies et al. 2001). Indiketiya (2019) also discussed propagation of erosion voids considering the geometry of the void and the relative location of the GWT. Similar studies have categorised the influence of GWT into two as pipe located above and below the GWT (Rogers 1986; Davies et al. 2001). However, the most important fact is the location of the GWT relative to the pipe defect. As crack or the opening in a pipe can be at the bottom or the crown, choosing the depth of pipe can be misleading for large diameter pipes. Therefore, in this model, sewer depth was categorised and scored into three sections as shown in Table 4.

Table 4. Criticality scoring for the GWT

Groundwater table	Attribute	Score
Well below the pipeline	Excellent	0
Closer to the pipeline	Poor	3
Above the pipeline	Worst	4

2.2.5 Effect of pipe defect size

Pipe defect size is one of the most governing factors which controls the rate of soil loss. Rogers (1986) first proposed a relationship between ground loss and the ratio of B/D_{85} for a variety of cohesionless soils under the one-way water flow. Where D_{85} is the size of sieve through which 85% by weight of a soil sample will pass and "B" is the crack width. Critical crack width for continuous migration of soil in monotonic water flow was expressed as $2.5D_{85}$ to $4.5D_{85}$. Indiketiya (2019) observed that the rate of soil loss is significantly smaller if the "B" is less than D_{max} or $2D_{85}$ of the backfill material and soil loss was critical when "B" was greater than $2D_{max}$. These findings are consistent with the studies available on granular flow through orifices. Based on these findings, pipe defects were categorised into different groups for critical scoring as given in Table 5.

Table 5. Criticality scoring for the pipe defect

B/D_{max}	B/D_{85}	Attribute	Score
<0.75	<1	Excellent	0
0.75-1	1-2	Fair	2
1-2	2-3	Poor	3
>2	>3	Worst	4

2.2.6 The magnitude of sewer exfiltration

Rogers (1986) performed a series of physical model tests to examine the soil loss from sewer exfiltration from pipe and groundwater infiltration into the pipe. It was revealed that in fine-granular soil, the frequency of sewer exfiltration or leakages with a smaller surcharge was more critical than having a single leakage with a larger surcharge. Therefore, even minor daily leakages through the pipe cracks can cause significant soil loss if the flow occurs cyclically through large defects. The hierarchy proposed in WRC (2001) for the magnitude and frequency of sewer leakages is used in this model by assigning criticality scores as shown in Table 6.

Table 6. Scoring for sewer exfiltration

The magnitude of exfiltration	Attribute	Score
Never	Excellent	0
Occasional, low magnitude	Good	1
Occasional, high magnitude	Fair	2
Frequent, lower magnitude	Poor	3
Frequent, high magnitude	Worst	4

2.2.7 The magnitude of rainfall

Kuwano et al. (2006) reported that majority of sinkholes in Japan are formed in the rainy season. Rise in GWT, frequent sewer overflows, and groundwater infiltration through existing cavities due to rain can accelerate the erosion process and sinkhole development. Referring to the classification introduced by WRC (2001) for sewer exfiltration which was presented in Table 6, a very similar approach was used in this model to classify the frequency and magnitude of rainfall. It is difficult to quantify the magnitude and the frequency of rainfall for each group as it is sensitive to location and the country. Therefore, the proposed qualitative classification in Table 7 can be adapted to any location based on a relative judgment.

Table 7. Scoring for the magnitude of rainfall

The magnitude of rainfall	Attribute	Score
No rainfall	Excellent	0
Occasional, light shower	Good	1
Frequent, light shower	Fair	2
Occasional, heavy rainfall	Poor	3
Frequent, heavy rainfall	Worst	4

2.3 Assigning critically scores for COE

The COE is a representation of values of financial or of life-loss, and it measures the effect of pipe failure regarding environmental, economic, and social consequences. There are various studies which predict the risk of consequences of pipe failures. Erosion void formation and ground subsidence have very similar consequences regarding environmental, social and economic impacts. Therefore, the four parameters used by Emilio (2015) for sewer pipe failures are used in this model.

The parameters include pipe diameter, distance from commercial zones, distance from critical infrastructure, and vehicular traffic volume as parameters for quantifying the environmental, economic, and social consequences. The scoring criteria for each of the four factors above are summarized below in Section 2.3.1 to 2.3.4.

Similar to LOE scoring, COE scoring is assigned under six attributes as excellent, very good, good, fair, poor and worst. The scores are assigned as 0, 1, 2, 3, 4, 5 respectively. Therefore, the overall risk of COE of erosion void formation closer to a pipe is scored out of 5 as $0 \leq \mu_i \leq 1$ and $\Sigma\mu_i = 1$.

2.3.1 The size of the pipe diameter

Pipe diameter is a crucial factor in COE function as it represents the volume of sewer flow, the amount of public coverage and the potential environmental consequences in a sinkhole event or rehabilitation work. For large diameter pipes, pipes cover a larger domestic and industrial buildings and if a pipe breaks the public inconvenience is higher. When the diameter is increased, the depth of the pipe is also higher, and the consequences of sinkhole formation will be greater as the size of the sinkhole is increasing with the depth (Guo et al. 2013). Therefore, the total cost, effort and time required for a repair are higher than in a smaller size pipe. Table 8 shows the scoring breakdown for the pipe diameter. This categorisation is referring Emilio (2015) and actual sewer pipe sizes available in real practice in Australia.

Table 8. Scoring for the size of the pipe diameter

Pipe Diameter (mm)	Attribute	Score
<150	Excellent	0
180 - 225	Very Good	1
250 - 375	Good	2
400 - 525	Fair	3
550-750	Poor	4
>750	Worst	5

2.3.2 The distance from commercial zones

In Australia, different states use different land zone classifications and Victoria's major zonings are residential, commercial, industrial and rural, in addition to sub-zones as specified by the State Government of Victoria (2014). In commercial zones, there are commercial activities which are essential for functioning of a city such as retail shops, offices and childcare centres. Therefore, the distance from the sinkhole to these commercial zones is important, the greater the distance, the lower the risk of consequences. Scores defined by Emilio (2015) are selected for this model as shown in Table 9. Based on the scoring, pipes which are 1500m away from commercial activities have less impact while those located closer than 300m have severe impact.

Table 9. Scoring for the distance from commercial zones

Distance from commercial zones (m)	Attribute	Score
>1500	Excellent	0
1200 - 1500	Very Good	1
900 - 1200	Good	2
900 - 600	Fair	3
300-600	Poor	4
<300	Worst	5

2.3.3 The distance from critical infrastructure

Critical infrastructure enables the provision of essential services such as food, water, health, energy, communications, transportation, emergency services and banking. Sinkholes, pipe breaks and the subsequent repairs may influence a city's ability to respond to emergencies. Emilio (2015) also counted schools as critical infrastructure in his model, as schools are large public gathering points that may be negatively affected. The same scoring breakdown used by Emilio (2015) is applied in this COE model as shown in Table 10 since pipe failures have very similar consequences to sinkhole events.

Table 10. Scoring for the distance from critical infrastructure

Distance from critical infrastructure (m)	Attribute	Score
>2500	Excellent	0
2499 - 2000	Very Good	1
1999 - 1500	Good	2
1499 - 1000	Fair	3
999-500	Poor	4
<500	Worst	5

2.3.4 The traffic volume/road type of the location

The type of the road or the volume of traffic where the sinkhole appears are crucial which affect the consequences of the event. However, as the traffic volume highly depends on the location, the city and the country, it is difficult to normalise the volume of traffic as an indicator for general practice. Therefore, road type would be beneficial as it is a relative gauge which can be easily replaced for different countries. There is a variety of classifications for road types, and no single variable is available to completely describe a class of roads. The road classification implemented throughout Victoria according to (Austroads 2005) are used here. According to this hierarchy, "M" routes deserve a higher critical score as it carries the highest traffic volume and has greatest connectivity within the road network. The scoring system proposed in this study is given in Table 11. Footpaths are also added with the lowest critical score as some sewer pipes are buried in footpaths which are not included in the national road numbering system.

Table 11. Criticality scoring for the road type

Distance from critical infrastructure (m)	Attribute	Score
Footpaths	Very Good	1
C	Good	2
B	Fair	3
A	Poor	4
M	Worst	5

2.4 Data acquisition for weighted influence factors

Two of the recommended methods for estimating influence factors (λ and μ values) in Equation 2 and 3 is to get the expert's judgment (Joseph et al. 2010) or iterative computation through field data (Emilio 2015; Kaddoura and Zayed 2017). As collecting actual field data related to defective sewer pipes and sinkhole events are extremely difficult, multiple experts are selected by considering the experience and confidence on the topic. As this theme is still quite new and thorough knowledge about the pipe deterioration and erosion process is required to fill up the questionnaire, 15 researchers were selected from various countries referring to their publications which indicates their expertise on this study area. All the information required for survey was provided and experts were requested to assign λ_i and μ_i values corresponding to parameters from their expertise so that $\sum(\lambda_i) = 1$ for LOE and $\sum(\mu_i) = 1$ for COE separately.

2.5 Data analysis and determination of weighted influence factors

The proposed λ_i and μ_i values by experts were scattered in a wide range. Therefore, the weighted average (Mean) and the mode of each data set for λ_i and μ_i are calculated and presented in Table 12 and Table 13 respectively. The mean and the mode of all seven λ_i values are close and consistent. Therefore, final λ values were designed clearly as closely following the mean and the mode values while satisfying the condition of $\sum(\lambda_i) = 1$.

However, all four μ_i, parameters are having higher standard deviations while mean and the mode values are also slightly different. Therefore, considering the mean, mode and the distribution of the normal frequency, judgment on final value was decided as presented in Table 13. Emilio (2015) had the same parameters in the COE model and the judgment was μ_1=0.3, μ_2=0.3, μ_3=0.2 and μ_4=0.2. These have been decided manually based on judgment where more emphasis was applied to social concerns because they directly affect the public.

Therefore, the final equations for LOE and COE with the proposed influencing factors can be written as shown below in Equations 4 and 5.

Table 12 The Mean, mode and proposed λ_i values

Parameter	λ		
	Mean	Mode	Proposed
λ_1	0.19	0.2	0.2
λ_2	0.11	0.1	0.1
λ_3	0.09	0.1	0.1
λ_4	0.18	0.2	0.2
λ_5	0.21	0.2	0.2
λ_6	0.12	0.1	0.1
λ_7	0.10	0.1	0.1
$\sum(\lambda_i)$			1.0

Table 13 The Mean, mode and proposed μ_i values

Parameter	μ		
	Mean	Mode	Proposed
μ_1	0.26	0.3	0.3
μ_2	0.25	0.2	0.2
μ_3	0.25	0.3	0.25
μ_4	0.25	0.2	0.25
$\sum(\mu_i)$			1.0

LOE = 0.2*(Soil type score) +0.1*(Relative density of backfill score) + 0.1*(Depth of sewer score) + 0.2*(Location of GWT score) + 0.2*(Effect of pipe defect size score) + 0.1*(Frequency and magnitude of sewer exfiltration score) + 0.1* (Frequency and magnitude of rainfall score) (4)

COE = 0.3 * (Environmental-pipe diameter score) + 0.2 * (Economic-commercial zone score) + 0.25 * (Social-critical infrastructure score) + 0.25 * (Social-traffic volume score) (5)

Table14. Risk level categorisation for ROE based on a risk matrix

Likelihood of erosion (LOE)	Consequences of erosion void formation (COE)					
	0 (Low)	1 (Low)	2 (Low to moderate)	3 (Moderate)	4 (High)	5 (Very high)
0 (Low)	0 Low	0 Low	0 Low	0 Low	0 Low	0 Low
1 (Low to moderate)	0 Low	1 Low	2 Low	3 Low	4 Low	5 Moderate
2 (Moderate)	0 Low	2 Low	4 Low	6 Moderate	8 Moderate	10 High
3 (High)	0 Low	3 Low	6 Moderate	9 Moderate	12 High	15 Very high
4 (Very high)	0 Low	4 Low	8 Moderate	12 High	16 Very high	20 Very high

Since the LOE is scored out of 4 and COE is scored out of 5, this model considers pipes with LOE of 3 to 4 as the higher vulnerability for ground subsidence with pipe failure and in need of urgent attention. Similarly, COE is scored out of 5 and pipes with COE score of 4 to 5 are considered as critical pipes which causes many social, economic and environmental consequences. Various studies have graphically illustrated the risk matrix system (Baah et al. 2015) which combines the probability and consequences for an event. Referring those studies, risk level for a pipe to develop an erosion cavity was categorised through the risk matrix based on the score as low, moderate, high and very high as illustrated with a colour code in Table 14.

3 VALIDATION

The model can be validated one of these methods: (1) comparison of the predicted risk with that of previous models, (2) validation based on real field data or (3) implementation of the model in a case study. Detailed reports of investigations of sinkhole accidents are extremely rare, as the relevant authority's primary goal is to restore the infrastructure as quickly as possible to minimise the public, economic and social inconvenience. General information about the events is usually published in media as news reports. All the attempts to access some field data to validate the model from local and international authorities were unsuccessful as the present research is a university-based study without any industrial collaborations.

The ROE model presented in this chapter was developed following a thorough study of previous research related to erosion through pipe defects, risk prediction models for pipe failures and the experimental investigations available in literature. The output of COE is closely aligned with Emilio 2015). Nevertheless, the LOE function needs to be validated before implementing it in industrial applications.

4 CONCLUSIONS

Based on the study, the following conclusions were driven.

- Seven key parameters which affect the likelihood of erosion void formation are identified. Of those parameters, the soil type, the size of the pipe defect and the location of the GWT have the highest relative weights.
  Four parameters which evaluates the consequences of erosion void formation were considered as the pipe diameter, the distance from commercial zone, the distance from critical infrastructure and the road type of the location
- Criticality scores for LOE function was scored out of 4 and COE function was scored out of 5. Therefore, the overall risk of erosion, ROE is predicted rating out of 20. Then the level of risk for a defective pipe to develop an erosion cavity is categorised according to a risk matrix based on the ROE score: low (0 to 4), moderate (5 to 9), high (10 to 14) and very high (15 to 20).
- Unfortunately, due to lack of published data, and the legal requirements of different institutes and countries, it proved impossible to access real data to validate the model. However, this model development contributes significantly to existing knowledge. Therefore, it can be validated and improved with collaboration from industry partners in a future study.
- Ultimately, this allows defective pipes to be ranked based on the risk of erosion void formation and consequences which assist to organise a maintenance and rehabilitation schedule by allocating the priority.

5 ACKNOWLEDGEMENTS

Authors would like to acknowledge:

- Swinburne University of Technology in supporting this research by offering Swinburne University Postgraduate Research Award.
- All the research experts who contributed for the survey to determine the weightage factors for the model.
- Chadwick Geotechnics in providing the financial support for publishing the article.

REFERENCES

Austroads. 2005. Towards a Nationally Consistent Approach to Route Numbering. Available from https://www.onlinepublications.austroads.com.au/items/AP-R224-03 2018].

Baah, K., Dubey, B., Harvey, R., and McBean, E. 2015. A risk-based approach to sanitary sewer pipe asset management. Science of the Total Environment 505: 1011-1017. doi: https://doi.org/10.1016/j.scitotenv.2014.10.040.

Balkaya, M., Moore, I.D., and Sağlamer, A. 2012. Study of non-uniform bedding due to voids under jointed PVC water distribution pipes. Geotextiles and Geomembranes 34: 39-50. doi: http://dx.doi.org/10.1016/j.geotexmem.2012.01.003.

Davies, J., Clarke, B., Whiter, J., and Cunningham, R. 2001. Factors influencing the structural deterioration and collapse of rigid sewer pipes. Urban Water 3(1): 73-89.

Emilio, C.R. 2015. Criticality and risk assessment for pipe rehabilitation in the city of Santa Barbara sewer system. M.Sc. Thesis, Department of Civil and Environmental Engineering, California Polytechnic State University.

Guo, S., Shao, Y., Zhang, T.Q., Zhu, D.Z., and Zhang, Y.P. 2013. Physical modeling on sand erosion around defective sewer pipes under the influence of groundwater. Journal of Hydraulic Engineering 139(12): 1247-1257. doi: Doi 10.1061/(ASCE)Hy.1943-7900.0000785.

Indiketiya, S. 2019. Erosion potential of pipe embedment materials through defective sewer pipes. PhD. thesis, Department of Civil Engineering, Swinburne University of technology, Australia,

Joseph, S.A., Adams, B.J., and McCabe, B. 2010. Methodology for Bayesian belief network development to facilitate compliance with water quality regulations. Journal of Infrastructure Systems 16(1): 58-65.

Kaddoura, K., and Zayed, T. 2017. Erosion Void Prediction Model for Sewer Pipelines. In International Congress on Underground Infrastructure, Water Management and Trenchless Technology, Istanbul. pp. 114-126.

Kuwano, R., Hiorii, T., Kohashi, H., and Yamauchi, K. 2006. Defects of sewer pipes causing cave-ins' in the road. In 5th International Symposium on New Technologies for Urban safety of mega cities in Asia (USMCA), Phuket, Thailand.

Moss, R.E.S. 2013. Applied civil engineering risk analysis. National Association of Sewer Service Companies, PACP Assessment Certification Program., Charleston: Shedwick Press.

O'Reilly, M.P., Rosbrook, R.B., Cox, G.C., and McCloskey, A. 1989. Analysis of defects in 180 km of sewer pipes in Southern water authority. TRRL Research Report, Transport and Road Research Laboratory, Berkshire, UK.

Renuka, I.H.S. 2012. Evaluation of ground loosening behavior and mechanical properties of loosened sand associated with underground cavities. M.Sc. thesis, Department of Civil Engineering, University of Tokyo

Rogers, C.J. 1986. Sewer deterioration studies the background to the structural assessment procedure in the sewerage rehabilitation manual. Water Research Centre, Swindon SN5 8YF, Great Britain.

Sato, M., and Kuwano, R. 2015. Influence of location of subsurface structures on development of underground cavities induced by internal erosion. Soils and Foundations 55(4):829-840.doi: http://dx.doi.org/10.1016/j.sandf.2015.06.014.

State Government of Victoria. 2014. Reformed zones for Victoria. Available from https://www.planning.vic.gov.au/policy-and-strategy/planning-reform/reformed-zones-for-victoria [accessed 29-07- 2021].

United States Department of the Interior. 1996. Pipe Bedding and Backfilling. In Geotechnical Training Manual No.7. Bureau of Reclamation, Technical Service Center, Geotechnical Services, Denver, Colorado.

Water Research Centre (WRC). 2001. Sewerage Rehabilitation Manual. Water Research Centre. Marlow, UK.

WSA 02-2002-2.3-MRWA Edition. 2002. Sewerage code of Australia, Melbourne Retail Water Agencies edition, Version 1.0 Melbourne, Australia.

Yan, J.M., and Vairavamoorthy, K. 2003. Fuzzy Approach for Pipe Condition Assessment. In New Pipeline Technologies, Security, and Safety. pp. 466-476

SESSION 2

INSTRUMENTATION AND MONITORING IN DESIGN

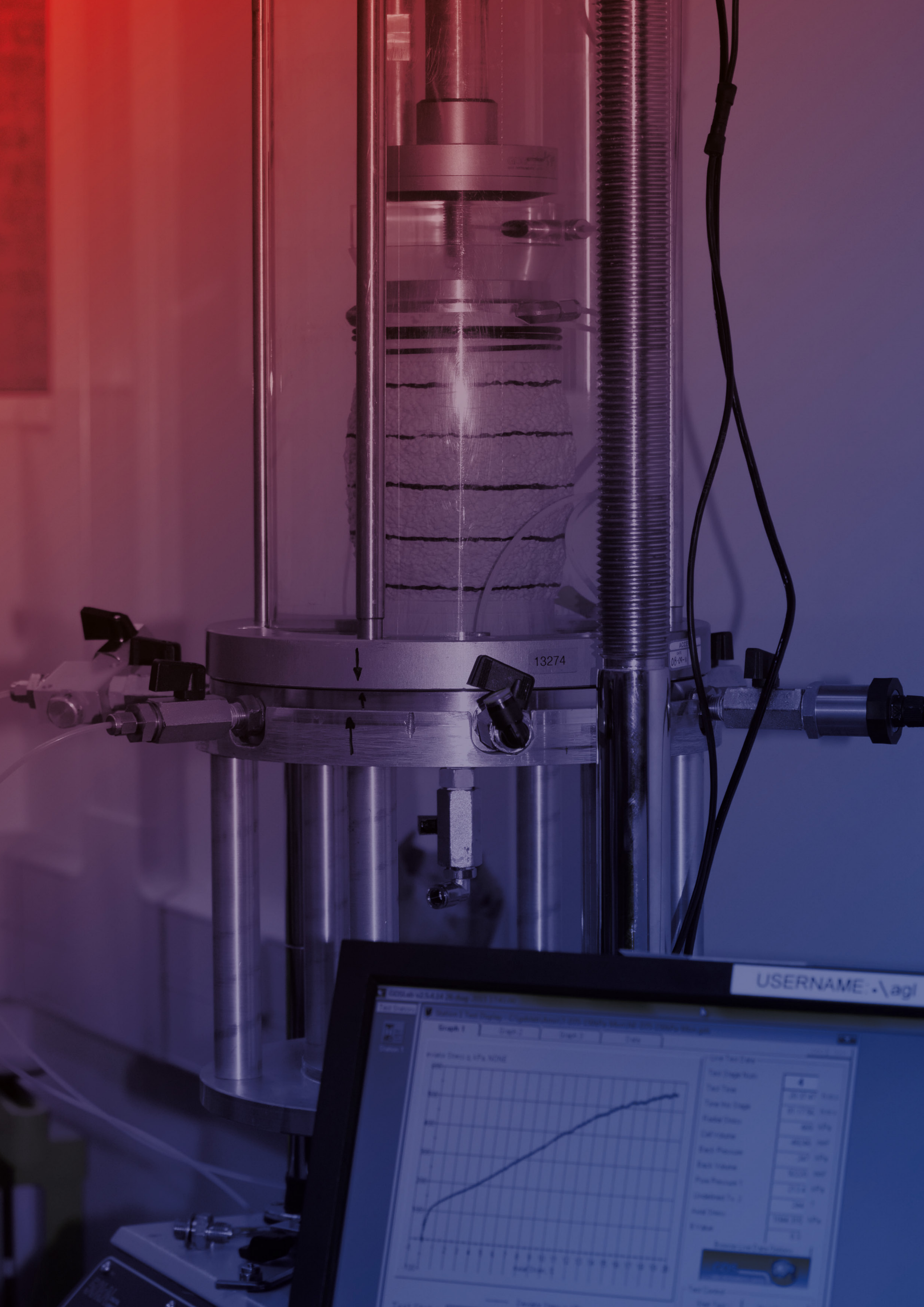
13274
USERNAME: .\agl

Keynote Address

Ground truth, control and design of driven piles: implementing old ways with a new twist

J. P. Seidel[1], CP Eng and D. Denes[2], CP Eng

[1]Foundation QA Pty Ltd, Managing Director, POBox 4280, Croydon Hills, Victoria, Australia, 3136; email: julian@foundationqa.com
[2]Golder Associates Pty Ltd, Foundation/Pile Testing Department, Building 7, Botanicca Corporate Park, 570 – 588 Swan Street, Richmond, Victoria 3121, Australia; email: Ddenes@golder.com.au

ABSTRACT

Piling design and verification is a fraught and risky business. The spread of pile capacity estimates submitted to conference predictions exercises is often staggering and sobering. This underlines why design of driven piles does not stop at the design engineer's desk but continues through construction, and relies on the valuable information provided by the installation process. Each installation blow is a test - a test of the ground response to hammer input delivered into the pile. Traditionally, pile capacity has been interpreted from this input-response relationship through various and many pile driving formulae. Five decades ago, measurement systems were first used to measure and interpret the stress waves in piles generated from the hammer inputs and reflected from the ground response to infer capacity in a more sophisticated and reliable way using wave mechanics principles. Today, PDA testing and wave matching are routinely accepted practice. However, each PDA test has direct relevance only to the individual pile which is tested. This paper will argue that our fundamental task as designers and supervisors is to establish ground truth, by synthesizing the results of PDA tests into a locally-evidenced and locally-targeted dynamic formula. Therefore, only dynamic formulae, properly modified and correlated, must be the vehicle for delivering local ground truth and ultimately being the basis for sign-off. On a foundation-wide basis, the role of PDA tests is critical but subservient, and principally to provide the evidence on which a correlated dynamic formula is developed. Consequent implications for the foundation sign-off process, and for a proposed new approach to establishing capacity reduction factors for driven piles will also be discussed.

Keywords: pile driving formulas, pile acceptance, PDA testing, capacity reduction factors, wave equation analysis

1 INTRODUCTION

Piling design is a fraught and risky business. The spread of pile capacity estimates submitted to conference predictions exercises is often staggering and sobering. Fellenius (2013) summarizes the results of such a prediction exercise for a continuous flight auger (CFA) pile installed in clay till with sand and gravel lenses. The predicted load-movement responses from 41 invited foundation engineers are shown in Figure 1 with the actual load test results. The test had to be terminated prematurely for safety reasons and two possible extrapolations are shown in the solid lines. 35 predictions included a full load-settlement curve; 6 provided only a capacity estimate at 50mm movement indicated by the black circles. The average capacity prediction was 1920kN, with the range of predictions between 700kN and in excess of 5000kN. For the purpose of this paper, the issue is not how well the predictions compare with the measured (and extrapolated) test response, but the extreme range of predictions of both pile capacity (7-fold) and pile stiffness (8-fold).

This paper is concerned with driven piles, and in contrast to CFA piles, there is another opportunity to evaluate capacity for individual piles based on monitoring of key installation characteristics. The potential uncertainty of geotechnical design underlines why design of driven piles does not stop at the design engineer's desk but continues through construction, and relies on the valuable information provided by the installation process.

For pile driving, each installation blow is a test. A test of the ground response to hammer input delivered into the pile. Traditionally, pile capacity has been interpreted from this input-response relationship through various and many pile driving formulae (e.g. Hiley, 1930; Chellis, 1961; Olson and Flaate, 1967; Fragaszy et al., 1989; Lawton et al., 1986; Allin et al., 2015) amongst many others. A particularly good summary can be found in Groom, (2019).

The underlying assumption of any pile driving formula is that it should reflect a universal ground truth and by application of this formula, pile capacity can be inferred by measurement or assumption of some key parameters. The many studies which assessed the comparative merits of different formulae by comparison with static load tests all indicated large scatter and poor reliability which resulted in recommended factor of safety of up to 6 (for the Engineering News Record formula).

However, it should be considered that at the time of many of these comparison studies, the effect of pile setup could not be assessed, and the true energy delivered by pile driving hammers could not be measured. These are critical factors which the authors of early studies did not have at their disposal, and would undoubtedly have influenced their finding

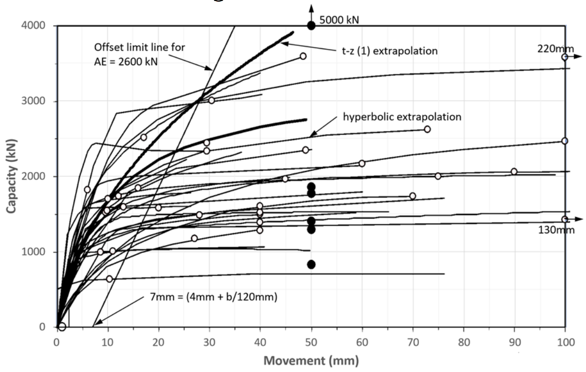

Figure 1. Load-movement predictions from Fellenius (2013)

Fifty years ago, electronic systems were first used to measure and interpret the stress waves in piles generated from the hammer inputs and reflected from the ground response to infer capacity in a more sophisticated and reliable way using wave mechanics principles (Rausche et al., 1972; Goble et al., 1975). Today, PDA testing and wave matching are routinely accepted practice (Hannigan, et al., 2016). But prior to 1985, pile driving acceptance was based only on static load testing and pile driving formulae.

Our fundamental task as designers and supervisors is to ensure that capacity and integrity of each pile installed meets the demands of the structure that it supports. To do this we need to establish a 'ground truth', albeit a locally-evidenced and locally-targeted ground truth capable of application to all piles in a foundation system. Dynamic formulae, properly modified and correlated, must be the vehicle for delivering local ground truth and ultimately being the principal basis for sign-off.

It is important to remember that each PDA test has direct relevance only to the individual pile which is tested. On a foundation-wide basis, the role of PDA tests is critical but subservient, and principally to provide the evidence of ground truth on which a correlated dynamic formula is founded.

Consequent implications for the foundation sign-off process, and for a new approach to establishing capacity reduction factors for driven piles will also be discussed.

2 ANALYSIS AND SYNTHESIS

The engineering design process can be generalized to comprise two phases

1. An analysis phase which includes collecting evidence, organization and processing of data
2. A synthesis phase in which the data collected and analysed is transformed into a connected design

Elsewhere analysis is defined variously as "The process of studying or examining something in an organized way to learn more about it, or a particular study of something" (Cambridge, 2021) or "The process of separating something into its constituent elements" (Oxford, 2021).

Similarly, synthesis is defined variously as "The act of combining different ideas or things to make a whole that is new and different from the items considered separately" (Cambridge, 2021) or "The combination of components or elements to form a connected whole" (Oxford, 2021).

2.1 Geotechnical design

The geotechnical design process is no different, and proceeds through the same analysis and synthesis phases. We explore, observe, sample and test (analysis) and then draw all this together as best we can in the design process, trying to transform the diverse information into simple models which are amenable to solution.

In this section, we will consider the design for a project to be supported on driven piles, and the process of designing a single pile to support a column load.

The purpose of this section is only to provide an analogy to a process that is well understood as a basis for subsequent argumentation regarding the role of dynamic pile formulae.

In the analysis phase of our pile design case, activities include:

- Desktop studies
- Site investigation
- Insitu testing
- Laboratory testing

The synthesis phase activities include:

- Development of simplified site stratigraphy
- Assigning characteristic properties to the layers
- Selecting and applying a pile design method
- Considering the structural loads to establish a design pile size and length

Let's suppose that the pile is a floating pile in a deep clay layer, and that the design method adopted is the α method, in which the pile adhesion, τ at any depth is computed based on the local undrained shear strength, c_u and an adhesion factor, α

$$\tau = \alpha c_u \qquad (1)$$

Figure 2, reproduced after Coduto (1994), is typical of design charts which relate α to c_u. The Coduto curve is similar to the design chart which was included in the Appendix to AS2159 (1978).

Such design curves are often used by designers in the belief that they are based on some universal truth, unaware of the significant scatter which lies behind this design relationship.

Figure 3, includes the 124 test results from which the Coduto relationship was developed. Based on the reference tests alone, it can be seen that if a designer uses this design curve, they could easily overestimate or underestimate adhesion by a factor of 2.

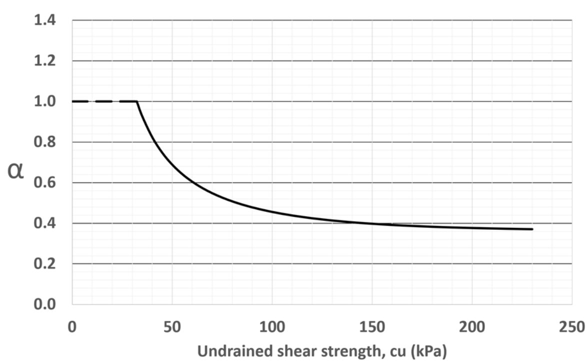

Figure 2. Adhesion factor α after Coduto (1994)

The scatter has an equivalent coefficient of variation (COV) of 29% about the best-fit curve, which is within the bounds of normal expectation for soil investigations. Kulhawy and Phoon (2002) suggest typical COVs of 10 to 30% for laboratory UU triaxial tests; 10-40% for field vane shear tests and 25 to 50% for SPT N tests, amongst others.

The development of this design curve is the embodiment of the synthesis process, in which the engineer necessarily has to reduce the diverse test results into a design algorithm, despite the up to four-fold range of the data on which the algorithm is based.

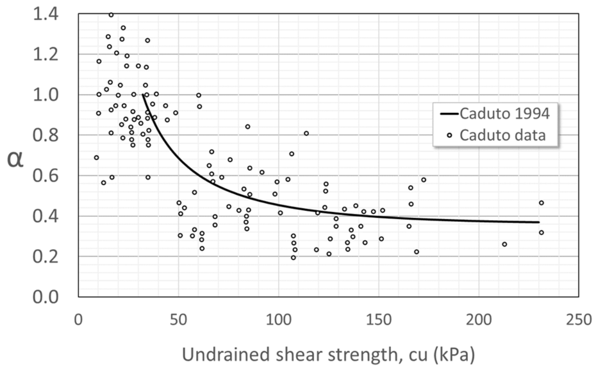

Figure 3. Data sets for adhesion factor α after Coduto (1994)

Coduto is only one of many researchers who have attempted to determine the relationship between α and c_u. Figure 4 compares the Coduto recommendations to other published relationships (Cherubini and Vessia, 2007).

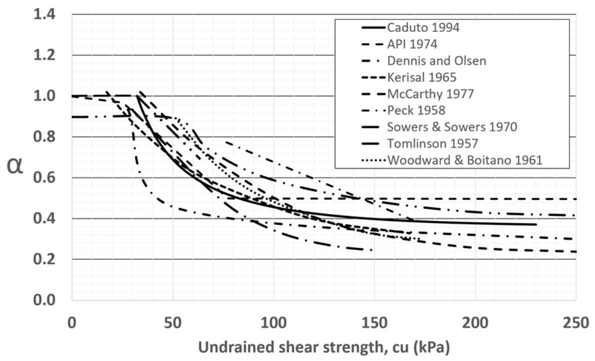

Figure 4. Comparison of published adhesion factor α relationships

It is clear that other researchers, investigating the same relationship but in other geologies and with other pile types have determined and propose distinctly different empirical relationships. This demonstrates that empirical relationships are not universal, but are limited to situations in which the prevailing conditions match the critical parameters on which that relationship are based.

Various authors have identified that α is not only dependent on undrained shear strength, but also a range of other physical properties such as clay mineralogy, Atterberg limits, moisture content, overconsolidation ratio, pile material, geometry, displacement ratio, and installation method.

Improved predictions of α are possible if some of the influencing factors are taken into account. Thus Nowacki et al. (1992) proposed the design chart shown in Figure 5. More sophisticated interpretations of data sets can lead to more reliable assessments with reduced uncertainty.

Putting aside whether the α method is the most suitable design method, it is clear that the variability of results will reduce as the number of variables decreases. By reducing the scope of a relationship to a specific site, or a small region within the same geological setting, the possibility of developing a more reliable relationship increases. Further, if that data is collected for a single pile type, then that will further increase the reliability of prediction.

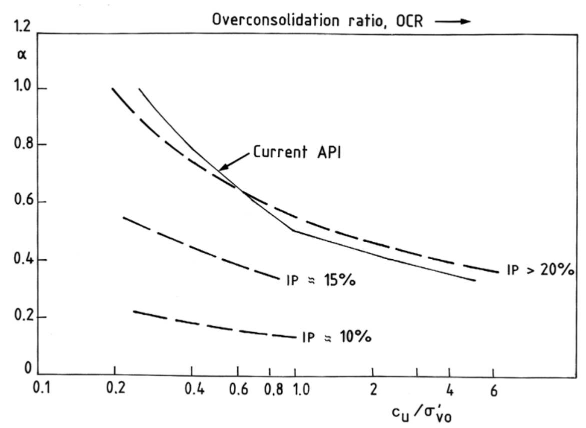

Figure 5. Prediction of adhesion taking into account OCR and plasticity index (IP)

It would be impractical for all but the most significant projects to undertake a program of static load tests to develop site-specific relationships. On the other hand, dynamic load tests conducted adjacent to bore locations provide a practical opportunity to develop the basis for evaluation of site-specific or region-specific α values. Our design-and-construct piling subcontractors have been doing this for decades in order to ensure that they can provide efficient and cost-effective designs. Of course, such an approach must be based on thoughtful, and geotechnically-informed Wave Equation analysis.

Figure 6 is a simulation of the sort of data set which might be generated for a set of tests within a particular geological formation and for a specific pile type. The coefficient of variation of this data set is now less than 5%. The grey zone represents the 95% confidence limit bounds. The lower bound aligns with the definition of characteristic value adopted in Eurocode EC7 (Bond et al., 2013).

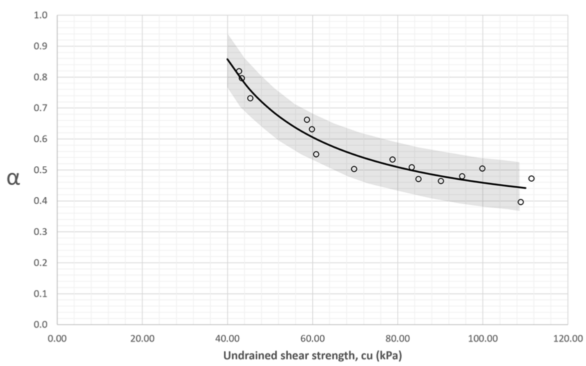

Figure 6. Simulated adhesion relationship for specific geology and pile type

2.2 Key findings

To summarize, the key findings (*kf*) from this review are :

kf1. Geotechnical design relationships are generally based on data sets with wide scatter

kf2. Geotechnical engineers using these relationships must understand and account for the inherent uncertainty in their design (with appropriate reduction factors)

kf3. Empirical relationships are by nature not universal, but are specific to the particular conditions existing at the sites used for data collection

kf4. The reliability of design recommendations can be improved by reassessment of data sets taking into account critical influencing factors

kf5. The reliability can also be improved by developing local relationships for a specific geological formation and particular pile type.

kf6. Statistical analyses can be used to evaluate confidence limits and to determine characteristic values for design. This is fundamental to developing realistic geotechnical reduction factors

kf7. Even in the face of significant variability and uncertainty, engineers necessarily synthesize the individual test results into a unifying relationship (design method) so that the test data can be extrapolated to locations not specifically tested

kf8. The synthesis of test results is fundamental to the design process

2.3 Dynamic Formulae and Pile Acceptance

As noted, the purpose of the previous section was only to provide an analogy to a process that is well understood as a basis for argumentation in this section regarding the role of dynamic pile formulae in regard to pile acceptance. Fragaszy et al., 1989 reviewed the reliability of 10 common pile driving formulae, including the Hiley Formula, in a study of 103 pile tests conducted in Oregon and Washington states by consultants and their departments of transport.

Because of the traditional use of the Hiley Formula in Australia, only the Fragaszy results in relation to this formula will be discussed here.

The Hiley formula is based on a simple theoretical model of pile driving characterized as the inelastic collision with coefficient of restitution, n of 2 masses (the hammer, W_h which drops from a height h with drop efficiency e_h and the pile and helmet, W_p). The pile experiences a permanent set, s , and three components of transient movement, C. Equation (2) predicts the pile capacity, R_u.

$$R_u = \frac{e_h W_h h}{s + (C_1 + C_2 + C_3)} \cdot \frac{W_h + n^2 W_p}{W_h + W_p} \qquad (2)$$

The basis of this equation is to estimate the striking hammer energy, determine the energy transferred to the pile, and then to equate that to the work expended in the transient and permanent movements of the pile. With the exception of the Gates Formula (Gates, 1957), pile driving formulae are based on some simplified energy balance equation.

That being said, two key parameters in the Hiley Formula – drop efficiency, e_h and coefficient of restitution, n can only be determined empirically[1].

Subsequent modifications of the traditional Hiley Formula, which substitute PDA-computed energy transfer, EMX, have been proposed by Broms (1989) and Paikowsky and LaBelle (1994). These modifications were well established in general practice prior to these publications, but with the addition of a correction factor, χ as shown in Equation (3)

$$R_s = \frac{EMX}{\chi.(s + C/2)} \qquad (3)$$

The empirical factor χ (a correction factor which correlates the formula to PDA or Wave Equation estimates of static resistance, R_s) is traditionally assumed to be constant, however, as will be shown, it can be any empirical function. Although the genesis of Eqn. (3) is theoretical, the use of a correlation factor implies a fundamental reliance on empiricism.

The comparison between Hiley Formula predictions (according to Eqn (2)) and static load tests reported by Fragaszy et al., 1989 are shown in Figure 7. The authors report that of the 103 tests, 38 were rejected because of incomplete data and 2 were rejected because the piles were broken. The remaining 63 usable tests included 6 timber, 20 prestressed concrete, 5 H-section, 4 pipe (open and closed), 7 concrete-filled pipe, 5 hollow concrete, and 16 Raymond step taper piles. Included in these tests were 41 piles driven in cohesionless soil, 11 in cohesive soil, and 11 where the sub-surface conditions consisted of layers of both cohesive and cohesionless soil.

In the case of Figure 7, the 63 individual test comparisons are shown against reference line of 1:1 correspondence – the 'design' line

$$\frac{R_{Hiley}}{R_{static}} = 1 \qquad (4)$$

Supplementary lines are also shown for factors of 2 and 3 overestimation and underestimation for reference.

This design line shown in Eq (4) and Figure 7 is equivalent to the α design line in Figure 3, and demonstrates the same key findings *kf*1, *kf*2 and *kf*3 (see Section 2.2).

Although on average the predictions have low bias (the average ratio of Hiley to static capacity is 0.985), the scatter is very wide which is reflected by the coefficient of variation of 72.6%.

Given that the basic premise of monitoring the installation of piles is to reduce the uncertainties inherent in pile design, such a high coefficient of variation undermines the very premise on which pile monitoring is based.

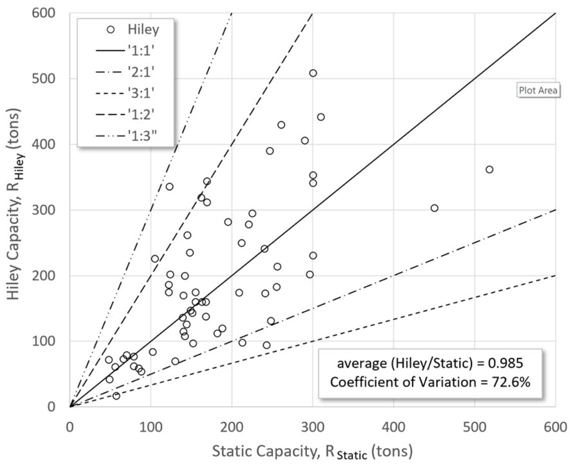

Figure 7. Hiley capacity vs Static capacity (after Fragaszy et al. 1989)

[1] And in practice are generally assumed rather than measured

Go to table of contents

Fragaszy et al. do not further analyse the data of Figure 7 in order to determine whether the spread is affected by pile type, hammer type or soil type.

The difficulties of comparing end of drive installation data (on which driving formulae are based) with static load tests undertaken some days or weeks later have been discussed elsewhere (Seidel, 2015a). The phenomenon of pile setup is well documented and is particularly associated with post-installation pile capacity increases in cohesive soils (Skov and Denver, 1998; Lee et al., 2010).

Ramey and Johnson (1978) report a data set of 153 piles comprising steel-H, steel pipe, concrete and timber piles. Five dynamic formulae, including Hiley Formula, are compared with static tests. All things being equal, one would expect the Hiley/Static capacity ratio to be relatively highest for the piles installed in cohesionless soils (which are generally not known for setup), and lowest for the piles exclusively in cohesive soils (for which end of drive capacity may be significantly less than the capacity measured later during static load testing).

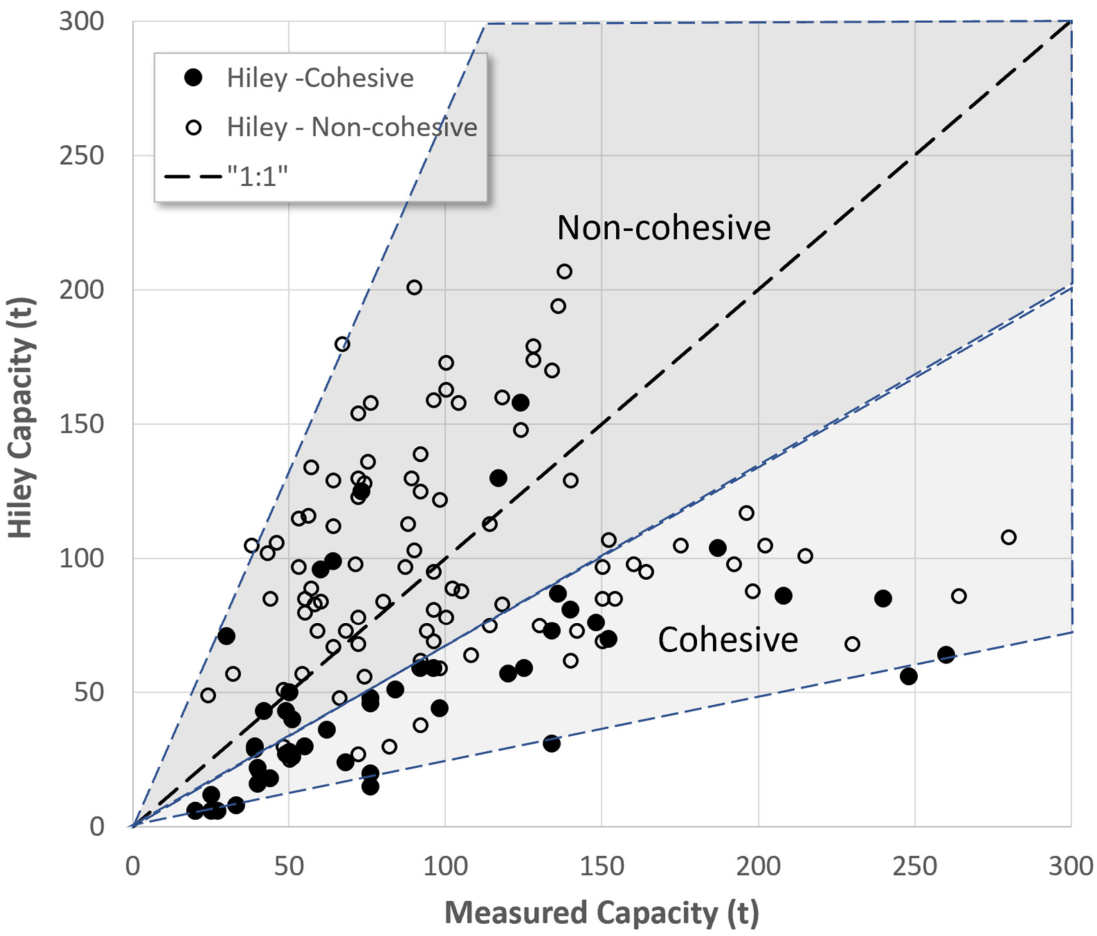

Figure 8. Hiley capacity vs Static capacity after Ramey and Johnson (1978)

Figure 8 shows that the spread of data is similar to the Fragaszy data set. However, the data broadly supports the expected differentiation of test results by soil type, with the spread of cohesive soil data generally being below the non-cohesive data, and showing the influence of pile set-up. Key findings *kf* 4 and *kf* 5 are demonstrated in Figure 8.

As noted in regard to the design parameter, α insightful consideration of the influencing factors (in that case overconsolidation ratio and plasticity index), can reduce uncertainty.

In order to further reduce the uncertainty in the application of dynamic formulae, it is important to understand that dynamic formulae do not predict static pile capacity but rather predict the total resistance of the soil to driving, R_t.

This resistance comprises two parts – a static component, R_s, and a transient dynamic component R_d. thus

$$R_t = R_s + R_d \quad (5)$$

As discussed in Seidel (2018a), the relative proportion of static and dynamic components of total driving resistance vary with the ease of driving. For hard driving, with low set, the total resistance is dominated by the static component. As driving becomes progressively easier (increasing set), the proportion of dynamic resistance increases as indicated schematically in Figure 9.

Referring to Equation (3), the correction function, χ[2] will be relatively small at low sets, and progressively increase as pile sets increase. χ can either be evaluated by wave equation analysis prior to piling, or evaluated empirically from dynamic pile testing, particularly at the commencement of a project.

[2] χ is referred to as Dynamic Reduction Function (DRF) in Seidel (2018)

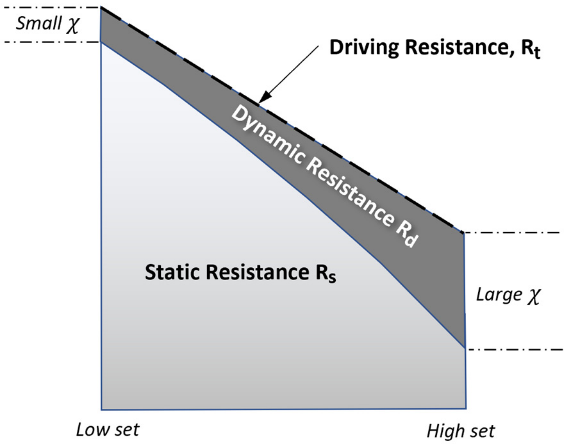

Figure 9. Schematic representation of resistance components during pile driving

The predicted relationship between Hiley Formula and static capacity, was evaluated using the Wave Equation program GRLWEAP (Rausche et al., 2004). for a near-shore piling project with a hydraulic hammer and steel pipe piles driven through bed sediments to refusal on variably weathered rock.

Figure 10 compares the uncorrected Hiley formula capacities inferred from the GRLWEAP predicted values of transferred energy, set and temporary compression with the analysed static capacities. The Hiley formula shown in Equation (3) was used with $\chi = 1$. Hammer strokes of between 0.6m and 1.5m were used in the analyses.

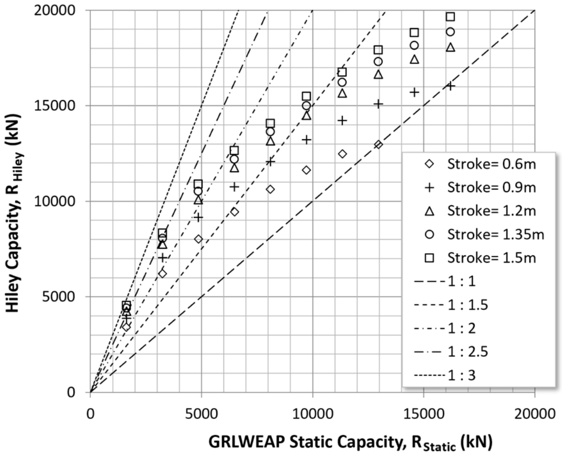

Figure 10. Comparison of Hiley Capacity and Static Capacity predicted by GRLWEAP

The similarity between Figures 7 and Figure 10 is noted. The Hiley formula overpredicts capacity by a factor of up to 3 at low capacities. Unlike the traditional Hiley Formula of Eqn (2), the modified Hiley Formula of Eqn.(3) generally does not underpredict capacity. It is evident that the degree of overprediction progressively decreases with capacity for each stroke, and approaches the equality line (Eqn. 4) at higher capacities.

It is clear that the ratio of Hiley capacity to Static capacity is not constant but varies between 1 and 3 even for a single project with defined soil model, pile type and geometry and hammer. Figure 11, plots the correction factor, χ as a function of pile set. There is a compelling dependency of χ on set across all hammer strokes analyzed, which results in a coefficient of variation of only 1%, and a very tight 95% confidence limit band.

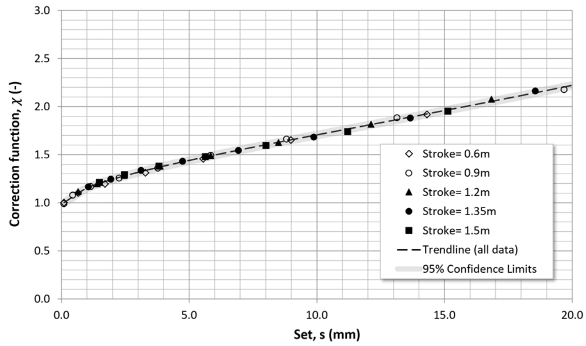

Figure 11. Correction factor function χ computed by GRLWEAP analysis

It is worth reinforcing that by understanding fundamentally the factors underlying the variability of Hiley Formula predictions (see Figure 7) it has been possible to develop a definitive correction factor and to adopt characteristic values which are only marginally below the best-fit relationship for the data (see Figure11). On the other hand, it is noted that the correction function computed here is theoretical. In practice, the data spread will inevitably be greater due to accuracy of set measurements (Denes et al. 2021), quality of PDA testing, uncertainty in wave equation matching (Seidel, 2015a) as well as inherent geotechnical variability. The confidence of any relationship will be reflected in the quality of these inputs. Figure 11 demonstrates the same key findings *kf*4, *kf*5 and *kf*6 (see Section 2.2).

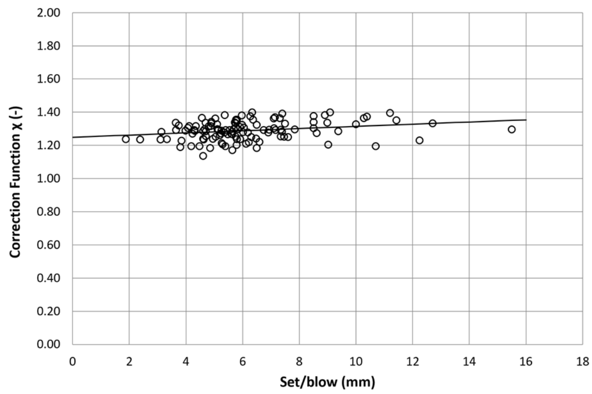

Figure 12. Correction factor function χ computed from project PDA data

Figure 12 presents correction function data for a large project. Each data point represents the wave matching solution for a PDA test. The spread is seen to be larger than for Figure 11, but a distinct trend is still shown. As χ is on the denominator of Equation (3), the upper bound of the confidence limit should be adopted as the characteristic value line.

The data represented in Figure 12 has a very low coefficient of variation (about the trendline) of only 4.2%. This was achieved with remote non-contact set measurements and with high quality PDA testing and mindful (non-automatic) wave equation matching. The consequence is the potential for higher capacity reduction factors (as discussed in the next section).

Figure 12 demonstrates the same key findings *kf*7 and *kf*8 (see Section 2.2). The PDA results are only relevant to the particular piles tested. It is necessary to synthesize these results into a unifying relationship from which a pile acceptance criterion can be developed. Locally correlated driving formulae provide the ground truth, and are fundamental to providing the basis for acceptance of any untested pile.

3 PILE ACCEPTANCE

The current practices in Australia for driven pile acceptance vary considerably. Generally, piles are driven to a capacity rather than a penetration criterion. What might be considered a normal practice is that a percentage of piles are PDA tested and matched with wave equation analysis, and this percentage defines the adopted capacity reduction factor, ϕ_g in accordance with the provisions of Section 4 of AS2159 (2009).

AS2159 (2009) introduced the concepts of a basic geotechnical reduction factor, ϕ_{gb}, an intrinsic test factor, ϕ_{tf} , and a testing benefit factor, K, which allowed the capacity reduction factor, ϕ_g to vary depending on the percentage of piles tested, p.[3]. For a typical project with low perceived risk category and low redundancy $\phi_{gb} = 0.56$, the computed capacity reduction factors are as indicated in Table 1:

Table 1: AS2159 (2009) Effect of increasing percentage of PDA tests

p (%)	3	5	10	25
ϕ_g (−)	0.69	0.72	0.76	0.80

Table 1 suggests that by the very act of testing, a reduced risk is imparted to the pile foundation system. The benefits of testing are manifest, and higher percentages of testing will increase the likelihood of detection of any piles with insufficient capacity. However, there is an implied assumption in AS2159 (2009) that the installation of the 75% to 97%[4] of piles not tested is informed by the results of the tests. This is generally not true, or is not implemented in a rigorous way.

One common practice is to treat the untested piles as unrelated to the tested piles. The tested piles must demonstrate a capacity in excess of the contractual requirement. The untested piles must pass a predefined acceptance criterion in the specification, such as the traditional Hiley Formula. In this approach, the valuable learnings of the PDA tests do not inform acceptance of the untested piles.

The second common practice is to adopt a maximum set criterion which corresponds to the set measured for a tested pile with the target capacity, or inferred if the tested capacity exceeded the target. This implicitly assumes that delivered energy efficiency is constant and that the set-capacity relationship is fixed with no variation. We will see in the next sections that neither of these assumptions is correct.

It will be shown (see Figure 14) that transferred energy cannot be assumed to be constant. Figures 10 to 12 demonstrate that the set-capacity relationship is not constant. Any acceptance criterion must take into account the demonstrated variability of both the energy delivered and of the set-capacity relationship.

3.1 Pile acceptance based on energy, set and temporary compression

Despite the certainty provided to the evaluation of χ , there still remain challenges in evaluation of static capacity, R_s, in Equation (3) which is reproduced here for convenience.

$$R_s = \frac{EMX}{\chi.(s + C/2)} \qquad (3)$$

There are a range of techniques for measurement of pile set and temporary compression. The possibilities, their benefits and limitations are discussed in Denes et al. (2021).

However, the most significant challenge to implementation is EMX, the energy transferred to the pile. Although some modern hammers measure and report kinetic impact energy, KE, these represent only a small percentage of the existing hammer fleet. Even for these hammers, the challenge still remains to evaluate the loss of energy, $KE - EMX$, through the helmet, particularly for concrete piles, for which the pile cushion can be highly variable in thickness and stiffness, especially when the cushion properties change during driving.

Flynn and McCabe (2016) compare EMX and KE measurements for hydraulic hammers on 5 projects, and demonstrate the uncertainties with inferring EMX from hammer energy measurements, as shown in Figure 13. The Flynn and McCabe data indicates that the percentage of hammer energy delivered to the pile typically varied between 75% and 100%, but in isolated instances was as low as 50%. This variability is just the transfer variability. The variability of the hammer stroke and kinetic energy is not even included in this assessment.

For uninstrumented hammers, transferred energy can only be estimated on the basis of estimated ram drop height, assumed hammer drop efficiency, and an assumed loss of energy in transferring from the hammer to the pile. As just noted, this can be particularly challenging for concrete piles.

Seidel (2018b) presents the energy measurements for a project in which 155 PDA tests were undertaken on prestressed concrete piles over the extent of a large bridge project. The project is distinguished by the requirement for all piling and all PDA tests to be undertaken with a drop height of 0.5m. Despite this control on drop height, delivered energies averaged 69.2kJ (88% efficiency), but with a range of 37.5 to 91.0kJ (48% to 116%[5] efficiency). The coefficient of variation of EMX was 15.4%. The three projects that the paper details demonstrate energy ranges of 36% and 40% for the steel pile projects, and 77% for the concrete pile project.

Li et. al., (2022) report in regard to another case study "The driving hammer energy efficiency recorded variations of up to 40%, casting doubt on the use of achieved set as a means of inferring pile capacities".

The histogram in Figure 14 presents the sequential EMX values for 51 of the 155 PDA tests.

[3] Up to a limit of p = 25(%) of piles PDA tested

[4] i.e. (100 – p)%

[5] Efficiency greater than 100% is physically impossible, indicating that the true drop height was significantly in excess of 0.5m

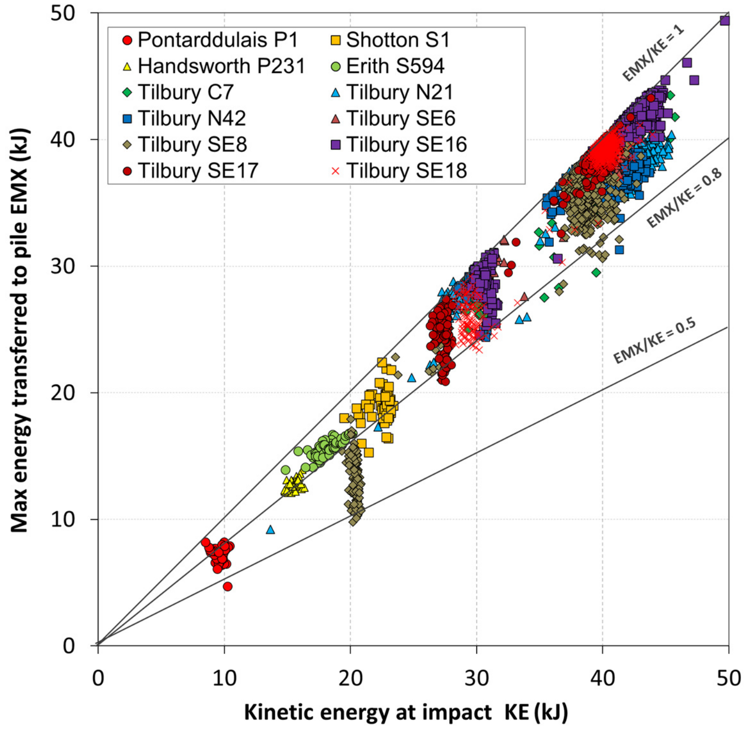

Figure 13. Relationship between kinetic energy at impact and energy transferred to pile

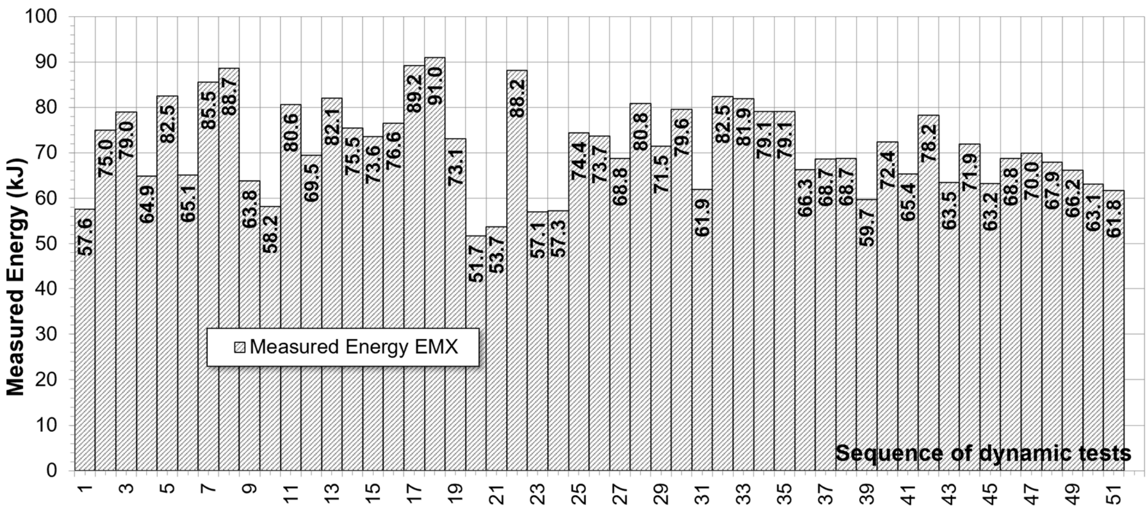

Figure 14. Longitudinal study of variability of delivered energy

The only possibility for individual pile energy measurements[6] is from high frequency remote non-contact displacement measurements. Peak pile velocities can be computed from differentiating the displacement-time signal. It is possible to identify low energy blows from low velocity measurements. Although EMX is related to the square of peak velocity VMX, the relationship is affected by variations in cushion stiffness, so that no unique and reliable energy can be computed in most cases.

Figure 15 is a representation of Figure 12, with upper and lower 95% confidence limits shown. Also shown are the implied geotechnical reduction factors based on a transferred energy uncertainty of 5%[7].

It is noted that the ϕ_g value of 0.70 is derived exclusively from a statistical assessment of the pile testing results and hammer performance and is independent of any assessment of the basic geotechnical reduction factor, ϕ_{gb}. This is a logical approach, because assessment of the installation process should be independent of any of the risk factors considered in developing project average risk rating, ARR and ϕ_{gb} in Table 4.3.2(C) of AS2159 (2009).

[6] Other than PDA testing or attachment of an accelerometer to each pile, both of which have practical issues

[7] The uncertainty in transferred energy evaluation, either from instrumented hammer or pile velocity measurements should be determined from each case.

Go to table of contents

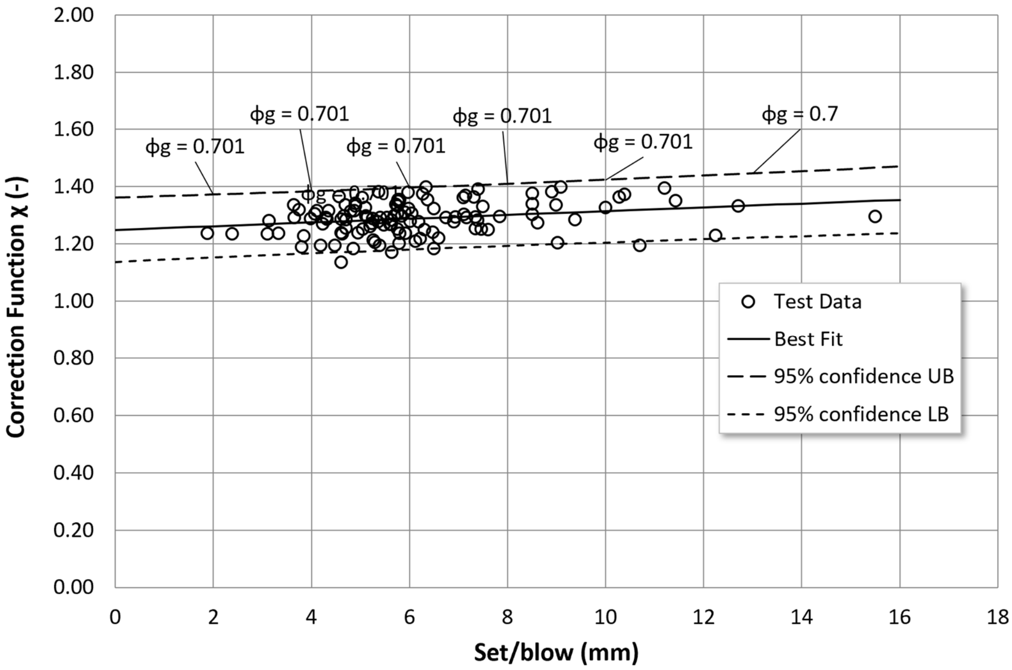

Figure 15. Confidence limits and inferred geotechnical reduction factors for Figure 11 data

3.2 Pile acceptance based on energy and set

Pile acceptance methods based on energy and set alone are fundamentally premised on use of bearing graphs correlated to field test results. Bearing graphs represent the relationship between capacity and pile set, which is of course dependent on hammer energy. Seidel (2015b) and Denes et al. (2021) discuss the importance of Energy-Capacity-Movement (ECM) relationships.

Figure 16 compares bearing graphs for 5 different hammer strokes. The inferred capacities at a blow count of 200 blows/m (5mm set) are shown for each stroke, ranging from 3525kN at 0.4m stroke to 5650kN at 0.8m stroke. Clearly, capacity can only be known if the delivered energy is known.

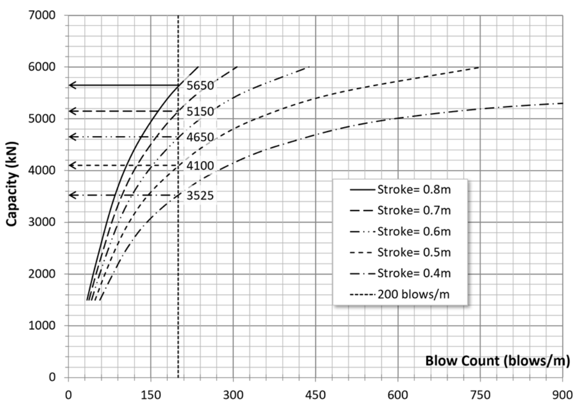

Figure 16. Traditional bearing graphs for a range of hammer strokes / delivered energies

As shown by Seidel (2018b) these bearing graphs can be normalized by the capacity at a specific blow count (in this case 200 blows/m). All the curves collapse to a near-unique relationship as shown in Figure 17, which is an interesting finding.

Three key points are shown on the graph at blow counts of 67, 200 and 870 blows/m (15mm, 5mm and 1.15mm set). What this graph shows is that for any given energy, the capacity at 15mm set will be 50% less than the capacity at 5mm set, and the capacity at 1.15mm set will be 50% more than the capacity at 5mm set. This relationship is unique to this data set, but equivalent relationships will hold for any site.

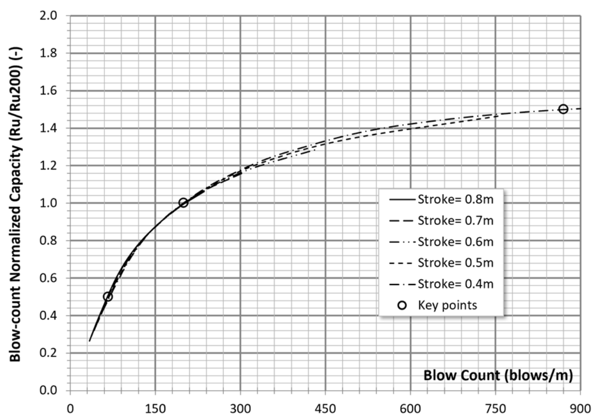

Figure 17. Normalized bearing graphs with normalization to capacity at nominated blow count

The benefit of this approach is that it does not require measurement of temporary compression.

However, all energy-based methods require determination of the energy delivered to the pile. The same comments regarding variability of transferred energy and the reliability of EMX estimates discussed in Section 3.1 apply equally to methods based on energy and set alone.

3.3 Pile acceptance based on force and set

Pile driving formulae are almost universally some expression of a Energy-Capacity-Movement (ECM) relationship, with assumed or measured energy being a fundamental input. As discussed, this is problematic, because of the potential variability of hammer performance, and the uncertainties involved in estimating energy transferred to the piles, even for instrumented hammers (Flynn and McCabe, 2016).

The Gates pile driving formula (Gates, 1957) is an empirical formula which is based not on energy, but the square root of energy, which leads to an equation which is not dimensionally correct. Regardless, the Gates formula, or derivatives of the Gates formula[8] continue to show comparatively the best performance in comparative studies in the United States where it is in common usage (Long, 2009).

To better understand why a non-dimensional equation performs well, consider Equation (6) for kinetic energy KE of the pile driving hammer with mass M_r, which strikes with velocity v_{imp} ,

$$KE = 1/2\, M_r v_{imp}^2 \qquad (6)$$

from which it follows that

$$\sqrt{KE} \propto v_{imp} \qquad (7)$$

Similarly, the energy transferred to the pile, EMX is computed from pile-top PDA measurements of force, $F(t)$ and velocity, $v(t)$ as

$$EMX = \int F.v.dt \qquad (8)$$

One dimensional wave mechanics provides the following relationship which holds between F and v at the commencement of the dynamic event when no reflections from the soil have reached the pile head.

$$F = Z.v \qquad (9)$$

where $Z = EA/c$ is the pile impedance, a function of the pile modulus, E, pile cross-section, A and pile wavespeed, c.

From Equations (8) and (9) it follows that there is an (imperfect) relationship between $\sqrt{EMX}$ and pile-top velocity, v, and pile-top force, F.

The Gates formula therefore effectively expresses a relationship between capacity and force or velocity. The FHWA Gates formula is

$$R_u = 1.75\sqrt{eE_r}\,\log(10N_b) - 100 \qquad (10)$$

Without detailing all the components, the influence of blow count, N_b in blows/inch on modifying the estimate of static capacity, R_u , is shown in Figure 18 which has been shows the relationship in equivalent mm set units.

Seidel (2018c) presented results from a parametric study of 194 Wave Equation simulations involving 20 different piling hammers ranging from 7 to 168 tonne ram weight; 25 concrete or steel pile sections varying from 0.2m square concrete to 3m diameter and 80mm wall thickness steel; cushion stiffnesses, short and long piles, and varying resistance quakes, damping factors and resistance distributions. The study therefore ranged across an extreme range of piling scenarios.

[8] For example FHWA-Gates, modified FHWA-Gates or WSDOT formulas
[9] Capacity normalized by the impact force, R_u/F_{imp}

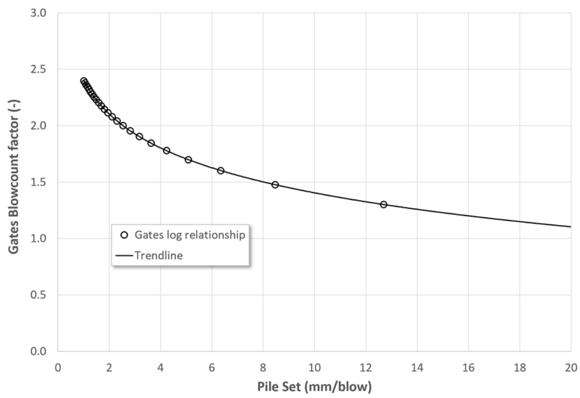

Figure 18. Gates blow-count capacity modifier

The purpose of the parametric study was to investigate the factors affecting normalized capacity with a view to developing reliable predictions of the relationship between normalized capacity[9] and pile set. Only moderate success was achieved, and a reliable prediction method is yet to be developed.

Figure 19 shows the results for 4 of the cases investigated. These cases include concrete and steel piles, and span ratios of (a) ram weights of 10.4, (b) pile impedances of 3.5; (c) damping factors of 3.4 and (d) quakes of 2.1. Despite these large variations in hammer and pile parameters, the indicated normalized capacity-set relationships have a limited range. Furthermore, in practice, the range of this relationship appears to be more limited than indicated by Figure 19, because the parametric study included hammer/pile combinations which could be considered extreme and outside the bounds of practical experience.

Regardless of whether it will be possible to reliably predict these relationships in advance with a simple algorithm, predictions for any project can be made in advance using wave equation analysis.

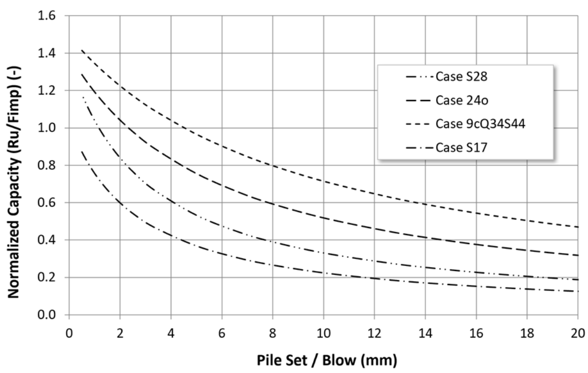

Figure 19. Wave Equation study of Normalized Capacity – Set relationship

Furthermore, any predicted relationship should be calibrated against the results of testing once piling commences. It is recommended that for the initial pile installations, PDA testing and wave matching analyses be undertaken at a range of pile sets – for instance at 10mm, 5mm and 2mm set per blow.

Figure 20 is an example drawn from a project covering multiple dispersed bridge sites. The data includes both end of drive and restrike tests, but is constrained to a single pile geometry (1200mm diameter steel pipe piles) and hammer system.

Figure 20 also shows the upper and lower 95% confidence limits, and the corresponding geotechnical reduction factors, ϕ_g, which vary depending on pile set and the spread of data. For typical acceptance criteria with sets below 5mm /blow, ϕ_g is in excess of 0.7 and as much as 0.74.

Of course, the relationship is premised on measurement of impact force, F_{imp} , for every (untested) pile. This is not practical, however, peak impact velocity, v_{imp} , can be used as a proxy for F_{imp}
using Equation (11).

$$F_{imp} = Z.v_{imp} \tag{11}$$

It is possible to measure v_{imp} with high frequency remote pile measurement devices (see Denes et al., 2021).

The basis for the popularity of the Gates formula can be seen in the similarity of the capacity-set relationships shown in Figures 18, 19 and 20. The empirical success of the Gates formula reinforces the essential validity of a force-based, but locally correlated acceptance criterion.

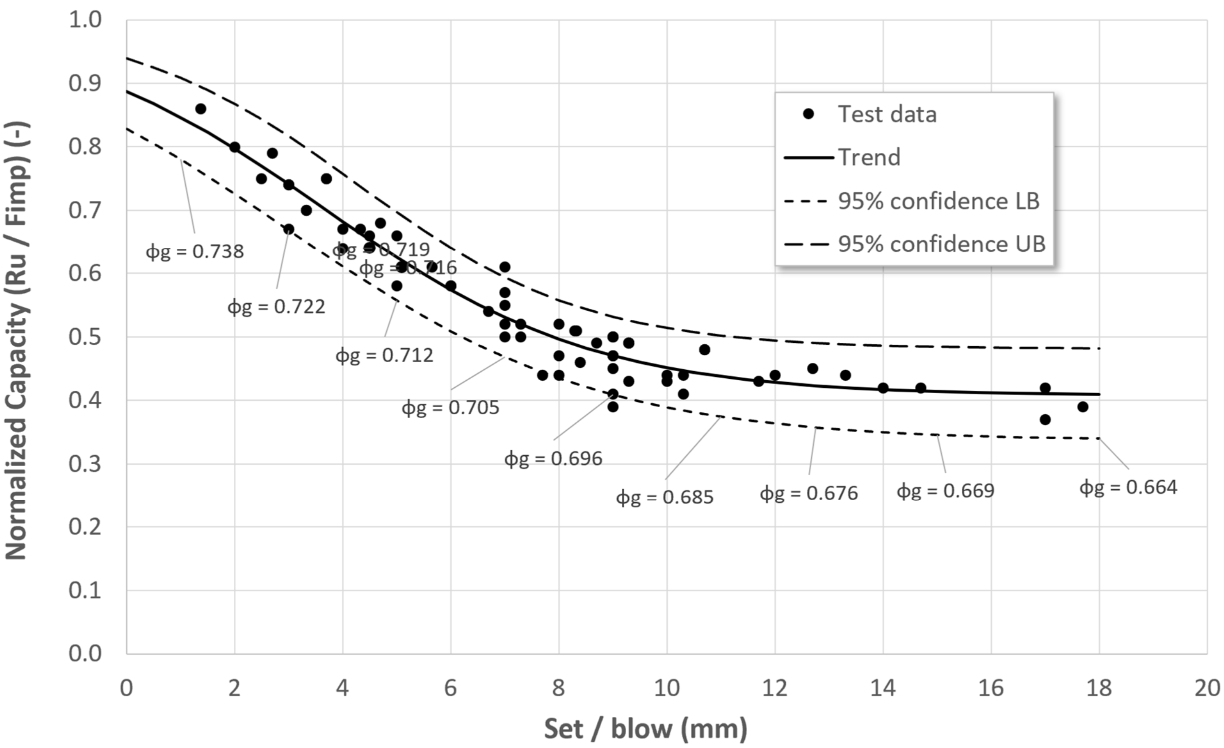

Figure 20. Normalized Capacity – Set relationship for multi-bridge project

4 CONCLUSIONS

Pile driving formulae have long been considered an unreliable approach to evaluation of pile capacity. Although this view may have had historical merit, it misunderstands the central role that pile driving formulae have in modern pile driving control.

Pile driving formulae are not universal truths, but are empirical formulations which have relevance only to the particular set of conditions (piling equipment, pile and soil) on which they are based.

In the modern context, pile driving formulae should have a central role in being the synthesis of the results of PDA testing and wave matching analysis. The pile driving formula, locally correlated against the test results is an expression of the local ground truth, and provides the basis for extension of the individual test results to all piles in the foundation system.

In order to undertake this successfully, the PDA tests must be of high quality and the wave matching must be conducted in a geotechnically relevant and thoughtful approach.

The paper has described three alternative approaches to implementation of pile acceptance criteria – two based on traditional energy-based approaches and a third based on measurement of pile impact velocity (being a proxy for impact force).

It has been shown here and elsewhere that the hammer energy delivered to piles can be extremely variable. The greatest challenge to implementation of the energy-based approaches is the evaluation of delivered energy to the pile for every pile. On the other hand, the alternative based on measurement of pile impact velocity (and pile set) is practically attainable.

Finally, it has been shown that these approaches provide a logical pathway to determining realistic capacity reduction factors, based on the reliability of the adopted empirical pile acceptance relationship, the reliability of the energy, force and movement measurements and the number of tests on which the relationships are based. These approaches do not rely on any evaluation of the basic geotechnical reduction factor defined in AS2159 (2009), which is in itself a logical outcome.

5 ACKNOWLEDGEMENTS

The authors acknowledge the important contributions of their ex-colleagues at FSG Geotechnics and Foundations, in particular Pearse Casey, Ben Kroenert, Nick Medley, Alireza Foroughi and Hossein Ahmadi, to the development and refinement of the novel pile acceptance methods presented here.

6 REFERENCES

Allin, R., Likins, G. and Honeycutt, J., 2015. Pile driving formulas revisited. In *IFCEE 2015* (pp. 1052-1063)

AS2159 (1978) SAA Piling Code. Rules for the design and installation of piling. Standards Australia

AS 2159-2009 (2009). Piling – Design and Installation. Standards Australia

Bond, A.J., Schuppener, B., Scarpelli, G., Orr, T.L., Dimova, S., Nikolova, B. and Pinto, A.V., 2013, June. Eurocode 7: geotechnical design worked examples. In Workshop "Eurocode (Vol. 7).

Broms, B. and Choo, L.P., 1988. A simple pile driving formula based on stress-wave measurements. In Proc. of the 3rd Intl. Conf. on the Application of Stresswave Theory to Piles (pp. 591-600).

Cambridge University Press 2021. Available at https://dictionary.cambridge.org/dictionary/english

Chellis, R.D. (1961) 'Pile Foundations'. 2nd (ed). New York: McGraw-Hill Book Company, Inc.

Cherubini, C. and Vessia, G., 2007. Reliability approach for the side resistance of piles by means of the total stress analysis (α Method). Canadian Geotechnical Journal, 44(11), pp.1378-1390.

Coduto, D.P. 1994. Foundation design, principles and practices. Prentice Hall Inc., Englewood Cliffs, N.Y.

Denes, D., Foroughi, A. and Seidel, J.P. 2021. Pile Testing Verification – an Alternative Approach. Australian Geomechanics Society Victoria Seminar, Oct. 2021.

Fellenius, B.H., 2013. Capacity and Load Movement of a CFA Pile: A Prediction Event. In *Foundation Engineering in the Face of Uncertainty: Honoring Fred H. Kulhawy* (pp. 707-719).

Flynn, K. and McCabe, B.A., 2016, August. Energy transfer ratio for hydraulic pile driving hammers. In Proc., Civil Engineering Research in Ireland Conf.

Fragaszy, R.J., Argo, D. and Higgins, J.D., 1989. Comparison of formula predictions with pile load tests. *Transportation Research Record*, *1219*, pp.1-12.

Gates, M., 1957. Empirical Formula for Predicting Pile Bearing Capacity, Vol 27, No. 3, March : 65-66

Goble, G.G., Likins Jr, G. and Rausche, F., 1975. *Bearing capacity of piles from dynamic measurements* (No. OHIO-DOT-05-75 Final Rpt.).

Groom, D. 2019. An Assessment of Dynamic Pile Driving Formulae for use by Military Engineers

Hannigan, P.J., Rausche, F., Likins, G.E., Robinson, B.R. and Becker, M.L., 2016. *Geotechnical Engineering Circular No. 12–Volume II Design and Construction of Driven Pile Foundations* (No. FHWA-NHI-16-010).

Hiley, A., 1930. Pile-driving calculations. The Struct. Eng, 8.

Kulhawy, F.H. and Phoon, K.K., 2002. Observations on geotechnical reliability-based design development in North America. In Foundation Engineering in the Face of Uncertainty: Honouring Fred H. Kulhawy (pp. 142-159). ASCE.

Lawton, E.C., Fragaszy, R.J., Higgins, J.D., Kilian, A.P. and Peters, A.J., 1986. Review of methods for estimating pile capacity. *Transp. Res. Record No. 1105: Struct. Foundations, Transp. Res. Board*, pp.32-40.

Lee, W., Kim, D., Salgado, R. and Zaheer, M., 2010. Setup of driven piles in layered soil. Soils and foundations, 50(5), pp.585-598.

Li, I., Vinod. M. and Hsi, J. 2022. Case Study: Lessons learned from large scale pile driving in Waikeria, New Zealand. Proc. 20th International Conference on Soil Mechanics and Geotechnical Engineering, Sydney 2022 (submitted for review).

Long, J.H., 2009. Comparison of five different methods for determining pile bearing capacities. Wisconsin Highway Research Program.

Olson, R.E. and Flaate, K.S., 1967. Pile-driving formulas for friction piles in sand. *Journal of the Soil Mechanics and Foundations Division*, *93*(6), pp.279-296.

Oxford University Press. 2021 Available at: https://www.lexico.com/definition/wake

Paikowsky, S., and LaBelle, V. 1994. Examination of the Energy Approach for Capacity Evaluation of Driven Piles. Proceedings of the International Conference on Design and Construction of Deep Foundations, December 6–8, Orlando, FL. FHWA, Vol. II, pp. 1133–1149

Ramey, G.E. and Johnson Jr, R.C., 1979. Relative accuracy and modification of some dynamic pile capacity prediction equations. Ground Engineering, 12(6).

Rausche, F., Liang, L., Allin, R. and Rancman, D., 2004. Applications and correlations of the wave equation analysis program GRLWEAP. In Proceedings, VII Conference on the Application of Stress Wave Theory to Piles (pp. 107-123).

Rausche, F., Moses, F. and Goble, G.G., 1972. Soil resistance predictions from pile dynamics. *Journal of the soil mechanics and foundations division*, *98*(9), pp.917-937.

Seidel, J.P., 2015a. Overview of the Role of Testing and Monitoring in the Verification of Driven Pile Foundations. In Proceedings on the 12th Australia New Zealand Conference on Geomechanics (ANZ2015).

Seidel, J.P., 2015b. Enhanced Use of Dynamic Pile Testing in Foundation Engineering. In Proceedings on the 12th Australia New Zealand Conference on Geomechanics (ANZ2015).

Seidel, J.P., 2018a. The normalized bearing graph and dynamic reduction function concepts in pile acceptance. DFI-EFFC International Conf. on Deep Foundations and Ground Improvement, Rome, Italy 6-8 June, 2018.

Seidel, J.P., 2018b. The importance of energy evaluation on an individual pile basis. DFI-EFFC International Conf. on Deep Foundations and Ground Improvement, Rome, Italy 6-8 June, 2018.

Seidel, J.P., 2018c. Mobilization of Pile Capacity and Pile Acceptance. Invited presentation to Australian Geomechanics Society, Victorian Chapter, 8 August, 2018.

Skov, R. and Denver, H., 1988. Time-dependence of bearing capacity of piles, Proc. 3rd International Conference on Application of Stress-Wave Theory to Piles, Canada, 1–10.

The Application of 3D Finite Element Method in the Design of Large Piled Foundation System - Case Study: Melbourne Cement Facility

K. Ranjbar Pouya[1], B. Collingwood[2] and A. Judi[3]

[1] FSG Geotechnics and Foundations, Unit 12, 71 Victoria Crescent, Abbottsford, VIC, 3067; email: kranjbar@fsg-geotechnics.com.au
[2] FSG Geotechnics and Foundations, Unit 12, 71 Victoria Crescent, Abbottsford, VIC, 3067; email: bcollingwood@fsg-geotechnics.com.au
[3] Wagstaff Piling Pty Ltd., 33 Nott Street, Port Melbourne, VIC, 3207; email: a.judi@wagstaffpiling.com.au

ABSTRACT

This paper provides an overview of the foundation design and analysis process carried out for the Melbourne Cement Facility silo located in Port Melbourne, Victoria, Australia. The proposed silo is a cylindrical multi-compartment cement storage facility supported on a 2.6m thick concrete ring beam with an external diameter of 38.5m. The ring beam is supported by a piled foundation system comprising 155 CFA piles in an annular pile layout. The site is underlain by Quaternary Sediments of Yarra Delta which are further underlain by Werribee Formation. This paper describes a detailed soil-structure interaction analysis performed using the finite element program PLAXIS 3D, which was used to assess the foundation performance with particular attention to global and differential settlement of the pile group. The study evaluated the complex load sharing between the piles and the ring beam, and the differences in load mobilisation between piles within the group. The results of this study highlight the capability of 3D FEM analysis for obtaining an optimised foundation design solution and understanding and addressing various technical challenges associated with silo foundation systems of this type.

Keywords: piled raft, piled foundations, foundation design, finite elements, storage facilities, settlement analysis

1 INTRODUCTION

Piled raft foundations can be a practical and economical solution for very tall budlings and heavy industrial facilities where substantial vertical loads will be transferred to the substructure. The proposed cylindrical multi-compartment cement storage facility weighs up to 922 MN when all compartments are fully loaded. Considering the size and loads of such large storage facilities, the settlement of the foundation system supporting the structure is often a governing factor in the design. It has been shown that piles can be successfully used as settlement reducers (Burland et al. 1977; Mandolini et al. 2005) with a contribution from the overlying raft. Moreover, in many cases the primary objective of including piles in the design of pile raft foundations is to control settlements as raft alone can provide sufficient bearing resistance (Davis and Poulos 1972; Randolph 1994). However, as Viggiani et al. (2012) identified in the case of a so-called *small pile raft*, the un-piled raft could not solely carry the vertical loads and, in contrast to the case of a *large piled raft*, the key requirement for including piles is to satisfy an adequate factor of safety against bearing failure.

A considerable body of literature has been focused on developing methods for piled raft analysis. Early analytical works for the piled raft analysis were carried out by Davis and Poulos (1972) and Randolph (1983, 1994). Davis and Poulos (1972) presented a simplified analytical approach to evaluate the role of piles as settlement reducers in combined piled raft systems. The first series of simplified numerical analyses emerged as in two distinct approaches of *strip on springs* (Poulos 1991) and *plate on springs* (Poulos 1994; Viggiani 1998; Russo and Viggiani 1998). Ta and Small (1996) developed the Finite Layer Method for the analysis of pile raft foundations resting on layered soil stratum. More recent attention has focused on three-dimensional analysis of piled rafts (Smith and Wang 1998; Katzenbach et al. 1998; Katzenbach et al. 2005; Lee et al. 2010). Recent advances in Finite Element Modelling (FEM) have made full three-dimensional piled raft analysis a robust tool to capture the realistic soil-structure interaction and load sharing behaviour among the piles and the raft. In this study, the FEM program PLAXIS 3D was employed to evaluate the performance of the foundation system in regard to both stability and serviceability requirements. A detailed soil-structure interaction analysis was carried out to evaluate and understand the contribution of the piles and the ring beam in the design of the foundation system.

2 SITE LOCATION, SILO STRUCTURE AND LOADING CONDITIONS

The cement silo facility proposed for construction by Melbourne Cement Facility (MCF) is a cylindrical structure with a number of segmented storage compartments and a total height of about 71m. The structure is located in Port Melbourne, Victoria, Australia. The site location and the proposed location of the new silo is shown in Figure 1. The structure has an internal diameter of about 31.4m and comprises circular reinforced concrete walls with thicknesses of around 0.5m to 1.2m.

Figure 1. Site location and the proposed location of the new silo - source: Google Earth

The silo structure is supported on a 2.6m thick annular ring beam which is shown in Figure 2. Loads coming from the superstructure will be transferred from the cylindrical silo walls to the ring beam and the piles constructed underneath. The foundation system is designed to perform as a piled raft as the ring beam has a large dimension (and contact area) and can contribute to the load-bearing of the system. A quantitative assessment of the contribution of the piles and ring beam to the foundation performance will be discussed in subsequent sections. The overall dead load and live load of the silo structure is in the order of 900 MN in total. The load critical load cases that were adopted in foundation modelling and design are summarised in Table 1.

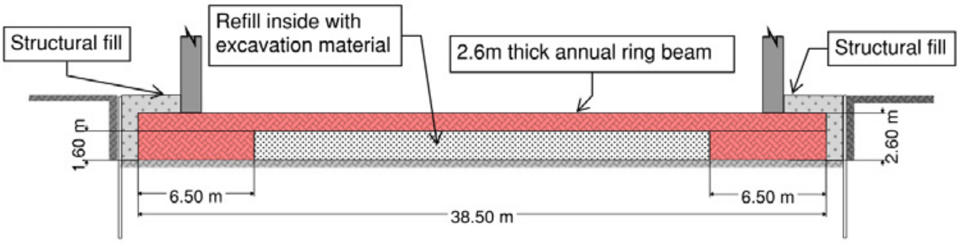

Figure 2. Silo ring beam geometry

Table 1: Summary of design load cases

Load Case	Description	Load Composition
SLS-1	Serviceability limit state for global settlement check – full silo loading	DL+LL
SLS-2	Serviceability limit state for differential settlement check – live loading on one half of silo only	DL across full silo LL on one half of silo
ULS-1	Ultimate limit state for maximum vertical loading based on AS 1170 load combination	1.2 DL + 1.5 LL
ULS-2	Ultimate limit state for earthquake loading based on dead & live vertical loads, shear force and overturning moment	DL + LL + EQ

Serviceability limit state load cases SLS-1 and SLS-2 were used for settlement assessment. It was assumed that all silo compartments are fully loaded for SLS-1. It is understood that some compartments of the silo can be either fully loaded or completely empty at times. Therefore, SLS-2 was adopted to account for the worst-case scenario in terms of differential settlements when half of the silo is empty (DL only) and the other half is fully loaded (DL+LL). Ultimate state limit load cases ULS-1 and ULS-2 were used to check the generated actions in piles against the structural capacity. ULS-1 was also used to check the overall geotechnical stability of the foundation system which will be discussed in more detail in the subsequent sections.

3 GROUND CONDITIONS

According to the Geological Survey of Victoria 1: 31, 680, the construction site is located in an area of recent Quaternary sedimentation which forms part of the well-known Yarra delta. Yarra delta sediments at the site are present beneath a fill layer, and comprise Port Melbourne Sand (PMS), Coode Island Silt (CIS), Fishermen's Bend Silt (FBS) and Moray Street Gravel (MSG). The Yarra Delta sediments are further underlain by Werribee Formation and Silurian age Siltstone of the Melbourne Formation. The groundwater level has been reported consistently at a depth range of 2.2m to 2.7m below ground surface, consistent with the adjacent river water levels. Ground models were developed based on the available site investigation data, which includes information from both borehole and CPTs. The ground conditions were found to be reasonably consistent with our general expectation of the Yarra Delta profile as described in many existing references, for example, Ervin (1992). A summary of the adopted ground model is presented in Table 2.

Table 2: Summary of geotechnical modelling parameters

Unit	Depth BGL (m)		Unit Weight (kN/m^3)	Effective Cohesion c' (kPa)	Friction Angle ϕ' (deg)	Young Modulus E' (MPa)
	From	To				
Fill	0	3.6	18	2	30	20
Port Melbourne Sand	3.6	6.5	19	2	30	20
Coode Island Silt	6.5	8	17	2	27	5
Fishermen's Bend Silt	8	29	19	7	27	50
Moray Street Gravel (interbedded clays and sands)	29	49.5	19	2 - 7	28 - 35	55 - 180
Werribee Formation (sand)	49.5	63.5	19	2 - 10	28 - 37	60 - 150
Siltstone, EW to HW	63.5	70	20	10 - 25	30 -32	60 - 200

4 FOUNDATION DESIGN

The large depth to siltstone rock meant that the piled foundations needed to be founded in the overlying soil profile at depths that could be readily achieved by an available piling plant. The size and significance of the silo structure, and the significant loading it imposes on the founding soils, meant that both geotechnical strength and serviceability requirements had to be carefully evaluated.

According to the adopted serviceability design criterion, calculated foundation settlements under the serviceability load combinations (SLS-1 and SLS-2) should not exceed the allowable settlements. Allowable settlements for silo were specified as below:

- Total settlement is not to exceed 300mm.
- Differential settlement under Load Case SLS-2 is not to exceed 60mm from one side of the silo to the other.

Design for geotechnical strength was based on the limit state design principles documented in the Australian Piling Code (AS 2159-2009). This requires piles to be designed in such a way that the design geotechnical strength (which is the ultimate geotechnical strength multiplied by an appropriate geotechnical strength reduction factor) will be not less than the design action effect. However, it has been well documented that applying such geotechnical criteria to each individual pile within a pile group can result in considerable conservatism in the design (e.g., Poulos, 2017). This is acknowledged in AS 2159-2009 in clause 3.2.2, which allows individual piles within the group to be overloaded for the ULS load case provided that the ultimate geotechnical design strength of the pile group satisfies the requirements of the code. To this end, the ULS-1 load divided by an appropriate Geotechnical Strength Reduction Factor (φ_g), was modelled with the acceptance criteria being that the pile group must maintain overall stability. This is indirectly a check on the overall factor of safety for the foundation system design and stability under this load case demonstrates that the requirements of AS2159-2009 are met with respect to strength.

The foundation system has the ring beam supported on 155 No. 900mm diameter reinforced concrete CFA piles with pile toes founded in the Moray Street Gravel (MSG) unit. The layout for the CFA piles includes five rows of piles from inside to outside of the ring beam. The pile spacing varies between rows, but averages about 2.1m.

Available site investigation data suggested that the MSG is comprised of interbedded sand and clay layers. To account for the lithological variation of interbedded granular and cohesive sublayers within the MSG unit and the possibility of encountering clay lenses at the toe of some of the piles, a series of sensitivity analyses were performed to evaluate the foundation performance with an appropriate range of ultimate base resistance values.

Appropriate pile design parameters for shaft friction and base resistance were determined in consultation with Wagstaff Piling, based on previous experience and available load test results from previous tests in similar ground profiles, ensuring that the selected values were reasonably expected to be achievable at the site for CFA piles installed with the available equipment. Table 3 presents the unit stresses that were adopted in our modelling.

Table 3: Summary of pile resistance parameters

Unit	Depth (m)		Ultimate Shaft Friction (kPa)	Ultimate Base Stress (kPa)
	From	To		
Fill	0	3.5	0	-
PMS	3.5	6.5	20	-
CIS	6.5	8	20	-
FBS	8	17	50 to 80	-
MSG	34	40	100 to 150	3000-5000*

** Sensitivity checks were carried out for the range of base stresses presented which cover the expected range of outcomes in practice.*

Using the estimated unit stresses, the ultimate geotechnical strengths of piles considered in the modelling process ranged between 9.2MN and 11.3MN, depending on the various founding assumptions.

5 NUMERICAL ANALYSIS

Recent advances in computational speed have facilitated the utilisation of relatively complex and detailed 3D analyses of piled raft foundations. Commercially available software packages, such as PLAXIS3D, can model complex ground conditions, pile arrangements and soil-structure interaction. In this study, modelling of the silo foundation system was carried out using the PLAXIS 3D software.

Simulation of piles in a sufficiently accurate and realistic manner is a key aspect of a piled foundation analysis. There are two distinct methods in PLAXIS for modelling piles in a 3D analysis. One involves modelling piles as volume elements with a user-defined interface. Although considered to be the more robust approach, the application of volume elements can be extremely demanding in terms of processing time for a large foundations system with a considerable number of piles.

The alternative option, which is adopted in this study, is the application of embedded beam elements in which the piles interact with the surrounding soil by means of special embedded interface elements. Lee et al. (2010) showed that the application of embedded beam elements can be considered a rigorous numerical approach as it results in very similar predictions compared to volume elements for pile rafts. Although pile shaft friction can be calculated automatically by the software (by relating the shaft profile to the strength properties of the soil), in this exercise the shaft resistance is manually defined to ensure the modelled ultimate geotechnical resistance of piles is consistent with the values given in Table 3.

A linear elastic perfectly plastic model with Mohr-Coulomb failure criteria was adopted for all soil layers. Effective stress analyses were carried out using drained material properties to evaluate the long-term settlement behaviour of the foundation system. Long term consolidation over the design life of the structure was also considered, by estimating the secondary compression of soils over the 50-year design life of the structure. The adopted geotechnical modelling parameters are summarised in Table 2. To ensure loading was accurately distributed to the foundation system, loads were converted to equivalent pressures on top of the ring beam. Figure 3 shows the model geometry and pile arrangements.

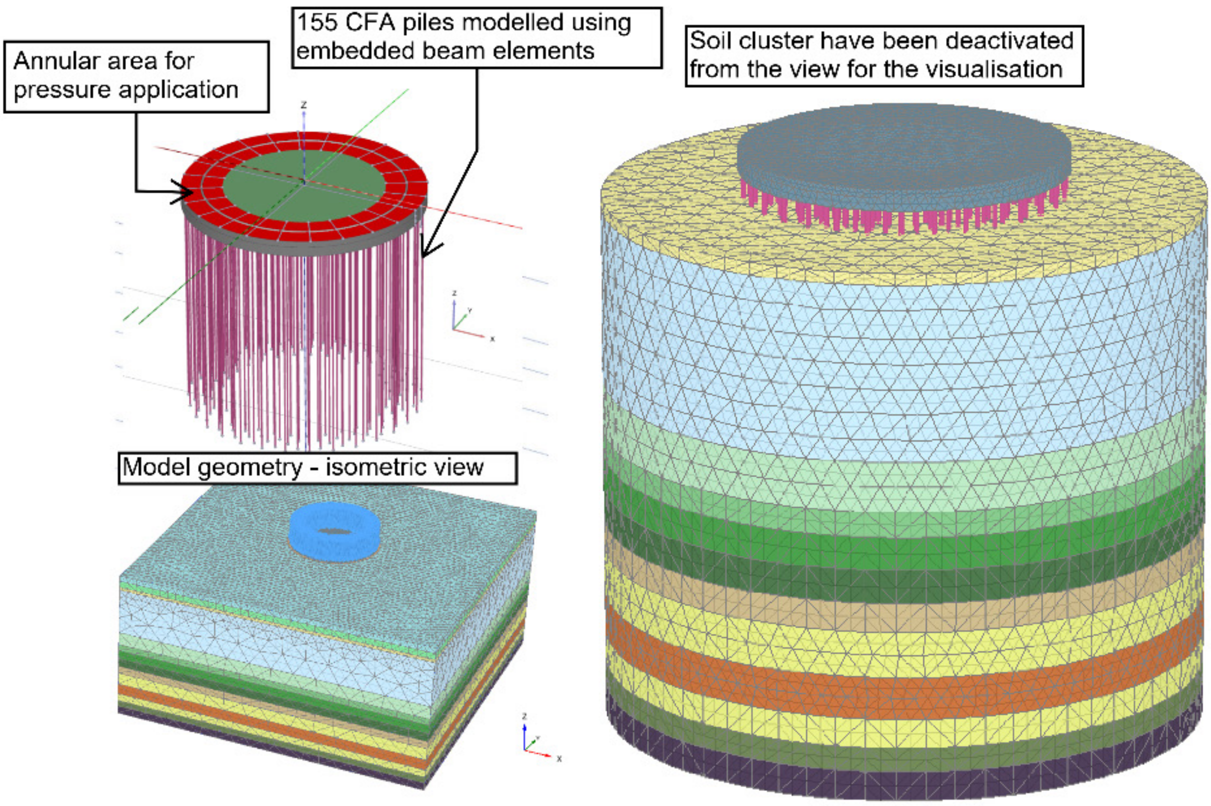

Figure 3. PLAXIS 3D model geometry for the silo foundation system

6 RESULTS AND DISCUSSION

Table 4 summarises the estimated total and differential settlements for the foundation system under SLS load cases, for each of the adopted founding levels and end bearing assumptions. It can be inferred from the data in Table 4 that the settlement performance of the foundation system is not greatly sensitive to the range of assumptions that were used. We consider this is likely to be because a significant proportion of the SLS loads are being resisted by shaft friction over the length of the piles, and shed to the surrounding ground. As a consequence, the load is distributed to a large soil mass and small differences in founding level and end bearing do not have a significant impact on settlements. Figure 4 presents the predicted absolute and differential settlement contours for load case SLS-1 and SLS-2 for founding condition case 4 specified in Table 4.

Table 4: Summary of calculated settlement from PLAXIS analysis

Founding Condition Case	Maximum calculated vertical settlement (mm) SLS-1	Maximum calculated vertical differential settlement (mm) SLS-2
1.Toe RL -38.5m, f_{bu}= 5MPa	93	50 (33 to 83)
2.Toe RL -36.5m, f_{bu}= 5MPa	100	56 (35 to 91)
3.Toe RL -38.5m, f_{bu}= 3MPa	94	51 (33 to 84)
4.Toe RL -36.5m, f_{bu}= 3MPa	101	58 (34 to 93)

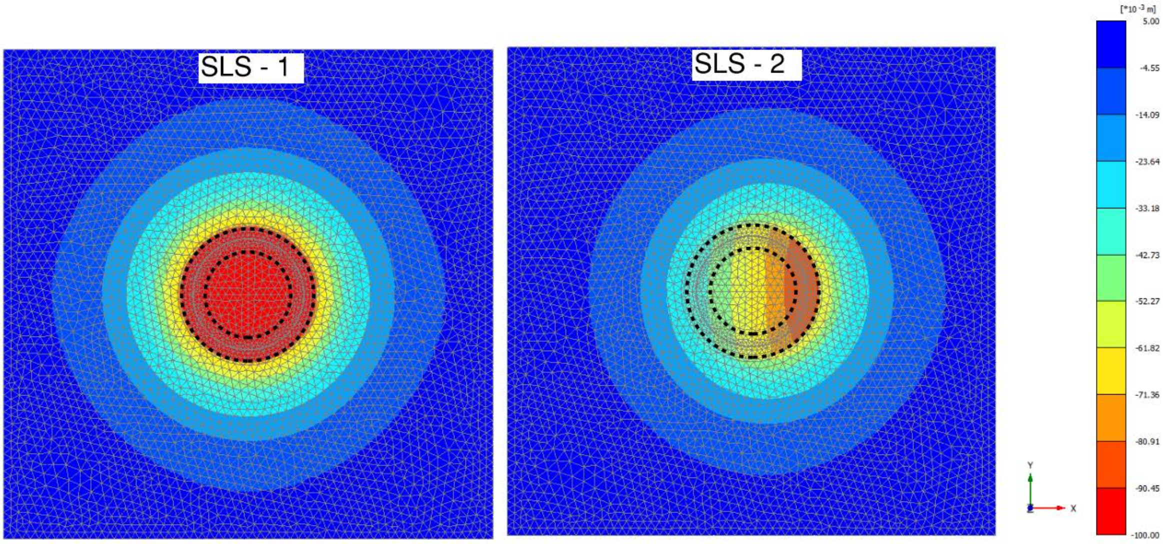

Figure 4. Absolute and differential settlement contours for load cases SLS-1 and SLS-2

The load sharing behaviour between the piles and the ring beam is summarised in Table 5, as the ratio of the sum of the pile head loads over the total load being applied on the foundation system. This is sometimes referred to as the combined piled raft foundation coefficient (Katzenbach et al. 2005). Table 5 indicates that the superstructure loads are mostly carried by the piles, with a bearing contribution of about 80%, and the remaining 20% of the loads are transferred to the subsoil directly through the ring beam contact area.

Table 5: Pile and ring beam load sharing

Case	Q_p/Q_t
SLS - 1	0.80
ULS - 1	0.78

Figure 5 illustrates the calculated pile head axial loads under ULS-1 for founding condition case 2. This Figure shows that the loads are unevenly distributed among piles, ranging from around 4.5 MN to 10 MN. It is noted that some of the variations in individual pile loads is thought to be attributable to the FEM modelling process; specifically localised meshing effects. For this reason, the variability in actual pile loads is expected to be less in practice than the model outputs would suggest.

Nonetheless, a large variation in individual pile loads has also been demonstrated in other studies (e.g., Poulos, 2017). A highly non-uniform distribution of loads among piles highlights the importance of considering group stability when assessing the ultimate limit state geotechnical capacity of the foundation system to avoid unnecessary over-conservatism in the design by designing all piles to the highest individual pile load.

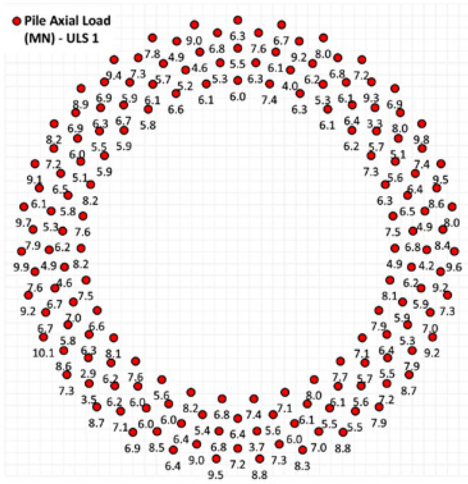

Figure 5. Calculated pile head loads, ULS-1

As mentioned in the preceding sections, an additional load case, based on the ULS-1 loading divided by the adopted geotechnical reduction factor (φ_g), was analysed for all founding condition cases and a satisfactory outcome was achieved. This demonstrated compliance with AS2159-2009 with respect to the ultimate geotechnical capacity of the pile group, and an adequate overall factor of safety for the foundation system design.

To account for the localised variability in individual pile loads (inferred to be due to meshing effects) in the design, our approach was to average the individual pile loads across a selection of adjacent piles for each row of piles. Table 6 presents the average maximum axial pile head loads across inside, middle and outer rows of piles under SLS-1 and ULS-1 load cases. It is noteworthy that the outside row piles attract significantly higher loads compared to the middle row and inner row piles.

Table 6: Summary of calculated pile head loads

Case	Maximum axial pile head load (kN)
SLS - 1	Outside Row = 9413 Middle Row = 3159 Inside Row = 5765
ULS - 1	Outside Row = 10050 Middle Row = 5747 Inside Row = 6591

To better understand the load sharing mechanism between piles in different rows, it is necessary to consider the differential movements between these piles and the surrounding soil. Figure 6 shows a cross-section of the vertical settlement contour plot through the midsection of the silo from the PLAXIS analysis.

This figure needs to be interpreted in conjunction with the tabulated values in Table 6. As shown in Figure 6, the soil mass enclosed inside the ring of piles settles much more compared to the soil mass outside the footprint of the silo. Due to the relative rigidity of the ring beam, the absolute settlements of all piles are very similar. Therefore, the outer row piles settle more relative to the surrounding soil mass, which results in mobilisation of higher shaft and end bearing resistances in these piles. In contrast, the soil mass inside the silo footprint undergoes a much larger settlement and the displacement of the inner row piles relative to the soil is correspondingly lower; hence, less resistance is mobilised in the inner row piles. The middle row piles mobilise the least resistance, as the soil mass around these piles is being loaded by adjacent piles in both the inner and outer rows; hence, middle row piles experience the least relative pile/soil displacement.

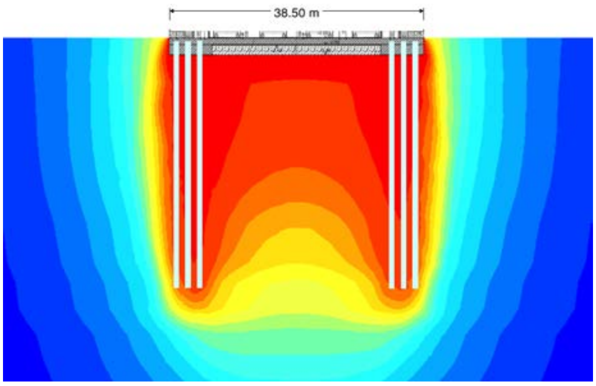

Figure 6. Vertical settlement contour plot

7 CONCLUSION

This paper presented the analysis undertaken as part of the design of the foundation system for a large cement silo storage facility. A satisfactory outcome was achieved in terms of both geotechnical strength and serviceability performance. The study showed that 3D FEM analysis can be employed to understand the group performance of the foundation system and the distribution of load to foundation elements. The results were used successfully to develop an optimised design solution for the piling scheme. The nature of the load transfer between the piles and the ring beam was able to be assessed, as well as the distribution of loads to individual piles and inner, middle and outer pile rows. The analysis indicated that the distribution of vertical loads was highly non-uniform among piles in different rows, which can be explained by the relative displacements experienced by piles in each row relative to the surrounding soil. The study illustrated the importance of considering the foundation system as a group, in order to avoid over-conservatism in the pile design.

8 ACKNOWLEDGEMENTS

The authors wish to acknowledge the contribution and assistance of Melbourne Cement Facility and Fitzgerald Construction (Australia) in the execution of the study and for allowing the publication of this technical paper.

REFERENCES

AS 2159-2009 Piling - Design and installation, Standards Australia.
Burland, J. B., Broms, B. B., and De Mello, V. F. B. (1977). “Behaviour of foundations and structures.” Proc. 9th int. Conf. on Soil Mech. & Found. Eng., 2, 495-546.
Davis, E. H., and Poulos, H. G. (1972). The analysis of piled raft systems. Aust. Geomech. J 2, 21-27.
Ervin, M.C., (1992), Engineering properties of Quaternary age sediments of the Yarra Delta, Seminar, Engineering Geology of Melbourne, 245–260.
Katzenbach, R., Arslan, U., Moorman, C., and Reul, O. (1998). “Piled raft foundation: interaction between piles and raft.” Darmstadt Geotechnics (Darmstadt University of Technology), 4, 279-296.
Katzenbach, R., Schmitt, A., and Turek, J. (2005). “Assessing Settlement of High-Rise Structures by 3D Simulations.” Computer-Aided Civil and Infrastructure Engineering, 20, 221-229.
Lee, S. W., Cheang, W. W. L., Swolfs, W. M., and Brinkgreve, R. B. J. (2010). “Modelling of piled rafts with different pile models.” Numerical Methods in Geotech. Eng. Benz & Nordal (eds), Taylor & Francis Group, 637-642.
Mandolini, A., Russo, G., and Viggiani, C. (2005). “Pile foundations: experimental investigations, analysis, and design.” Proc. 16th Int. Conf. on Soil Mech. & Geotech.l Eng., 12–16 Sep, Osaka, Japan, 177-213.
Poulos, H. G. (1991). “In computer methods and advances in geomechanics (eds Beer et al.), 183-191. Rotterdam: Balkema.
Poulos, H. G. (1994). “An approximate numerical analysis of pile-raft interaction.” Int. J. for Numerical and Analytical Methods in Geomechanics, 18, 73-92.
Poulos, H. G. (2017). “Tall Building Foundation Design.” CRC Press, Taylor & Francis Group.
Randolph, M. F. (1983). “Design of piled foundations.” Proc. Int. Symp. on Recent Development in Lab. & Field Tests & Analysis of Geotech Problems, Bangkok, 525-537.
Randolph, M. F. (1994). “Design methods for pile groups and piled rafts: state-of-the-art report.” Proc. 13th Int. Conf. Soil Mech. Found. Eng., New Delhi 5, 61-82.
Russo, G., and Viggiani, C. (1998). “Factors controlling soil-structure interaction for piled rafts.” Intern. Conf. on Soil-Structure Interact. in Urban Civil Eng., Ed. Katzenbach, R., and Arslan, U., Darmstadt, 79-102.
Smith, I. M., and Wang, A. (1998). “Analysis of piled rafts.” Int. J. Numer. Anal. Meth. Geomech., 22, 777-790.
Ta, L. D., and Small, J. C. (1996). “Analysis of piled raft systems in layered soils.” Int. J. for Numerical and Analytical Methods in Geomech., 20, 57-72.
Viggiani, C. (1998). “Pile groups and piled rafts behaviour.” Proc. 3rd Int. Geot. Seminar on Deep Foundations on Bored and Auger Piles, Ghent, 77-94.
Viggiani, C., Mandolini, A., Russo, G. (2012). “Piles and Pile Foundations.” Spon Press, Taylor & Francis Group.

Pile Testing Verification – an Alternative Approach

D. Denes[1], CPEng., A. Foroughi [2], BEng., J. Seidel [3], PhD., CPEng.

[1]Golder Associates Pty Ltd, Foundation/Pile Testing Department, Building 7, Botanicca Corporate Park, 570 – 588 Swan Street, Richmond, Victoria 3121, Australia; email: Ddenes@golder.com.au
[2]Golder Associates Pty Ltd, Senior Engineer, Building 7, Botanicca Corporate Park, 570 – 588 Swan Street, Richmond, Victoria 3121, Australia; email: AForoughi@golder.com.au
[3]Foundation QA Pty Ltd, Managing Director, POBox 4280, Croydon Hills, Victoria, Australia, 3136; email: julian@foundationqa.com

ABSTRACT

Dynamic pile testing is undertaken for a number of reasons including: 1. To confirm that the pile meets serviceability and geotechnical capacity requirements; 2. To assess pile integrity, either during installation (driven piles) or after construction (cast-insitu piles) and 3. To verify that the piling hammer delivers the energy required to satisfy the design criteria and that stresses during testing are kept within acceptable limits. In addition, testing allows us to establish and calibrate acceptance criteria - relationships such as resistance vs set curves, and/or correlated pile driving formulas. These relationships are premised on the interrelationship of capacity (C), transferred energy (E) and pile movement (M) which is represented primarily by pile set. These ECM relationships allow capacity to be inferred from measurement of transferred energy and pile movement and are used to infer the capacity of untested piles. However, for a variety of reasons, transferred energy can vary significantly between piles which, being undetected, undermines the reliability of ECM relationships. An alternative approach to using ECM relationships is proposed based on pile set and pile force (F). We demonstrate through parametric studies and review of project data, that these FCM relationships are reliable alternatives which bypass the problems with variable energy transfer. Of course, impact force will also vary with hammer performance, but impact force can generally be accurately determined from the measured impact velocity as a proxy. Pile velocity can be measured by attaching a single accelerometer to the pile, or by using a high frequency displacement monitoring device. FCM-based acceptance criteria have the significant advantage that both the necessary force (F) and displacement (M) inputs can be verified by simple measurements on all untested piles.

Keywords: Pile Testing, Pile Verification, Dynamic Formulae, PDA, Case Study

1 INTRODUCTION

The intent of this paper is to discuss an alternative approach to estimate the resistance of untested driven piles. The traditional methods of pile verification for these piles are almost universally based on Energy-Capacity-Movement relationships. Pile driving formulae are various forms of ECM relationship (Seidel, 2018, 2021). Without these relationships every pile would need to be tested.

An alternative Force-Capacity-Movement (FCM) approach has been developed which relates pile capacity to the pile head force generated by the driving hammer and to pile set. In application, this approach involves measuring pile impact velocity (as a proxy for pile impact force). In all but exceptional cases, pile-top force and pile velocity are related by pile impedance at the time of impact. The benefit of the FCM approach is that pile-top impact force can be inferred from simple measurements for each pile, whereas transferred energy (in ECM relationships) can only be assumed. The FCM approach is therefore intrinsically more reliable than traditional ECM approaches.

This paper will focus on demonstrating the nature of the relationship between pile head force and pile capacity using data generated from both a GRLWEAP (Goble et al., 1988) wave equation parametric study and also from actual piling data.

2 BACKGROUND

Deep foundations are constructed to transfer loads from a superstructure into the ground. There is an inherent uncertainty associated with the interaction between the piles and the ground in which they are installed or constructed. In order to reduce the risk of failure for these foundation elements, design methods take into account this uncertainty. In order to reduce this uncertainty, and benefit from higher capacity reduction factors, driven piles are tested during installation.

Pile testing is undertaken to confirm that the pile meets serviceability and geotechnical capacity requirements. Depending on the type of test, the structural integrity of the pile may also be assessed to ensure that the pile is intact and free of damage. Testing can further provide information on the performance of the driving system. In summary, testing is a quality control process which helps increase confidence that the test pile meets the design intent.

The uncertainty of a particular pile capacity evaluation is related to the intrinsic reliability of the test method used. However, the benefit of any test has indirect benefit to the evaluation of other similarly installed piles. Under AS2159-2009 the applicable geotechnical reduction factor (φg) for untested piles is determined from a risk assessment in conjunction with the proposed type of pile test and percentage of piles being tested. The so-called testing benefit factor increases with the percentage of piles tested.

Static pile testing is the traditional and direct method of pile testing where the movement of the pile is monitored and recorded as the pile is gradually loaded to the desired capacity. Due to practicality, time and cost implications of static pile testing, only a limited number of piles are usually tested (Rausche et al., 2008), which is not ideal for large projects, especially for sites with significant geological variability as there is a significant risk where test piles may not be representative.

The focus of this paper is on driven displacement piles which allow a wider range of testing opportunities, including high strain dynamic testing (commonly referred to as PDA testing). PDA testing has been used in Australia and New Zealand since the early 1980's. PDA testing has substantial cost and time advantages relative to static testing, and this allows more testing to be conducted for the same testing budget. PDA testing therefore allows statistically significant, and widely distributed testing to be conducted – a significant benefit compared to traditional static testing.

Typically, less than 15% of piles on a project are tested, leaving the remaining 85% of piles untested. The verification of the untested piles can be done in several ways. For example, by simply comparing installation data of untested piles to installation data of tested piles and ensuring that the untested piles have been driven to similar or harder conditions. In practice, dynamic formulae, such as the Hiley formula (Hiley, 1930) are often used for this verification. Hiley formula is recognised in AS2159-2009 and is also in the Auckland Structural Group Piling Specification (2002). However, academic debates from as early as 1941 (American Society of Civil Engineers, 1941) and to this date (Allin, 2015) continue to discuss the inaccuracies of the use of dynamic formulae. Allin recommends using wave equation analyses instead of generic dynamic formulae for the assessment of untested piles. Seidel (2015) proposes the use of site-specific dynamic formulae, which are to be calibrated based on test data, which has been further investigated with success (Damen & Denes 2017, Denes & Kroenert 2019). Nevertheless, the use of dynamic formulae in projects may lead to mis-guided results and inaccuracies and should be used with a correct understanding and informed approach.

Regardless of whether a dynamic formula, a modified dynamic formula or a wave equation analysis is used for comparison between tested and untested piles, the capacity of a pile is related to the applied energy (or hammer drop height) and the pile movement (or set). This is discussed further below in detail.

3 PILING RELATIONSHIPS – CURRENT PROCEDURE

There is a requirement for most driven piling projects to provide a driving (or installation) criterion prior to commencement of pile driving to ensure the required pile capacity is achieved. This is usually in the form of graphical correlation between pile capacity, applied hammer energy and measured permanent movement (set) from a single (or a specific number of) hammer stroke(s). This graphical representation is usually referred to as a bearing graph. Bearing graphs can be generated from either the traditional dynamic formula (e.g. Hiley) or Wave Equation Analysis Programs (e.g. GRLWEAP). Dynamic formula use simplified empirical relationships relating to energy transfer between two bodies. Wave Equation Analysis Programs simulate the driving sequence and estimate the energy applied to the pile considering a much wider range of factors including stiffness and dimension of the pile and striking weight, hammer and piling cushions, etc.

Once a bearing relationship has been developed for pre-piling, the first installed piles are tested to confirm the bearing relationship. The bearing graph may be further calibrated based on observed field results taken during end of initial drive or restrike testing. At the end of the test piling process, the aim is to use the pile test results to produce a relationship that reliably predicts resistance of the untested piles to the tested piles.

The result of Wave Equation analysis is a relationship between pile capacity and pile set, which is energy dependent – i.e. a form of ECM relationship. This is traditionally presented as one or more curves relating capacity to blow count (blows/metre) called a bearing graph, as shown in Figure 1.

The problem with this traditional form, is that at very low pile sets (high blow counts), blow counts become excessively high and the relationship below 1.0mm set (1000 blows/m) is difficult to evaluate. Therefore, in the following, the bearing graphs shown will relate capacity to set, as shown in Figure 2 which represents the same data shown in Figure 1.

3.1 Set and Hammer Energy Measurements

In order to use the bearing graph for pile capacity verification, measurements of the pile set and hammer energy are required. Different methods can be used to measure pile set, with various degrees of accuracy. The traditional method used to measure set involves a person (a) standing beside a pile and marking a piece of paper attached to the pile

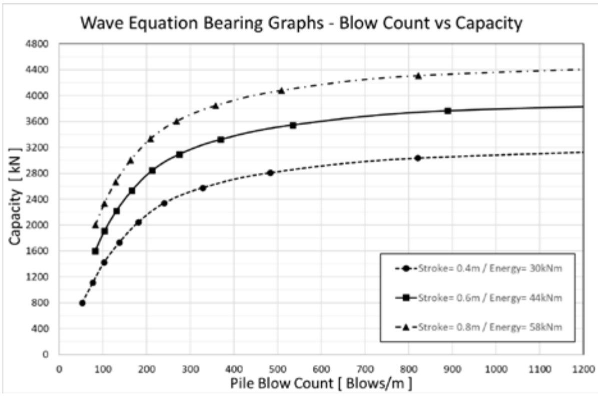

Figure 1. Bearing graph relationship – blow count

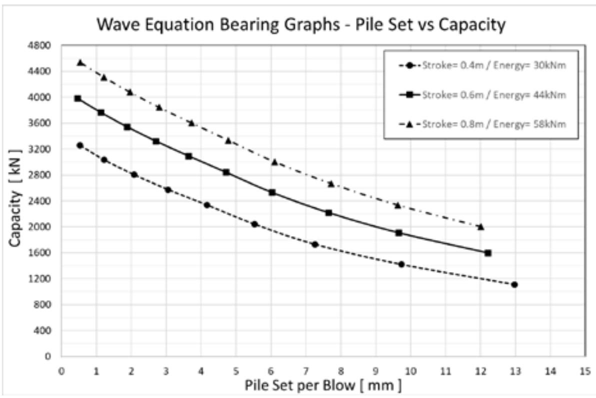

Figure 2. Bearing graph relationship – pile set

during each hammer strike. Due to safety concerns associated with standing and working beside a hammer, this method has mostly been replaced with one of the following methods: (b) monitoring using surveying equipment; (c) manually marking the pile prior and subsequent to the final 10 hammer blows; (d) onboard piling hammer instrumentation (such as the iPilier system by Junttan or NDT lazer & computer system); (e) counting the number of hammer strikes for the pile to move a certain distance (blow count); (f) non-contact high frequency displacement monitoring devices, such as the Pile Driving Monitor (PDM) which has sub-0.1mm accuracy.

It can be unreliable to rely on options (a) to (d), especially when pile set is small. Ideally, more focus towards set measurement using digital equipment should be embraced, as anything that involves manual pile marking and/or counting is likely to introduce an element of error.

Set is usually measured over a sequence of 10 blows. It is important that these blows be consistent so that the average set is meaningful. Any 'warm up' blows to reach the specified drop height should be discarded from consideration. In summary, set is a fundamental measurement used in all ECM relationships, so it is important that set measurement is reliable.

It is noted that temporary compression measurement is used in the Hiley Formula. This can only be measured using methods (a) and (f) above. Method (a) is not recommended for safety reasons, as discussed.

Hammer energy for an untested pile can be estimated from the potential energy of the ram which is a function of the weight and drop height. The drop height of a hammer is usually recorded for the full sequence of pile driving (referred to as pile driving record) which can be used to estimate the energy applied to the pile. The actual delivered energy to the top of the pile is often less than the potential energy of the ram due to frictional losses in the hammer, energy losses in the hammer and pile cushion, energy losses during impact, and restrictions on energy transfer that are functions of the pile material, cross-section, length and driving resistance. There have been several papers that document and emphasize the high variability in energy transfer from impact hammers and caution for the sensitivity of driving formulae and wave equation analyses to this parameter (Allin (2015), Seidel (2015b), Flynn & McCabe (2016)). Given the sensitivity of driving formulae to this parameter, a calibration using either measurements of actual energy in the test piles or an energy efficiency factor based on previous performance of the hammer is usually recommended for estimation of hammer energy. However, the performance of a hammer, including the efficiency, can vary from pile to pile and over time. Various factors such as hammer alignment, pile-hammer contact surface and hammer maintenance frequency can also affect the energy transferred to the pile which in turn affect the accuracy of the bearing graph correlation. Further to this, there can be errors in identifying the actual hammer drop if it is undertaken visually when the hammer is in operation.

Seidel (2015) has reported in one comprehensive study for a major project that the measured energy observed from PDA testing on the same pile type (and hammer) varied by +/- 33% about the median energy. The first author's experience has often seen variation in energy ranging between +/- 15 %. This demonstrates the uncertainty associated with estimation of the delivered energy to untested piles.

Using Seidel's observation, and assuming a 5mm set per blow, if we apply a +/- 33% variation to the 44 kNm energy example in Figure 2, the resistance acting on the pile can range between 2200 kN and 3050 kN which is an unacceptably large range.

4 AN ALTERNATIVE APPROACH - FORCE

As noted, an alternative approach to using the standard ECM relationship has been developed using the pile set and the force applied to the top of the pile. This FCM approach was first discussed and presented by Seidel (2018).

In simple terms, the general principle that applies to piling is similar to driving a nail into timber. For a nail to drive into timber, the force applied must overcome the force resisting the nail to move. If the nail does not move under the force of the hammer, one can assume that the force resisting the nail to movement is equal to or greater than the force from the hammer. On the other hand, if the nail moves, then resisting force is expected to be less than the force applied by the hammer. This is often seen with pile testing. If the pile movement is zero under a hammer strike, one can infer that the resistance acting on the pile is equal to or greater than the applied force.

Based on the principles of one-dimensional wave theory pile force and velocity are related by pile impedance for as long as there is only a single wave in the pile. Under those conditions, the following holds true.

$$F = vZ \qquad (1)$$

where F is the pile-top force, v is the pile-top velocity and Z is a constant of proportionality called the pile impedance, and

$$Z = EA/c \qquad (2)$$

where E is the pile modulus, A is the cross-sectional area, and c is the pile wave-speed.

During impact, and generally up to the time of maximum impact force and velocity, this proportionality between F and v can be reliably assumed. Therefore, knowing Z, the peak pile-top impact velocity can be used as a proxy for measurement of peak impact force.

it is important to distinguish between capacity and resistance in relation to pile driving. The resistance to penetration that the pile experiences when struck by the hammer is called the driving resistance. Driving resistance comprises a dynamic component due to the velocity of the pile movement, and a static component, which is the (static) capacity of the pile at the time of impact, and would be the expected capacity if it were possible to undertake an instantaneous static load test.

The parametric study and case studies described relate to the relationship between pile capacity, C, and peak impact force, F. The capacity/force (C/F) ratio is dependent on hammer, soil and pile characteristics, and is also shown to be a function of pile set, being maximum at low set, and progressively decreasing as pile set increases (and dynamic resistance represents a progressively larger proportion of the driving resistance).

Figures 1 and 2 presented the results of a GRLWEAP analysis for a 9t hammer hitting a 400mm square concrete pile from drop heights of 0.4m, 0.6m and 0.8m. The three curves in each Figure relate capacity to blow count or set for each of the three drops/ energies. The parametric study takes this one step further by normalizing the capacities by peak impact force.

The same data presented in Figures 1 and 2 is shown in Figure 3 in normalized form – i.e. the FCM relationship - C/F ratio vs set. What is striking is that all three curves reduce to a single and unique relationship between C/F ratio and set, regardless of drop height.

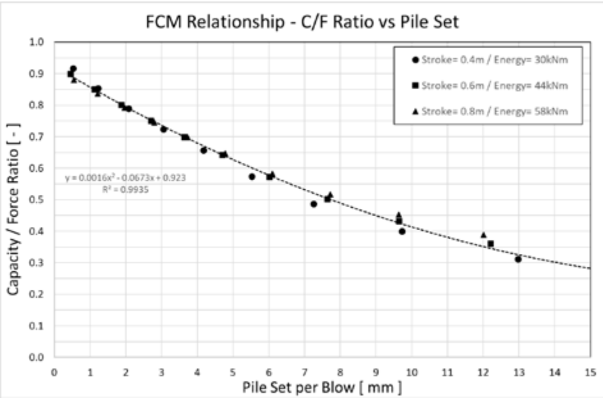

Figure 3. Normalized bearing graph (FCM relationship: C/F ratio vs pile set)

5 CASE STUDY CORRELATIONS

Two case studies will be presented for historical piling projects. PDA testing equipment from Pile Dynamics (PDA-PAX and 8G systems) were used to collect the pile force and velocity data. The data was analysed using CAPWAP to determine pile capacity.

In each case, the CAPWAP results were normalized using the PDA-measured peak impact force and the data presented as data points on a C/F ratio vs set plot.

The FCM relationship has also been computed using GRLWEAP based on the site hammer, pile and soil characteristics using representative resistance distribution, damping and quake values determined in the CAPWAP analyses.

5.1 Case Study One – Open Ended Steel Tube Piles

The project used for case study one is the upgrade of an existing berth. At this project the soil stratigraphy consisted of dense clayey sand and very stiff to hard sandy clay layers. All piles were open ended 610mm steel tubes with 16mm wall thickness each with a total length of 35m and an average penetration of 16m (ranging between 13m to 18m). The end of drive sets were between 5mm and 22mm using 1200mm drop height. The piles were driven with a 9t hammer. All piles were restrike tested between 4 to 18 days after installation using the same hammer with 1.5m drop height. The restrike sets ranged between 0.5mm and 10mm and estimated CAPWAP resistances varied between 3500kN to 6800kN. GRLWEAP analyses were undertaken replicating all relevant characteristics as noted above.

Figure 4 compares the C/F ratio vs set data from PDA tests and the FCM relationship from GRLWEAP analysis. At pile sets less than 1mm per blow, the inferred capacity is approximately equal (96%) to the peak impact force. At sets of 5mm, the achieved capacity is only 70% of the peak impact force; at 10mm the ratio reduces to 55% and at 15mm pile set the ratio drops further to 44%.

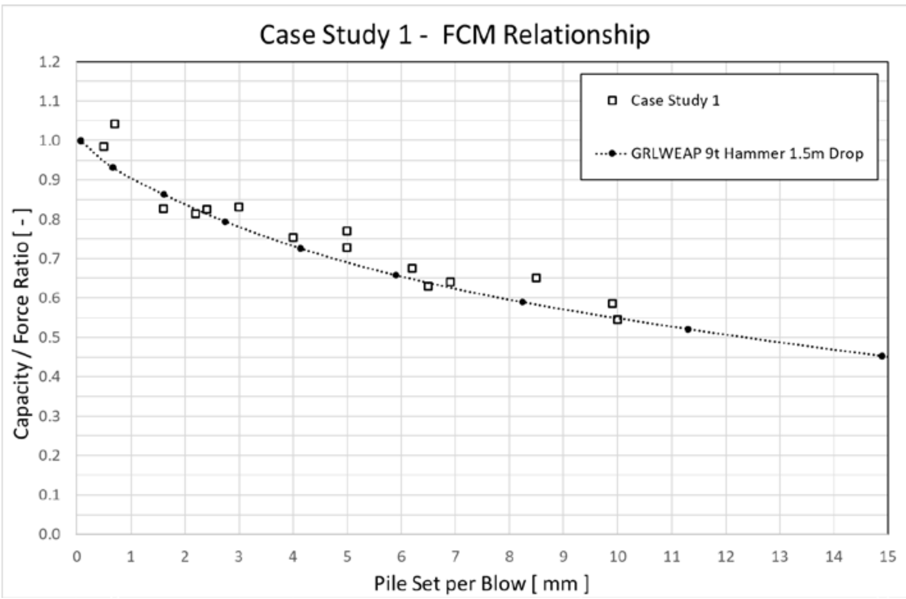

Figure 4. Case study 1 - data comparison to FCM relationship

It is clear that there is very good correlation between the site data and the theoretical prediction. There are two important findings relating to this case study.

1. If the GRLWEAP parameters can be reasonably estimated in advance, then the FCM relationship can be predicted, and initial target sets can be established in advance of piling.
2. The FCM approach offers a piling control and acceptance method which can accommodate large variations in hammer efficiency without impacting reliability. The capacity of all non-PDA tested piles, can be estimated with greatly improved accuracy provided that the set and pile velocity can be measured accurately.

5.2 Case Study Two – Precast Concrete

The project used for case study two is the construction of 13 bridge pier foundations for a river crossing. At this project the soil stratigraphy consisted of very stiff to hard sandy clay layers. All piles were 400mm square simply-reinforced precast concrete with total lengths ranging between 20m to 41m and penetration ranging between 18m to 36m. The end of drive sets were between 1mm and 13mm using 300mm to 500mm drop height. The piles were driven with a 9t hammer. All piles were restrike tested between 1 to 24 days after installation using the same hammer with drop heights between 400mm and 800mm. The restrike sets ranged between 0.3mm and 9mm and estimated CAPWAP resistances varied between 1100kN to 4500kN. Timber ply was used as a pile cushion for all tests.

For the GRLWEAP models, three different drop heights were used for assessment. The reason is related to the practicalities of driving precast piles where different drop height may need to be applied due to varying soil/ground conditions, controlling driving stresses (especially tension stresses) and/or different load requirements.

Figure 5 presents the correlation between the C/F ratio and pile set for PDA/ CAPWAP data compared to the GRLWEAP models with 3 different drop heights. Similar to Case 1, the correlation between the C/F ratio and pile set can be clearly seen from these results. It is also evident that GRLWEAP models can predict the correlation with reasonable accuracy if the necessary parameters for the GRLWEAP models are available.

Nevertheless, there is some increase in scatter evident which may result from minor PDA data issues (proportionality), accuracy of the manual set measurement especially at small sets or variable pile cushion stiffness.

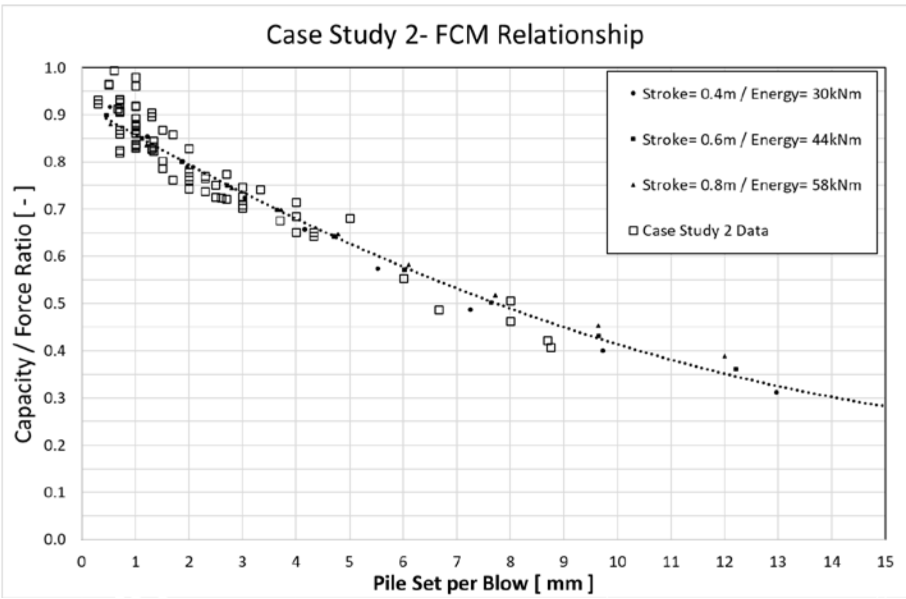

Figure 5. Case study 2 - data comparison to FCM relationship

The general form of the FCM relationship is similar for both Case 1 and Case 2, albeit with different specific values, and again, predictable by theoretical analysis using relevant analysis parameters.

For Case 2, at pile sets less than 1mm per blow, the inferred capacity is slightly less (92%) of the peak impact force. At sets of 5mm, the achieved capacity is only 63% of the peak impact force; at 10mm the ratio reduces to 42% and at 15mm pile set the ratio drops further to 29%.

The results also confirm that the use of different drop heights has little effect on the correlation between C/F ratio and measured set.

6 RECOMMENDED FCM RELATIONSHIP PROCEDURES FOR A PROJECT

The FCM relationship can be developed using the following method:

1A. Undertake a GRLWEAP analysis with estimated driving parameters from site investigation using proposed pile and driving hammer details.

1B. Undertake PDA testing and CAPWAP analysis on the first pile. Analysis to be undertaken at various different pile sets (e.g., 12mm, 6mm and 2mm).
2. Use data from either step 1A, 1B or both, to establish a site correlated FCM relationship.
3. Measure pile velocity and pile set for untested piles.
4. Estimate pile force using the measured velocity and calculated pile impedance
5. Use the site correlated FCM curve to find the C/F ratio for the measured set and then calculate resistance using the force estimated in step 4.

Ongoing pile testing with CAPWAP analysis should also be undertaken on a percentage of piles to check the relationship. Minor adjustments/refinement may be required as more data is collected.

7 FURTHER DISCUSSION

7.1 Measuring Velocity

There are only two known methods currently undertaken to measure the velocity during pile driving. The first is by using accelerometers recording the acceleration of the pile which can then be used to obtain the velocity.

Examples of equipment used are accelerometers from the PDA system (PDI / Allnamics).

The second is by measuring displacement and differentiating with respect to time to calculate velocity. An example is the Pile Driving Monitor (PDM). PDM is a device that records the displacement of the pile with high frequency and can therefore accurately measure pile set and pile velocity, and hence, can be further used to estimate pile resistance for all untested piles from a FCM relationship created from tested piles or GRLWEAP modelling.

7.2 Set Limitation

Similar to dynamic formulae, bearing graphs, PDA testing and CAPWAP analysis, the pile set that is recommended to be used for the FCM correlation has a range and should be between 2 mm and 12 mm. Sets outside this range may provide results that do not have the required level of accuracy.

Small sets (less than 2mm) can be a sign that the full resistance of the pile may have not been mobilized during driving which can lead to under-estimation of the static capacity.

Large sets (greater than 12mm) during driving can generate large dynamic component of resistance which may lead to over-estimation of the static capacity.

7.3 Pile Cushion

As discussed earlier, the calculated pile force is a function of pile impedance and velocity. Hence, the change in cushion stiffness does not affect the relation between velocity and force.

The importance of this is to note that although the pile cushion 'stiffness' does not affect the pile head force calculation but it may alter the relationship between the force applied and the pile resistance.

This will be further researched by the authors and presented at a later date.

However, the authors do note that there are cushions available in the market which claim to have a very consistent modulus or 'stiffness' form the start to the end of the cushion life. This may have significant benefits to a project as this will provide a higher level of confidence to the FCM relationship.

8 CONCLUSION

An alternative approach to pile verification using a force base relationship with respect to pile set has been generated using GRLWEAP. Two case studies on two very different pile types show very good correlation between the theoretical GRLWEAP results and the field results.

The determination of force and consequently capacity using pile velocity provides more confidence when untested piles are concerned. The use of this velocity correlation removes the reliance on hammer energy and the inaccuracies associated with estimating hammer energy which are the result of variable hammer performance from pile to pile and from time to time.
Recording pile velocity using readily available equipment is quick and easy, with some equipment able to record both the pile set and velocity. Pile set is an important aspect of this force base verification and an accurate measurement of set should always be a strict requirement.

The use of this force relationship for projects should follow the same process used for standard bearing graph relationships. That is to undertake a GRLWEAP analysis prior to piling works to establish an initial correlation. Then once the first pile(s) has(have) been PDA tested, refinement of the relationship is required for application to the remaining piles. Ongoing testing should also be undertaken to identify the need for further refinements as the project progresses.

REFERENCES

AS 2159-2009 (2009). Piling – Design and Installation. Standards Australia.
Allin, R., Likins, G. and Honeycutt, J. (2015) Pile driving formulas revisited. Proceedings of the International Foundations Congress and Equipment Expo 2015. San Antonio, Texas. Eds. M. Iskander et al.
American Society of Civil Engineers (1941) Pile driving formulas. Progress report of the committee on the bearing value of pile foundations. Proceedings of the American Society of Civil Engineers. Vol. 67, No. 5, pp853-866.
Damen, R. & Denes, D. (2017) Improving site specific modified driving formulae using high frequency displacement monitoring. Proc. 20th NZGS Geotechnical Symposium. Eds. GJ Alexander & CY Chin, Napier.
Denes, D. & Kroenert, B. (2019). A Case Study of Pile Testing and Verification. Berth 4 Upgrade - Port of Townsville. Australasian Coasts & Ports 2019 Conference – Hobart, 10-13 September 2019.
Flynn, K.N., McCabe, B.A. (2016) Energy Transfer Ratio of Hydraulic Pile Driving Hammers. Civil Engineering Research in Ireland (CERI 2016).
Goble, G. G., F. Rausche, and G. E. Likins. "GRLWEAP–Wave Equation Analysis of Pile Driving." (1988).
Hiley, A. (1930). Pile-driving calculations with notes on driving forces, and ground resistance. The Journal of the Institution of Structural Engineers. pp 246-259 (part 1, July) and pp278-288 (part 2, August)..
Pile Driving Monitor PDM. Website: https://www.foundationqa.com/pile-driving-monitor. Foundation QA (2019). Pile Driving Monitor, Because Every Pile Is Important, General Specifications. Melbourne, Australia.
Rausche, F., Nagy,M. and Likins, G. (2008). Mastering the Art of Pile Testing. Proc. of the 8th Int'l Conf. on the Application of Stresswave Theory to Piles. Lisbon. J.A.Santos (ed) : 19-32.
Seidel, J.P. (2015) Overview of the Role of Testing and Monitoring in the Verification of Driven Pile Foundations. Proceedings on the 12th Australia New Zealand Conference on Geomechanics (ANZ2015). Wellington. Ed. G. Ramsay. pp389-396.
Seidel, J.P. (2018) Mobilization of Pile Capacity and Pile Acceptance. Australian Geomechanics Society Victoria Meeting Presentation August 8, 2018.
Seidel, J.P. (2021) Ground truth, control and design of driven piles – implementing old ways with a new twist. Australian Geomechanics Society Victoria Seminar October 21, 2021.

SESSION 3

OPTIMIZATION OF RISK AND SAFETY IN DESIGN

Keynote address

Using geotechnical innovation to reduce project risk

Chris Lyons[1], Cameron Cairns[2]

[1]Principal Geotechnical Engineer, Suburban Rail Loop Authority, 80 Collins Street, Melbourne, 3001, Victoria, email: chris.lyons@srla.vic.gov.au
[2]Manager Minerals Geoscience, Geological Survey of Victoria, Level 17, 1 Spring St, Melbourne, Victoria 3000, email: Cameron.Cairns@ecodev.vic.gov.au

ABSTRACT

Project risk is commonly defined as an uncertain event or condition that, if it occurs, has a positive or negative effect on a project's objectives. As the construction industry continues to deliver larger and more complex projects, improving how we manage project risk is a key priority for clients, contractors and designers. Within this digital age, innovation and change in our industry will play a key part in how we manage risks and deliver projects. This paper considers how we can define 'innovation' and how innovation can be promoted within organisations and on projects. The classification of something as innovative can vary widely depending on its novelty and context. The journey from creativity (an idea) to a productive solution (innovation) is difficult and frequently does not materialise. Three examples of innovation are presented to highlight the range of productive solutions that can be considered as innovation within their context.

1. The development and benefits of public Geotechnical Databases; novel within the context of Victoria
2. Incremental innovation in the use of InSAR satellite monitoring.
3. Radical/modular innovation using automated processed to import piling construction records back into project models to validate QA and geotechnical ground models.

Keywords: Innovation, InSAR, Geo-database, piles, risk

1 DEFINING INNOVATION

There are many definitions and concepts around innovation. The definition of innovation varies according to the context and field of application such as organisational structure, customer service or technical fields. Across the many definitions and fields, two main dimensions of innovation can be considered (Edison, et al., 2013):

1. the degree of novelty (new to a firm, new to a market, new to the industry or new to the world), and
2. the kind of innovation (whether it is a process, product, or service system innovation)

Within this framework, innovation can take many forms and in particular, the degree of novelty means the technology systems which are well developed elsewhere, can still be considered as innovation providing there is a productive outcome.

1.1 Technical innovation

Within technical fields, a commonly adopted framework divides innovation into four types (Henderson & Kim, 1990):

- **Radical innovation:** Establishes a new dominant design and, hence, a new set of core design concepts embodied in components that are linked together in a new architecture (e.g., the establishment of Finite Element Modelling (FEM)).
- **Incremental innovation:** refines and extends an established design. Improvement occurs in individual components, but the underlying core design concepts, and the links between them, remain the same (e.g. improvement in viewing FEM results)
- **Architectural innovation:** innovation that changes only the relationships between them core design concepts (e.g. ability to import ground profiles into a FEM)
- **Modular Innovation:** innovation that changes only the core design concepts of a technology (e.g. improved algorithms for resolving FEM)

Each of these fields could have different kinds of innovation (process, product or service) noted above.

1.2 Creativity Vs Innovation

While creativity and innovation are related, they should not be confused as the same thing. Creativity is the ability to generate new ideas or plans, whereas innovation is the ability to apply the ideas in a productive manner. Early models of innovation (Utterback, 1971) considered three phases of innovation: 1) creative idea generation 2) turning the idea into reality (i.e., an invention) and 3) having an economic impact through implementation.

1.3 Delivering innovation

Successfully taking creativity and delivering it into innovation depends greatly on the environment within an organisation. A culture which both embraces innovation and has a process for delivering innovation is required. To successfully develop an innovation, first a specific need must be identified, macro and meso trends must be understood, competency must be developed (people and technology) and financial support provided. Goals and aligned actions must be defined, supported and tracked using metrics during development.

Once an innovation is developed, the lifecycle and impact on the market changes over time as the product is first established, then widely adopted, incrementally developed as it matures and eventually declines is usage (Figure 1). Businesses and industry which rely on innovation require a succession plan of innovation projects moving through the product lifecycle.

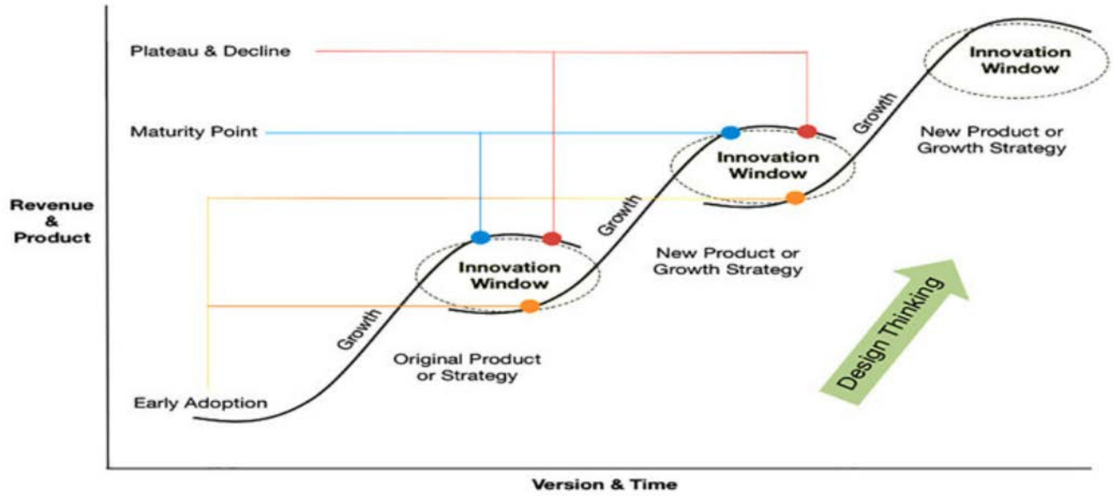

Figure 1. Innovation life cycle showing with succession planning within a market for continued high performance (Mazouz, et al., 2019).

1.4 Opportunities for Innovation

Within this digital age, the opportunities for innovation to revolutionise how we operate are emerging into all facets of our industry. Opportunities include;

- Automated processes ranging from simply eliminating repetitive activities, to scripting complex models to parametric design process.
- The evolution of Digital Twins connected to the Internet of Things (and conversely their Evil Twin, bloated with excess data) (Hannel, 2019).
- Machine Learning and Artificial Intelligence are changing our use of data and design processes.
- Robotics and drone automation as our construction sites become smarter, with autonomous trains, vehicles, and drone 'swarms'
- Virtual reality and augmented reality
- 3D printing
- Big Data, Blockchain and Cloud technologies supported by 5G and Wi-Fi 6 networks

For this paper, three examples of innovation have been selected to show different ranges of activities which could be defined as innovative. A key feature of all three are the degree of novelty, the kind of innovation (process, product, service) and the generation of productive outcomes.

1. The development and benefits of public Geotechnical Databases.

2. Incremental innovation approaches for the use of InSAR satellite monitoring.

3. Radical innovation in adopting construction monitoring data into digital models, akin to integrating the Internet of Things into construction. The Smart Piles platform presented is modular application of the broader concept, which is globally novel from a design and QA perspective

2 SHARED GEOTECHNICAL DATABASES

Innovation can be classified as the adoption of existing technology or system and applying them within a local market. Within the Melbourne market, there is a gap in the collation, management and delivery of geotechnical data that supports industry and maximises the return on public investment. Public geotechnical borehole databases, and associated geoscience datasets acquired as part of geotechnical investigations, are a relatively common structure in other States within Australia and globally, although the structure and sophistication of the databases vary. The Geological Survey of Victoria (GSV) is working with government partners to scope the development of a Victorian geotechnical database. The aim of the database is to augment existing free public resources delivered by the GSV such as GeoVic, the online mapping application that enables users to build their own maps, using an array of datasets, perform searches and access data, the GSV catalogue, and the Victorian Drill Core Library located in Werribee.

2.1 Benefits of public geotechnical databases

The following are the key benefits generally identified with public geotechnical data bases, many of which directly assit reducing project risk:

- The greater the availability of geotechnical information to inform design and construction, the more efficient and less wasteful design and construction can be. This logic would be shared by most geotechnical practitioners.
- Increased information and knowledge of wider geotechnical conditions mitigates the risk of project delays, cost over runs and environmental impacts.
- Databases present geotechnical logs and other information in a single accessible location and thereby reducing data management inefficiency, optimise site investigation planning and support scoping, early-stage design and feasibility stage geotechnical risk assessments.

Go to table of contents

- Reduce the cost of projects both by reduced investigations and less conservative designs with more informed geological (3D) modelling.
- Provide a cost-effective way of compiling and sharing information, opening opportunities for cumulative crowd sourcing from smaller, private projects, which reduces inefficiencies in retrieving achieved files and relying on historic knowledge of projects when planning investigations.
- The data lives on in the public domain following the end of the project and/or agency.
- Facilitate the research into geotechnical properties of materials, geological profiling, and education.
- The re-purposing of geotechnical investigation data from projects for other areas of public good geoscience, examples in greater Melbourne include improved understanding of sea level rise and fall and volcanic eruption frequency.

It is estimated the total site investigation saving for residential property from the Christchurch Geotechnical Database is in the order of $50-$100 million NZD (Scott, et al., 2015). This excludes savings in infrastructure and commercial development project and qualitative benefits such as the improved confidence in project risk and more efficient delivery.

2.2 Geotechnical database examples

A of review of relevant geotechnical data bases is summarised, demonstrating the recognised benefit to the construction industry:

- In the 1970's the Urban Geotechnical Automated Information System (UGAIS) was developed in Canada, funding the creation of geotechnical databases for 27 cities involving records from over 110,000 boreholes. While several of the data bases are no longer in use, many still are. The Ontario databases includes data from over 90,000 boreholes and in 2015 was accessed on average almost twelve times every workday (Thompson, 2016).
- The British National Geotechnical Properties Database was launched by the British Geological Survey (BGS) in 1992. The database includes over 100,000 boreholes and the web viewer portal is accessed over 60,000 times a month (Thompson, 2016).
- The Perth, Australia Central Business District (CBD) database was created in 2004 with 649 boreholes from the 1970's.
- The Canterbury Geotechnical Database (CGD) was created to generate efficiencies in sharing geotechnical information following the earthquakes of 2010 and 2011 around Christchurch. In addition to hosting over 26,000 borehole and CPT records, it also includes regional assessments and maps of liquefaction susceptibility. The CDG assisted with the design and construction of residential, commercial and infrastructure rebuilds, as well as city planning and enabling the insurance industry to understand and manage development risks. In 2016 the New Zealand Ministry of Business and Innovation launched the New Zealand Geotechnical Database (NZGD), which combined the CGD with other regional databases. The NZGD has over 130,000 data points and is used by over 6,000 users.
- The Queensland Geotechnical Database (QGD) was launched in 2017 with a view to consolidate primarily tax and toll payer subsidised exploratory investigations. The database holds over 1,600 geotechnical investigation records.
- The NSW government is currently working on the Government Geotechnical Repot Database Project (GGRD) to collate geotechnical investigation records.
- Progressive European nations have recognised the value and importance of geoscience (geotechnical investigation) data and knowledge (urban geology models) in infrastructure planning and development for sustainable cities. Sub-Urban group compiles data and models from multiple European Geological Surveys, Cities and Researchers (including international partners) http://sub-urban.squarespace.com/

2.3 Development of a Victorian geotechnical database

There have been recent changes to Victoria's public construction guidance. When procuring services for geotechnical investigations, or Works or Services that may require geotechnical investigations, Agencies must ensure that their contracts provide for the ownership and custody of geoscience data collected for the project to be transferred to the State of Victoria, where:

- 'geoscience data' includes geological, geotechnical and environmental information, reports, maps, images, recordings, survey results and drill core, drill cutting and associated materials embodied in any form; and
- 'geoscience data collected for the project' includes geoscience data generated, placed, stored, processed, retrieved, printed, accessed, or produced using data supplied by the Principal, for the purpose of the contract.

Within Victoria, the GSV is in the process of scoping the compilation and public delivery of all geotechnical investigation physical (i.e. drill core) and digital geoscience data acquired as part of geotechnical investigations undertaken as part of State of Victoria infrastructure projects.

The GSV are working through agreements with current major projects and stakeholders on the transfer and release of geotechnical data. The Suburban Rail Authority Loop Authority (SRLA) is coordinating with GSV to provide data from 560+ geotechnical investigations already completed for Stage One of the project. Discussions are ongoing for the provision of construction stage face mapping and geological records to supplement the project investigation data.

3 DEVELOPMENT OF INSAR MONITORING

Interferometric Synthetic Aperture Radar (InSAR) is a radical, innovative satellite-based ground movement monitoring system that is increasing become commonly place on major infrastructure projects and forensic studies. It significantly enhances and complements traditional survey monitoring approaches.

Satellite based InSAR has been applied across a range of major infrastructure, mining, forensic and geohazard assessment projects. Within the sphere of metro rail tunnel projects, InSAR came to prominence in Europe slightly over 10 years ago on multiple projects (Crossrail in London, Paris Metro Line 4, Barcelona Metro, Warsaw Metro). Within the Victorian context it was adopted on the Metro Tunnel Project in Melbourne and has been procured by the Suburban Rail Loop project to baseline and understand existing historic ground movements.

InSAR measures ground movements by comparing two or more Synthetic Aperture Radar (SAR) images of an area to identify surface movements over time (refer Figure 1). InSAR enables ground movements to be monitored over spatially extensive areas to a high level of accuracy (typically 1-3mm). Radically innovative technology considering the data comes from satellite hundreds of kilometres above the earth. Benefits of InSAR include:

- Extensive spatial coverage which is suitable for assessing regional ground movement trends.
- Can assess seasonal shrink/swell effects, thermal effects (e.g., bridges) existing consolidation and/or groundwater related settlement.
- Satellites have been collecting and storing data over most urban centres in Australia for more than seven years, enabling historic data to be processed from time periods prior to project commencement and assist with establishing baseline ground movements; and
- Monitoring can cover sensitive urban areas and structures, mitigating the need for access (e.g., rail corridors) and approval (e.g., heritage structures).

Limitations with InSAR include:

- Satellites typically collect data every 7-14 days and, therefore, more conventional automated systems are required to assess movements during construction. Additionally, data requires processing, which is typically undertaken in batches of 3-to-6-month intervals.
- The location of monitoring points cannot generally be controlled. The processing requires consistent backscattering to develop a reliable data point for processing (such as kerbs, outcrops, or structures) and may not be reliable over vegetated areas. On Crossrail the X-band data generated one monitoring point approximately every 40m2 (Garcia, et al., 2016); and
- "Unwrapping" errors if rapid ground movements occur between satellite passes. Where large settlement (i.e. <10mm) occurs between satellite passes the comparison of SAR images can assess the data as heave instead of settlement. Unwrapping errors in data can be easily re-calibrated with manual settlement monitoring if required.

While InSAR can't replace automated systems, it can successfully complement them, providing historical ground movements, assessing regional settlement/heave, reduce the extent of conventional monitoring and provide cost effective long-term monitoring. On the Crossrail project the procurement and data management of InSAR was in the order of a magnitude cheaper than maintenance and data management of automated data monitoring (Gonzalez, et al., 2017).

InSAR's massive spatial coverage, high accuracy, regular readings, and ability to model historical movements make it a radically innovative approach to surveying.

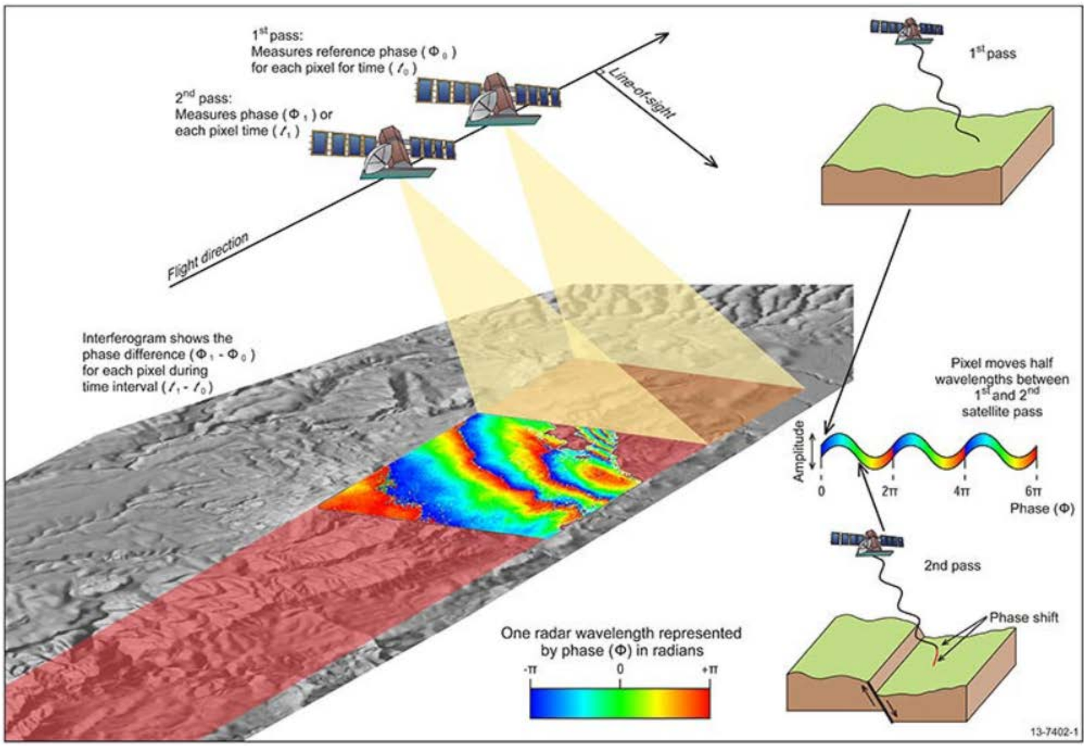

Figure 2. Two SAR images of the same area are acquired at separate time intervals and the phase shift in the reflected wavelength is used to assess the differential movement (Geoscience Australia, 2021)

3.1 InSAR incremental innovation

Incremental innovative improvement of InSAR is ongoing to expand its use and application. Two examples are provided.

3.1.1 Artificial Reflectors to monitor areas of low coverage

The Suburban Rail Loop Project is collating historic InSAR data to baseline existing ground movements and identify areas of existing ground movement risk. Part of the project includes the construction of stabling yards over areas which have a history as former mixed landfill sites (Suburban Rail Loop, 2021). It could be reasonably expected that historic landfills have an ongoing settlement risk. These areas would be a perfect application for InSAR monitoring, however there is very poor spatial coverage due to the vegetated nature of the area and ongoing site activities.

Suburban Rail Loop Authority, working with our technical advisors and Sixense Oceania have established a series of InSAR artificial reflectors over the site (Figures 3 and Figure 4). The reflectors generate a strong and reliable image which can be readily recognised in SAR data. The adoption of artificial reflectors grassed areas overcoming one of the traditional limitations of InSAR and facilitates accurate, frequent and access free monitoring at a significantly cheaper cost compared with traditional survey approaches.

Figure 3. InSAR reflector installed at the SRL stabling yards (courtesy of Sixence Oceania).

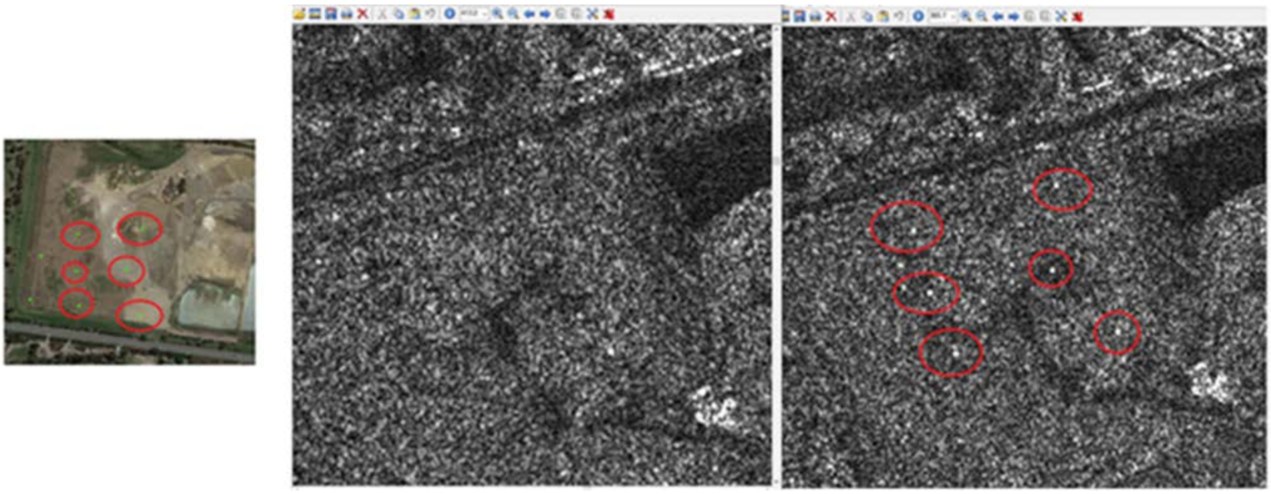

Figure 4. InSAR reflectors installations being picked up clearly within a grassed area (before and after images courtesy of Sixense Oceania).

3.1.2 Commercialisation of space

The miniaturisation of satellites combined with the increasing availability and affordability of commercial space payloads has significantly reduced the cost of launching satellites. Subsequently the number of commercial satellites orbiting the earth is quickly increasing, enabling incremental innovation in the use of InSAR monitoring.

Within the context of InSAR, the increased number of satellites relates to an increased frequency of readings. Currently InSAR reading using a single satellite are typically recorded on a two-week frequency (8-14 days), which is one of limitations compared with traditional survey approaches. However, commercial organisation such as Capella Space are rapidly launching additional satellites and within three years, by using readings from multiple satellites the monitoring frequency may reduce to daily, or even multiple times per day. Subject to the InSAR image overlay and batching process becoming more automated, this increased frequency has the potential to significantly alter how InSAR monitoring integrates with traditional monitoring approaches. This higher frequency of monitoring has the potential to move InSAR through a subsequent cycle of innovative growth.

Within a broader industry context, the commercialisation of space with increased frequency and higher resolution of satellite imagery may have large impacts in fields such as coastal engineering, hydrology and tracking construction progress, particularly when combined with advanced in artificial intelligence and data-driven models.

4 CONSTRUCTION DATA TO DIGIAL DATA

While advances are being made in developing existing asset data and designs into digital models and digital twins, to complete the data cycle we need to look at integrating construction data directly back into our models. Currently construction data collection and automation are typically targeted around increased productive to reduce construction costs and programme. One of our next steps as an industry must be integrating these digital systems directly into our digital design models to validate geotechnical models, improve quality control systems, manage geotechnical risks and provide efficiencies in automated development of as-built records.

Collection and use of data from sensors, aka the Internet of Things (IoT), is already rapidly occurring within other industries such as healthcare, manufacturing, agriculture and energy. The construction industry is not as advanced, but the use of automation and machine learning processes are advancing rapidly. The industry already has many established systems ranging from data collation on automated monitoring platforms, robotics in construction (e.g. drilling for tunnel ferrules), autonomous mining trucks, UAV surveys, tracking materials/supplies and GPS positioning of plant.

Adopting IoT construction solutions has the potential to improve workplace safety (e.g. wearable IoT devices, fall detection apps), resources management, reporting and maintenance, reduce insurance premiums, mitigate wastage and theft. However, the industry also faces challenges including employee privacy, data security, cost vs benefit and collection of all data vs useful data. For the time being it is likely that advances in IoT construction solutions will come from large building and infrastructure projects where the benefit will outweigh the effort to implement new systems.

4.1 Smart piles

Smart Piles is an innovative product which has been developed by Arup as a tool for collating and using data from piling rigs. The tool collects site data from piling rigs to visualise progress, undertake quality checks and integrate construction record data back into project geotechnical models. Research within Arup has played a fundamental role in identifying and leveraging business opportunities, with a structured, global approach to research engaging over 1,900 staff across 500 research projects annually (Arup, 2021).

Most modern piling rigs have sensors which record data with depth for piling, soil mixing and ground improvement activities. Examples of data types include penetration depth, inclination, drilling torque, rate of progress and concrete pressure (see example in Figure 1). Traditionally these records are provided as hard copy PDFs for a review of quality (embedment depth, grout pressure etc) or as a record of construction. However, this digital information can also be uploaded to a cloud-based server relatively easily akin to an Internet of Things (IoT) approach, opening various avenues of digital manipulation.

Within the construction industry, many operators have already similar approaches to extract digital piling rig data to provide insights into construction productivity and quantities. Smart Piles takes the same data and uses automated processes to provide:

1. Automated quality control reviews.
2. Verification and development of project geological models,
3. Interrogation of data during construction and visualisation of piling data into BIM as-built models.

4.2 Quality control reviews

Quality reviews of piling records by designers are typically complete at the end of the project or when zones of the work are completed. Designers normally check grout pressure and embedment depths to confirm that the as-built records meet the design requirements. Smart Piles uses automated processes to review piling construction records to verify the quality of each pile as it is constructed to provide early warning of construction issues (Figure 5). The system effectively completes all necessary QA checks, reducing input from engineers reviewing logs and providing confidence in the works.

4.3 Verification of project design models

Manual reviews of piling records will often look at changes in drilling penetration/torque to help validate ground models and design assumptions. This is particularly important in lateral loading designs including lateral spreading associated with liquefaction, where the depth to a firm layer is a key design assumption. On sites with variable geological profiles, pile layouts may change across the site according to changes in subsurface profiles.

Smart Piles uses automated process to review logs during construction, enabling changes in construction conditions to be assessed immediately once pile records are completed and integrated back into the geological models. This is a more proactive approach to identifying ground changes and managing ground risks, particularly on complex sites.

4.4 Interrogation of digital pile data

Once pile data is available in a digital format, it opens new opportunities for construction reviews. Within the piling industry some organisations are using digital piling records to review construction programmes and assess the rate of piling productivities.

Smart Piles can take the automated quality control and design verification process and integrate them spatially into digital models. This enables the automated quality and design verification processes and checks to visually communicated across the site, enabling both issues to be address early in the construction process and opportunities for refinement to be identified early enough so that they can have a material impact on the works.

Smart Piles also enables digital as-built models of the piling works to be produced in an automated manner, providing cost savings and improved quality to produce LoD 500 BIM models.

Smart Piles is a step towards closing the gap from ‘design’ to ‘as-built’, using modern digital technologies in an automated and innovative way.

Go to table of contents

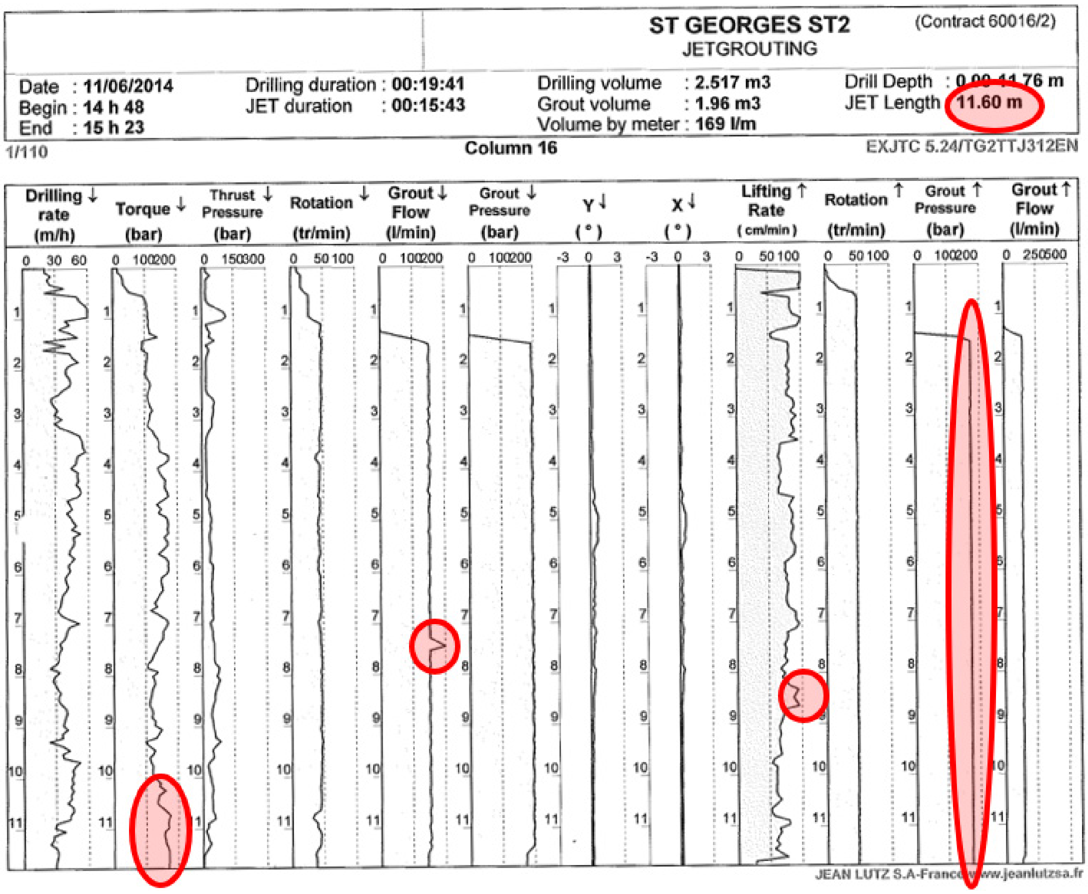

Figure 5. Example of a piling rig installation records where checks can be completed on consistency or variations in the data.

5 MANAGING PROJECT RISK THROUGH INNOVATION

Project risk is commonly defined as an uncertain event of condition that, if it occurs, has a positive or negative effect on a projects objectives. As the construction industry continues to deliver larger and more complex projects, improving how we manage project risk is a key priority for clients, contractors, and designers. Introducing ideas, practices or object that are new (aka innovation) are a central component to improving how we manage project risk.

The three examples presented show different ways in which innovation will continue to shape our industry within Victoria ranging from adopting established systems, implementing emerging technology and looking forward to the development of future tools and processes. The innovations described all improve our knowledge on project and reduce the potential for errors and uncertainty, effectively assisting us in reducing project risk. Added benefits of innovation also generally include program and cost savings.

However, experience shows that the process of taking creative ideas, developing them into reality and then successfully implementing within the industry is difficult, requiring focus and effort. The journey from creativity (an idea) to a productive solution (innovation) is difficult and frequently does not materialise. Typically of the small number of innovations which do emerge, very few make a significant impact on our industry. To continue to support innovation we need to establish a culture of embracing innovation and processes to support innovation though its lifecycle.

6 CONCLUSIONS

There is a range of ways in which innovation can be implemented to reduce project risk. In defining innovation, the degree of novelty is an important concept, ie adopting an established system which is new to its local context can still be considered innovative. Similarly, we can differential between radical and progressive innovation as we progress through a products lifecycle.

Three examples of innovation have been presented to highlight the range of ways innovation can be applied on projects. 1) The development of public geotechnical databases within Victoria is an adoption of an established structure as a novel tool into an existing market. 2) InSAR satellite monitoring is an established radical innovation for ground movement monitoring which becoming increasing adopted on projects. Innovation with InSAR technology is being incrementally developed with the potential for a subsequent significant growth cycle. 3) Emerging innovation using data-driven automated systems to integrate construction data into digital models using tools such as Smart Piles. These innovations improve our understand of project hazards, reduce uncertainty, and subsequently enable us to manage and reduce project risks through planning, design and delivery stages.

Within this digital age, innovation will continue to play a key part in how we manage risks and deliver projects. The journey from creativity (an idea) to a productive solution (innovation) is difficult and frequently does not materialise. Successful continued delivery of innovation within organisation and the industry requires a culture of embracing innovation and a commitment to processes to deliver innovation.

REFERENCES

Arup, 2021. Research at Arup. [Online]
Available at: https://research.arup.com/
Edison, H., Ali, N. & Torkar, R., 2013. Towards innovation measurement in the software industry. Journal of Systems and Software, pp. 1390-1407.
Garcia, J. R., Black, M. & Gomar, B. S., 2016. Correlation Study Between In-Situ Auscultation and Satellite Interferometry for the Assessment of Nonlinear Ground Motion on Crossrail London. [Online]
Available at: https://learninglegacy.crossrail.co.uk/documents/correlation-study-situ-auscultation-satellite-interferometry-assessment-nonlinear-ground-motion-crossrail-london/
Geoscience Australia, 2021. Interferometric Synthetic Aperture Radar. [Online]
Available at: http://www.ga.gov.au/scientific-topics/positioning-navigation/geodesy/geodetic-techniques/interferometric-synthetic-aperture-radar
Gonzalez, J. M., Nevard, S. & Sanchez, J., 2017. The Use of InSAR (Interferometric synthetic aperture radar) to complement control of construction and protect third party assets. [Online]
Available at: https://learninglegacy.crossrail.co.uk/documents/use-insar-interferometric-synthetic-aperture-radar-complement-control-construction-protect-third-party-assets/
Hannel, A., 2019. The Evil Digital Twin. [Online]
Available at: https://hannellbim.com/2019/08/07/the-evil-digital-twin/
Henderson, R. M. & Kim, C. B., 1990. Architectural Innovaion: The Reconfiguration of Existign Product Technologies and the Failure of Established Firms. Administrative Science Quarterly, pp. 9-30.
Schumpter, J., 1983. The Theory of economic development: an inquiry inot profits, capital, credit, interest and the business cycle. New Brunswick, New Jersey: Transaction Publishers.
Scott, J. W., Stannard, M., Van Ballegooy, S. & Lacrosse, V., 2015. The benefits of a shared geotechnical database in the recovery of Christchurch following the 2010 - 2011 Canterbury earthquakes and the potential benefits of expanding it into a national database. Wellington, Australian Geomechanics Society .
Suburban Rail Loop, 2021. Stage One train stabling. [Online]
Available at: https://suburbanrailloop.vic.gov.au/Planning/Stage-One-train-stabling
Tarde, G., 1903. The laws of imitation. New York: H. Holt & Co.
Thompson, T., 2016. A 2016 case for public geotechncail databases. Gold Coast, Queensland, Australia, Australian Geomechanics Society, pp. 1045-1050.
Utterback, J., 1971. The Process of Technoiological Innovation Within the Firm. Academy of Management Journal, pp. Vol 14, pp78.

Design methodology and input parameters applicable to foundation design for large complex towers

Y.Y. Tay[1], BEng (Hons), PhD, CEng, FICE, FIEAust, CPEng; A. K. C. Smith[2], MA, PhD, MBA, CEng, FICE, CGeol, FGS; and C. Haberfield[3] BSc, BE (Hons), PhD, FIEAust, CPEng, RPEQ

[1, 3] Golder Associates Member of WSP, Building 7, Botanicca Corporate Park, 570-588 Swan Street, Richmond, Victoria 3121, Australia; email: ytay@golder.com.au, chaberfield@golder.com.au
[2] Coffey Geotechnics Ltd., Gardner House, Hornbeam Park Avenue, Harrogate, UK, HG5 8NA, email andrew.smith@coffey.com

ABSTRACT

As buildings are progressively getting taller, traditional methods of design that generally relied on considerations of the vertical load-carrying capacity of the foundation system, assessed by empirical methods and a lumped factor of safety, have been largely replaced by serviceability-based methods of design which typically result in an optimised foundation design. Serviceability-based designs typically rely on powerful commercial software packages to enable advanced numerical analysis of foundation systems. This paper briefly discusses case studies of foundation design processes including soil-structure interaction analyses adopted for the serviceability design of tall towers. In order to obtain accurate building movement prediction from complex computer analysis, it is imperative that materials and ground stiffness properties be accurately characterised and measured. This paper presents ground stiffness properties measured from various types of tests at different strain levels (i.e., geophysical testing, pile load tests, pressuremeter and laboratory tests) that have been adopted as input parameters in the numerical analyses. The higher allowable shaft friction values from serviceability analysis compared to those from traditional methods, are further justified on the basis of bi-directional static pile testing.

Keywords: serviceability-based design, ground stiffness, mobilised pile skin friction

1 INTRODUCTION

Serviceability-based methods of design are based on the performance and movements of building foundations rather than strength that renders the building unusable. Therefore, it is imperative that ground stiffness properties are accurately measured and appropriately adopted for foundation design. This paper presents the tests carried out in-situ and in laboratories for ground stiffness measurements of weak carbonated rock in Dubai, such as unconfined compressive strength tests with stiffness measurements, pressuremeter, geophysical and bi-directional static pile load tests. It attempts to address the strain levels at which the different tests were undertaken, amongst other variables, and therefore producing different measured stiffness range. These test strain levels were also compared to levels determined from numerical analysis of pile group foundations of tall towers when axially loaded.

2 SUBSURFACE CONDITIONS

Bedrock across the emirates of Dubai for engineering purposes is the Barzaman Formation Miocene Age rocks overlain by the more recent Quaternary Age Ghayathi Formations. The ground conditions discussed herein underlie four plots at a master development in Dubai, typically comprising superficial deposits, overlying weak calcarenite/ sandstone (Ghayathi Fm), followed by calcisiltite/ siltstone and conglomerate (Barzaman Fm). Only rock properties are discussed in this paper.

The carbonated rocks are typically weak with unconfined compressive strength (q_c) between 1.5 MPa and 4 MPa as shown in Figure 1. There is little increase in strength with depth, and no discernable difference in strength between calcarenite and calcisiltite layers (interface at around RL -25 m Dubai Municipality Datum, DMD). This was likely the result of unconfined compressive strength (UCS) tests performed without confinement and the swelling tendency of calcisiltite/ siltstone when extruded from ground at depth.

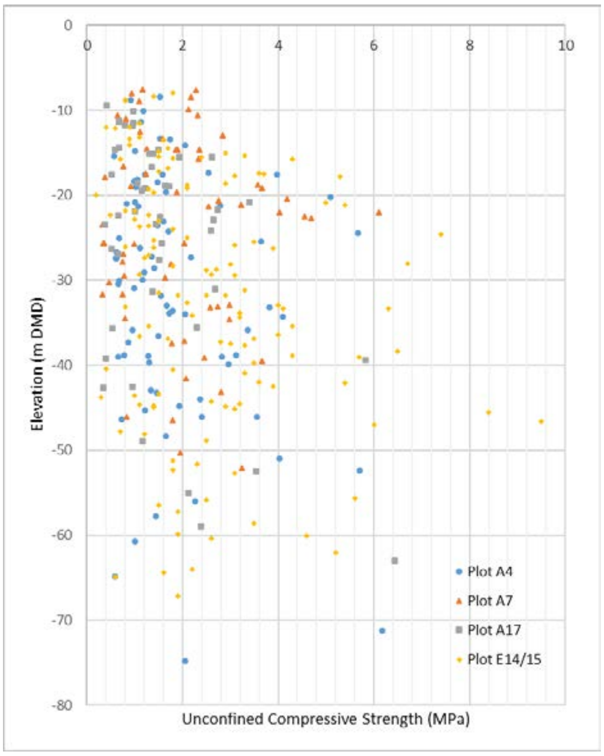

Figure 1. q_c vs depth at Plot A4, A7, A17, E14/15

3 LABORATORY AND IN-SITU TESTING

3.1 Ground stiffness measurements

In the laboratory, E_{LAB} was determined from the displacement of rock samples in UCS tests. Similar to the

Go to table of contents

q_c profile with depth, E_{LAB} values of the four plots tend not to increase significantly with depth (Figure 2).

In-situ Young's modulus (E_{PMT-H}) was measured by pressuremeter tests with unload reload cycles. The subscript "H" used here refers to measurements taken in the horizontal direction. Unload-reload $E_{PMT-H-ur}$ values from pressuremeter tests were about 4 times higher than the initial $E_{PMT-H-ini}$ (Figure 2), the main reason being that the latter was an elasto-plastic measurement where part of the expansion was irrecoverable.

Intuitively, E_{PMT-H} from pressuremeter tests which test a larger rock mass compared to intact rock samples tested in laboratory, should be smaller than E_{LAB} because of the scaling effect and the fact that the bigger rock mass is likely to consist of more imperfections, noting rock mass in Dubai do not have much fractures. However, Figure 2 shows initial $E_{PMT-H-ini}$ to be around 2.5 times higher than E_{LAB} and unload-reload $E_{PMT-H-ur}$ to be around 9 times higher than E_{LAB}. In addition, E_{PMT-H} increases with depth and the difference between E_{LAB} and E_{PMT-H} is more pronounced at depth. It is likely that E_{LAB} measurements were underestimated as a result of the lack of confinement in UCS testing and that the calcisiltite samples extruded from deeper depths were disturbed as they swelled. Other explanations of the difference between E_{LAB} and E_{PMT-H}, aside from the above and scaling effects are likely anisotropy of rock and test strain levels discussed in the following sections.

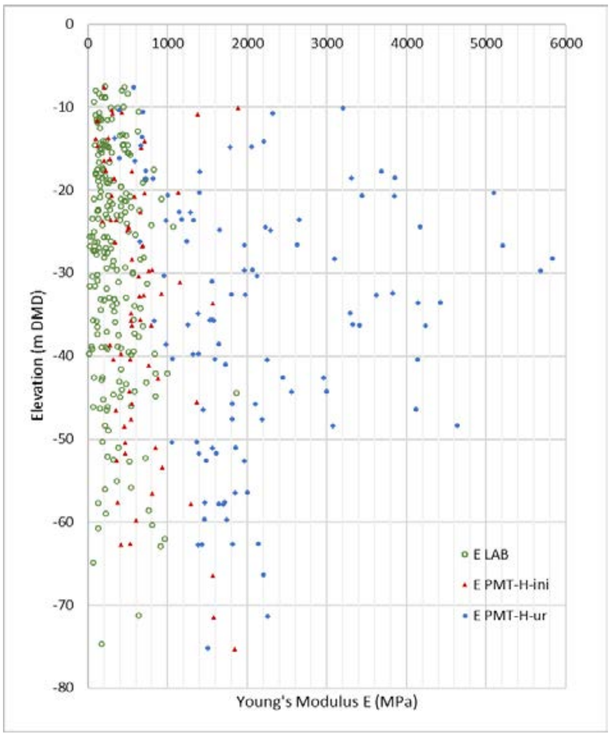

Figure 2. E_{LAB} and E_{PMT} vs depth

3.2 Correction for anisotropy

The rock mass in pressuremeter tests is loaded in the horizontal plane, and the tests give horizontal shear stiffness (G_{HH}). Whilst this may be directly applicable to the analysis of radial compression or pile lateral movement assessment, it may not be applicable for axially loaded piles where the piles and rock are deformed in the vertical plane. In the absence of direct measurements of G_{HH} and vertical shear stiffness (G_{VH}) measured from geophysical testing for anisotropy assessment, G_{HH} from pressuremeter presented in the following sections have been corrected to G_{VH} assuming anisotropy is due to the differences in normal stress acting in different directions. Therefore, stiffness in any direction is a function of K_0 as shown by the following equations from first principles:

$$G_{HH} = E_H / [2(1+\nu_{HH})] \quad (1)$$

For undrained expansion,

$$\nu_{HH} = 1 - K_0 / 2 \quad (2)$$

where $K_0 = E_H / E_V$ (3)

E_{PMT-V} is conservatively assumed to be E_{PMT-H} / 2 in this paper, as K_0 measured from pressuremeter tests was greater than 1.5. Correction of anisotropy of rock may partly explain higher E_{PMT-H} compared to E_{LAB}.

3.3 Stiffness and strain relationship

Cavity strain measured from the expansion of borehole in pressuremeter tests was converted to shear strain. Shear strain is the constant area ratio as shown in Figure 3, therefore shear strain of the pressuremeter tests is determined from (4) below:

$$\text{Shear strain} = 1 - [\, 1/ (1+\varepsilon_c)^2 \,], \quad (4)$$

where ε_c is the cavity strain.

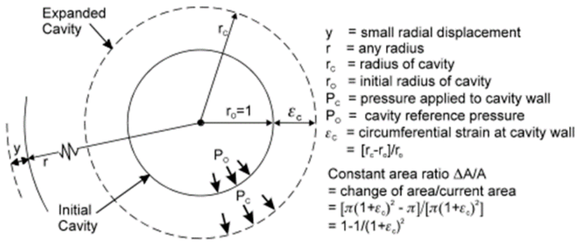

Figure 3. Pressure and straining around an expanding cavity

Figure 4 shows initial and unload-reload E_{PMT-V}, corrected for anisotropy, versus shear strain. The figure also shows combined in-situ and laboratory E measurements (i.e. E_{PMT-V}, E_{DYN} from geophysical downhole and crosshole testing and E_{LAB}) of the four plots versus their respective shear strain levels. As E values are generally consistent at strain levels less than 0.001%, maximum and minimum E_{DYN} measured was plotted at 0.001% strain in Figure 4. The shear strain of E_{LAB} has been assumed to be the strain at 50% peak stress.

From Figure 4, E values increase with decreasing shear strain which partly explains higher $E_{PMT-V-ur}$ than $E_{PMT-V-ini}$ and E_{LAB}.

4 BI-DIRECTIONAL PILE LOAD TESTS

Large scale bidirectional static load tests to failure, using Osterberg cell (O-cell), were carried out at the four plots for the assessment of pile-settlement behaviour and pile ultimate skin friction. Osterberg cell tests are increasing in popularity in Dubai. They eliminate many of the safety risks of static load tests using kentledge or tension piles. They also have the significant advantage of enabling test piles to be short enough such that full mobilisation of skin friction between the piles and ground (i.e. failure) can be achieved. The full range of the anticipated pile depths can be tested by the simple expedient of having O-cells at different depths.

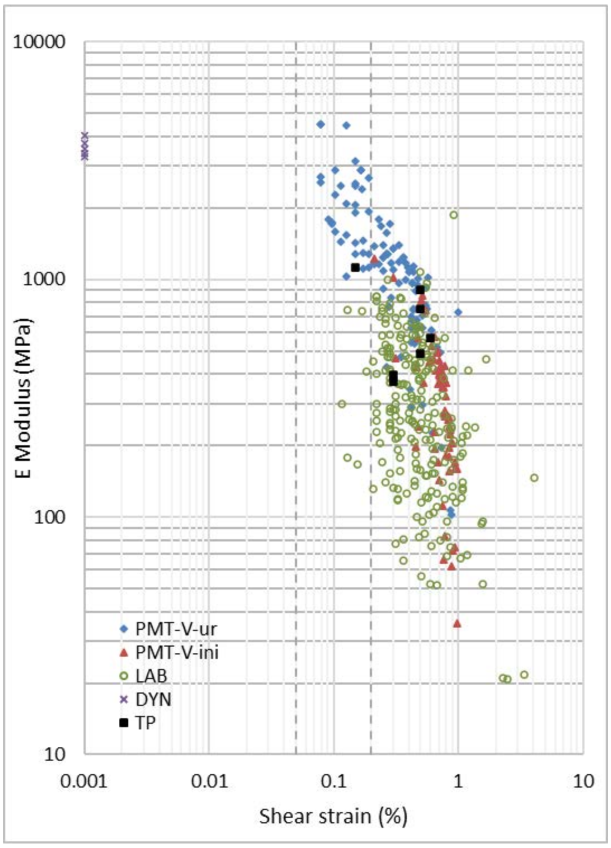

Figure 4. E Modulus versus shear strain

Each test pile carried out comprised an upper and lower segment. The segments were generally 5 to 10 m long. The test pile segments were embedded within selected depths of the rock based on strata and rock strength profiles, covering the anticipated pile depths between RL -10 m and -30 m DMD.

The test pile diameters were 1.2m at Plots A7 and A17; and 1.5m at Plots A4 and E14/15 and maximum test loads applied were 48.0MN, 53.5MN, 81.6MN and 81MN respectively. For each test pile, a number of O-cells were located at a single level separating the upper and lower test segments. The maximum test load was dependent on the number of O-cells that could be arranged across the pile section at a single level, and maximum jacking load of each O-cell that was used for testing.

A diagram showing the test pile arrangement and instrumentation is presented in Figure 5, noting that a "soft toe" had been included in majority of the test piles such that end bearing is not engaged during the testing (Figure 6).

4.1 Back analysed ground stiffness

A total of 7 no. pile tests were carried out at the four plots. Movements of the upper and lower segments of each test pile were measured as the segments were jacked apart by the O-cell. These movements were converted into an equivalent top-loaded pile-settlement curve for each test. Stiffness E_{TP} from the pile tests were back-analysed by numerical modelling a single isolated pile using Plaxis 2D (axis-symmetry model) and matching the pile-settlement in the model to that measured. E_{TP} and average shear strain along the pile, obtained from the model at pile head settlement of 1% pile diameter are included in Figure 4. The E_{TP} values fit within the range of the values determined from other tests carried out.

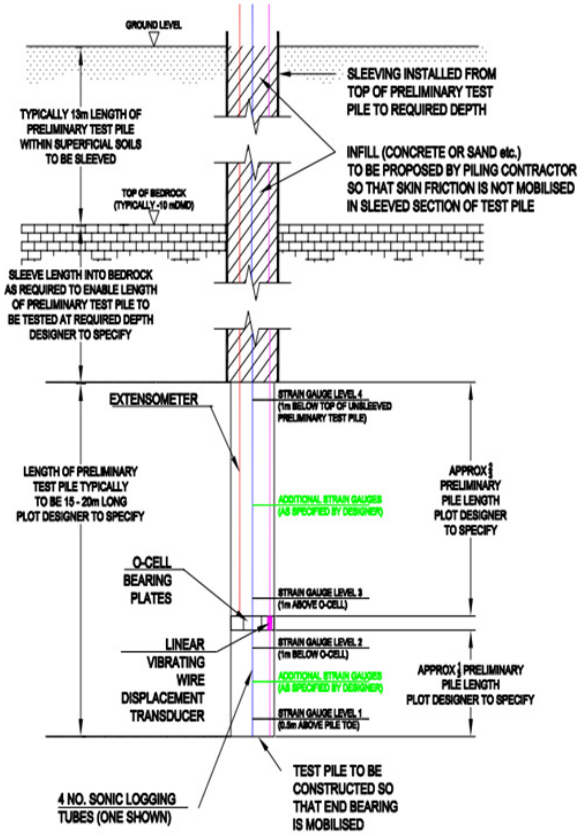

Figure 5. Diagram showing the pile arrangement

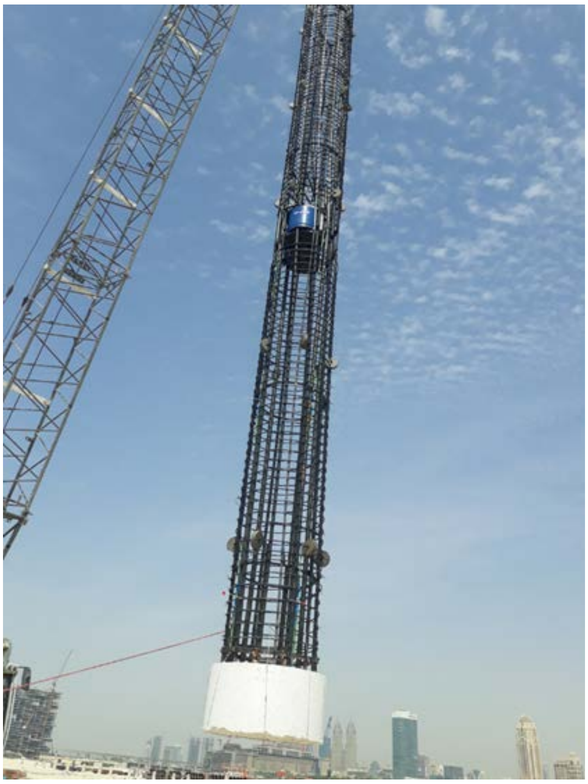

Figure 6. Photo showing lowering of reinforcement cage with 0.5m thick polystyrene 'soft toe' attached to the base

4.2 Measured pile skin friction

Average mobilised skin friction values along the upper and lower test segments of each test are shown in Figure 7. Test piles at Plots A17 and E14/15 had longer upper test segments (10m) than the lower segments (5m), the average measured values were lower for the upper segments as they were not fully mobilised. The maximum measured skin friction (near full mobilisation) at each site ranged between 1250 and 1700 kPa.

Expressions for ultimate skin friction as a function of q_c have been derived by several authors, some of which are shown in Table 1. These can typically be normalised, as shown in (5):

Ultimate skin friction = $x\sqrt{}(q_c)^{0.5}$ (5)

Where x = 0.25 to 0.4

q_c = unconfined compressive strength

Table 1. Correlations of ultimate skin friction and qc

Correlations	Reference
$0{\cdot}375\ (q_c)^{0{\cdot}515}$	Rosenberg and Journeaux (1976)
$0{\cdot}22\ (q_c)^{0{\cdot}6}$	Meigh and Wolski (1979)
$\alpha\beta\ (q_c)$	Williams and Pells (1981)
$(0{\cdot}20 \text{ to } 0{\cdot}30)\ (q_c)^{0{\cdot}5}$	Horvath et al. (1983)
$0{\cdot}45\ (q_c)^{0{\cdot}5}$	Rowe and Armitage (1987)
$0{\cdot}15\ (q_c)$	Carter and Kulhawy (1987)
$(0{\cdot}15 \text{ to } 0{\cdot}2) \times (q_c)^{0{\cdot}5}$	Reese and O'Neil (1988)
$(0{\cdot}40 \text{ to } 0.8) \times (q_c)^{0{\cdot}5}$	Zhang and Einstein (1998)

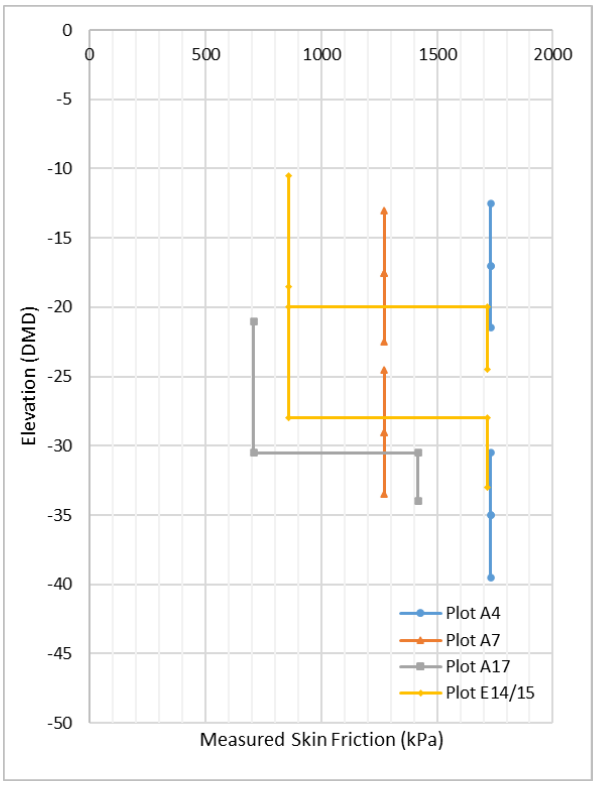

Figure 7. Average measured skin friction along test segments

Considering a mean q_c of 1.83MPa from Figure 1, ultimate unit skin friction determined from (5) would range between 450 and 730 kPa with x = 0.25 and 0.4, respectively. These values are considerably less than the measured test values, which would mean that (5) yields conservative ultimate skin friction and/or q_c values measured from UCS tests were underestimated.

5 DESIGN METHODOLOGY

The design methodology adopted for the four plots follows two slightly different but related means of achieving optimised foundation solutions by justifying serviceability analysis, also associated with higher stiffness values derived in part from pile testing; and by justifying the use of higher allowable shaft friction values on the basis of pile testing to failure.

5.1 Serviceability assessment

For serviceability-based design, soil-structure interaction modelling of foundations is key. Soil-structure interaction essentially requires compatibility between a structure, its foundation and surrounding soil/ rock. This requires two key fundamentals to be achieved, which is load equilibrium amongst the structure, foundation system and soil; and compatibly amongst displacement of structure, pile head and ground at the interfaces. The approaches to undertake soil-structure interaction assessment are:

1. 3D finite element modelling which incorporates the ground, foundation and structure.
2. Split the ground, foundation and structure into two models (structural and geotechnical models) and iterate between the models until compatible displacements at the interface of the models have been achieved.
3. 3D finite element modelling which incorporates the ground and foundation system; and column/ wall loads input as point/ line loads on the foundation system.

Assessment using Approach 1 and 2, will account for structure, foundation system and ground stiffnesses. However, structure stiffness will not be accounted for in Approach 3. Furthermore, redistribution of column loads (if any) as a result of foundation displacement will not be captured. The robustness of design is often inversely proportional to the duration required to construct the model for assessment. Therefore, whilst Approach 1 provides the most robust of designs, it is often impracticable for use given that the project timeframe is usually short. It will also require both structural and geotechnical engineers working on a single model to ensure specific elements are correctly modelled. The following discusses methodology and input parameters adopted for Plot A4. A similar process was followed for all other plots.

A non-linear strain dependent stiffness curve is ideal as input for assessment by Approach 1. However due to time constraints, Approach 2 with characteristic $E_{PMT\text{-}H\text{-}ini}$ values was adopted for the pile group design, noting that the geotechnical software used did not allow for non-linear stiffness analysis. Characteristic $E_{PMT\text{-}H\text{-}ini}$ values were not corrected for rock anisotropy, and were assumed to lie between $E_{PMT\text{-}V\text{-}ini}$ and $E_{PMT\text{-}V\text{-}ur}$ as shown in Figure 8.

The strain range of axially loaded pile groups determined from numerical assessment is around 0.2%, which is at the higher end of typical strains for foundation indicated by Atkinson (2000) as shown in Figure 9.

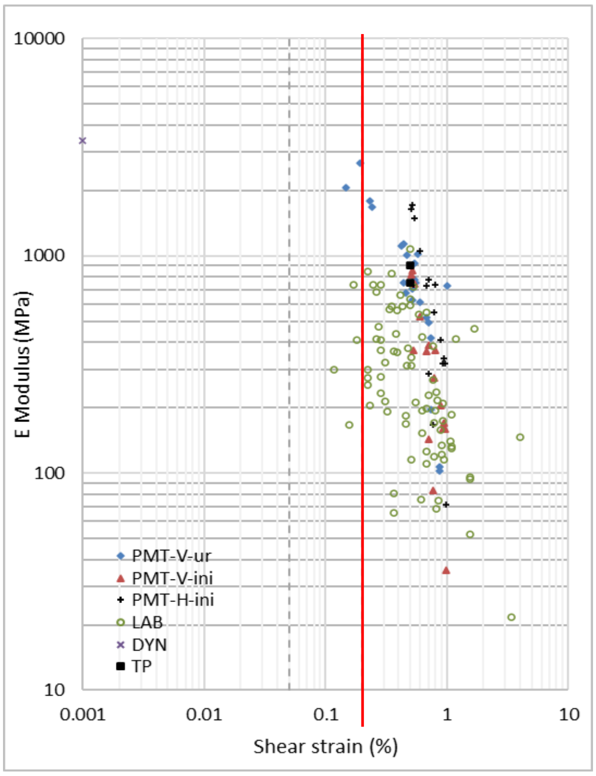

Figure 8. E Modulus versus shear strain - Plot A4

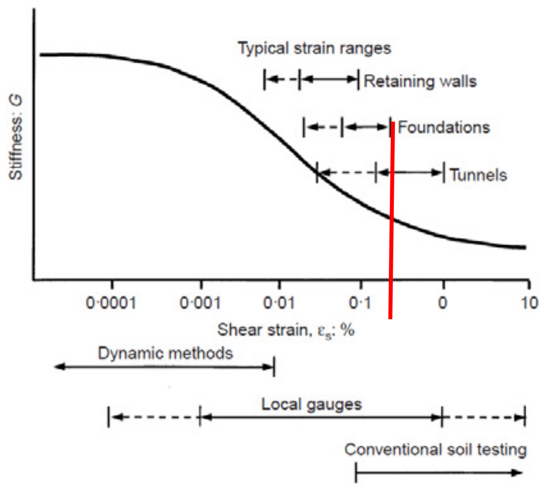

Figure 9. Typical strain ranges for geotechnical structures (Atkinson, 2000)

Considering stiffness E associated with the strain range of pile group foundations (around 0.2%) and the back-analysed E_{TP} from pile tests (see Figure 8), the use of $E_{PMT\text{-}H\text{-}ini}$, (uncorrected for anisotropy) in the design is justified.

5.2 Pile skin friction

Allowable skin friction (fs) values for Plot A4 were determined based on the following methods for comparison purpose:

1. Traditional method of applying a lumped factor of 2.5 to ultimate f_s determined from (5) with q_c from site investigation.
2. Back-analysed from serviceability analysis adopting $E_{PMT\text{-}H\text{-}ini}$ and a limiting total building settlement of 50mm.
3. Applying a factor of safety of 2.5 to measured skin friction from pile testing to near failure. The factor of safety includes the additional design criterion that attempts to avoid the full mobilisation of shaft friction along the piles to reduce the risk that cyclic loading will lead to degradation of shaft capacity for tall tower foundations (Poulos, 2017), especially those embedded in weak carbonated rock.

Figure 10 shows allowable pile skin friction determined from the three methods, and values from Method 1 were conservative. Serviceability analysis (Method 2) offers a more economical design, where the lengths of the piles were shorter with higher allowable skin friction compared to Method 1. Should higher allowable building settlement (i.e. > 50 mm) be considered, the pile design may be further revised. However, allowable friction values from Method 2 should not exceed values from Method 3, in which potential pile skin friction degradation is considered. Adopting factored friction values from pile tests (Method 3) alone without settlement checks, would result in movements outside the limiting tolerance as the piles were tested to failure.

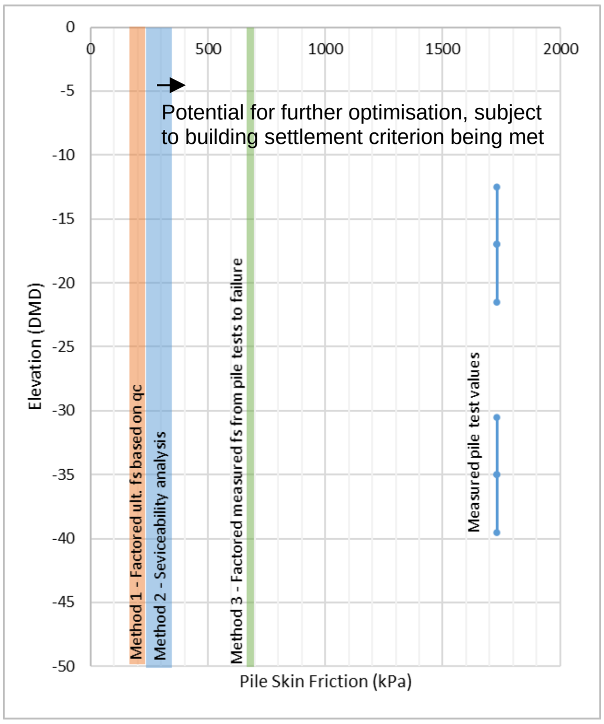

Figure 10. Pile skin friction – Plot A4

6 CONCLUSION

This paper discusses the design methodology that follows two slightly different but related means of achieving optimised foundation solutions by justifying serviceability analysis with the use of high stiffness values and by justifying the use of higher allowable shaft friction values on the basis of pile testing.

A brief overview of soil-structure interaction assessment methods is presented, along with ground stiffness measurements from various testing at different strain levels for serviceability analysis. Case studies show that allowable skin friction values determined from serviceability analysis were higher than those from empirical formula with a lumped factor of safety. The use of allowable skin friction from serviceability analyses were further justified by measured skin friction values, from large scale bi-directional static pile tests to failure, which were reduced to avoid the full mobilisation of shaft friction along the piles. This is partly to reduce the risk associated with cyclic loading that will lead to degradation of shaft capacity for tall tower foundations embedded in carbonated weak rock.

7 ACKNOWLEDGEMENTS

The work presented in this paper was carried out by the authors on projects in Dubai with the support of their colleagues at Tetra Tech Coffey. They are thankful to Antone Dabeet and Nabeel Bux who provided expertise that greatly assisted the projects.

REFERENCES

Atkinson JH (2000), "Non-linear soil stiffness in routine design." Géotechnique, 50(5), 487–508.

Carter JP and Kulhawy FH (1987), "Analysis and Design of Foundations Socketed into Rock". Geotechnical Engineering Group, Cornell University, Ithaca, NY, USA, Res. Rep. 1493-4.

Horvath RG, Kenney TC and Kozicki P (1983), "Methods of improving the performance of drilled piers in weak rock". Canadian Geotechnical Journal 20(4), 758-772.

Meigh AC and Wolski W (1979), "Design parameters for weak rock". Proceedings of 7th European Conference on Soil Mechanics and Foundation Engineering. British Geotechnical Society, London, UK, vol. 5, pp. 59–79.

Poulos HG (2017), "Tall Building Foundation Design." CRC Press, Boca Raton, USA.

Reese LC and O'Neill MW (1988), "Drilled Shafts: Construction Procedures and Design Methods". US Department of Transportation, Dallas, TX, USA, FHWA-HI-88-042.

Rosenberg P and Journeaux NL (1976), "Friction and end bearing tests on bedrock for high capacity socket design". Canadian Geotechnical Journal 13(3), 324–333.

Rowe RK and Armitage HH (1987), "Theoretical solution for axial deformation of drilled shaft". Canadian Geotechnical Journal 24(1), 114–125.

Williams AF and Pells PJN (1981), "Side resistance rock sockets in sandstone, mudstone, and shale". Canadian Geotechnical Journal 18(4), 502–513.

Zhang L and Einstein HH (1998), "End bearing capacity of drilled shafts in rock". Journal of Geotechnical and Geoenvironmental Engineering 124(7), 574–584.

Optimisation of temporary support design for the Northern portal cut & cover tunnel

J. Zeerak[1], Dr. M. Wei[2], J Roper[3], B Clarke[4]

[1]Associate Principal-Geotechnics, EIC Activities Pty Ltd, 567 Collins Street, Melbourne, Australia; email: Jawad.Zeerak@eicactiv.com
[2]Technical Principal-Geotechnics, EIC Activities Pty Ltd, 567 Collins Street, Melbourne, Australia; email: Michael.Wei@eicactiv.com
[3]Principal-Structures, EIC Activities Pty Ltd, 567 Collins Street, Melbourne, Australia; email: Jeff.Roper@eicactiv.com
[4]Engineering Manager, John Holland Group, 180 Flinders Street, Melbourne, Australia; email: Ben.Clarke@jhg.com.au

ABSTRACT

The West Gate Tunnel Project is a city-shaping project that will deliver a vital alternative to the West Gate Bridge, provide quicker and safer journeys, and remove thousands of trucks off residential streets. Delivery of the WGTP project is currently underway by a joint venture of CPB Contractors and John Holland Group. Northern Portal cut and cover tunnel is one of the major structures on the project which requires excavations to a depth of 22 m to allow the launch of the twin 15.6m diameter Tunnel Boring Machines (TBM). Design of the retention system comprised 900 – 1500 mm diameter secant pile wall supported with multiple levels of temporary steel struts. A detailed Soil-Structure Interaction (SSI) analysis together with a review of proposed construction methodology indicated that a two-level propping arrangement as opposed to propping at three levels, which is what would normally be expected for a structure of this scale, would be adequate. The opportunity to remove one level of the proposed steel struts with the potential for a significant reduction in materials and time was considered critical to the completion of this critical path structure. Removal of one level of props would result in a reduction of steel tonnage in excess of 1,000 tons, in addition to improving constructability, productivity and safety. This paper discusses technical aspects of the analysis which enabled the development of the above optimised solution. In addition, the results of the instrumentation and monitoring and performance of the constructed portal structure will be discussed.

Keywords: WGTP, Cut & Cover Tunnel, Deep Excavation, Secant Pile Wall, Soil Structure Interaction, FEM, Value Engineering

1 INTRODUCTION

The West Gate Tunnel Project (WGTP) is a city-shaping project that will deliver a vital alternative to the existing West Gate Bridge, provide quicker and safer journeys, and remove thousands of trucks off residential streets. In addition to the construction of twin large diameter (15.6 m) tunnels the project will deliver:

- Widening of the West Gate Freeway from 8 to 12 lanes
- Multiple crossings across the Maribyrnong River, connected to an elevated viaduct along Footscray Rd, and
- Multiple bridges, entry and exit ramps across the eastern and western zones of the project.

The project is currently in the delivery phase in Melbourne by a construction Joint Venture of CPB Contractors and John Holland Group.

2 NORTHERN PORTAL CUT & COVER TUNNEL

The Northern Portal (NP) cut and cover tunnel at WGTP is one of the major packages of the works on the project. The portal is used in the temporary condition to facilitate the launch of twin TBM machines for the bored tunnels and forms the final cut & cover tunnel (tunnel portal) after completion of the TBM launch and construction of the permanent structural lining. The portal structure is over 330m in length and up to 22.2 m in depth at the interface of the cut & cover tunnel and the TBM tunnel. Temporary support for the northern portal excavation comprised the following retention systems:

- Secant pile walls supported with heavy steel strutting & waling
- Anchor supported sheet pile walls
- Base slab
- Tension piles

Propped secant pile wall was adopted for the deeper parts of the cut & cover tunnel at the interface with the TBM tunnels, transitioning to the anchored sheet pile wall as the excavation depth reduces towards the open trough structure. Multiple design types were incorporated in the design to suit excavation depths and ground conditions along with the portal structure. The portal structure was designed as a tanked structure (undrained) for the full length of the portal to minimise disturbance to the regional groundwater regime. Figure 1 presents a general layout of the northern portal.

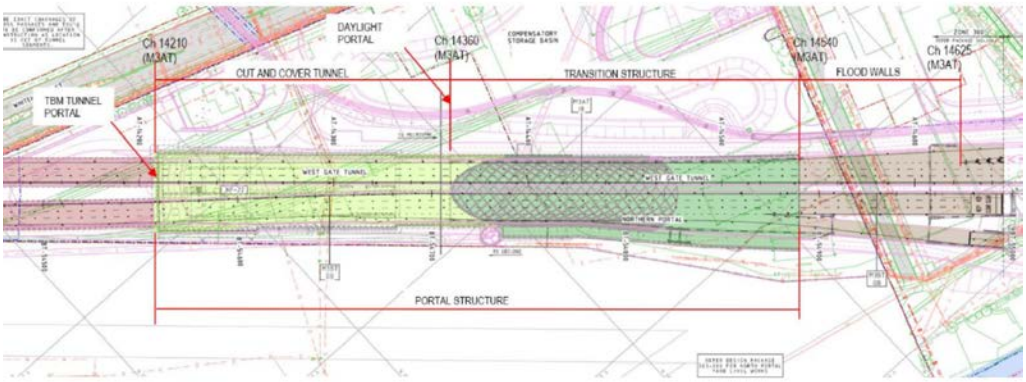

Figure 1. Northern portal site layout

It is worth noting that the northern portal cut & cover tunnel is a major structure comprising propped secant pile wall in the temporary and a structural lining wall constructed on the inside in the long term. The two structure types combined forms the cut & cover tunnel with a significant interaction between the two structure types. Discussions in this paper are limited to the analysis conducted for the structure in the temporary condition only before construction of the permanent structural lining. It is further noted that the discussion presented in this paper are based on the analysis, which are limited in nature conducted as part of a value engineering and optimisation exercise, detailed design of the structure were undertaken by others.

2.1 Geological Conditions & Geotechnical Parameters

Figure 2 presents surface geology of the general project area highlighted on an extract from the Geological Survey of Victoria's Melbourne Mapsheet.

The geological conditions at the Northern Portal consists of an upper unit comprising man-made Fill overlying a thin veneer of the soft and compressible Coode Island Silt (light green in Figure 2, not shown in Figure 3). These thinner units are underlain by a more substantial layer of Quaternary alluvial outwash, and deeper alluvial infill to a paleochannel crossing the northern end of the Northern Portal (green/dark green in Figure 3). Variable thicknesses of the Brighton group unit (yellow in Figure 3) are encountered in parts of the northern portal. The older volcanics rock (pink in Figure. 3) comprises the bedrock in the area of the portal where most of the piling and excavation works within the deeper ends of the northern portal occur.

Variable degrees of weathering of the older volcanic units were encountered during piling which comprised residual soils to extremely and highly weathered rock. Tertiary aged Werribee formation sediments underly the Older Volcanics rock. A typical geological section at the northern portal is shown in Figure 3. Groundwater levels vary along with the portal structure and ranges typically between RL0 mAHD to RL-4 mAHD. The lower levels were associated with the long-term depressurisation effects of local drains e.g. North Yarra Sewer Main. The portal structure was designed as a tanked structure with the retention structure comprising predominantly a secant pile wall which is considered watertight. It is worth noting that a row of recharge wells was proposed along the perimeter of the excavation to minimise the impact of works on the local groundwater regime. Given the secant wall system, any groundwater inflow was expected to be through the foundation rock which was expected to be minimal.

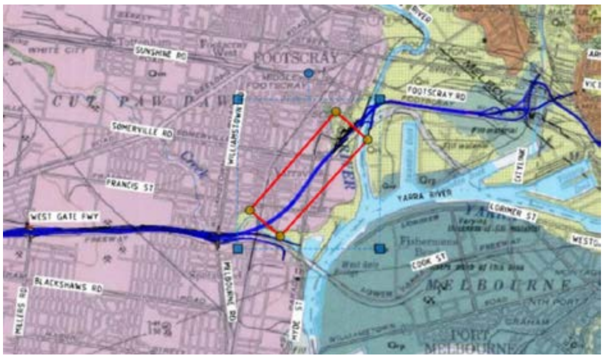

Figure 2. Geological Survey of Victoria, Melbourne Mapsheet, (1:63,360)

Geotechnical parameters adopted in the finite element analysis were derived from site investigation data, laboratory testing, published literature and past experience. Parameters for the soil units were generally derived from laboratory testing, typical correlations, and past experience. While rock mass parameters for use in the design of excavation support were assessed using the generalised Hoek-Brown strength criterion using the Roclab (RocData) software by Rocscience. Adopted parameters are summarised in Table 1.

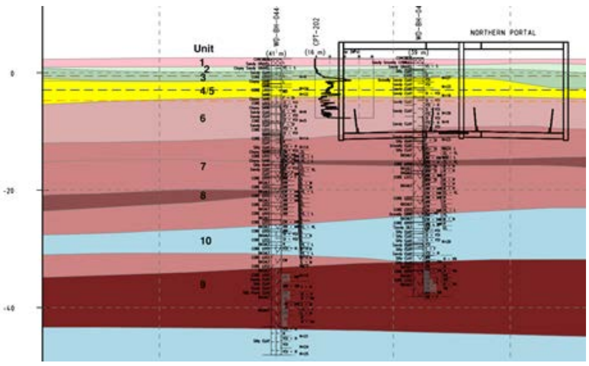

Figure 3. Northern Portal Geological Profile

In the analysis, both drained and undrained parameters were utilised relevant to each stage of the construction. In general, short term or undrained parameters were used in the short term i.e. during top down excavation to the final excavation level and casting of the base slab after which soil parameters were changed to drained parameters relevant to long term conditions.

The above covers two extremes of soil behaviour.

Table 1: Adopted Geotechnical Parameters

Unit	Unit	r [kN/m^3]	Su [kPa]	c' [kPa]	Phi' [º]	E' [MPa]	ν'
1	Fill – General	17	20	2	26	12	0.3
2	Alluvium Outwash	18	-	1	33	25/20/75	0.2
3	Paleochannel Alluvium	18	120	10	28	25/20/75	0.2
4	Brighton Group-Clays	19	150	10	30	40	0.35
5	Brighton Group-Sands	20	-	1	34	60	0.3
6	Older Volcanics-Residual Soil	20	150	15	28	60	0.2
7	Extremely weathered older volcanics	21	250	30	28	200	0.3
8	Highly weathered Older Volcanics	21	-	50	40	800	0.3
9	Slightly weathered Older Volcanics	28	-	400	55	6000	0.2
10	Werribee Formation	20	200	20	28	50/40/150	0.2

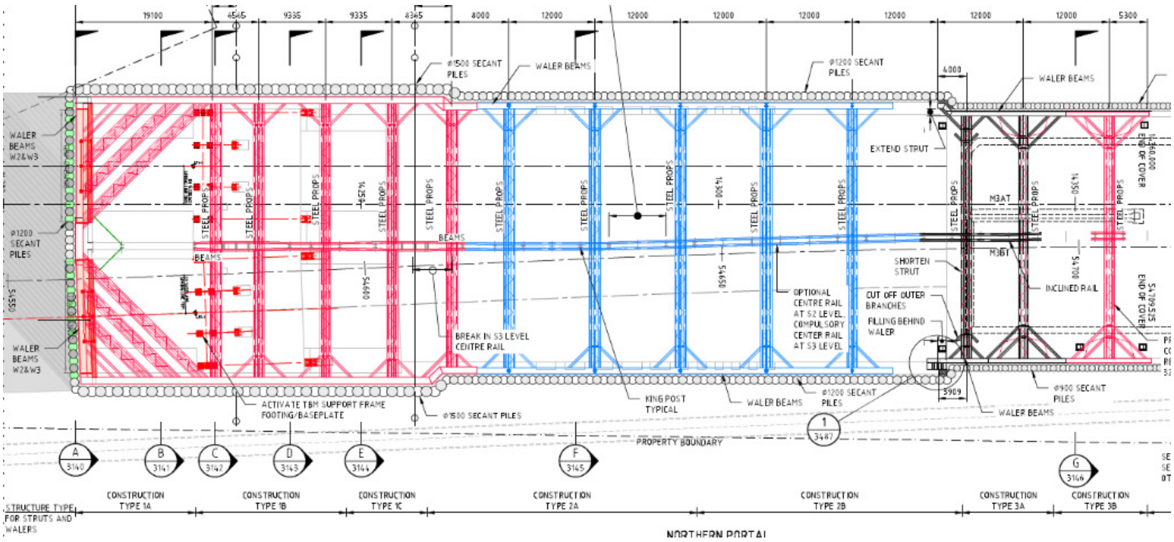

Figure 4. Northern Portal strutting layout

In reality, the soil behaves in a lot more complex manner than that in the modelling. For the purposes of covering critical cases in terms of forces on the retention structure and support elements, various sensitivity checks were carried out with changing soil properties from undrained to drained at various constructing stages. The impact of the above sensitivity checks on the overall design was found to be negligible in this case.

Excavation works are essentially ‘unloading’ problems. This behaviour is best captured using the constitutive soil model Hardening Soil (HS) model in a finite element analysis e.g. PLAXIS. The HS model is an advanced soil model that is able to generate a more realistic soil response in terms of non-linearity, stress dependency and inelasticity of soils. The model requires three stiffness parameters (E50/Eoed/Eur) as shown in the E’ column in Table 1. In the analysis, in general an unload/reload modulus (Eur) of 3 x Secant modulus (E50) was adopted based on literature and common practice. Although experience and some cases studies in literature indicate that this ratio can be significantly higher than 3 in some cases. This may also explain the better than predicted deflection results for the structure which will be discussed in later sections.

3 NORTHERN PORTAL RETENTION DESIGN

The adopted retention system for the majority of the cut & cover structure comprised 900 mm to 1500 mm secant piles propped with multiple layers of steel struts. A secant pile wall option was required to provide a watertight structure as required by the project technical specifications. The larger diameters 1200 mm and 1500mm diameter piles were adopted for the deeper parts of the excavation in a hard-hard pile configuration, while the smaller 900 mm diameter piles were adopted for the shallower excavation depths with a hard-soft arrangement. It is noted that a hard-hard pile arrangement was incorporated in the design for constructability reasons i.e. to reduce reinforcement congestion and ease of installation.

The proposed design of the propping for the secant pile wall comprised 3 levels of steel strutting connected to a waler system against the secant pile walls. The largest steel struts comprised double 1200WB steel sections connected to a double 1200WB walers system attached to piles. Steel struts were supported in the middle using a row of king posts supported on bored piles socketed to rock. The initial strutting layout at S2 level is shown in Figure 4 with a typical section shown in Figure 5.

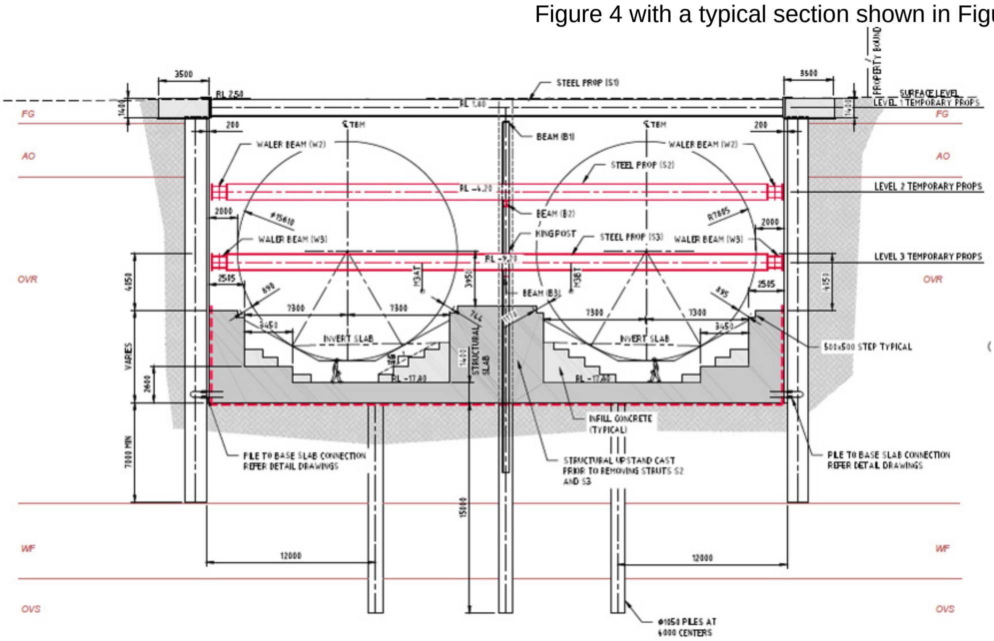

Figure 5. Typical retention design – Northern Portal

The assessment criteria relevant to the design of retention system in the temporary condition included:

- Stability during excavation
- Wall deflection and settlement behind the wall
- Crack widths
- Strength checks

Stability, deflection, and settlement checks were assessed as part of the soil-structure interaction (SSI) analysis discussed in this paper, while strength and crack widths along with other criterion relevant to structural design were assessed under several load combinations as part of a detailed structural analysis, which are outside scope of this paper.

4 SOIL STRUCTURE INTERACTION

As noted earlier, in the temporary condition the portal structure was intended to facilitate the TBM launch for the twin bored tunnels. In other words, the portal structure was on the critical path for the project. Given the required excavation depths, length, size and type of structure, there was a considerable scope of piling and strutting required. Any improvement in the construction program (and cost savings) was seen critical to the success and timely completion of the works. The above warranted a detailed review of the structure in particular the temporary support system. The review targeted geotechnical parameters, improvements in the finite element analysis (FEA) modelling approach, construction sequencing as well as piling methodology some of which is described in brief here.

The portal structure comprised a secant pile (1200 diameter for sections discussed in this paper) wall retention system in the temporary to retain the soil and water before a permanent lining structure was constructed on the inside. The temporary retention piles and final structural lining was constructed over several stages. During the top-down construction, steel props (typically 2x1000WB) were used to support the retention piles. As the final structural lining was constructed progressively in a bottom-up approach, permanent supports comprising a base slab, road deck and roof slab replaced the temporary props. Given the relatively complex nature of works and associated construction stag, involving installation and removal of multiple supports, a detailed Soil-Structure Interaction (SS) model was developed using the finite element software program PLAXIS 2D. A SSI analysis such as one described above, is able to capture interaction between structural elements (retention piles), ground and water loads particularly as the loads changes during the staged construction and locked in stress are generated at various stages. In addition to above, there is also a significant interaction between the retention piles and the permanent structural lining as the permanent lining is progressively installed and temporary supports removed. PLAXS analysis showed that loads on the retention piles (and supports) were greatest in the short term before installation of the permanent supports. This was expected given the limited support points in the temporary condition in contrast to the final configuration when the structure is propped at multiple levels with road deck, roof slab and base slab. Once the structural lining and permanent supports were installed, there is a load redistribution and load sharing occurring between the retention piles and the lining structure. Given the focus of the current paper is on the temporary supports system until excavation of the final excavation level and installation of base slab and upstand walls as shown in Figure 7, discussion on the interaction of permanent and temporary structure will be limited to the above.

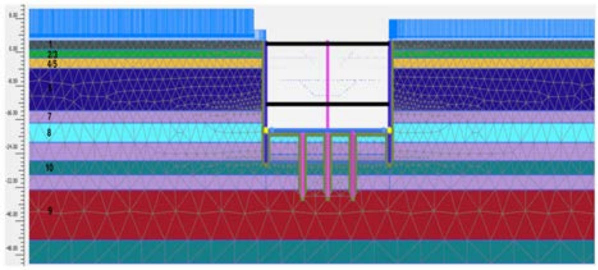

Figure 6. Typical PLAXIS 2D Model

In the PLAXIS model, all construction stages were simulated based on the proposed sequence until completion of the excavation and installation of the base slab and removal of the S3 prop. The above stages can generally be summarised as below:

- Installation of retention piles
- Progressive excavation and installation of temporary steel props
- Construction of base slab and casting of upstand walls (partially completed permanent wall)

Figure 7. View of northern portal temporary strutting towards TBM headwall

The level for S1 prop was generally fixed at the caping beam level for the portal structure as they are most effective in controlling pile head deflections and from a constructability point of view. The aim of the above exercise was to eliminate S2 prop from a design where feasible. Therefore, the configuration for the S3 (lowest level prop) was of significant interest in order to optimise the propping design. An optimum arrangement of S3 prop was considered to be one which would allow removal of S2, while limiting wall deflections and providing adequate support to the retention piles in what would be considered a significant unpropped height between the S1 and S3 (with S2 removed).

To achieve the above goal, various iterations were run in the PLAXIS analysis to test and assess the most optimum configuration for S3 prop. From the iterations of the PLAXIS analysis, it became clear that a lowered S3 prop would generally be a lot more effective in providing lateral support to the retention piles. However, the extent on how much the S3 props could be lowered was constrained by the working space required for the base slab and construction of the partial upstand walls. Therefore, the prop was lowered as far as feasible for practical purposes.

It is also noted that small section of the permanent structural lining was constructed in early stages after casting of the base slab which was called 'Upstand Walls'. The analysis also showed that it was critical that the partial upstand walls were constructed prior to removal of the S3 prop. These upstand walls would prop the retention piles at a higher level and therefore reduce additional forces generated in the piles. Analysis indicated that this would result in an increase of forces within the base slab and upstand walls slightly, however, the benefits would outweigh the small increase in forces. The above were relatively simple, yet critical modifications required to enable a two-level strutting system for spans of over 15 m between the two props which were considered unprecedented in author's experience.

In addition to the above, various refinements and improvements were also made in the finite element modelling resulting in improvements of the overall analysis outcome. In the recent versions of PLAXIS 2D, the software allows the input of flexural stiffness as 'elastoplastic' moment-curvature diagram instead of the more 'traditional' way of defining flexural stiffness of the plate elements as a linear elastic material. With the improved moment-curvature (M-K) input feature, it was found that forces generated within the retention piles were more optimised and considerably lower than those which would have been obtained using the traditional 'EI' values reduced by a factor to account for short- and long-term cracking of the concrete. The combined effects of the above led to the possibility of the S2 (middle props) being removed from the design leaving two levels S1 and S3. Although there were differences in the pile forces at individual stages, PLAXIS analysis indicated that retention pile structural actions envelopes generally remained similar between a two-strut configuration and a three-strut system. Proposed prop sizes also remained adequate for the slightly increased loads with the S2 props removed. Figure 8 shows a view of the northern portal temporary works completed.

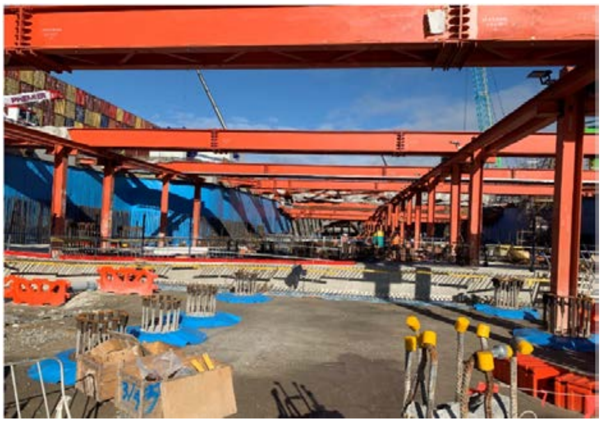

Figure 8. View of northern portal temporary strutting

5 INSTRUMENTATION AND MONITORING RESULTS

Given the size and scale of the portal structure, a detailed and comprehensive Instrumentation and Monitoring regime was recommended as part of the design. The following instruments were installed on piles and struts along the portal:

- In Place Inclinometers at regular intervals
- Reflectorless prims at multiple levels on the piles
- Settlement markers behind the excavation at regular intervals
- Groundwater monitoring wells; and
- Strain gauges on selected steel props to monitor forces on the steel struts.

The I&M requirement was a critical part of the design allowing the wall and strutting system to be monitored during progressive excavation and installation of strutting system. This was in particular critical where the S2 level props were omitted. The recommendation was that retention piles and S1 level props would be monitored continuously, and wall deflections and prop forces compared against design predictions.

The monitoring system would allow for early intervention should the monitoring results indicate a need based on the wall performance during construction. Accordingly, wall deflections were monitored continuously during bulk excavations and installation of the steel props until base slab excavation. Based on the PLAXIS analysis, a maximum wall deflection of 55mm was expected in the final stage, upon removal of the S3 prop after the base slab had been constructed. Inclinometer readings obtained during construction indicated maximum wall deflections of 20mm which was well below the design predicted value and set trigger levels. Typical inclinometer profiles showing horizontal wall deflections are shown in Figure 9.

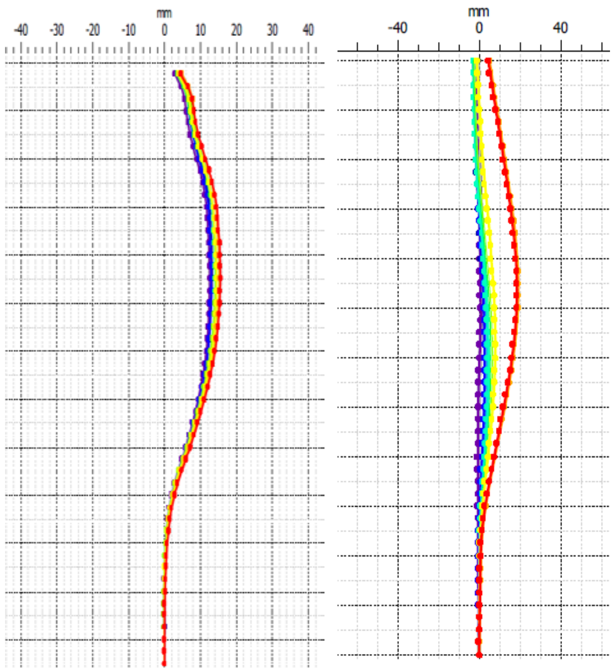

Figure 9. Typical inclinometer profile (horizontal wall movements)

Similarly strain gauges installed on the steel struts were monitored during construction to obtain prop forces and comparison against design predictions. Monitoring results indicated strut forces within the range predicted in the PLAXIS analysis. There were variations in the peak forces as shown in Figure 10. These fluctuations in the forces were attributed to the changes in the atmosphere temperature levels causing expansion and contraction of the steel struts. Progressive and real-time monitoring results obtained at each stage of the construction provided confidence in the suitability and adequacy of the design.

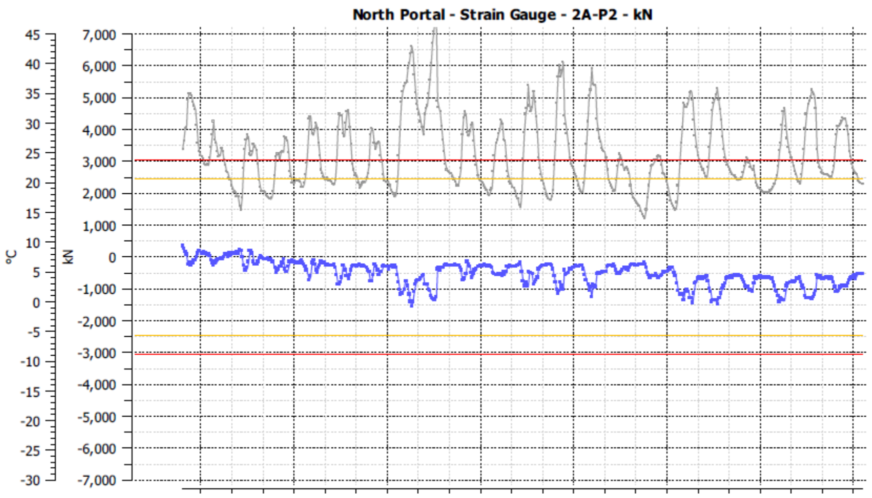

Figure 10. Strain gauge data

Observations made from the monitoring results were that significantly lower wall deflections were recorded compared to those predicted in the design and calculated in PLAXIS analysis. This is in part attributed to some level of prudent conservatism in the design as would expected for the scale and size of the excavation described in this paper. However, other observations and lessons learnt relating to better-than-expected performance of the excavation support system, particularly the retention piles could be attributed to factors stated below:

- Stiffness parameters for various rock units were assessed using the Roclab software using lower bound and upper bound test results. In the PLAXIS analysis, typically lower bound parameters were used given the scale and size of excavation, associated risks and to cover inherent variability and uncertainty associated with ground conditions. It appears, that encountered ground conditions have responded considerably better than those assumed in the analysis which has resulted in better performance of the retention system. Greater levels of confidence can be reached with additional targeted geotechnical investigations and laboratory testing to optimise parameters further during design stages.

- As noted earlier, an unload/reload (Eur) modulus of 3xE50 was adopted in the design. It is also possible that in this Eur/E50 ratio is higher than 3, potentially greater than 5. Pressuremeter testing can be undertaken to obtain more accurate estimates of the Eur/E50 ratio.

- There is a propping effect at the two corners where the portal structure meets the TBM headwall. Based on experience from other similar structures, the corner effects can be significant due to soil arching in the corners, but also the propping effect of the end walls (TBM headwall in this case) to the side walls. Given the limitations associated with a 2D plane strain analysis, this was not captured in the analysis undertaken for this structure. However, these beneficial effects can be captured well using a 3D type analysis.

6 CONCLUSION

As part of a value engineering exercise, a detailed soil structure interaction (SSI) and review of construction methodology indicated possibility of removal of one level of props for a major portal structure on the WGTP. The SSI was completed using the finite element software package PLAXIS 2D. Results of the FE analysis indicated that a two-level strutting arrangement opposed to propping at three levels, would provide adequate support to the 22 m deep excavation at the portal structure. Level of the lowest strut (along with other improvements discussed in this paper) was found to be critical in optimising the temporary support requirements for the portal structure. A thorough and continuous instrumentation and monitoring regime prescribed as part of the design, enabled a close monitoring of the performance of the structure and provided confidence during construction with the suitability and adequacy of the proposed design. Results of the ongoing monitoring indicated a generally better performance of the retention design than expected. This may be attributed to the 3D nature of the structure towards the deeper ends of the portal which was not captured in the 2D analysis and encountering better ground conditions in particular better rock stiffness than those assumed in the design. This underlines the significance of adequate site investigation and testing to enable detailed assessment and adoption of refined geotechnical parameters. The adoption of an optimising strutting design at two levels as opposed to three levels which would normally be seen reasonable for excavation depths such as those required at the northern portal, provided significant cost savings to the project in addition to an efficient, smoother and safer construction program.

7 ACKNOWLEDGEMENTS

As noted in the introduction, the discussions presented in this paper are based on limited analysis conducted as part of a value engineering and optmisation exercise. Detailed design of the structures are by others. Authors wish to acknowledge inputs and support provided by the WGTP tunnel zone personnel during design and construction phases of the northern portal structure. without whose support this paper would not have been possible. Finally, authors wish to thank Dr. Jeff Hsi of EIC Activities for a peer review of this paper.

REFERENCES

GSV, (1974), “Melbourne Mapsheet 1:63,360”, Geological Survey of Victoria.

SESSION 4

THE ROLE OF DESIGN IN INFRASTRUCTURE PROJECTS

Supporting Innovative Design and Construction

S. R. Taylor[1], CPEng, FIEAust.

[1]Major Road Projects Victoria, Level 25, 180 Lonsdale Street, Melbourne; email scott.taylor@roadprojects.vic.gov.au

ABSTRACT

Innovation is at the core of the engineering profession. Innovation is driven largely by the need to increase efficiency, reduce costs, or respond to increasing complexity. In today's context, these drivers appear to be converging, with efficiency, cost and increased complexity almost a baseline for all projects, and the impacts of climate change, sustainability and the circular economy a significant influence on the future of transport infrastructure. To seek the benefits of innovation on transport infrastructure projects, Major Road Projects Victoria's (MRPV) aims to facilitate the minimisation and removal of barriers and obstacles to innovation. The barriers to innovation include a risk-adverse culture, limited capacity and capability of resources (both within industry and government), leadership, regulatory requirements and a bureaucratic culture, and rewards and incentives for the implementation of innovation. Through a series of new initiatives, this presentation will outline how MRPV is supporting innovation in design and construction of major road projects in Victoria. To address barriers associated with risk-aversion and capacity, MRPV have implemented a new delivery model that focuses on a program of projects with incentives for innovative solutions. For barriers associated with leadership, regulatory requirements and bureaucratic culture, MRPV is leading a program of modernising and updating standards and specifications including trialling intelligent compaction, and creating of a new technical specific for recycled organics.

Keywords: innovation, transport infrastructure, standards, specifications

1 INTRODUCTION

Innovation is a corner stone of engineering. Clear technological and engineering advancements can be associated with human development. Similarly, in the transport infrastructure sector, often, innovative design and construction facilitates significant step changes industry wide. Without innovation, many of the currently projects being delivered would not be possible or even conceivable. Therefore, innovation must be fostered and encouraged by all participants (whether from government or industry) in the delivery of projects.

Innovation in the context of projects, organisations and industry can be viewed differently, and has differing lasting impacts. The transport infrastructure sector is comprised of a number of organisations (including government, contractors, suppliers, consultants etc), which in turn form smaller teams to deliver projects. Diagrammatically the relationship between projects, organisations and industry can be represented in Figure 1. When considering the impact of innovation, targeting the broader industry will obviously result in the greatest outcome as the benefits are realised over the greatest number of projects.

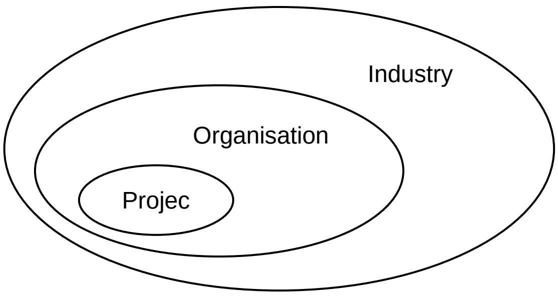

Figure 1. Relationship between projects, organisations and industry.

This paper begins by exploring the drivers and barriers to innovation in the transport sector, with a focus on identifying the barriers to implementation of innovation at the industry level. The paper then explores two key initiatives being undertaken at Major Roads Projects Victoria (MRPV) that aim to reduce and remove barriers to innovation and enable innovation to be realised across the entire industry. The specific initiatives being undertaken by MRPV include the Program Delivery Approach (PDA) used to deliver projects, and a program of modernising and updating standards and specifications.

2 DRIVERS FOR INNOVATION

Scholarly articles relating to "drivers for innovation" in engineering number in the multiple hundreds of thousands. It is clearly a well-researched and commented topic. Common themes in the transport infrastructure sector have been identified by a range of authors including Wipulanusat et al. (2019), Ozorhon and Oral (2017), and Salter and Torbett (2003). The drivers of innovation include;

- Innovations developed to increase efficiency and effectiveness.
- Innovations to reduce costs.
- Innovations in response to increasing complexity which can be derived from both internal or external sources. The rise of the 'mega' project is also a large source for innovations driven by a complex environment,
- Innovations in response to an external crisis which is becoming more commonly related to climate change, sustainable practices and the circulate economy.

When returning to the levels of projects, organisations and industry, there is no known documented evidence of the amount of innovation done at the different levels – possibly due to the fact it would be difficult to categorically assign innovations solely to a project, organisation or industry. Yet at the project level, drivers for innovation would occur more regularly, but the likelihood of the innovations carrying through to the organisation or even the industry would be less common. That is, an individual project may develop an innovation, no matter how small, but fail to pass that innovation onto other projects within their organisation, or onto other projects within different organisations. This means the risk of losing innovation done by a project is significant, as once the project finishes and the team is disbanded, there is little incentive or desire for the project learns to pass their innovations onto the next project. In the transport infrastructure sector this is largely driven by the competitive nature of projects, where organisations will tend to protect innovations from the broader market.

For the full benefits of any innovation to be realised by the broader industry, it requires an industry wide agency to oversee innovation for the industry. This is a role State Governments in Australia have significant part to play. Governments set the regulatory and policy environment within which industry operates. They are also the major purchaser of civil infrastructure within Australia. Therefore, it is within government's interest to ensure innovations succeed at the industry level so that their benefits can be fully realised.

3 BARRIERS TO INNOVATION

Likewise for drivers, barriers to innovation can equally have a significant impact on the success of innovations and the development of an innovative culture.

Wipulanusat et al. (2019) provided a framework for defining barriers and obstacles to innovation. The context they have defined barriers are those in the public sector which impede and delay government agencies from adopting and implementing innovations successfully. They propose barriers to innovation in the public sector include a risk adverse culture, limited resources, failure of leadership, regulatory requirements, few rewards and incentives, and a bureaucratic culture. Each of these barriers is discussed future in the following sections.

3.1 Risk Adverse Culture

Wipulanusat et al. (2019) proposed that due to the negative ramifications of risk-taking in the public sector, such as political damage to the government or public criticism, the public sector tends to have a risk adverse culture. In the context of innovation, this results in diminishing likelihood by government agencies of taking risks through the adoption of new technology. In the transport infrastructure sector, this is further compounded by the increasingly complex legal and commercial environments, where uncertainty in new technology, systems or processes leads to the suppressing of innovation at project, organisation and industry level.

A symptom of a risk adverse government culture is the creation of an overly conservative and prescriptive regulatory and legal environment. This then means innovations are constrained by the limitations and boundaries imposed by technical standards and specifications.

3.2 Limited Resources

Capacity can be considered in both the context of people and funding. Often innovation will require development and funding without knowing the outcome of the research being undertaken. Government's, however, operate on clear funding cycles and productive use of resources, leaving little space for the ability to innovate.

While this may be a reality of government entities, this is not such a barrier for private industry who are more willing to invest in innovation without the certainty of success. Therefore, to effectively remove this barrier, government and industry need to partner in a manner that makes best use of the limited resources, while still allowing individuals the freedom to explore new ideas or concepts.

3.3 Failure of Leadership

Wipulanusat et al. (2019) comment that leadership plays an important role in fostering a culture of innovation. "Leaders must find mechanisms to encourage the generation, adoption and implementation of innovations," (Wipulanusat et al. 2019). While the leaders don't need to be the creative force behind innovations, they are critical in supporting and championing innovation to ensure its success.

In a highly technical area such as transport infrastructure, this also requires leaders to have a level of technical literacy that they are able to identify innovation and encourage its growth. At MRPV this has been achieved by establishing a strong leadership team that consists of all the necessary skills required for successful project delivery in the transport infrastructure sector.

3.4 Regulatory Requirements

Change and approval processes within government are heavily controlled and regulated (Wipulanusat et al. 2019). Further, in the engineering context, standards and specifications play a significant role in defining acceptable minimum requirements. Many of these standards and specification are prescriptive in nature, which inherently limit the ability of innovators to use products, systems and processes that lie outside these defined boundaries.

An innovation within or for a government project will never be successful if it does not meet the wide range of regulation, guidelines, policies, standards and specifications. Further, where innovations use new technologies that lie outside current regulatory requirements there is the risk they will not be accepted as they cannot be measured against a set of requirements to determine if they are suitable of use.

A significant factor in much of the regulatory requirements that exists are they are prescriptive in nature, and as a result the product, process or system needs to fit within the framework and boundaries of the requirements very neatly. An alternate approach is to develop performance-based requirements, where the performance requirements are defined and testing procedures described, however the parts that constitute the final output are not defined. This enables individuals to innovate knowing their product, system or process only needs to achieve the output performance requirements.

3.5 Few Rewards or Incentives

Wipulanusat et al. (2019) comment that in government innovators rarely received feedback or a reward for their success, however "if the innovation fails or does not prove to be efficient, the innovators are responsible for all the costs." When translated into the transport sector, particularly for traditional D&C delivery models, there is little incentive for contractors and designers to share innovations beyond their projects, meaning they can be short lived and not widely adopted.

Therefore, a key feature of delivery models that foster a culture of innovation are those that contain some element of reward and recognition for new technology, processes, or systems.

3.6 Bureaucratic Culture

The barrier related to a bureaucratic culture relates strongly to leadership and the risk adverse culture within government. Governments tend to be hierarchical in decision-making, as well as restrained in their promotion of innovation due to their inherent tendency towards regulation and certainty (Wipulanusat et al. 2019).

To overcome the barrier of a bureaucratic culture, MRPV has partnered with industry to delivery projects through the Program Delivery Approach (PDA) which has enabled projects to offer innovative solutions that address performance-based regulations, standards, and specifications. This ensures industry suppliers with new technology, process or systems can successfully implement their innovative solutions within the constraints of government requirements.

4 INITIATIVES TO ENCOURAGE INNOVATION

To increase and encourage new technology, systems, and processes within road projects, MRPV has been working on a number of initiatives that aim to remove and reduce the barriers to innovation. The next sections outline two key initiatives, namely the Program Delivery Approach (PDA) used to deliver projects, and a program of modernising and updating standards and specifications.

5 PROGRAM DELIVERY APPROACH

In mid-2020, MRPV implemented a new project delivery model called the Program Delivery Approach (PDA). The PDA offers the ability for a portfolio approach to the delivery of projects. The objectives of the PDA are to;

- Create a more sustainable contractor market, by engaging with the appropriate industry partner based on their capacity and capability.
- Improve the efficiency of project procurement resulting in saving time and minimising State and contractor costs.
- Improve project outcomes, contractor performance and optimise value through a more collaborative approach to procurement and delivery, by incentivising contactor performance, both financially and via future opportunities.

The PDA model awards projects to pre-qualified contractors and designers based on their capability, capacity, past performance, and ability to deliver value-for-money solutions. These pre-qualified companies have been assigned to MRPV's Construction and Design Panels. The panels divide industry partners into broad groups based on their capability.

Once selected, a contractor will follow a two-staged delivery model under the PDA, entering into a Project Development Phase to determine the scope and value of the project, and then the Project Delivery Phase once contracts are executed. A designer is engaged by the contractor in a sub-contract agreement similar to a traditional D&C model. The appointment is made after the award of the project to a contractor and before the start of the Project Development Phase, such that MRPV, the contractor and design all work collaboratively through both phases of the delivery model.

At its core, the PDA approach features elements of both the Alliance, and Design and Construct (D&C) project delivery models. The initial Project Development Phase is similar to Alliancing, whereby scope, risks and opportunities are shared and resolved with input from MRPV, contactors and designers. Once the contract is executed, the model converts to more of a traditional D&C, however payment is through an Incentivised Target Cost (ITC) payment mechanism, which reimburses direct costs and includes cost and non-cost incentives through a performance regime. However, a significant difference of the PDA model from current forms of delivery models is the projects are managed as a program of works enabling a more sustainable contractor and designer market.

The benefits of the PDA model for industry include;

- a more sustainable supply of projects for industry partners and their supply chain;
- creation of long-term competition based on performance rather than short term, cost driven competition;
- improved cost certainty through the reimbursement of all direct costs;
- better sharing and allocation of risk to the party best able to manage the risk;
- streamlined procurement processes leading to reduce procurement time and costs;
- streamline procurement processes and, in so doing, maximise efficient engagement of contractors and consultants of all tiers to perform works;
- enable more Front End Engineering and Design (FEED), investigations and assessment of project specific risks; and,
- better integrated project planning and project delivery through collaboration between government and industry.

When considering barriers to innovation, the PDA model has a number of key features that foster and enable creativity and allow new technology to be more easily adopted by projects, as well as shared with the broader industry. The key features of the PDA model to enable innovation are explored further in the following sections and include increased collaboration, risk mitigation and sharing, and incentivisation for innovation.

5.1 Collaboration

A significant feature of the PDA model is the closer collaboration between industry (both contractors and designers) and government, as well as the supply chain partners critical to the projects delivery.

By engaging a single team through the project development phase, risk and opportunities can be rigorously assessed and mitigated, which would not normally be achieved in a more traditional D&C projects. Further, the collaboration between government and industry means that risks can be assigned to the party best able to mitigate those risks. It also enables a greater adoption of innovation, with industry and key suppliers able to bring forward ideas, with MRPV facilitating and enabling the adoption of the innovation.

5.2 Risk Mitigation and Sharing

Risk and risk management is dealt with very differently in the PDA model when compared with traditional D&C contracting. Considering only a single contractor and designer is taken through the project development phase with MRVP to develop a target outturn cost (TOC), it enables a shared understanding and contribution to risk mitigation. The eventual aim of the TOC development is to understand and eliminate risk by utilising resources, knowledge and relationships across both government and industry. Traditionally, in a D&C environment a contractor would assign a cost to items or scope they could not effectively mitigate or eliminate the risk. Whereas, in the PDA model, with input from MRPV, project teams work to identify and mitigate or eliminate all risk during the TOC development.

When considering the barriers to innovation, this model enables novel problem solving and innovative solutions to reduce or remove risk during the development phase of the project. Further, MRPV is able to draw on innovative solutions from across the industry to facilitate solutions for individual projects.

5.3 Incentives for Innovation

The final feature of the PDA model that encourages innovation is the use of financial and non-financial incentives for those projects that develop and adopt innovative solutions. Specifically, there is a KPI (key performance indicator), for both contractors and designer who develop innovative initiatives for not only the project, but that can be adopted more broadly in the industry. The assessment of the innovation KPI is based on the type of innovation(s) adopted, and defined as;

- **Continuous improvement** is defined as an initiative which is a continuous improvement initiative within the project. This is the lowest level of innovation that will trigger the KPI.
- **Innovation adoption** is an initiative which is adopted from another project. This is the starting point for more broader industry wide innovation and encourages teams to look at the practices of other projects to implement a new technology, process or system.
- **Industry application** is the highest level achievable within the KPI and is defined as an initiative which has industry wide application.

Contractors and designers are judged on the number and type of innovations adopted by the project, and given short term financial incentives, as well as longer non-financial incentives related to their ongoing performance.

6 MODERNISING STANDARDS AND SPECIFICATIONS

The second key initiative MRPV are undertaking to drive innovation at the industry level is through a program of modernising and updating standards and specifications. It is acknowledged that much of the work associated with this initiative is done in conjunction with the Department of Transport (DoT), who are the owner and operator of the assets delivered by MRPV.

A significant barrier to new products and new technologies is that standards and specifications don't allow or even consider the application of these emerging materials or concepts. This is a result of standards and specification being largely prescriptive in nature, where the minimum requirements define the inputs and describe what must be done to achieve the requirements. Prescriptive standards and specifications are best suited to situations where a high level of control is required and appetite for risk is low. However, under this framework, changes in technology or methodologies can not be easily adopted as it is unlikely the prescriptive standards or specification would have accounted for future innovations.

In an innovative culture, regulations (including standards and specifications) should be flexible and adaptive to enable changes in technology and new practices. This is achieved using performance-based standards and specifications which focus on the requirement outcome. Under this framework, products much achieve a minimum performance using which ever means they wish. Typically, the performance-based standard or specification will require a series of tests to be undertaken to verify the product, process or system achieves the minimum requirement. The risk with this approach is that the suite of performance requirements may not account for a behaviour or outcome that was not intended to be achieved.

In practice, it is very difficult to write a standard or specification entirely using a performance-based framework. Therefore, what more commonly happens to enable an innovative culture, is that standards and specifications are written predominantly with performance-based requirements and use more prescriptive-based requirements for elements deemed high risk.

Looking back at the barriers to innovation, the move towards largely performance-based standards and specifications enables removal of barriers associated with risk-aversion, regulatory requirements and bureaucratic culture. The basic premise of defining the performance outcome rather than prescriptive requirements means the basic elements that have led to risk-aversion, regulatory requirements and bureaucratic culture are retained, in that risk and uncertainty are managed, however the performance-based approach enables suppliers to propose new technologies, techniques and processes.

6.1 Key Standards and Specifications

The range of standards and specifications MRPV is working on with DoT is diverse and covers the full range of technical disciplines within the road transport sector. It includes new and updated standards and specifications for plastic noise walls and slip form barriers, as well as guidelines for application of spray seal pavements. However, the focus of this paper is a couple of initiatives associated with geotechnical aspects of road infrastructure, including trialling the use of intelligent compaction for road pavement, and creating a new technical specification for recycled organics.

6.1.1 Intelligent Compaction

Compaction is the process whereby material is placed in layers and compressed to increase the density and uniformity of the pavement material. Compaction is achieved by a roller and applied to all layers within a road profile (e.g. subgrade through to asphalt).

Currently, the most widely used technique used to confirm the achievement of compaction is a combination of in-situ spot test with a nuclear gauge density device and proof rolling. These methods are limited in that they only evaluate a small portion of the entire road composition (e.g. approximately 1 %) and as a result may miss weak or unqualified compaction areas.

Intelligent Compaction (IC) is a compaction technology that uses "vibratory rollers equipped with the real-time kinematic (RTK) Global Positioning System (GPS), roller-integrated measurement system (normally accelerometer-based), feedback controls, and onboard real-time display of all IC measurements," (Chang et al., 2011). It is starting to be adopted in Europe, Japan and North America.

The benefits of IC include (Chang et al., 2011);

- IC allows mapping of each compaction layers to enable real-time identification of weak spots for corrective actions prior to the compaction of the upper layers.
- IC provides the means to maintain a consistent rolling pattern for 100% coverage of a construction area.
- IC enables consistent rolling patterns under lower visibility conditions such as night paving operations.
- IC technology enables digital record collection for future investigation.

In 2019, DoT developed guidelines for IC trials (Papacostas and Walker, 2019). The guidelines describe how to set-up production trial work lots for placement, compaction, testing and assessment for a single material type. Previously, the requirements within VicRoads Technical Specification 204 were prescriptive in their requirement to undertake some type of nuclear gauge testing and proof rolling.

Through support from DoT, MRPV engaged the Australian Road Research Board (ARRB) to develop a set of guidelines for project to successfully implement IC monitoring. The guidelines build on DoT's work and assist projects in the development of the testing procedure, including suggesting IC equipment, quality control processes, and supporting onsite construction methodologies.

Currently there are a few IC trials underway on MRPV projects resulting in the innovation being adopted across the industry. Further, the flexibility of the guidelines enables projects to utilise as little or as much of the IC technology as they wish.

6.1.2 Recycled Organics

As waste becomes an ever-increasing problem for governments, the Victorian Government has developed the Recycled First Policy, whereby projects are encouraged to optimise the use of recycled and reused materials. The obvious weakness of this policy is that prescriptive standards and specifications can limit the type of materials used in civil infrastructure projects. To conform to a highly prescriptive-based standard or specification, recycled materials must achieve the same inputs as their virgin material counterparts which can be unrealistic.

In the landscaping discipline, this is particularly relevant for recycled organic materials. The Australian Standard AS 4454 (2012) Composts, Soil Conditioners and Mulches specifies the "requirements for organic products and mixtures of organic products that are to be used to amend the physical and chemical properties of natural or artificial soils and growing media." The standard is largely a prescriptive-based set of requirements, where physical and chemical requirements of nominated virgin materials are described.

Recycled organic materials don't easily conform with requirements of their virgin counterparts. Specifically, recycled organic materials can vary in quality largely due to the (i) the extent of impurities within the recycled material (e.g. plastics, paper etc), and (ii) the extent of processing time allowed to create the compost or soil conditioner. To enable recycled organic materials to be used on civil infrastructure projects, MRPV in collaboration with DoT and ARRB, are in the process of developing a technical specification for recycled organics. The intent is to define the performance requirements for a range of uses of recycled organic material, that link back to the classifications used within AS 4454 (2012). These include for landscaping (e.g. planting, hydro-mulch, turf topdressing, soil conditioning, fertiliser), erosion control (e.g. soil compaction mitigation, filter berms, and compost blankets), and biofiltration (e.g. filter media). By developing a technical specification, the innovative use of recycled organics is available for all projects within the industry.

7 CONCLUSION

Government has a significant role to play in ensuring innovations flourish and thrive across industry. The risk of innovations developed by industry and suppliers being stifled by barriers imposed by government are significant. The case of encouraging innovations is compelling with drivers for innovative solutions including increased efficiency and effectiveness, reduced costs, the ability to respond to increasingly complex environments, and the ability to respond to external crisis.

To facilitate innovation, several barriers must be overcome including the public sector risk adverse culture, limited resources, failure of leadership, regulatory requirements, few rewards and incentives, and a bureaucratic culture.

MRPV has initiated two key programs that aim to reduce and remove barriers to innovation. The specific initiatives being undertaken by MRPV include the Program Delivery Approach (PDA) used to deliver projects, and a program of modernising and updating standards and specifications.

8 ACKNOWLEDGEMENTS

The author wishes to acknowledge a number of people and organisations who have been instrumental in the development and implementation of both the PDA model and modernising standards and specifications. These include Allen Garner (MRPV's CEO) and Steve Cornish (MRPV's COO) for their leadership of the MRPV PDA model, Leon Choo (MRPV's Quality Manager) for his leadership of the Intelligent Compaction trials at MRV, and ARRB and DoT support of both the Intelligent compaction trials and development of the recycled organics technical specification.

REFERENCES

Wipulanusat,W., Panuwatwanich, K., Stewart, R. A., and Sunkpho, J. (2019), "Drivers and barriers to innovation in the Australian public service: a qualitative thematic analysis." Engineering Management in Production and Services, Vol 11 (1), 7-22.

Ozorhon, B., and Oral, K. (2017) "Drivers of Innovation in Construction Projects." Journal of Construction Engineering and Management, 143 (4).

Chang, G., Xu, Q., Rutledge, J., Horan, B., Michael, L., White, D. and Vennapusa, P. (2011) "Accelerated Implementation of Intelligent Compaction Technology for Embankment Subgrade Soils, Aggregate Base, and Asphalt Pavement Materials." Federal Highway Administration, Report No. FHWA-IF-12-002.

Papacostas, A. and Walker, A. (2019), "Guidelines for Intelligent Compaction (IC) Construction Trials." Department of Transport, Victoria.

VicRoads, (2015) "Technical Specification 204: Earthworks." Department of Transport, Victoria.

Australian Standard, (2014) "AS 4454 (2012) Composts, Soil Conditioners and Mulches."

BIM to Numerical Modelling Interoperability for Geotechnical Design of Underground Metro Station

M. Q. Huang[1], X. L. Chen[2], T. J. Sia[3] and Q. B. Zhang[4]

[1]Monash University, VIC 3800, Australia, email: Mengqi.Huang@monash.edu
[2]Monash University, VIC 3800, Australia, email: Xilin.Chen@monash.edu
[3]SMEC, Melbourne, VIC 3008, Australia, email: TongJoo.Sia@smec.com
[3]Monash University, VIC 3800, Australia, email: Qianbing.Zhang@monash.edu

ABSTRACT

Building Information Modelling (BIM) is one of the important processes being adopted by the construction industry as it provides a collaboration platform in conjunction with technical standards for interoperability over the lifecycle of an asset. However, geotechnical analysis engaging numerical tools has yet to leverage the BIM benefits due to the lack of effective interoperability means, which not only results in unnecessary remodelling and rework at a cost of labour and computational waste, but also with possibility of errors, misinterpretation and omission of information. Using a trinocular underground station as an example, a workflow underpinned by heuristic techniques is proposed to enhance the interoperability between a BIM design authoring tool (Revit) and a numerical modelling tool (FLAC3D) for geotechnical analysis. A BIM-based multiple LoD (levels of detail) model framework is proposed to represent different information requirements for different purposes of BIM use throughout the project lifecycle. Leveraging the associated geometry and semantics, techniques of parametric modelling, data manipulation via visual and traditional programming are engaged to bridge BIM and numerical modelling for geotechnical analysis on different design scenarios. The simulated results are visualised through a backward automation cycle to Revit for design optimisation. The presented solution offers and automates an error-free design-to-design workflow solution and therefore enables efficient exploration of design scenarios and design optimisation.

Keywords: Building Information Modelling (BIM), numerical modelling, automation, underground, metro station

1 INTRODUCTION

Building Information Modelling (BIM) is one of the important processes being adopted by the construction industry as it provides a collaboration platform in conjunction with technical standards for interoperability over the lifecycle of an asset (Azhar, 2011; Gu and London, 2010). While many analyses are now performed in computational environments capable of 3D representation and object-based design, there remain limitations of model-based collaboration and multidisciplinary integration in the underground construction processes, such that activities of disciplinary analyses are still performed in non-BIM environment, for example spatial coordination of geological model and infrastructure model often conducted in geographical information system (GIS) and structural analysis in numerical modelling programs (Huang et al., 2021). One important process often being excluded from the BIM environment while bearing significance to engineering success of underground construction is the geotechnical assessment based on analytical, empirical or numerical models. Heterogeneous applications are often used to complete this task without referencing to the BIM model that is supposedly the single source of information. This inadequately coordinated workflow not only results in the iterative, manual retrofitting with high labour and computational cost, but also inherits great risks of misinterpretation and omission of information (Ninic, 2021). Therefore, this paper proposes to build a link between BIM and numerical modelling to enable the prediction of geomechanical consequences of design variations via the parametric BIM modelling, parameter visualisation and optimisation, and programming. This paper focuses on improving interoperability between BIM design authoring and numerical simulation-based geotechnical analysis for an underground station from several perspectives, including identification of the information requirements on the exchange scenario of BIM design to numerical simulation for geotechnical analysis of underground station, the development of a multi-level BIM parametric station model considering the varying richness of information requirements, and the innovation of an intermediary solution based on automating information interchange workflow between design and numerical simulation for geotechnical analysis.

2 RELATED STUDIES

This section provides a brief literature review on aspects of information modelling in underground construction, multi-arch cavern design, stability analysis and existing interoperability efforts of information and numerical modelling.

Information modelling platforms developed with a modular or layered structure have been proposed in existing research (Huang et al., 2021, Koch et al. 2017, Zhu et al., 2017). The importance of geological and geotechnical information is well understood for underground construction design. However, much of this data is either proprietary or stored in formats requiring specific software to view. In order to make such information more accessible for future project planning and preliminary-stage design, some online infrastructures are built that allow public to interactively search, view and use borehole data according to their geolocations. Figure 1 illustrates an example of this type of platforms using the “Data and Information on the Dutch Subsurface (DINOloket Netherlands, 2019)”. With the increasing accuracy and data type coverage, future engineering design for underground construction could better leverage the open-source geological and geotechnical data.

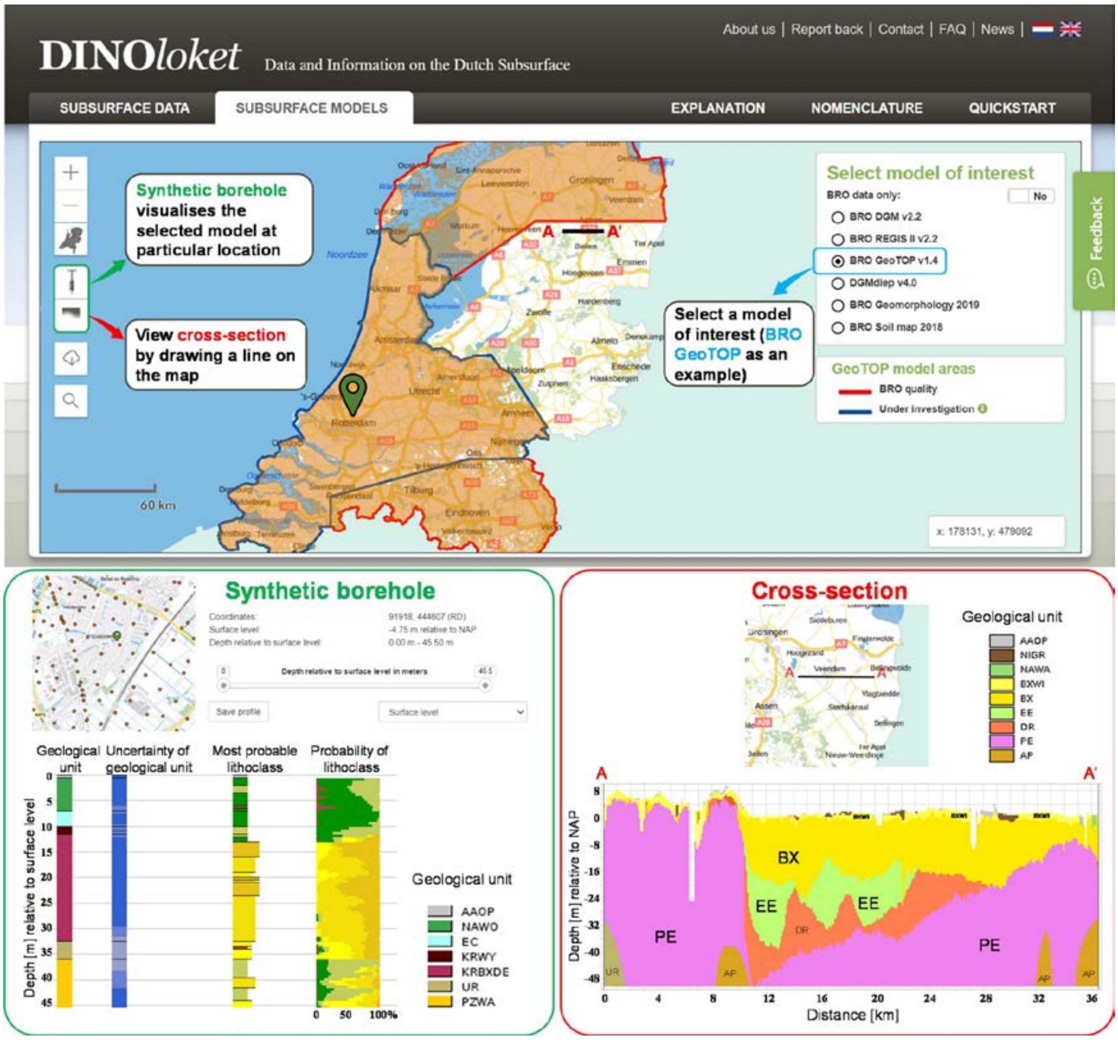

Figure 1. Demonstration of creating synthetic borehole and cross-section (Top: the main interface for user inputs including selection of model of interest, locating synthetic borehole and viewing custom-defined cross-section; bottom left: the resulted information of synthetic borehole including relevant geographical and geological data; bottom right: the cross-sectional geological information). (Huang et al., 2021)

A multi-arch cavern is a common structure adopted for underground metro stations with columns and walls providing support to the wide-span. Examples of stations using such structure include Moscow Mayakovskaya station (Shilin et al., 2016), Tokyo Kiyosumi-shirakawa Station (Konda, 2003), and Beijing Badaling Great Wall station (Li et al., 2020). Figure 2 illustrates an example of typical triple arched cavern and support systems. The construction methods or philosophies, such as sequential excavation method (SEM), sprayed concrete lining (SCL), New Austrian Tunnelling Method (NATM), and the 'Analysis of the Controlled Deformation in Rocks and Soils (ADECO-RS)' emphasised the significance of excavation and construction with adequate observation and support measures. The components prescribed in these methods should be modelled. Their mechanical properties should be taken care of given the information modelling approach is undertaken.

The stability analysis of the cavern structure is essential to geotechnical engineering. With computer software and information technology becoming easily accessible, numerical modelling methods such as the Finite Element Method (FEM), Finite Difference Method (FDM) and Discrete Element Method (DEM) have been used as common means to simulate different engineering scenarios of underground excavation and structure short-term to long-term stability. Since BIM models consist of geometry and semantics, BIM could act as a pre-modeller and post-viewer for numerical modelling, the BIM-numerical modelling interoperability, therefore, allows an error-free exchange of information between the two interfaces.

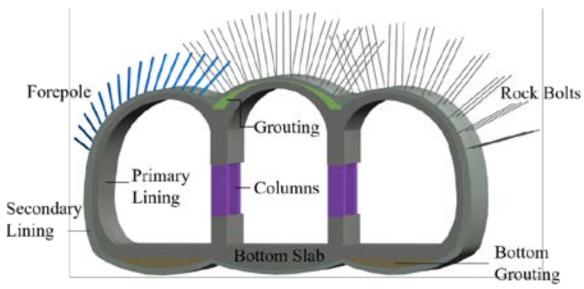

Figure 2. Example of a typical triple-arched cavern and support systems.

BIM encompasses a set of tools, technologies and processes ranging from parametric modelling (Ninic et al.,

2021) to project lifecycle management (Wang and Zhang, 2021) that are driving the digital transition of the Architecture, Engineering and Construction (AEC) industries. Many of the benefits suggested by adopting BIM and digital information technologies, such as improved visualisation and cross-disciplinary communication and collaboration, are desired for underground construction. For example, the downstream application of BIM has been investigated for tunnels. In Ninić et al.(2018, 2020 a and b), BIM-to-FEM and BIM-to-IGA workflows were developed, incorporating machine learning techniques, to deliver solutions that focus on automating model generation and simulation for numerical analysis on shield tunnelling induced settlement and decision aid on parameter optimisation in soil condition. Fabozzi et al. (2021) has also studied BIM-to-FEM and FEM-to-BIM interoperability via the use of several software tools, including commercially available rail design modelling package.

The existing research demonstrates the necessity and achievement to date of BIM uses in underground construction and solutions of bridging information modelling and numerical modelling. Nevertheless, the outlined prototypes and modelling methods have yet been generalised to facilitate the information modelling of all underground space usages. Besides, among those considered the interoperability between the information and numerical modelling, the engaged software tools may not have the built-in constitutive models to characterise the materials that make up the model or not necessarily capable of representing the large deformation of wide-span cavern structure. More specially, the workflow of Ninić et al focuses on circular tunnel in soil conditions, indicating relatively simple geometrical efforts and singular support structure (lining) involved in both BIM and numerical modelling process, and the specific meshing tool (GiD) and the research-oriented open-source simulation software program (Kratos) are engaged. Whereas the solution proposed by Fabozzi et al. (2021) is based on use of a commercialised software suite designed for railway, which could be leveraged for analyses in similar condition but may lack the versatility given that the required design or analysis exceeds the capability of the software packages.

This paper is therefore founded on the need of examining solutions to enhance interoperability between BIM authoring tool and numerical modelling software codes that are particularly suitable for cavern stability problems.

3 METHODOLOGY

Using a tri-arch underground station as an example, the information exchange between two main interfaces investigated in this paper are Revit and FLAC3D. A tri-arch station BIM model will be established under the multiple levels-of-detail (LoD) framework that intents to represent the different information requirements for the BIM model throughout the lifecycle of the construction. Leveraging the associated semantics, data mapping and parameterisation is achieved via visual programming, which also facilitates visualisation of numerical results back in the BIM environment. The two-way workflow was automated via the use of Python interface. Figure 3 illustrates the proposed workflow, which incorporates BIM-based alignment selection, visual programming generating parametric station models along with other project data to feed the exchange enabler and to allow setting of meshing parameters, initial and boundary conditions, and excavation and ground support properties.

3.1 Multi-LoD station BIM

The station model adopts the concept of "Level of Detail (LoD)", which specifies what objects are included in the model and the degree of detail with which each object is modelled (Sacks, 2018).

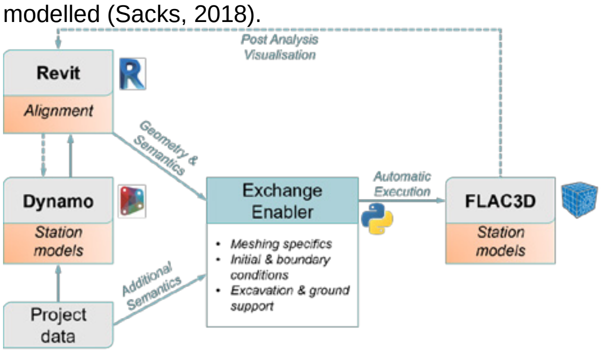

Figure 3. Workflow proposed in this paper

The LoD required for 3D modelling varies depending on the specific BIM goals and the types of model used throughout the project's lifecycle. The modelling process for any large infrastructure project, such as erecting a skyscraper in the urban centre, or constructing a train tunnel running between opposite ends of a city, often involves structures with widely differing scales, geometric appearances, and spatial arrangements. Therefore, it requires the participating engineers and designers to define carefully the LoDs for the to-be-modelled objects in order to address this peculiarity of infrastructure design.

Figure 4. demonstrates examples of a triple-arch station model with different LoD emphasising the variation of model content in terms of excavation support. At a low level of detail, it mainly includes the spatial illustration of excavation support means such as the major primary and secondary support while the high LoD-model includes physical elements of the primary (e.g. forepoling and rock bolts) and secondary support (e.g. cast-in-place concrete lining). In this study a LoD300 model is adopted for the use case of geotechnical analysis.

3.2 Parametric modelling

From a historical perspective, BIM model generation and design technology are evolved and matured based on 3D solid modelling, which represents the ability to generate and revise arbitrary 3D solid, and reaching its climax in object-oriented parametric geometry modelling. The then-state-of-art method integrated two forms of 3D solid modelling techniques, namely the boundary representation (B-rep) and the Constructive Solid Geometry (CSG), to realise functions of editing, visualising, measuring, clash detection as well as other non-editing uses (Sacks, 2018). Thereafter, the solid modelling computer-aided design (CAD) systems were improved by recognising the connectivity of shapes through sharing parameters and building links. Eventually, the realisation of automatic update and rebuilt of shapes via parametric relations marked the era of parametric geometry modelling.

Parametric modelling is adopted for reusability and extensibility, which refers to establishing intelligent objects and object assemblies described with parameters. The to-be proposed methodology largely relies on computational design concepts, which have been in use for architectural designs since emerging in the 60s, and has more or less influenced the development of BIM tools. Both parametric design and generative design are popular terms considered in the scope of computational design (Caetano et al., 2020). Establishing a component (referred to as a family in the selected BIM software), for example a bolt, based on constraints of parameters and rules denotes parametric design for a single element.

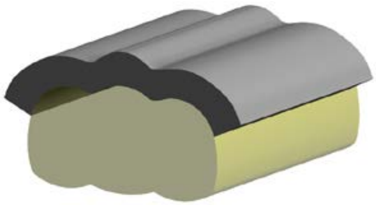

(a) LoD 100

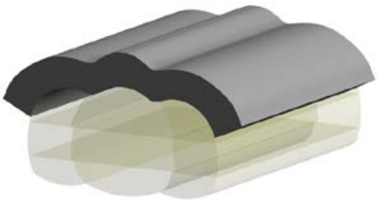

(b) LoD 200

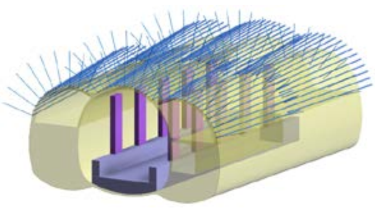

(c) LoD 300

Figure 4. A triple-arch station model with LoD 100 to LoD 300 (construction sequence and support systems are modelled)

Parametric modelling is adopted for reusability and extensibility, which refers to establishing intelligent objects and object assemblies described with parameters. The to-be proposed methodology largely relies on computational design concepts, which have been in use for architectural designs since emerging in the 60s, and has more or less influenced the development of BIM tools. Both parametric design and generative design are popular terms considered in the scope of computational design (Caetano et al., 2020). Establishing a component (referred to as a family in the selected BIM software), for example a bolt, based on constraints of parameters and rules denotes parametric design for a single element.

BIM applications and BIM enabled platforms usually provide an extensive set of predefined parametric object classes and families while allowing users to customise when a desired parametric object does not exist in the specific BIM tool. However, underground infrastructure such as the metro station often do not reflect the target functionality of most BIM tools designed for architectural and building modelling, constructing custom parametric objects and families is inevitable. Several design-based parametric families are created for this study, mainly concerning the geotechnical analysis that will be performed. Example of an outer shell and rock bolts as forms of excavation support are illustrated in Figure 5. The triple arched primary lining as the outer shell is essentially created by extrusion, which is a simple parametric modelling procedure.

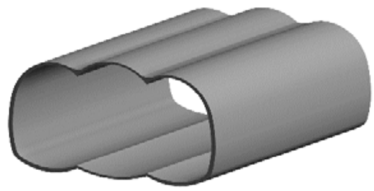

(a) Primary Lining

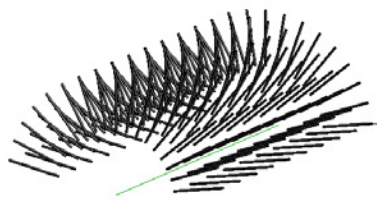

(b) Rock Bolts

Figure 5. (a) Primary lining family as a type of support and(b) assembly of rock bolt family instances.

Then, we propose to use computational design approach in conjunction with parametric modelling and visual programming to account for assembly and construction constraints. This approach holistically considers the elements and variations of elements implying regional geological conditions, excavation sequence and support installation, so that design flexibility and convenience of modification and retrofit can be achieved. Figure 6 illustrates the layout of visual programming procedures engaged to create a station model ready for geotechnical analysis.

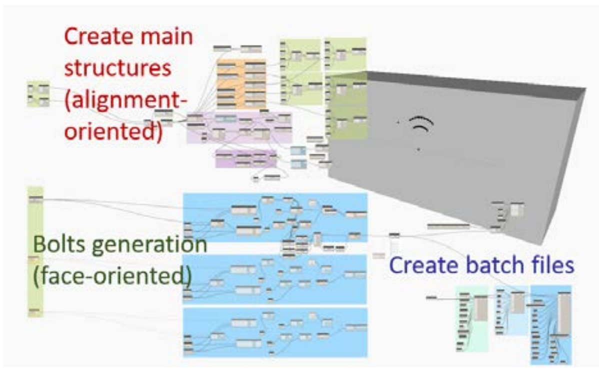

Figure 6. visual programming layout of instantiating lining, ground and rock bolts (controlled by alignment and faces) and generation of batch files for numerical simulation.

3.3 Model semantic enrichment

As aforementioned, geological and geotechnical quantification is of paramount importance to numerical simulation for ground stability analysis. The process of assigning or embedding related attributes in the geometries is regarded as semantic enrichment in BIM. In this study, we dedicated another visual programming algorithm to achieve this goal. The stored parameters for a rock bolt as an example could include density, grout-cohesion, grout-friction, grout-stiffness, yield-compression, yield-tension, and young's modulus. These properties are then read and input by Python script into numerical simulation program to perform calculation concerning geotechnical problems such as ground settlement, structural deformation and yielding.

3.4 Information exchange and process execution

The interface selected for numerical simulation for geotechnical analysis is FLAC3D, which supports a command-driven program execution and allows the use of data files (.dat format) to describe the model (Itasca, 2019). This supposedly outdated program design is actually favoured in information exchange scenarios as it makes the complete automation of program execution possible.

An exchange enabler is proposed to facilitate exchange of BIM model and automate the execution of numerical simulation. The enabler is realised by a set of Python scripts under a modular structure to allow future extensions and convenient modifications. The modules are constructed in accordance with the general solution procedure of the numerical modelling program. The processes of data file generation and process execution is illustrated in Figure 7.

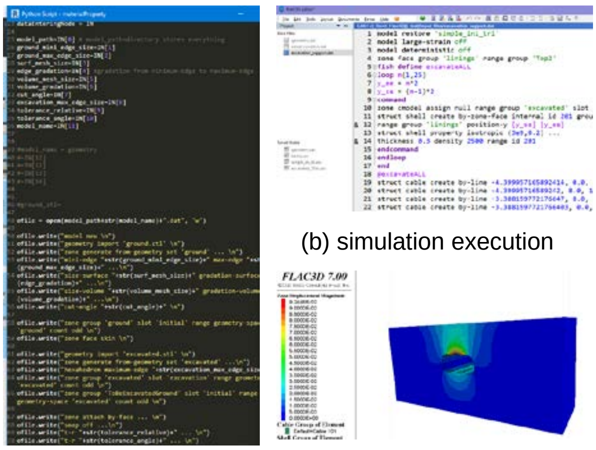

Figure 7. (a) batch file generation enabled by the exchanger; (b) program execution and (c) simulation result plotted in the numerical simulation interface.

3.5 Results Visualisation

A back-analysis loop is enabled also through a dedicated algorithm to help visualise the impacts of underground construction in the BIM native environment. By combining the settlement effect with existing structures such as buildings, existing tunnels, or geological structures, design variations could be proposed and tested following the same procedure.

Both coloured contour and mesh distortion are achieved to visualise the settlement results obtained from numerical simulation. Since parametric modelling is used, parametric study could be easily facilitated by adapting, for example, the overburden thickness, station cavern shape, lining thickness and installation pattern of ground support systems.

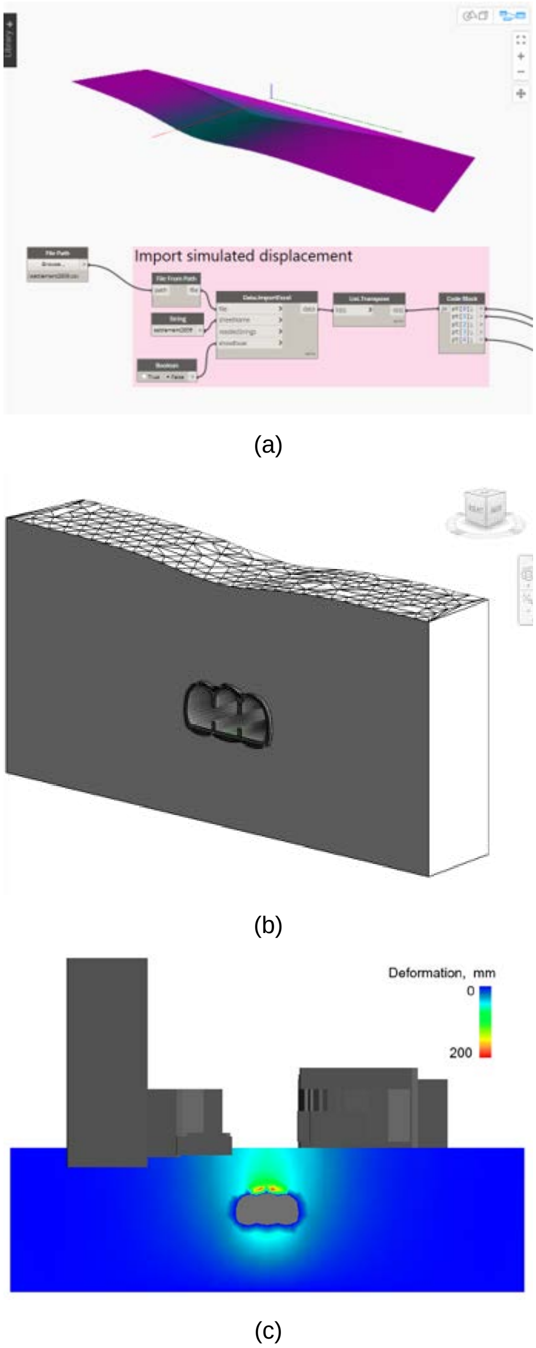

Figure 8. Visualisation with (a) contour coloured map in visual programming interface, (b)mesh distortion and (c) contour coloured map illustrating deformation of a cross-section via cutting plane perpendicular to the triple-arch cavern.

4 DISCUSSION

The workflow consisted of three parts: (1) generation of structural model of underground metro station encompassing both geometries and semantics via parametric modelling and visual programming; (2) automation of model exchange and calculation commanding by python scripts; and (3) development of a reverse loop to visualise numerical calculation results in BIM environment for further analysis, parameter optimisation and scenario refitting. The workflow is marked by its modularity and extensibility that could be easily adapted for further development. Each part is valid as a single system while creating an efficient BIM-to-numerical modelling loop for geotechnical analysis. Currently, the exchange module is developed for the specific interfaces that it is connecting, this means that certain adaptations are required if other software tools are employed for BIM and numerical simulation. Another limitation the current exchange module may suffer from is the level of complexity in meshing. The success of FEM or FDM simulation largely relies on the quality of meshes while examples used to testify the workflow have only involved relatively simple geometrical structures without comprehensive set of interfaces. A potential approach that would be investigated in the next stage is to engage a meshing program as a middle-ware or to experiment with the octree mesh in FLAC3D. Ultimately, proper translators could be developed based on BIM data schema, such as the industry foundation class (IFC). There is yet standard for underground construction based on IFC while research and development efforts are ongoing by buildingSMART, an international industry body aiming at improving interoperability between software applications used in the construction industry, cooperating with other organisations focusing on subsurface utilisation, such as the International Tunneling and Underground Space Association (ITA-AITES).

5 CONCLUSION

This study aims to provide a solution to tackle the problem of lacking open standard data models that cover the context-specific knowledge required for underground construction. By leveraging the parametric modelling technique of BIM, the workflow could mitigate the efforts of numerically retrofitting and re-modelling at feasibility and earlier design stage. The enabled a design-to-design workflow with the reversed visualisation loop creates opportunity for backanalysis and design optimisation.

6 ACKNOWLEDGEMENTS

This work was financially supported by the ARC Nanocomm Hub (IH150100006). The first author would like to acknowledge the Australian International Postgraduate Research Scholarship and Monash Graduate Scholarship. The technical information and photos used in this paper are from the Metro Tunnel Project in Melbourne (https://metrotunnel.vic.gov.au), and the models are partially supported by the Government and Industries.

REFERENCES

Azhar, S., 2011. Building Information Modeling (BIM): Trends, Benefits, Risks, and Challenges for the AEC Industry. Leadership and Management in Engineering 11, 241-252.

Caetano, I., Santos, L., Leitão, A., 2020. Computational design in architecture: Defining parametric, generative, and algorithmic design. Frontiers of Architectural Research 9, 287-300.

DINOloket Netherlands, 2019. Data and Information on the Dutch Subsurface, Data en Informatie van de Nederlandse Ondergrond (DINO), p. 10. https://www.dinoloket.nl/en/subsurface-data

Fabozzi, S., Biancardo, S.A., Veropalumbo, R., Bilotta, E., 2021. I-BIM based approach for geotechnical and numerical modelling of a conventional tunnel excavation. Tunnelling and Underground Space Technology 108, 103723.

Gu, N., London, K., 2010. Understanding and facilitating BIM adoption in the AEC industry. Automation in Construction 19, 988-999.

Huang, M.Q., Ninić, J., Zhang, Q.B., 2021. BIM, machine learning and computer vision techniques in underground construction: Current status and future perspectives. Tunnelling and Underground Space Technology 108, 103677.

Koch, C., Vonthron, A., König, M., 2017. A tunnel information modelling framework to support management, simulations and visualisations in mechanised tunnelling projects. Automation in Construction 83, 78-90.

Konda, T., 2003. Reclaiming the underground space of large cities in Japan, Proceedings of the ITA World Tunnelling Congress, pp. 1-13.

Li, R., Zhang, D., Fang, Q., Liu, D., Luo, J., Fang, H., 2020. Mechanical responses of closely spaced large span triple tunnels. Tunnelling and Underground Space Technology 105, 103574.

Ninic, J., Alsahly, A., Vonthron, A., Bui, H.-G., Koch, C., König, M., Meschke, G., 2021. From digital models to numerical analysis for mechanised tunnelling: A fully automated design-through-analysis workflow. Tunnelling and Underground Space Technology 107, 103622.

Ninić, J., Bui, H.G., Meschke, G., 2020a. BIM-to-IGA: A fully automatic design-through-analysis workflow for segmented tunnel linings. Advanced Engineering Informatics 46, 101137.

Ninic, J., Giang Bui, H., Meschke, G., 2018. Parametric Design and Isogeometric Analysis of Tunnel Linings within the Building Information Modelling Framework. CEUR Workshop Proceedings.

Ninić, J., Koch, C., Vonthron, A., Tizani, W., König, M., 2020b. Integrated parametric multi-level information and numerical modelling of mechanised tunnelling projects. Advanced Engineering Informatics 43, 101011.

Sacks, R., Eastman, C., Lee, G., Teicholz, P., 2018. BIM handbook: A guide to building information modeling for owners, designers, engineers, contractors, and facility managers. John Wiley & Sons.

Shilin, A., Kirilenko, A., Znajchenko, P., 2016. Complex reconstruction project of Mayakovskaya metro station in the centre of Moscow. Structural Analysis of Historical Constructions—Anamnesis, Diagnosis, Therapy, Controls; Van Balen, K., Verstrynge, E., Eds, 1736-1741.

Wang, G., Zhang, Z., 2021. BIM implementation in handover management for underground rail transit project: A case study approach. Tunnelling and Underground Space Technology 108, 103684.

Zhu, H., Wu, W., Li, X., Chen, J.Q., Huang, X.B., 2017. High-precision acquisition, analysis and service of rock tunnel information based on iS3 platform. Chin. J. Rock Mech. Eng. 36. 2350–2364.

On best practices for trackbed design

N. Yousefpour, PhD, PE[1]

[1]Department of Infrastructure Engineering, The University of Melbourne; Arup, Melbourne, VIC, Australia; email: negin.yousefpour@unimelb.edu.au

ABSTRACT

This paper reviews the best practices of trackbed design for railway projects. Various existing methods have been studied and recommendations for more economical design are provided. The analytical/empirical methods from various standards such as UIC, AREMA, British Rail, and Australian standards, as well as other commonly used methods such as Raymond and Li-Selig are compared based on a typical track embankment cross section. The outcome was then evaluated against 2D and 3D numerical models. Incorporating numerical methods is shown to render considerable reductions in the required prepared subgrade/structural fill materials and allow for assessment of long-term design issues, such as subgrade shear failure due to excessive plastic deformations.

Keywords: Trackbed Design, 3D Numerical Modelling, Best Practices, Railway Standards

1 INTRODUCTION

With major ongoing and emerging rail projects across the world and in Australia, the rail infrastructure industry seeks innovative solutions to provide sustainable and cost-effective design solutions. Proper engineering design of track-bed and track formations is one of the key components for effective design and operation of railways and minimizing the construction and maintenance costs.

This paper presents a review on various common analytical and empirical methods and standards for track-bed and track formation design. The variations in the design outcomes using these methods are investigated. In addition, the application of innovative solutions including advanced nonlinear finite element method (FEM) analysis and subgrade stabilisation for optimizing the track formation design is discussed.

2 TRACKBED AND TRACK FORMATION

A typical track embankment cross-section is presented in Figure 1. The main function, typical dimensions, and typical material properties for all the required layers are defined in Table 1. Ballast and subballast are normally defined as “trackbed” laying on top of the ‘track formation,” which is the natural subgrade [1].

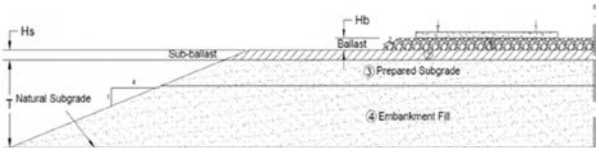

Figure 1. Trackbed and formation typical section

3 ANALYTICAL AND EMPIRICAL DESIGN METHODS AND STANDARDS

3.1 UIC method

UIC [1] requires the following items to be considered in dimensioning the track bed layers:

- Problems of frost protection
- Bearing capacity of subgrade
- Type and spacing of sleepers
- Traffic characteristics

The UIC method of estimating the suggested minimum thickness of the trackbed layers including is depicted in Figure 2. Table 2 provides the method of determination of subgrade bearing capacity class and required prepared subgrade class and thickness.

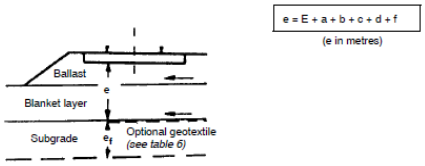

Fig. 15 - Calculation of minimum thickness (e) of track bed

E	= 0,70 m	for soils of bearing capacity class P1[a]
E	= 0,55 m	for soils of bearing capacity class P2[a]
E	= 0,45 m	for soils of bearing capacity class P3[a]
a	= 0	for UIC groups 1-4[b]
a	= - 0,10 m	for UIC groups 5 and 6[b]
b	= 0	for wooden sleepers of length 2,60 m
b	$= \frac{2,50 - L}{2}$	for concrete sleepers of length L (b in m, L in m; b possibly negative if L > 2,50 m)
c	= 0	for usual dimensions
c	= - 0,10 m	special case for difficult working conditions on existing lines
d	= 0	when the nominal maximum axleload of hauled vehicles does not exceed 200 kN (see *UIC Leaflet 700*)
d	= + 0,05 m	when the nominal maximum axleload of hauled vehicles does not exceed 225 kN (see *UIC Leaflet 700*)
d	= + 0,12 m	when the nominal maximum axleload of hauled vehicles does not exceed 250 kN (see *UIC Leaflets 700 and 724*)
f	= +	the track bed should include a geotextile if the prepared subgrade is formed from soils of quality class QS1 or QS2[c]
f	= 0	(no geotextile is required) if the prepared subgrade is formed from soils of quality class QS3[d]

a. The bearing capacity classes are defined in table 6.
b. The UIC groups are defined in UIC Leaflet 714 (edition of 1.1.89) (see Bibliography).
c. See NB in point 2.6 - page 40
d. The UIC soil quality classes are defined in table 5.

Figure 2. UIC method of calculating the minimum thickness of trackbed layers [1]

3.2 AREMA method

AREMA [2] recommends the Talbot equation for estimating the thickness of the granular trackbed (i.e. ballast + sub-ballast). This method was developed based on field tests conducted in 1910s and 1920s. Subgrade conditions, heavier axle loads, dynamic effects, and granular material quality are factors that have not been considered in this method.

$$H = 0.24\ (P_m/P_c)^{0.8}$$

Where,
H is the granular material thickness (Ha + Hs),
P_c is the allowable subgrade stress (138 kPa recommended by AREMA), and P_m is the vertical stress applied on the ballast surface.

Table 1: Trackbed and formation layers

Track layer	Main functions	Typical thickness	Typical material
Ballast	-Transfers and distributes loading from the ties to the underlying subballast or subgrade of the track structure at a tolerable level. -Provides drainage through the support structure and away from the track	300 – 450 mm	Crushed rock/aggregates with maximum size of 63.5 mm (2.5 in)
Subballast/Capping	-Providing a filter/buffer between subballast and subgrade -Drainage	150 mm	Crushed rock/aggregates the maximum grain size of the subballast shall not exceed the maximum grain size of the track ballast and no more than 5% of the subballast shall pass the No. 200 sieve.
Prepared Subgrade/Structural Fill	An additional layer on top of the fill or natural subgrade to further reduce the stress on subgrade and also to provide sufficient overall stiffness	0-500 mm (varies depending on the subgrade strength)	Varies with different standards: well-graded coarse-grained material with low to medium plasticity and maximum 15% to 30% fine-grained
Embankment Fill	Provide the required track level	Depends on the track level design wrt the existing ground	Should be free of unsuitable material: -Materials containing stumps, weeds, leaves, coals, peats, ashes, grasses, and other organic materials. -Contaminated soil -Material with soaked CBR[1] <2% and swell index[2] >3 %
Natural Subgrade	Foundation to the trackbed	NA	Must have a minimum of CBR=2 %; Should be free of unsuitable material as per above

1. 95% Standard compaction – 9 kg Surcharge
2. ASTM D4546 – 14e1 “Standard Test Methods for One-Dimensional Swell or Collapse of Soils”, Test Method A.

Table 2: Determination of subgrade bearing capacity and prepared subgrade thickness

Subgrade/ Fill Soil Quality[1]	Min. CBR[2] (%)	Req. Bearing Class for Subgrade[1]	Prep Subgrade Quality Class	Prep Subgrade Min. CBR[3]	Min. thickness: “ef” (m)
QS1	2-3	P2 P2 P3	QS2 QS3 QS3	5 10-17 10-17	0.5 0.35 0.50
QS2	5	P3	QS3	10-17	0.35
QS3	10-17	P3	QS3	10-17	NA

1. QS0: “Unsuitable”, QS1/P1: “Poor”, QS2/P2: “Average”, QS3/P3: “Good”. Refer to [1] for details
2. CBR of the in-situ (soaked)
3. CBR of remoulded samples (soaked)

3.3 Raymond Method

Raymond (1985) [3] modified the design method recommended by AREMA. Figure 3 shows the design chart developed by Raymond for vehicles weighing 70-125 tons. The following assumptions have been made in the development of this method:

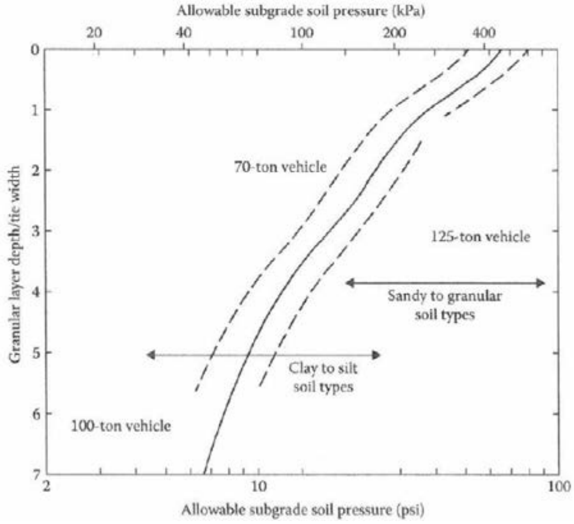

Figure 3. Raymond design chart

- Ballast, sub-ballast + subgrade act together as a single homogenous layer
- Uses a single value of axle load disregarding the amount of cumulative tonnage

3.4 British Rail Method

Heath et al. (1972) [4] developed a threshold stress design method for selecting the granular layer thickness. The threshold stress is the limit stress in the subgrade to protect the subgrade from progressive shear failure (See Figure 4).

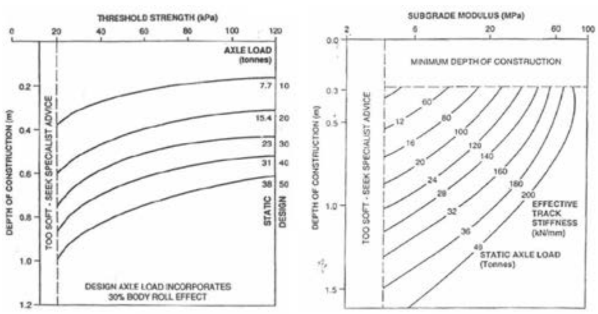

Figure 4. Subgrade threshold stress for selecting granular layer thickness [4]

3.5 Li-Selig Method

The Li-Selig Method (1998) [5,6] can be used based on the allowable stress at the subgrade surface (allowable cumulative plastic strain), as well as the allowable subgrade deformation. Figure 5 provides examples of design charts. In these charts, H is granular material thickness. I_ε and I_p are referred to as the strain influence factor and the deformation influence factor, respectively:

$$I_\varepsilon = \frac{\sigma_{da} A}{P_d}$$

$$I_\rho = \frac{\rho_a / L}{a(P_d/\sigma_s A)^m N^b} \times 100$$

Where, σ_{da} is the allowable deviator stress at the subgrade surface, ρ_d is the allowable total subgrade plastic deformation for the design period, N is the total equivalent number of load repetitions during the design period, P_d is the design dynamic wheel load, σ_s is the soil compressive strength, a, m, and b are the material parameters dependent on soil type, A is the area factor selected to make deformation influence factor dimensionless, (0.64m^2, 1000in^2), and L is a factor to make charts dimensionless (6in, 0.152m).

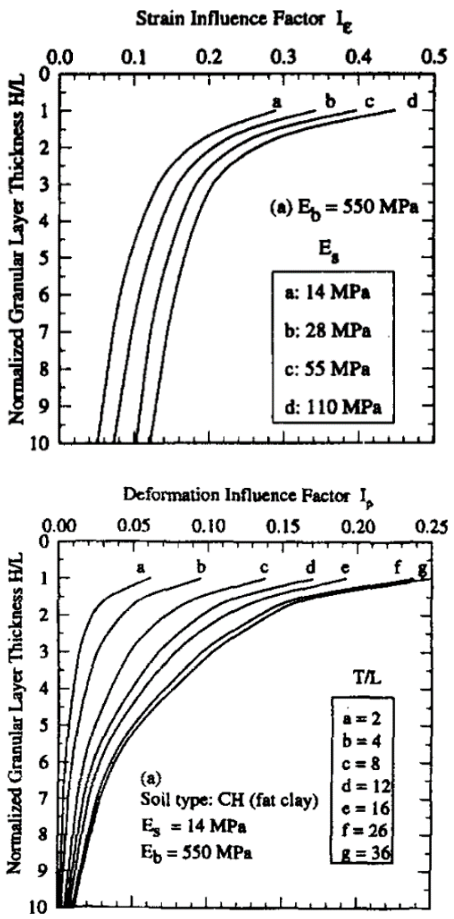

Figure 5. Li-Selig example design charts [5]

Two main failure mechanisms were considered for the development of this approach:

1) Subgrade progressive shear failure (Figure 6): This has been reported by the European railways and in the United States for track under heavy axle loads especially on fine-grained soils without sufficient granular layer thickness. This normally causes a heave at trackside which can block the proper drainage. Water coming from the granular layer can be trapped in the subgrade depression areas which can aggravate the failure.

2) Excessive Plastic Deformation due to Repeated Loading: This can cause ballast pockets under the track (Figure 7) and happens predominantly in soft soil subgrades.

Other types of failure include mud pumping, excessive consolidation settlement, and slope stability failure. The granular layer thickness does not influence these [5].

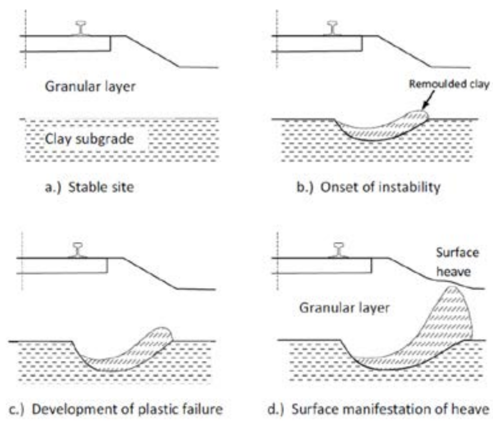

Figure 6. Subgrade progressive shear failure

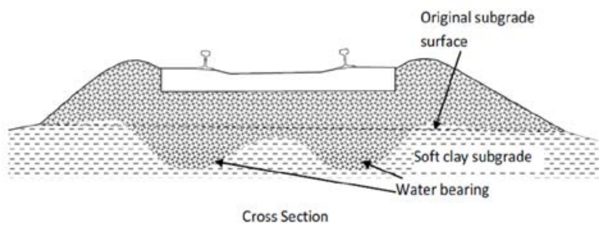

Figure 7. Excessive plastic deformation due to repeated loading [5]

3.6 Australian Standards

ARTC and ASA [7,8], VLine [9] and MTM [10] standards provide relatively similar guidelines for trackbed design. A minimum of 0.3m ballast and 0.15m subballast or capping is recommended (total granular layer thickness of 0.45m). Typical thickness/depth for the prepared subgrade/structural fill layer is provided based on the CBR of the natural subgrade as presented in Table 3.

Table 3: Structural Fill/Prepared Subgrade Depth (m) per Australian Standards

Subgrade/Fill Material Soaked CBR (%)	ARTC/MTM[1]	VLine
1-2	1	NA[2]
2-3	1	1
3-5	0.5	0.5
5-7	0.5	0.3
≥8	0.5	0/0.2

1. Minimum subgrade CBR is 3% by MTM, 2% by VLine, 1% by ARTC
2. Minimum fill CBR is 2% by VLine
3. 0mm for subgrade, 200mm for fill

Go to table of contents

3.7 Comparison of Methods

An example is worked based on the discussed methods in this section to compare the required thickness of the granular layer (H=Hb+Hs) from different methods. The example is based on an axle load of 160 kN. It is assumed that granular layer will lay on an underlaying layer with QS2 soil quality with CBR~5% (~150kPa). Table 4 provides the estimated required thickness ranging between 0.4m to 0.5m.

Table 4: Granular layer thickness from various methods/standards

Method	Ballast+Sub-ballast Thickness (m)
UIC	0.5
AREMA	0.4
Raymond	0.4
British Rail	0.45
Li-Selig	0.45
Australian Standards	0.45

The required prepared subgrade thickness is 0.35m based on UIC specifications. Based on Australian standards a thickness of 0.5m is required.

4 FINITE ELEMENTS METHOD

4.1 Finite Element Method

In the previous sections, it was shown how various methods and standards can result in different thickness values for trackbed layers.

With the current computational capabilities, 3D finite element methods (FEM) can help engineers with more economic and more reliable design. Following sections provides the result of a 3D train embankment model using LS-Dyna in comparison with a 2D Plaxis model. The impacts of cyclic degradation in subgrade has not been considered.

4.2 Geometry

Figure 8 presents the isometric and cross section view the 3D model for a track embankment cross section from a project in Victoria. The length of the model is about 25m equal to the length of a train car. The trackbed includes a 0.3m ballast, underlain by a 0.15m subballast/capping layer over a prepared subgrade/structural fill. The natural subgrade is assumed to have a CBR=3.

As shown in the analytical example above, this condition renders a structural fill of 0.5m according to Australian standards. However, in this case, a 0.3m of prepared subgrade from stabilised subgrade material with CBR=15 has been proposed to replace the structural fill to save on cost. Using a Ls-Dyna model, the proposed design is being validated by checking the stress and strain developed in the subgrade and by checking for bearing failure.

The train loading assumes a 23 tons axle load (two bogies, four axles per car), resulting in 450kN/m linear load for each wheel applied on top of the rail track over the length of a sleeper (0.25m) (see Figure 9).

4.3 Material Model

An Elasto-Plastic, Mohr-Coulomb constitutive model was implemented, adopting material parameters as per Table 5. The water table was not considered within the model, assuming a dry subgrade (zero pore water pressure).

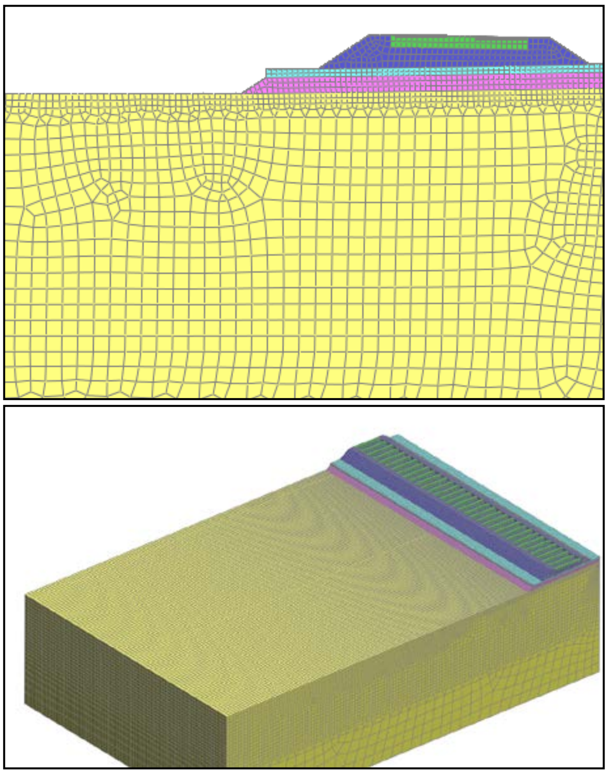

Figure 8. Isometric and cross section view of the track formation

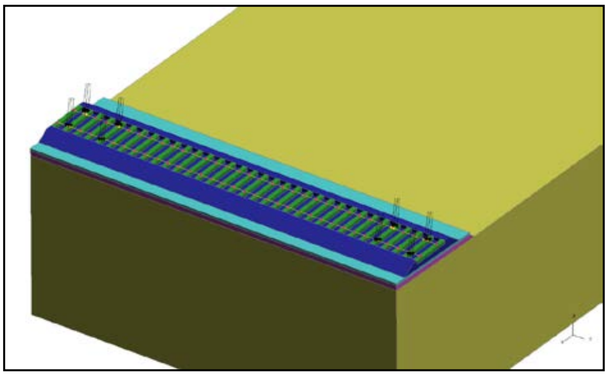

Figure 9. Train loads

4.4 Results

A summary of model outputs, including stress and strain distribution, as well as deformations and plastic strains are provided below (see Figures 10 to 14). The shear stress within the subgrade is below 15 kPa and the vertical stress is below 50 kPa, the subgrade allowable stress, hence no plastic stain is observed. The deformation at the sleeper level shows to be less than 5 mm, which is below the common acceptable criteria of 10 mm (1/2 in). This validates the proposed design of 0.3m prepared subgrade with higher CBR, instead of the 0.5m structural fill with CBR=8 required by Australian standards.

Results of LS-Dyna model was then compared with an equivalent Plaxis 2D model of the longitudinal cross section. As shown in Figure 15 and 16, the 2D model shows a maximum stress of 140 kPa in ballast, about 20% lower stress as compared with 3D LS-Dyna. Similarly, looking at the shear stress distribution, from Ls-Dyna the maximum shear stress is around 15 kPa in the subgrade and around 27 kPa in the prepared subgrade layer, whereas Plaxis shows maximum of 12 kPa in subgrade and 40kPa in the prepared subgrade. The 2D model underestimated the maximum stress, hence the deformations, in the trackbed layers.

Table 5: Track formation material properties

Layer	Friction Angle	Cohesion	Undrained Shear Strength	Unit Weight	Young's Modulus	Poisson's Ratio
	Deg	kPa	kPa	kN^3/m	MPa	
Ballast	40	0	0	23	280	0.3
Sub-ballast	35	0	0	23	150	0.3
Prepared Subgrade (CBR=15)	0	0	250	20	200	0.3
Natural Subgrade (CBR=3)	0	0	50	19	30	0.3

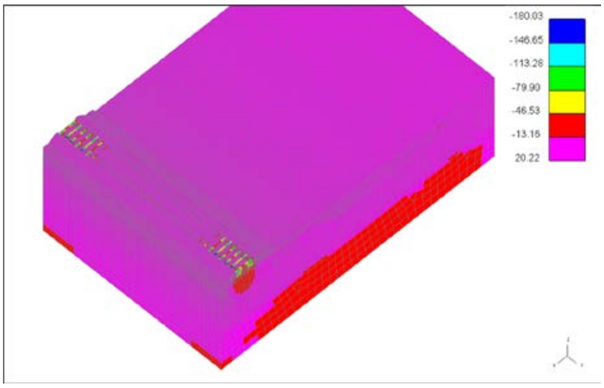

Figure 10. Stress under the sleepers

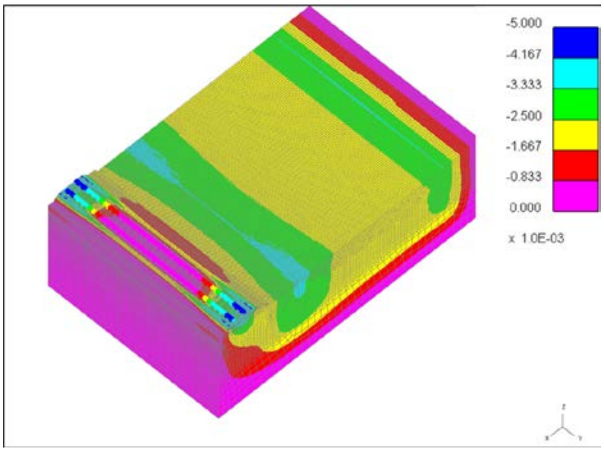

Figure 11. Vertical deformations

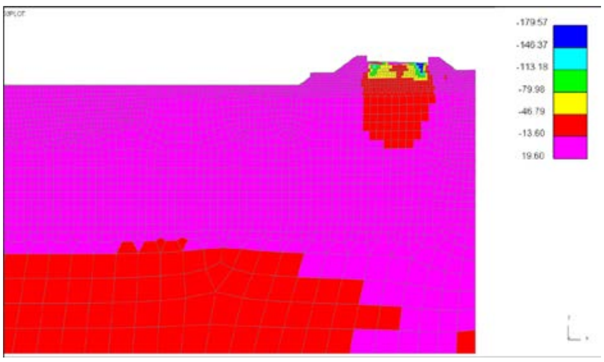

Figure 12. Vertical stress

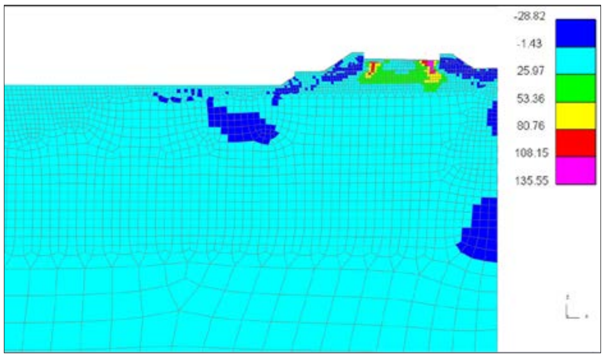

Figure 13. Von-Mises stress (=2 × shear stress)

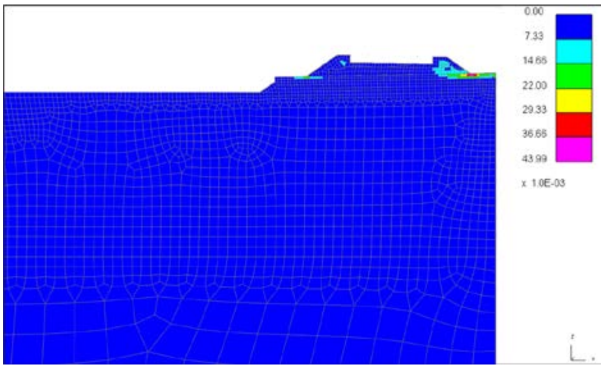

Figure 14. Plastic strains

5 CONCLUSIONS

Among the discussed analytical design methods, Li-Selig is the only method that considers both allowable stress and deformation at subgrade with respect to the train loading cycles, providing a more reliable trackbed design. Incorporating 3D numerical

simulations, can further improve the design, by providing a more accurate assessment of stress distribution and deformations in the subgrade, resulting in potential reduction of the required depth for the structural fill/prepared subgrade layer on soft natural subgrades.

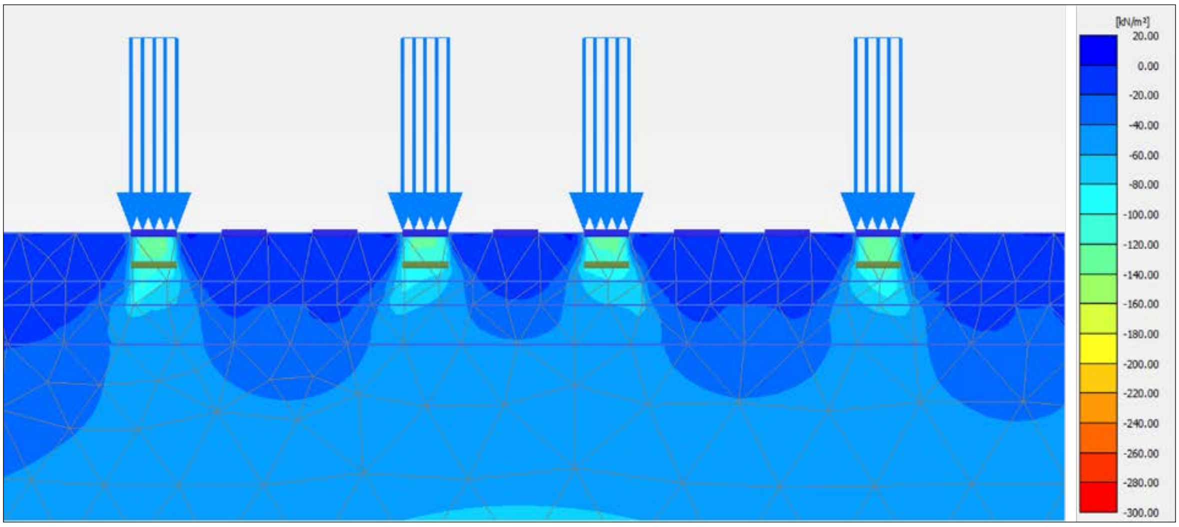

Figure 15. Vertical stress – Plaxis 2D

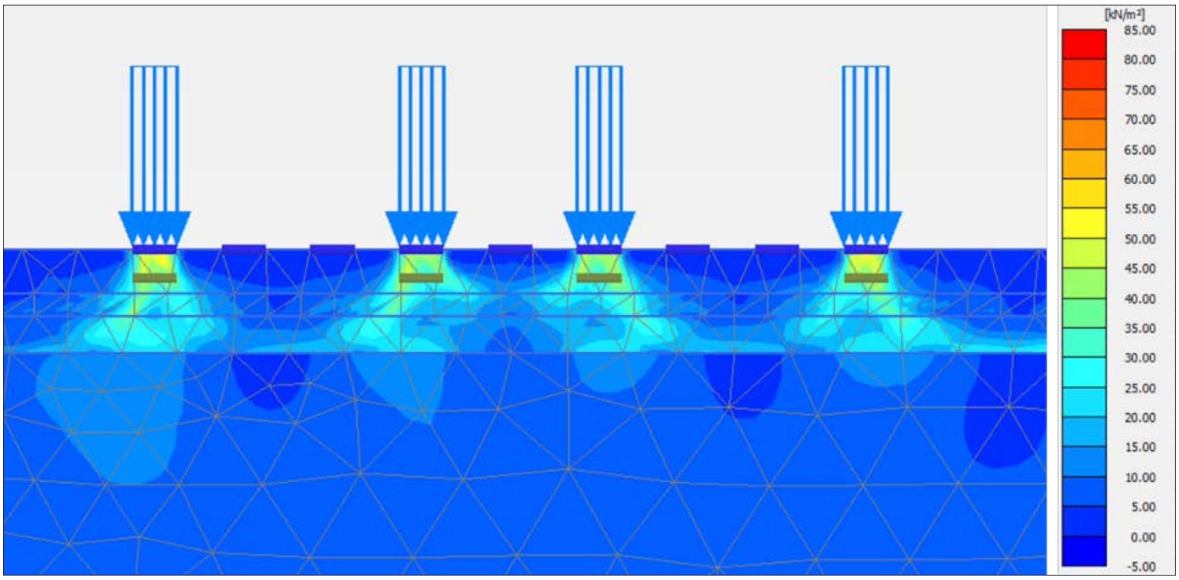

Figure 16. Shear stress – Plaxis 2D

These methods also allow for identifying potential long-term issues with bearing failure or excessive plastic strain due to cyclic loading. Although it is common for clients to demand compliance with standards, there is often provisions for applying more rigorous design methods beyond the standards by getting client approvals for derogations in early phases of a project.

6 ACKNOWLEDGEMENTS

This study was sponsored by Arup University.

REFERENCES

UIC (International Union of Railways), Earthworks and Trackbed for Railway Lines, Code 719, 3rd Edition, 2008.

AREMA (American Railway Engineering and Maintenance-of-Way Association), 2015.

Raymond, G. P., design of railroad ballast and subgrade support, Journal of the Geotechnical Engineering Division, ASCE, Vol. 104, No. GT1, 45-59, 1985.

Heath, D. L., Shenton, M. J., Sparrow, R. W., and Waters, J. M., Design of Conventional Rail Track Foundations, Proceeding of Institution of Civil Engineering Vol. 15, 251-267, 1972.

Li, D. and Selig, E., Method for Railroad Track Foundation Design. I: Development, Journal of Geotechnical and Geoenvironmental Engineering, ASCE, 316-322, 1998.

Selig, E. and Waters, J. M., Track Geo-technology and Substructure Management, Thomas Telford, 1995.

ARTC (Australien Rail Track Corporation), Track & Civil Code of Practice, Railway Earthworks - Supplementary Appendix, ETC-08-02, 2006.

ASA (Asset Standards Authority) Earthworks and Formation Standard, Version 1.0, 2018. Supplementary Appendix to ARTC.

VLine, Network Infrastructure Standard (NIST) 2659, Earthworks and Drainage Standard, 2019.

MTM (Metro Train Melbourne), Earthwork and Formation Specification, L1-CHE-SPE-178, Version 2.0, 2018.

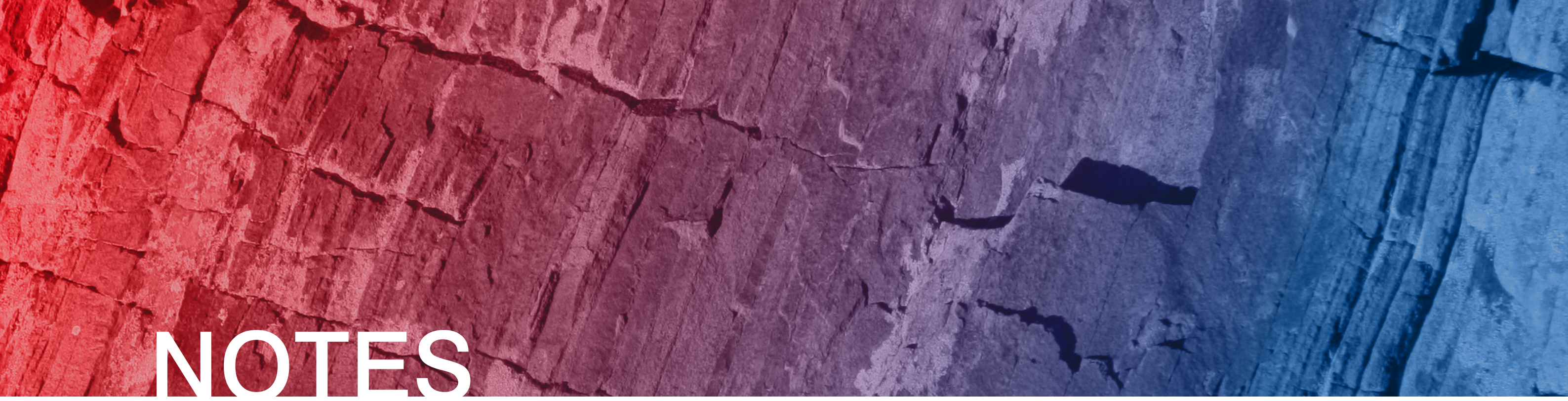

NOTES

2021 AUSTRALIAN GEOMECHANICS SOCIETY
VICTORIAN SYMPOSIUM

Innovations in Geotechnical Design

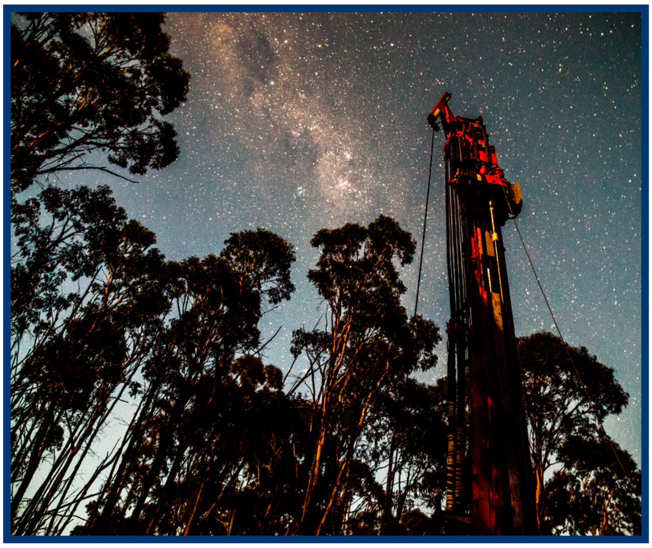

AUSTRALIAN GEOMECHANICS SOCIETY
VICTORIA CHAPTER